MINERALS

ECONOMIC & REGIONAL DEVELOPMENT AGREEMENT

Canada

Manitoba

MG-13097A

RESEARCH AND DEVELOPMENT IN MANITOBA MINES
TASK 2 - GROUND STABILITY EVALUATION WITH PARTICULAR REFERENCE TO AN EN ECHELON LENSED OREBODY DESIGN GUIDELINES

FINAL REPORT

by

HUDSON BAY MINING & SMELTING CO., LIMITED

in association with

INTERNATIONAL MINING SERVICES

DSS File Number: 14SQ.23440-4-9147-1
DSS Contract Serial Number: OSQ84-00330
CANMET Project Number: 4-9147-1

CANMET Scientific Authority: Dr. Somchet Vongpaisal

August 1989

90-01334/

RESEARCH AND DEVELOPMENT IN MANITOBA MINES
TASK 2 - GROUND STABILITY EVALUATION WITH PARTICULAR REFERENCE TO AN EN ECHELON LENSED OREBODY DESIGN GUIDELINES

FINAL REPORT

by

HUDSON BAY MINING & SMELTING CO., LIMITED

in association with

INTERNATIONAL MINING SERVICES

Work on the Project was Conducted Under the Auspices of the Canada Centre for Mineral and Energy Technology, Energy, Mines and Resources Canada (CANMET) Under the Canada/Manitoba Mineral Development Agreement

DSS File Number: 14SQ.23440-4-9147-1
DSS Contract Serial Number: OSQ84-00330
CANMET Project Number: 4-9147-1

CANMET Scientific Authority: Dr. Somchet Vongpaisal

August 1989

EXECUTIVE SUMMARY

This study is a culmination of five years of research that has been jointly sponsored by Hudson Bay Mining & Smelting Inc., CANMET and the Department of Mines of Manitoba under the Canada/Manitoba Mineral Development Agreement. The overall objective was to undertake ground stability evaluation with particular reference to an en echelon lensed orebody. Design guidelines were developed at Ruttan that enabled individual stopes to be designed and subsequently extracted under controlled and predicted conditions.

This study evaluates the factors that influence the stability of large, open stopes for an existing mining operation. The Ruttan mine, a 6000 tpd base metal operation, has mined by open stoping methods since 1979. This has resulted in a large data base of information which includes forty-three (43) stopes at various stages of extraction, thereby yielding 133 observations of:

Rock Mass Rating (footwall, hangingwall, ore)
Stope Dimensions (height, width, length)
Observed Dilution
Excavation Rates
Stope Configuration (isolated, rib, echelon)
Mining Sequence/Method

In addition, the observations were supplemented with in-situ measurements, structural mapping, stress and deformation monitoring and historical observations. A test stope was monitored and the results employed for purposes of verification of design guidelines presented in this study. It was concluded through numerical modelling, observation and measurement that the hangingwall and footwall of the individual stopes are in a state of relaxation, thereby enabling structural blocks to be released. This would generally be the case for most stope geometries whose major in-situ stress direction lies perpendicular to the long dimension of the opening. Consequently, the critical parameters were quantified in terms of their effect on dilution by employing multivariate analysis. The relationships derived were entirely confined to the Ruttan operation as they were empirically delineated and quantified.

The Ruttan operation is a multi-lensed orebody with individual stopes dipping at 70 degrees. The following empirically derived relationships were found to correlate strongly with the observed dilution:

a) Isolated Stope (61 observations)

Dil. = 8.6 - 0.09(RMR) - 13.2 (Exp.Rate) + 0.0038(Area Exp.)
r = 0.79 s = $\pm$ 3%

b) En Echelon Stope (44 observations)

Dil. = 10.3 - 0.13(RMR) - 14.8(Exp.Rate) + 0.003(Area Exp.)

r = 0.83 s = $\pm$ 2%

c) Rib Stope (28 observations)

Dil. = 15.8 - 0.18(RMR) - 7.7(Exp.Rate) + 0.0026(Area Exp.)

r = 0.8 s = $\pm$ 4%

where:

Dil.(%) - refers to predicted stope dilution (tonnes waste/tonnes reserves).

RMR(%) - Rock Mass Rating of the critical wall contact, generally the hangingwall.

Exp. Rate(x 1000m^2/mth) - refers to the rate at which the hangingwall is exposed (excavation rate/stope width).

Area Exp. (m^2) - refers to the exposed surface area of the hangingwall.

r,s - refers to the correlation coefficient and the unbiased standard error of estimate respectively.

The empirical relationships were related to stopes mined subsequent to the study and yielded errors of estimate of predicted dilution to within 2 - 4% of the observed dilution. The blast induced dilution was subsequently added to the predicted dilution. This value is difficult to estimate and is presently recorded as the dilution that is observed as the slot is being excavated. The design equations were based on a relatively large data base, considering that the works of Bieniawski (1973) and Barton (1974) were based on 49 and 200 case histories respectively.

It is suggested that the empirical methods of design outlined in this study be attempted at other operations where structural failure is the main factor contributing to stope dilution.

This would augment the data base and extend its applicability. Parameters unique to Ruttan that were employed in establishing the data base are as follows:

hangingwall and footwall of all stopes are in relaxation
groundwater is not a factor
mean stope inclination = 68° ± 9°
mean stope dilution = 10% ± 6%
mean RMR = 56% ± 20%
mean exposure rate = 0.18m² ± .09m² (x 1000)/mth
mean excavation rate = 2700m³ ± 1300m³/mth
mean span = 31m ± 13m
mean stope width = 15m ± 8m
mean stope height = 68m ± 20m
mean exposed surface area = 2250m ± 1120m
mean stope depth = 360m ± 48m below surface
mean blast correction factor = 3% ± 6%

Further observations and conclusions derived from this study can be summarized as follows:

a) Mine Sequence: Due to the en echelon nature of the deposit, the most optimum mining direction must be determined, that being the footwall stopes mined first progressing to the hangingwall or vice versa. Modelling of the above with BESOL (Chapter 4) had shown that both sequences would generate similar results. This is based upon an elastic solution. The F/W to H/W option would result in the least risk option based on the following assessment:

* the H/W of the producing stope will always be in virgin rock resulting in a more competent longitudinal pillar;
* the filling of the previously mined en echelon stope would result in fill below the present workings which is generally a safer situation.

b) Fill was found to limit the exposed span through ensuring that caving will not progress from one stope to an adjacent stope. It is a confining medium rather than a stress transfer medium. It was found to limit further stope deterioration due to wall slough. Benefits in terms of filling were not observed to be statistically significant when the Ruttan data base was evaluated in terms of dilution on adjacent stopes where one stope did not break into the adjacent work area.

c) Pillars at Ruttan were observed to yield when cut to remnant dimensions (6m in strike length x 10m in width x 60m in height). The pillars retained their post failure strength and acted as boundary pillars separating the dilution from one stope from affecting the dilution from the adjacent stope.

Crown Pillars at Ruttan have been designed to yield and subsequently monitored employing early warning devices during extraction.

The Ruttan operation has adopted the methods proposed in this study. It has been able to better predict stope dilutions, and design optimum stope spans to better forecast mining costs incurred due to wall stability. It is suggested that the empirical method of design outlined in this study be attempted/calibrated for other operations where similar failure mechanisms prevail.

RÉSUMÉ À L'INTENTION DE LA DIRECTION

Le présent rapport constitue le point culminant de cinq années de recherches parrainées conjointement par la Hudson Bay Mining and Smelting Inc., CANMET et le ministère des Mines du Manitoba, dans le cadre de l'entente Canada-Manitoba sur la mise en valeur des minéraux. Ces recherches visaient globalement à évaluer la stabilité des roches, en particulier d'un massif de minerai lenticulaire en échelon. Des lignes directrices de conception élaborées à Ruttan ont permis de concevoir des chantiers qui ont été par la suite exploités dans des conditions surveillées et prévues.

Le travail évalue les facteurs qui influencent la stabilité des grands chantiers ouverts d'une exploitation minière actuelle. Depuis 1979, la mine de Ruttan qui produit quotidiennement 6000 tonnes de minerais de métaux de base a été exploitée selon la méthode d'abattage par Chantiers ouverts. Cela a permis de mettre sur pied une importante base de données sur 43 chantiers, à diverses étapes d'extraction, de façon à recueillir 133 observations sur les points suivants :

La classification du massif rocheux (mur, toit, minerai)
Les dimensions des chantiers (hauteur, largeur, longueur)
La dilution observée
Les taux d'excavation
La configuration des chantiers (isolés, à piliers de paroi, en échelon)
La séquence et la méthode d'exploitation

Ces observations ont été en outre complétées par des mesures in situ, des observations structurales, des travaux de surveillance des contraintes et des déformations et des données historiques. Un chantier d'essai a été mis sous observations et les données utilisées pour vérifier les lignes directrices de conception contenues dans la présente étude. La modélisation numérique, les données d'observation et les mesures font ressortir que le toit et le mur de chaque chantier se trouvent en état de relaxation, permettant ainsi aux blocs structuraux d'être dégagés. Cela devrait être en général le cas de la plupart des chantiers caractérisés par une géométrie dont la direction principale des contraintes in situ est perpendiculaire à la direction de l'ouverture. Par conséquent, les paramètres critiques ont été quantifiés en fonction de leurs effets sur la dilution en recourant à une analyse multivariée. Les relations dérivées n'ont été appliquées qu'à la mine de Ruttan, étant donné qu'elles ont été délimitées et quantifiées à partir de données empiriques.

Ruttan exploite plusieurs lentilles, en chantiers inclinés à 70 degrés. Les relations empiriques suivantes correspondent étroitement à la dilution observée :

a) **Chantier isolé (61 observations)**

Dil. = 8,6 - 0,09 (CMR) - 13,2 (vit. exp.) + 0,0038 (surf. exp.)
r = 0,79 s = ± 3 %

b) **Chantier en échelon (44 observations)**

Dil. = 10,3 - 0,13 (CMR) - 14,8 (vit. exp.) + 0,003 (surf. exp.)
r = 0,83 s = ± 2 %

c) **Chantier à piliers de paroi (28 observations)**

Dil. = 15,8 - 0,18 (CMR) - 7,7 (vit. exp.) + 0,0026 (surf. exp.)
r = 0,8 s = ± 4 %

où :

Dil. (%) - désigne la dilution prévue en chantier (tonnes de stériles/tonnes de réserves)

CMR (%) - classification du massif rocheux au contact de la paroi critique, en général l'éponte supérieure.

Vit. exp. (x 1000 m^2/mois) - désigne la vitesse à laquelle est exposée l'éponte supérieure (vitesse d'excavation/largeur du chantier).

Surf. exp. (m^2) - désigne la surface exposée de l'éponte supérieure.

r, s - désignent respectivement le coefficient de corrélation et l'erreur type d'estimation non biaisée.

Les relations empiriques ont été utilisées dans les chantiers exploités après la réalisation de l'étude et les valeurs observées de dilution se sont maintenues entre 2 et 4 % de la dilution estimée. La dilution due au sautage a été par la suite ajoutée à la dilution prévue. La dilution due au sautage est difficile à préciser, et elle est estimée en fonction de la dilution observée pendant l'excavation du front de Taille Vertical. Les équations de conception étaient fondées sur une base de données relativement importante si l'on tient compte du fait que les travaux de Bieniawski (1973) et Barton (1974) comportaient respectivement 49 et 200 histoires de cas.

Il est proposé que les méthodes de conception empiriques, dont il est question dans la présente étude, soient mises à l'essai dans d'autres exploitations où les paramètres structuraux sont le principal facteur de dilution en chantier.

Ceci pourrait accroître la base de données et étendre son utilisation. Les paramètres particuliers à la mine Ruttan qui ont servi à mettre sur pied la base de données sont les suivants :

Le toit et le mur de tous les chantiers sont en état de relaxation
L'eau souterraine n'est pas un facteur à considérer
Inclinaison moyenne des chantiers = 68° ± 9°
Dilution moyenne des chantiers = 10 % ± 6 %
CMR moyenne = 56 % ± 20 %
Vitesse d'exposition moyenne = 0,18 m^2 ± 0,09 m^2 (x 1000)/mois
Vitesse d'excavation moyenne = 2700 m^3 ± 1300 m^3/mois
Portée moyenne = 31 m ± 13 m
Largeur moyenne des chantiers = 15 m ± 8 m
Hauteur moyenne des chantiers = 68 m ± 20 m
Surface moyenne exposée = 2250 m ± 1120 m
Profondeur moyenne des chantiers = 360 m ± 48 m sous la surface
Valeur moyenne du facteur de correction pour le sautage = 3 % ± 6 %

La présente étude a produit d'autres observations et conclusions qui peuvent se résumer comme suit :

a) Séquence d'exploitation : Étant donné la disposition en échelon du gisement, la direction d'exploitation optimale doit être déterminée de façon à ce que les chantiers de l'éponte inférieure, exploités en premier lieu, progressent vers l'éponte supérieure ou vice-versa. La modélisation de ce qui précède en recourant à BESOL (chapitre 4) avait montré que les deux séquences donneraient les mêmes résultats en se basant sur une solution élastique. La progression de l'éponte inférieure vers l'éponte supérieure présenterait moins de risques, compte tenu de l'évaluation suivante :

   * le toit du chantier exploité se trouverait toujours dans la roche vierge de façon à produire un pilier longitudinal plus compétent;
   * le remblayage du chantier en échelon déjà exploité donnerait un remblai au-dessous de l'exploitation en cours, ce qui, en général, constitue une situation plus sûre.

b) Le remblai a pour effet de limiter la portée exposée en empêchant le foudroyage de progresser d'un chantier à l'autre. Ce n'est pas un milieu de transfert de contraintes, mais bien un milieu de confinement. Le remblai limite donc la détérioration des chantiers due à l'effritement des parois. Le remblayage ne présentait pas d'avantages statistiquement importants lorsqu'on a évalué la base de données de Ruttan en fonction des effets de la dilution de chantiers adjacents, lorsque le chantier ne défonce pas dans des excavations adjascentes.

c) Selon les observations recueillies à Ruttan, les piliers cèdent lorsque découpés aux dimensions minimales (6 m longitudinalement x 10 m de largeur x 10 m de hauteur). Les piliers conservent leur résistance après rupture et jouent le rôle de piliers limites, empêchant la dilution d'un chantier d'affecter celle du chantier adjacent.

À Ruttan, les piliers de surface ont été conçus pour céder et être par la suite sous observation, pendant l'extraction, au moyen d'appareils de prédétection.

Les méthodes proposées dans la présente étude ont été appliquées à l'exploitation de la mine de Ruttan où l'on a été en mesure de mieux prévoir la dilution en chantier et de concevoir des portées de chantier optimales, afin de prévoir avec plus de précision les coûts d'exploitation dus à la stabilité des parois. Il est proposé que la méthode de conception empirique présentée soit mise à l'essai et calibrée dans d'autres exploitations où des mécanismes de rupture semblables sont observés.

TABLE OF CONTENTS

		Page
EXECUTIVE SUMMARY		i
TABLE OF CONTENTS		v
LIST OF TABLES		viii
LIST OF FIGURES		ix
ACKNOWLEDGEMENTS		xiii
CHAPTER 1	INTRODUCTION	1
1.0	GENERAL	1
1.1	SCOPE OF STUDY	1
1.2	INTRODUCTION	3
CHAPTER 2	THE RUTTAN MINE	7
2.1	INTRODUCTION	7
2.2	GEOLOGY OF THE RUTTAN DEPOSIT	8
2.2.1	LOCAL GEOLOGY	8
2.3	OREBODY GEOMETRY	10
2.4	MINING PRACTICE	10
2.4.1	STOPING METHOD	11
2.5	OBSERVATIONS/CONCLUSIONS	13
CHAPTER 3	STOPE DESIGN METHODOLOGY	25
3.1	INTRODUCTION	25
3.2	LITERATURE REVIEW	25
3.3	DESIGN PHILOSOPHY	28
3.4	SURVEY OF OPEN STOPE OPERATORS	30
3.4.1	DILUTION ASSESSMENT	31
3.5	CONCLUSIONS	32
CHAPTER 4	STRESS	40
4.1	INTRODUCTION	40
4.2	IN-SITU STRESSES AT RUTTAN	40
4.3	STRESS CONFIGURATION	41
4.3.1	NUMERICAL MODELS	41
4.3.1.1	Methods Available	42
4.3.1.2	Two Dimensional Boundary Integral Model	43
4.3.1.3	Three Dimensional Boundary Integral Model	44
4.3.1.4	Three Dimensional Displacement Discontinuity Method	44
4.3.2	MODEL INPUT PARAMETERS	44

TABLE OF CONTENTS (CONT.)

		Page
4.3.3	MODEL GEOMETRIES	44
4.3.4	EFFECT OF LENGTH/WIDTH RATIO	45
4.3.5	EFFECT OF DEPTH AND STRESS VARIATION	45
4.3.6	EFFECT OF MINING GEOMETRY AND SEQUENCING	46
4.3.7	COMPARISON OF MODELLING METHODS	47
4.3.8	STOPE 800-26J	48
4.4	CONCLUSION	48
CHAPTER 5	ROCK MASS CHARACTERIZATION	68
5.1	INTRODUCTION	68
5.2	ROCK MASS CLASSIFICATION	68
5.3	STRUCTURAL ASSESSMENT	71
5.3.1	KINETIC ANALYSIS	73
5.4	OBSERVATIONS/CONCLUSIONS	74
CHAPTER 6	DILUTION	84
6.1	INTRODUCTION	84
6.2	DEFINITION	84
6.3	OBSERVED DILUTION	86
6.3.1	VOLUME TRAMMED VERSUS STOPE DIMENSIONS MINED	87
CHAPTER 7	DATABASE	91
7.1	INTRODUCTION	91
7.2	STATISTICS	91
7.2.1	DEFINITION OF STATISTICAL TERMS	92
7.3	DISTRIBUTION OF DATABASE	96
7.4	IDENTIFICATION OF CRITICAL PARAMETERS	100
7.4.1	PARTIAL CORRELATION	104
7.5	QUADRATIC/LINEAR INTERPRETATION	105
7.6	OBSERVATIONS/CONCLUSIONS	106
CHAPTER 8	STOPE DESIGN	131
8.1	INTRODUCTION	131
8.2	STOPE CONFIGURATION	131
8.3	BLAST CORRECTION FACTOR	132
8.4	PREDICTIVE EQUATIONS (GOVERNING EQUATIONS)	133

TABLE OF CONTENTS (CONT.)

		Page
CHAPTER 9	APPLICATION	141
9.1	INTRODUCTION	141
9.2	CALIBRATED DATABASE	141
9.3	OTHER METHODS	141
9.4	TEST STOPE	143
9.4.1	INTRODUCTION	143
9.4.2	TEST STOPE 800-26J	144
9.4.2.1	Stope Geometry	144
9.4.2.2	Production History	145
9.4.2.3	Instrumentation	145
9.4.2.3.1	Extensometers	145
9.4.2.3.2	Stress Meters	147
9.4.3	EMPIRICAL DESIGN	147
9.4.3.1	Design Parameters	148
9.4.4	CONCLUSIONS	150
CHAPTER 10	MINE DESIGN GUIDELINES	169
10.1	INTRODUCTION	169
10.2	STOPE AND PILLAR DESIGN	169
10.2.1	STOPE DESIGN	169
10.2.2	PILLAR DESIGN	169
10.3	MINE SEQUENCE	170
10.4	SUPPORT	171
10.4.1	FILL	171
10.4.2	MECHANICAL SUPPORT	172
10.5	CROWN PILLAR EXTRACTION	173
10.5.1	CASE HISTORY - WEST LENSES	173
10.6	INSTRUMENTATION	176
CHAPTER 11	CONCLUSIONS	184
11.1	CONCLUDING REMARKS	184
LIST OF REFERENCES		186
APPENDICES		

LIST OF TABLES

		Page
Table 3.1	Rock Mass Classification Systems - Applications	34
Table 3.2	Limitations of the Major Rock Mass Classification Systems - Mining Applied	34
Table 3.3	Summary of Parameters Used in Rock Mass Classification Systems - Hard Rock Mining	35
Table 4.1	Numerical Codes	49
Table 4.2	Numerical Model - Input Parameters	50
Table 4.3	Summary of Numerical Analysis Performed	50
Table 5.1	Core Logging Format - Ruttan	75
Table 5.2	Intact Rock Strength Parameters	76
Table 5.3	Summary of Rock Mass Parameters	76
Table 7.1	Values of Correlation Coefficient for Different Levels of Significance	107
Table 7.2a	Isolated Stopes Data Base	108
Table 7.2b	Echelon Stopes Data Base	109
Table 7.2c	Rib Stopes Data Base	110
Table 7.3	Data Base - Statistical Summary	110
Table 7.4	Isolated Stopes Data Base	111
Table 7.5	Isolated Stopes Data Base - Comparison Quadratic and Planar Surface Empirical Equations	112
Table 8.1	Comparison Predicted/Observed - Isolated	134
Table 8.2	Comparison Predicted/Observed - Echelon	135
Table 8.3	Comparison Predicted/Observed - Rib	135
Table 9.1	Calibrated Database - Stopes Mined Subsequent to Study	151
Table 9.2	Calibrated Database - Predicted Dilution	152
Table 9.3	Blast Production Record - 800-26J	153
Table 9.4	Stope Worksheet - Empirical Approach to Design	154

LIST OF FIGURES

		Page
Figure 2.1	Location Map	14
Figure 2.2	Longitudinal of Ruttan Mine	15
Figure 2.3	Regional Geology	15
Figure 2.4	Island Arc Development	16
Figure 2.5	Schematic Section Showing the Formation of the Ruttan Deposit	16
Figure 2.6	Tectonic Evolution	17
Figure 2.7	Isometric Diagram - Ruttan Deposit	17
Figure 2.8	Local Geology	18
Figure 2.9	Plan or Ore Lenses - 260 m Level	18
Figure 2.10	Typical Section - 2650E	19
Figure 2.11	Ore Delineation Pattern	19
Figure 2.12	Isometric - 320 m Level	20
Figure 2.13	Typical Stope Dimensions	20
Figure 2.14	Stoping Method	21
Figure 2.15	Sequence of Extraction - Conventional	22
Figure 2.16	Sequence of Extraction - VCR + Slash	23
Figure 2.17	Categorization of Stopes - Plan View	24
Figure 3.1	Beam Theory	36
Figure 3.2	Voussoir Arch	36
Figure 3.3	Numerical Solution	36
Figure 3.4	Mathews Method of Stope Design	37
Figure 3.5	Hangingwall and Footwall Beam Deflection	37
Figure 3.6	Stress Trajectories - 320 m Level, Plan View	38
Figure 3.7	Structurally Controlled Failure - Section of Typical Stope	38
Figure 3.8	Plan View of Two Adjacent Stopes	39
Figure 4.1	Vertical Stress vs Depth	51
Figure 4.2	Horizontal Stress vs Depth	51
Figure 4.3	Suggested Direction of Compression During Tectonic Deformation and Measured Principal Stresses from Overcoring Plotted in Lower Hemisphere of Equal Area Net	52
Figure 4.4	Modelled Stope Configuration/Sequences - Plan View	53
Figure 4.5	Horizontal/Vertical Stress Ratio (k)	54
Figure 4.6	Tangential HW/FW Stress vs Span/Width	54
Figure 4.7	Stress Configuration - Parametric Study	55
Figure 4.8	Lateral Extent of Tensile Zone	56

LIST OF FIGURES (CONT.)

		Page
Figure 4.9	Effect of "k" on Tangential Stress in the FW/HW	56
Figure 4.10	Extent of Lateral Tensile Zone with Variance in "k"	57
Figure 4.11	Base Case - Stress Configuration	57
Figure 4.12	Stress Configuration - Rib Stopes	58
Figure 4.13	Stress Configuration - Echelon Stopes	59
Figure 4.14	Variation of Lateral Extent of Tensile Extent with Number of Openings	60
Figure 4.15	BESOL - Rib Stope Analysis - Stope "A" Mined	60
Figure 4.16	BESOL - Rib Stope Analysis - Stope "A & B" Mined	61
Figure 4.17	BESOL - Rib Stope Analysis - Stope "A, B, C," Mined	61
Figure 4.18	BESOL - Echelon Analysis FW/HW	62
Figure 4.19	BESOL - Echelon Analysis HW/FW	62
Figure 4.20	BITEM - Echelon Analysis - Instantaneous Excavation	63
Figure 4.21	Isolated Stope Analysis - Comparisons of Modelling Methods	63
Figure 4.22	Longitudinal (Paraiiel to Strike) Presentation of Test Stope 800-26J	64
Figure 4.23	BESOL Analysis - Hangingwall Displacement on 730 m L of 800.26J	65
Figure 4.24	BESOL Analysis - Hangingwall Displacement on 760 m L of 800.26J	65
Figure 4.25a	BESOL Analysis - Horizontal Cross-Section Stress Configuration on 760 m L, 800-26J	66
Figure 4.25b	BESOL Analysis - Horizontal Cross-Section Stress Configuration on 760 m L, 800-26J	67
Figure 5.1	Stope Characteristics	77
Figure 5.2	Rock Mass Distribution	78
Figure 5.3	Photograph Identifying the Major Sets at Ruttan	79
Figure 5.4	Photograph Showing the Continuity of Structure	80
Figure 5.5	Design Sets	81
Figure 5.6	Conditions for Sliding and Toppling of a Block on an Inclined Plane	82
Figure 5.7	Stereonet Showing the Potential for Failure in the FW of the "B Lenses" on the 430 m Level	82
Figure 5.8	Base Friction Model	83
Figure 6.1	Definition of Dilution	88
Figure 6.2	Cumulative Dilution vs Volume Excavated	88

LIST OF FIGURES (CONT.)

		Page
Figure 6.3	Volume Trammed = L1 x W x H	89
Figure 6.4	Longitudinal Showing a Typical Extraction Sequence	89
Figure 6.5	Inferred Measurement of Stope Span	90
Figure 7.1	Scatter Diagram	113
Figure 7.2	Example of Standard Error of Estimate	113
Figure 7.3	Distribution of Stopes - Data Base	114
Figure 7.4	Shape Factor (Hydraulic Radius)	115
Figure 7.5	Minor and Major Stress Contours Surrounding Stopes at Ruttan - Plan View	115
Figure 7.6	Stope Dilution - Blasting	116
Figure 7.7a	Distribution of Parameters Comprising Isolated Data Base	117
Figure 7.7b	Distribution of Parameters Comprising Isolated Data Base	118
Figure 7.7c	Distribution of Parameters Comprising Isolated Data Base	119
Figure 7.7d	Distribution of Parameters Comprising Isolated Data Base	120
Figure 7.7e	Distribution of Parameters Comprising Isolated Data Base	121
Figure 7.8a	Distribution of Parameters Comprising Rib Data Base	122
Figure 7.8b	Distribution of Parameters Comprising Rib Data Base	123
Figure 7.9a	Distribution of Parameters Comprising Echelon Data Base	124
Figure 7.9b	Distribution of Parameters Comprising Echelon Data Base	125
Figure 7.10	Critical Parameters	126
Figure 7.11	Rock Mass Analysis	127
Figure 7.12	Criteria for Sensitivity	127
Figure 7.13	Governing Equations - Derivation for Isolated Stopes	128
Figure 7.14	Governing Equations - Derivation for Echelon Stopes	128
Figure 7.15	Sensitivity Analysis - Data Base = All Stopes	129
Figure 7.16	Partial Correlation	129
Figure 7.17	Comparison - Type of Equation (Linear/Quadratic)	130

LIST OF FIGURES (CONT.)

		Page
Figure 7.18	Quadratic/Linear Correlation - Isolated Stopes	130
Figure 8.1	Governing Equations	136
Figure 8.2	Stope Configuration - All Stopes	137
Figure 8.3	Stope Configuration - Combined	137
Figure 8.4	Span Derivation	138
Figure 8.5	Incorporating Blast Correction Factor	138
Figure 8.6	Stopes with "BCF > 0" Omitted From Data Base	139
Figure 8.7	Predicted vs Recorded Dilution	139
Figure 8.8	Cumulative Relative Frequency vs Dilution Difference	140
Figure 9.1	Augmented Data Base	155
Figure 9.2	Mathews Method of Span Determination	156
Figure 9.3a	Laubsher Approach to Span Determination	157
Figure 9.3b	Barton Approach to Span Determination	157
Figure 9.3c	RMR Method of Span Determination	158
Figure 9.4	Voussoir Beam Method of Span Determination	159
Figure 9.5	Isometric Test Stope 800-26	160
Figure 9.6	Longitudinal 800-26J (Blast Sequence)	161
Figure 9.7	Plan 730 m L Location - 800-26J Stope	162
Figure 9.8	Sections Instrumented	163
Figure 9.9	Longitudinal Record	164
Figure 9.10	Stope Dilution	165
Figure 9.11a	Displacement vs Time - X7301	165
Figure 9.11b	Displacement vs Time - X7302	166
Figure 9.11c	Displacement vs Time - X7303	166
Figure 9.12a	NS Stress Meters	167
Figure 9.12b	EW Stress Meters	167
Figure 9.12c	Vertical Stress Meters	168
Figure 9.13	Incremental Dilution	168
Figure 10.1a	Modelled Geometry - Plan View	178
Figure 10.1b	Modulus of Deformation vs RMR	178
Figure 10.2	Stress Trajectories at Various Stages of Pillar Failure	179
Figure 10.3	Mining Sequence	180
Figure 10.4	Vacuum Pump Employed at Ruttan	180
Figure 10.5	Numerically Modelled Crown - Section	181
Figure 10.6a	Displacement Monitoring Instrumentation	182
Figure 10.6b	Stress Monitoring Instrumentation	183

ACKNOWLEDGEMENTS

The authors would like to express their appreciation to the management of the Ruttan mine for providing assistance in the development and implementation of guidelines developed through this study. Special gratitude is extended to Dr. S. Vongpaisal of CANMET for his technical review and guidance throughout the project.

The Ruttan operation gratefully acknowledges the research effort that is being conducted and sponsored jointly by CANMET, Department of Mines of Manitoba, and Hudson Bay Mining & Smelting Inc.

The project team acknowledges Mr. Andy Gottzmann who initiated the study and Dr. Rimas Pakalnis, Todd Madill and Brad Lantz who conducted the research.

CHAPTER ONE
INTRODUCTION

1.0 GENERAL

This report largely concludes the individual Work Tasks as commissioned by CANMET under the Canada/Manitoba Mineral Development Agreement. The overall objective was to undertake ground stability evaluation with particular reference to an en echelon lensed orebody. Design guidelines were developed at Ruttan that enabled individual stopes to be designed and subsequently extracted under controlled and predicted conditions. This study encompasses five project stages which commenced on January 14, 1985 and were completed on March 31, 1989.

The design guidelines have been implemented in the final two years of the project and assessed in terms of their predictive capabilities.

1.1 SCOPE OF STUDY

Hudson Bay Mining and Smelting Company Limited has been commissioned by the Canada Centre for Mineral and Energy Technology under the CANMET/Manitoba Mineral Development Agreement to undertake the following Task:

"Ground Stability Evaluation With Particular Reference To An En Echelon Lensed Orebody".

This Task is to encompass five project stages which commenced on January 14, 1985, and were completed on March 31, 1989.

The Sub-Tasks to be evaluated were as follows:

1. Review various rock mass classification methods and identify the most suitable which will have practical application for Underground Mining Operations.

   This project was completed and the final report submitted in June, 1985, to the Scientific Authority.

   (REFER: PROJECT 1 - REVIEW OF ROCK MASS CLASSIFICATION SYSTEMS RELEVANT TO UNDERGROUND MINES/JUNE, 1985)

2. Determine and establish a database which includes Static and Dynamic Mechanical Properties of Mine Rocks, In-situ Fill Properties, In-situ Stresses, Failure Criteria, Ground Water Conditions and Other Relevant Geologic Information for Modelling and/or Back Analysis Purposes.

   This information was employed to derive the guidelines for the design of open stopes at Ruttan and is summarized in this report. It is discussed in detail in Interim Report - Project 2/3 Database/Remote Monitoring.

3. Develop a Remote Monitoring Program Underground to forewarn of any failure. The equipment shall be capable to transmit data to surface via an underground communication network. A remote "Rod Extensometer" was installed in 800-27J to monitor the footwall. The data was transmitted to surface via the radio communication network. This part of the study is summarized under a separate project task "Communications in Underground Mines" CANMET PROJECT NUMBER: 4-9147-2.

   A "Local Remote" system was employed which warned the operator of excessive movement through the triggering of a flashing hazard light located in the vicinity of his work area. The "Local Remote" system is described in Chapter 10.6 - Instrumentation.

4. Identify the stabilizing effect that fill has on the individual stopes and to identify its effectiveness for overall mine stability. This project has been summarized in Chapter 10.4 - Fill Support.

5. Install rock mechanics devices which include shear strips, multi-wire extensometers, Irad gauges and pressure load cells in test stope areas in order to evaluate ground and fill stability. The information was employed to verify assumptions made in deriving stope design guidelines and is summarized in Chapters 9 and 10.

6. Conduct back analysis of field data and validate geo-numerical models; two and three dimensional boundary element programs were employed. In addition, "BESOL", a 3D-displacement discontinuity code was employed to derive stope design guidelines. This information is reviewed in Chapter 4 - Stress.

7. Develop design guidelines for mining a multi-lensed orebody, which include relevant parameters such as pillar and stope dimensions, crown pillar sizes, mining sequences, ground support, fill requirements and instrumentation (Chapter 10).

1.2 INTRODUCTION

This report is the culmination of three years of CANMET/Ruttan involvement in a research project whereby the objective was to delineate and to quantify the factors that influence the stability of large, open stopes for an existing mining operation. This would enable the ground control engineer to better design mine openings after having a more complete understanding of the factors affecting mine stability.

The study addresses the areas of concern at Ruttan which include crown pillar extraction, mine sequencing, support and monitoring. The most critical area of investigation was developing a rational approach to the design of stope spans in jointed materials. This forms the focus for the study where the associated areas of investigation will evolve upon developing an understanding of how rock behaves in a jointed medium. It will be shown in this study that the "optimum stope geometry can be quantified in terms of the rock quality, the rate of extraction, blasting effects and the resultant stress regime". This will be the formulating assumption that the study will attempt to justify.

Optimum is defined as that stope geometry that would yield a minimal acceptable dilution. Dilution is a measure of the quality of the design since it records the amount of hangingwall and/or footwall slough with respect to the stope reserves expected to be removed. The Ruttan Mine, a 6,000 tpd underground operation, is located in Northern Manitoba, 760 km North of Winnipeg and 20 km East of the town of Leaf Rapids. The Ruttan copper-zinc orebody is a multi-lensed, steeply dipping (70°) en echelon deposit. Individual lenses have a maximum strike length of 350 meters with widths varying from 7 to 61 meters. The mining method is open stoping with delayed backfilling which extends from surface to 860 meters below surface. Stope spans at the Ruttan Mine were initially designed employing classical beam theory. Failures at the mine were found to be controlled primarily by structure, and this could not be explained by the previous homogeneous model. There exists no accepted design method of predicting stope spans in jointed materials. Beam theories, numerical models and empirical criteria have been employed in the past with some degree of success, however, the major drawback is that much of our classical design approaches have been based on the assumption that homogeneous, isotropic, elastic conditions do exist.

Forty-three (43) stopes at the Ruttan Operation were analysed in terms of deriving the factors most critical to design. This database represents 432 stope geometries and resultant dilutions as recorded by the mine. The prevailing stress conditions at Ruttan cause the hangingwall (HW) and footwall (FW) to be in a relaxed state. The cases involved at Ruttan are for that particular stress regime which would cause the rock mass in the vicinity of the ore contacts to be in a state of relaxation.

The term "zone of relaxation" is employed rather that a zone of tension. While it is true that this region is unconfined, it may not be in pure tension. The reason being that in order for tensile stresses to be sustained in the rock mass, the rock mass must have a tensile strength which is generally assumed to be non-existent. An ore contact that is in a high state of shear or compression will result in entirely different failure modes. The deviations that may occur from the Ruttan database will be addressed and discussed, however, the study will generally be applicable only to a Ruttan type situation whereby:

* hangingwall and footwall of an individual stope is in a relaxed state;

* stope plunge ranges between 60 to 70 degrees;

* stope is not choke blasted (i.e. stope is void prior to blasting next cut).

This report is divided into relevant chapters which by themselves can stand alone, however, are ultimately incorporated into a cohesive unit in formulating the solution to the work scope stated previously.

The chapters will be as follows:

A) **The Ruttan Mine:** This will be a general chapter summarizing the ore geometry, lithology, stope configuration, mining method and history.

B) **Stope Design Methodology:** This chapter outlines the complexity of the Ruttan deposit with respect to arriving at a methodology for stope design. It also summarizes a literature search that assesses the state of the art of: a) stope design in jointed materials and b) of existing rock mass classification systems. A survey conducted by the author which reviews the present state of stope design as is practised by open stope operators throughout Canada is summarized and presented in Chapter 3.4.

C) **Stress:** This chapter assesses the influence of stress on the stope geometries at Ruttan. Individual stopes were modelled by employing a two dimensional "boundary element numerical code" and a post-processor developed for this study.

Nomograms are employed in estimating the stresses given a particular stope length/width dimension. A two dimensional analysis is employed and compared to observational and quantifiable measurements made throughout the mine. A three dimensional boundary element program, modified for the

Ruttan Operation, compares the validity of modelling stopes at Ruttan by the 2D process. The 3D displacement discontinuity program "BESOL" was employed to calibrate the test stope (800-26J) monitoring. It was employed to verify the above observations and to determine:

* Mining Sequence
* Backfill Effects
* 2D versus 3D Modelling Relationships at Ruttan

D) **Rock Mass Assessment:** The Ruttan Operation, including all forty-three (43) stopes, has been assessed in terms of a suitable rock mass descriptor. A selection of the most suitable classification was chosen upon identifying the relevant rock quality parameters with respect to the Ruttan database. The most critical parameters were evaluated in terms of resultant dilution. This is the "control" parameter that will enable the critical parameters to be quantifiably assessed. All development areas, mined stopes and future mining areas were assessed a Rock Mass Rating.

E) **Dilution:** This parameter is a measure of the quality of the stope design. It is a parameter that is recorded by most open stope operators in Canada. It is a measure of the degree of wall slough with respect to the expected stope reserves mined. Various definitions exist and are summarized in this chapter. Dilution is recorded for all mined stopes at Ruttan at various stages of extraction. These will be statistically correlated to the rock quality parameters identified as critical in order to evaluate a governing equation that attempts to predict optimum stope spans. Dilution is a quantifiable assessment of stope design, however, it is assessed in most instances by observation and calibrated by measurement.

F) **Database:** Upon the assessment of the significant factors affecting dilution, a database is derived for the individual mined stopes at Ruttan. The database is comprised of stope dimensions (span, height, width), stope configuration, stope depth, inclination, extraction rate, observed dilution, rock mass rating of the critical wall contact, and observed damage due to blasting. This database is comprised of 43 mined stopes yielding 432 recorded stope geometries which were subsequently averaged into 133 case histories. Mine sequence, fill requirements, among other parameters is assessed as to their significance to design.

G) **Stope Design Assessment:** The best fit parameters are incorporated through single/multiple correlation testing. Linear, planar, linear hyper-surface, and quadratic curved lines and surfaces are fitted to the relevant parameters in

order to assess the level of acceptance of the proposed hypothesis. Statistical assessment in terms of multiple and partial correlation coefficients, levels of significance, and confidence limits are determined for the best fit surface. It is concluded at this stage that stress is not significant in terms of dilution since numerical modelling indicated that the hangingwall and footwall of individual stopes at Ruttan are in a state of relaxation, thus resulting in rock mass controlled failures. This statement will be further reinforced through measurement and observational approaches.

H) **Application:** This chapter analyzes the relationships derived from the existing database to stopes subsequently mined. A brief comparative analysis is made between the most prospective existing methods of stope design and the empirical method proposed in this report. Stopes mined subsequent to the implementation of the original database were compared to the design equations.

I) **Mine Design Guidelines:** A rational approach to mine design is now possible upon developing a better understanding of how jointed rock behaves upon extraction. Incorporating this information into the mining of the Ruttan orebody, the following is attained:

* Stope Span and Pillar Design
* Mine Sequencing (Sequence of Extraction of Individual Lenses)
* Crown Pillar Extraction
* Support and Instrumentation Requirements

The above is achieved through the implementation of the program of study developed through this combined research effort.

CHAPTER TWO
THE RUTTAN MINE

2.1 INTRODUCTION

In order to understand the parameters involved in developing a method of stope design for the Ruttan orebody, it is important to know the history, geology, mining practice and the mine geometry. Studying the influencing factors requires that the methodology be integrated into the overall mine regime. This involves, in addition to numerical and analytical analyses, a coordinated field effort drawing from all the available information, and re-analyzing that information from a different perspective. This chapter describes the first stage of developing a database which will outline the associated geometric complexities associated with the Ruttan orebody.

The Ruttan Mine is located in Northern Manitoba, 760 km north of Winnipeg and 20 km East of the town of Leaf Rapids, Figure 2.1. The Ruttan copper-zinc orebody is a multi-lensed, steeply dipping (70°) en echelon deposit. Individual lenses have a maximum strike length of 350 meters and widths varying from 7 to 61 meters. The mining method practised is blasthole open stoping with delayed fill. Production, Figure 2.2, commenced by open pit in April, 1973 and continued until December, 1980. The pit at this time was 1000 meters long, 600 meters wide and 200 meters deep.

The Ruttan orebody is considered to be open at the 860 meter level (below surface). The underground operation was developed to 430 meters below surface and is commonly referred to as the "Upper Mine". Production from the Upper Mine commenced in March, 1979 and is presently at 6000 tonnes per day. The removal of the entire surface crown pillar in the summer of 1988 will complete the mining of the Upper Mine. Delineated reserves exist to the 860 meter level yielding tonnages sufficient for mining until 1992 at a production rate of 8000 tonnes per day. The "Lower Mine" is defined as that portion of the operation that exists between the 430 meter level and the 860 meter level. In October, 1985 mining of the Lower Mine commenced while the Upper Mine was phasing down.

A significantly large database of information is available from the Upper Mine, containing approximately 68 stopes of which 48 have been mined at the time of the completion of this study. It was decided to terminate the data gathering stage in February, 1986 with the subsequently mined stopes (20) serving to calibrate the predictive design equations.

2.2 GEOLOGY OF THE RUTTAN DEPOSIT

The Ruttan orebody is a copper-zinc rich, exhalative, massive sulphide deposit contained within a sequence of Proterozoic volcanic rocks and their derived sediments. Ruttan is located within the Churchill Geologic Province of Manitoba, Figure 2.3.

This geologic province is characterized by two east-west trending volcanic arc belts, the Wasekwan Group to the north and the Amisk Group to the south, separated by a wide sedimentary basin termed the Burntwood River Suite, Figure 2.3. This is particularly important in relating the orogeny of the deposit to its present configuration and stress regime. The Ruttan deposit is Aphebian in age and is interpreted to be a synclinal deposit associated with island arc development. This is graphically shown in the subsequent section concerning the tectonic history of Ruttan. The Wasekwan Group consists of a conformable sequence of volcanic flow, tuffs, agglomerates, breccias and volcaniclastic sediments. Overlying this package of rocks are the shallow water sediments of the Sickle Group. Archean basement borders the Wasekwan and Sickle Groups to the north.

The volcanic rocks of the Wasekwan and Sickle Groups have been considerably altered during regional metamorphism to lower amphibolite, amphibolite, and greenschist facies. Basic volcanic rocks and sediments have been converted to schists and banded gneisses locally characterized by epidote, hornblende, biotite, chlorite, garnet, staurolite, cordierite and andalusite alteration.

2.2.1 LOCAL GEOLOGY

The Ruttan Mine is thought to be a geosynclinal deposit associated with island arc development. This is where a plate of lithosphere is slowly plunging downwards into the mantle. The volcanism that builds the volcanic mountains is presumably caused by the melting of the downgoing plate, Figure 2.4. Therefore, the Ruttan deposit is assumed to have been formed along a flank of a large volcano. This volcanic arc trends east-west as shown in Figure 2.3. A schematic section, drawn perpendicular to the trend of the island arc, is employed to describe the sequence of events leading to the formation of the Ruttan deposit, Figure 2.5. It is best summarized as follows:

* Ruttan was formed beneath sea level as a result of magma being vented within a granitic host.

* Basalt flows were deposited then subsequently overlain by a sequence of volcanically derived sediments. Pillow structures are found within the basalt

unit indicating that this unit was emplaced at a rock-water interface. The footwall volcaniclastics are as a result of acid volcanism and its subsequent erosion. The rock is quite uniform, thinly to thickly bedded, relatively unaltered and composed of fine grained, intermediate, clastic fragments. This unit grades into the footwall altered volcaniclastics which is characterized by increased alteration and the presence of cordierite, staurolite and magnetite.

* The mine rhyolites (quartzites) follow in sequence. They are the products of erosion from the flanks of the volcano. These rhyolites were interbedded with channelways of mud deposits. This is a felsic rock which was subsequently replaced by copper and zinc rich solutions originating from the mineralized vent. The mud zones were hydrothermally altered to chlorite and chlorite-talc schist on both the footwall and hangingwall contacts of the ore lenses.

* Overlying the mine rhyolite is the exhalite horizon which was formed as a precipitate resulting from the mixing of the hydrothermal fluids and seawater on the sea floor. The zinc rich lenses of the Ruttan deposit are found in the Exhalite unit and are characterized by pyrite-sphalerite-silicate and chert banding. Well bedded detrital sediments dominate the upper portions of this horizon. The sulphide lenses formed are sedimentary in formation unlike the igneous origin of the lenses within the mine rhyolites.

* Finally, low (sediments) and high energy (turbidites) volcanically derived deposits settled over the exhalative horizon. It (PM unit) consists of interbedded graywackes and volcanic (erosion) derived conglomerates. Subsequent deformation was in the form of shearing of the weaker sulphide deposits and the further intrusion of a system of dykes throughout the above horizons.

The above sequence of events are sedimentary in nature resulting in flatly dipping deposits. It is postulated that, after the deposition of the Ruttan deposit, the Churchill province had subducted underneath the Superior province. This tectonic activity resulted in the inclination of the orebody to that shown in Figure 2.6. The combined tectonic activity of the initial island arc development and the subsequent subduction resulted in a late phase of regional metamorphism to influence the Ruttan deposit. This late phase of metamorphism converted the basic volcanic rocks to hornblende, plagioclase schists and banded gneisses with variable amounts of epidote, biotite and chlorite. The sediments were converted to biotite, muscovite, quartz schists and gneisses. An alteration zone is associated with the Ruttan deposit which is dominated by a bifurcating shear zone. The shear zone at Ruttan is

oriented at N70° E dipping at 68° SE. It is up to 30 meters wide and bifurcates into three main shear zones: Art's Fault, North Wall Shear and East Shear, Figure 2.7. The overall effect of the shearing was to significantly change the geometry of the ore lenses and alteration zones. The individual mine rock units will be further described in the context of "rock mass characterization", Chapter 5. Figure 2.8 is a geologic plan of the Ruttan area.

2.3 OREBODY GEOMETRY

The Ruttan orebody comprises nine ore lenses, all subparallel in attitude and en echelon in nature, Figure 2.7. The orebody strikes N70° E, dips 70° SE and plunges 70° to the east. The maximum dimensions of the ore zone are 120 metres wide by 700 metres long. An open pit lies immediately above the underground workings to a depth of 210 meters.

The geometry of the lenses is such that to the west of the east shear, five major lenses form a zone with a strike length of 350 meters at the 260 meter level (below surface) which narrows to 200 meters at the 430 meter level. These are known as the "west lenses" and the width of the individual lenses range from 7 to 35 meters. The west lenses bottom out at the 660 meter level whereas the "east lenses" continue to a yet unknown depth. These lenses lie east of the east shear and are comprised of four lenses.

Generally, the ore contacts are irregular both in plan and section and pinch and swell down dip, thereby enclosing narrow bands of waste, Figure 2.9, 2.10. Consequently, in order to properly delineate the stope geometry, diamond drilling is conducted on a 15 meter by 15 meter pattern along the ore contact, Figure 2.11. The complexity of the ore geometry is indicated by Figure 2.12. Individual stopes are defined by draw level, a letter designating the lens and a number defining the stope within the lens. An example is 320-11B. This stope is drawn off the 320 meter level, is a "B" lens as defined in Figure 2.9 and is stope number "11" within that lens. Generally, a stope having a similar number is located either in the footwall or hangingwall of the preceding stope. The "B" lenses are located in the footwall of the "C" which are located in the footwall of the "D" lenses. This terminology will be useful in identifying areas of the mine. Stope numbers increase from west (7 to 16) to east (17 to 22).

2.4 MINING PRACTICE

The Ruttan orebody is a complex arrangement of ore lenses. These lenses are located in close proximity to each other and join in certain locations. Such complexity and irregularity of ore outlines require that mining of the individual

lenses be carried out in a predetermined sequence in order to ensure maximum ground stability. The stoping method is blasthole open stoping with delayed fill. Two variations of open stoping are used. In one, conventional small diameter (51 mm) holes are drilled from levels spaced at 30 meter vertical intervals. In the second, large diameter (165 mm) holes are drilled from levels spaced at 60 meter vertical intervals. The blasting sequence in these "large diameter stopes" is a combination of vertical crater retreat and slash.

Stopes and pillars are laid out on a regular pattern and resemble the dimensions outlined in Figure 2.13. In general, stopes and pillars are approximately 30 meters and 15 meters in length respectively. Pillar recovery is an integral part of the normal stoping progression. When a stope is mined out, it is planned to be backfilled using classified mill tails. The adjacent stope is mined back to the predetermined pillar line, then the remaining pillar is blasted into the open stope leaving a 6 meter remnant of ore to retain the fill. In practice, this is generally not the case since the filling cycle is well behind schedule, thereby not enabling the filling of stopes prior to the mining of the adjacent stope. Consequently, the rib pillar is blasted to the 6 meter remnant without the benefit of fill. After removal of the broken pillar ore, the stope and pillar void is then backfilled with mill tails. The fill forms the draw level for the next mining lift.

Drawpoint levels are established at 60 meter vertical intervals. Active draw levels are currently at the 260 meter, 320 meter, 370 meter and 430 meter levels. Due to the irregularity of the ore lenses, it is sometimes necessary to locate additional drawpoints on levels other than the main levels. This consequently results in stope heights being less that 60 meters. Intermediate drill levels are driven between the main levels, creating a 30 meter level interval in stoping areas where small diameter blastholes are utilized. All production blasting is with ANFO and packaged water gels. Non-electric delays are used to effect proper sequencing of initiation.

2.4.1 STOPING METHOD

Generally, transverse open stoping is employed at Ruttan leaving a remnant pillar as shown in Figure 2.13. Mine practice dictates that where the ore width exceeds 30 meters, a longitudinal pillar is left, thereby ensuring that the stope width does not exceed 30 meters. These values have been determined empirically through trial and error.

As previously indicated, the Ruttan operation employs two variations of open stoping. Figure 2.14 depicts the conventional method of open stoping employing 51 mm diameter holes. Initially, the undercut is silled out for a vertical height of 12 meters from footwall to hangingwall and remnant to remnant pillar. The

2 meter x 2 meter slot is mined either conventionally or raisebored to a 12 meter height above the upper drill level. In addition to slot development, it is required to develop a footwall and hangingwall drive which are normally located at the ore contact. It is the practice at Ruttan that a single drill drive be driven through the centre of the stope if the ore width does not exceed 15 meters. Similar development occurs on the intermediate level. The 2 meters x 2 meters slot raise is subsequently slashed to 3.7 meters x 3.7 meters for the full stope height. Subsequently, the slot is slashed full width from hangingwall to footwall. Rings are then slashed into the void for the full stope width on either side of the slot, assuming access exists on either side. Normally, the rings that are blasted from the intermediate level correspond to a similar set of rings on the upper drill level, thereby ensuring that a continuous void extends from the draw level to 12.2 meters above the upper drill drive. The stope is generally drilled off prior to the commencement of slot blasting. The uphole on the intermediate and draw level are required to ensure that proper "inter-leaf" coverage between drill holes occurs between levels. Normally, the rings are spaced at a spacing of 1.5 meters and a toe burden of 2.1 meters, and only a sufficient number of holes are drilled for that particular blast.

The second method, Figure 2.14, involves a modified form of "vertical crater retreat" and slash. Large 151 mm diameter holes are employed, thereby allowing longer holes to be drilled by using in-the-hole hammer type of drill equipment. This enables the deletion of intermediate levels. Similarly, an undercut is taken as with the conventional method. The "vcr slot" is drop raised from the upper drill level to a 3.7 x 3.7 meter raise. The slot is not necessarily taken through to the upper level prior to production blasting. The production blasting requires the widening of the slot to 6.1 x 6.1 meters and subsequently slashing full stope width from hangingwall to footwall. The main tonnage is achieved through slashing decked charges into the void. The decked rings are blasted full stope width as in the conventional method described previously. The rings are spaced 3 meters apart with a toe burden of 4.2 meters. The slot, therefore, is the only part of the stope that is advanced employing the "vertical crater retreat" method of mining, which is characterized by spherical charges (6:1 = L/D).

Deviations of the above methods lie in the following:

* The initial slot is bored by machine from the draw level to the upper drill level.

* The VCR-Slash method may have the slot entirely complete prior to commencement of slashing. Subsequently, long parallel rings will be blasted for the full height of the stope.

The stope is ultimately filled to 12.2 meters above the upper drill level. Upon fill consolidation, the previous upper drill drive will form the draw level for the next lift. The draw cones are formed out of the fill. The sequence of extraction for an individual stope is as summarized by Figures 2.15, 2.16. The extraction sequence for an individual lens is generally from the hangingwall lens to the footwall and from the centre of an individual lens to the extremities. This again is not generally followed since production requirements necessitated changes to individual mining areas. The significance of mining sequence will be analysed in Chapter 4 (Stress).

2.5 OBSERVATIONS/CONCLUSIONS

This section was included to document the difficulties that will present themselves in trying to categorize the individual stopes into a database, or to even commence analysing by a suitable numerical code. The following categories of stopes generally occur at Ruttan, Figure 2.17:

* isolated
* rib: stopes exist along strike
* echelon: stopes exist along dip

The variance in mining sequence, Figures 2.15, 2.16 is not systematic or methodical but is primarily a function of production requirements. This is the case in most mining operations in Canada. The controlled experiment that one would like to achieve for a research project now is starting to accumulate many variables. An experimental stope would yield quantitative and qualitative observations. The difficulty arises in extrapolating the results to other areas of the mine exhibiting different rock qualities, stope configurations and mining practices. The database would have to be enlarged, which would mean an "experimental mine" rather than an individual stope would have to be instrumented. At the time of the study, the Upper Mine was in an advanced stage of extraction and had reserves for only three more years. A test stope, that would be isolated from adjacent workings, was not available. A further restriction was that it takes approximately ten (10) months for a stope to be completely excavated and another seven (7) months to fill. The approach taken was to analyze the existing database and to derive, if possible, critical parameters and areas to be further studied. A rock mechanics program at Ruttan had been implemented from inception which basically included stress gauges and extensometers. Stopes, as they have been extracted, were evaluated in these terms with minor success.

A test stope (800-26J) in the Lower Mine had has been instrumented (Oct/85) at Ruttan where an isolated stope configuration was monitored in order to prove or disprove the theories and ideas brought forth in this study.

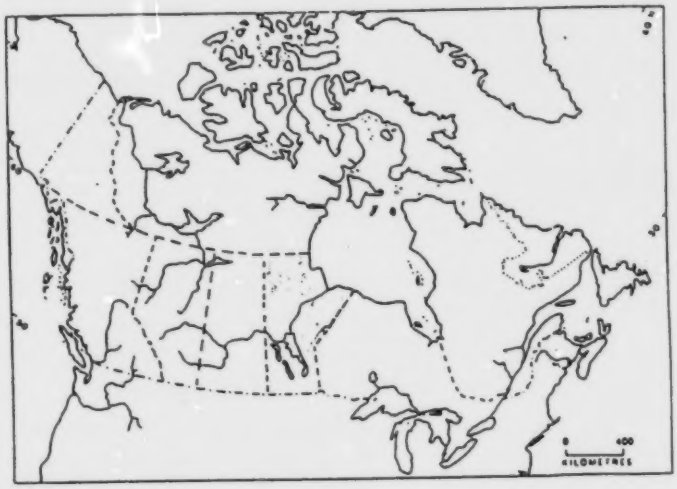

Map of Canada

Map of Manitoba

Figure 2.1: Location Map

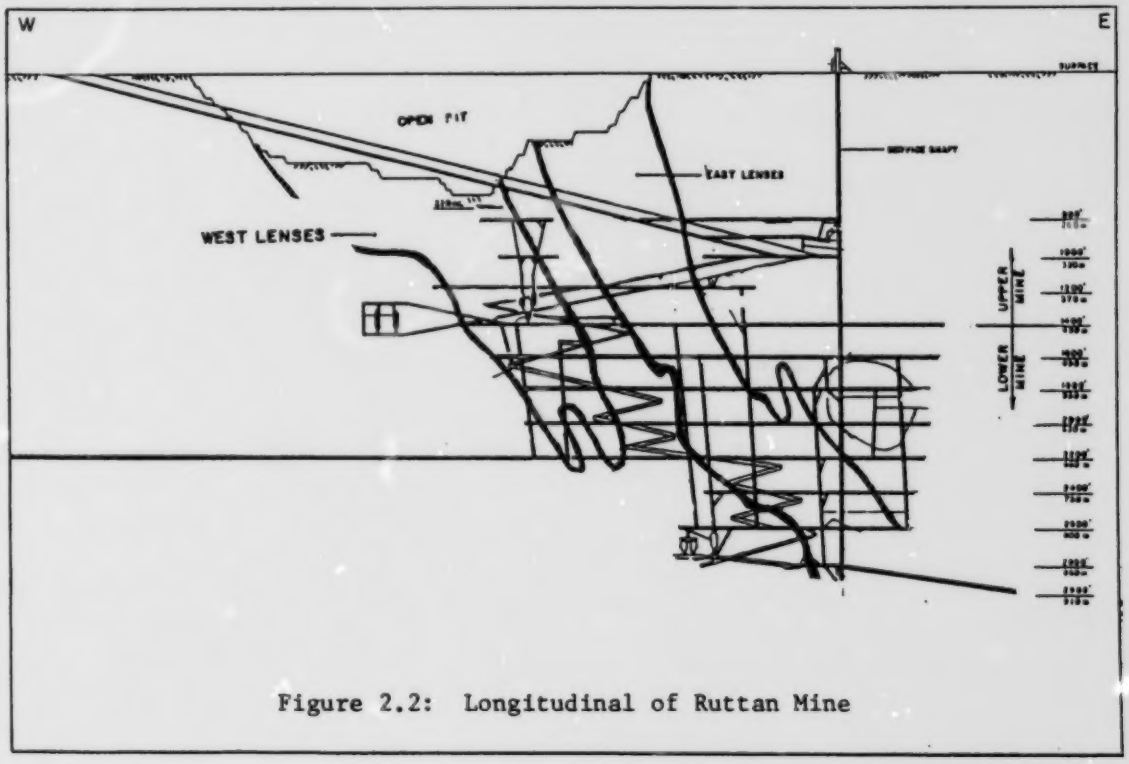

Figure 2.2: Longitudinal of Ruttan Mine

(Speakman et al, 1976)

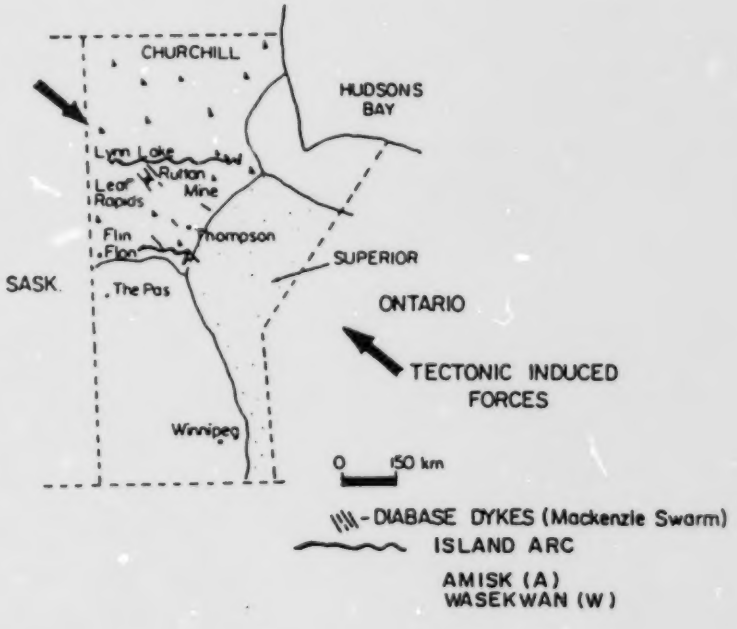

Figure 2.3: Regional Geology

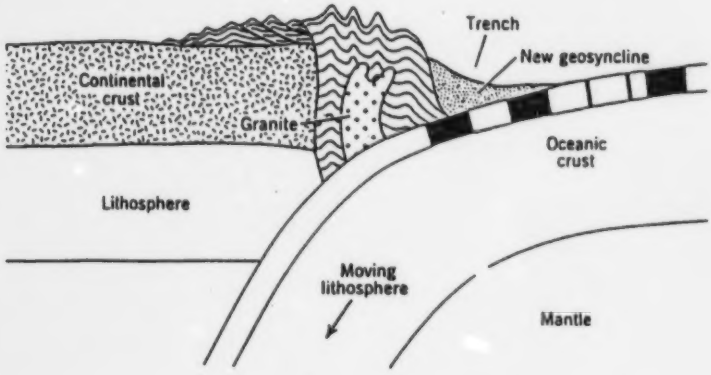

Figure 2.4: Island Arc Development

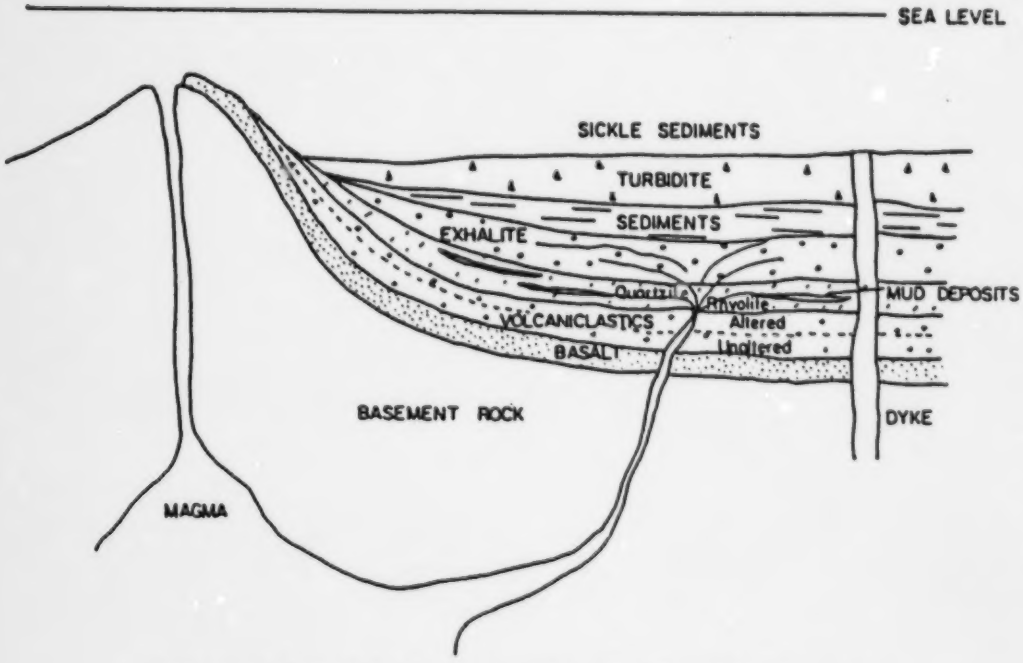

Figure 2.5: Schematic Section Showing the Formation of the Ruttan Deposit

(Speakman et al, 1976)

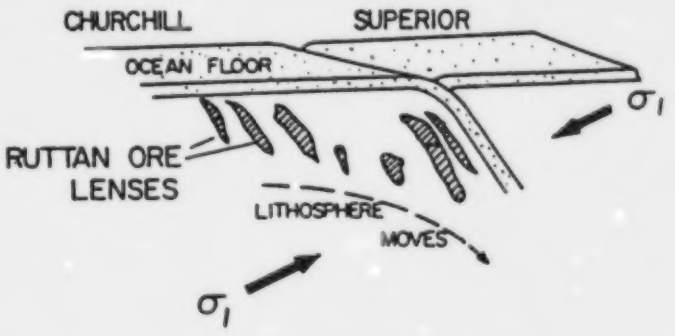

Figure 2.6: Tectonic Evolution

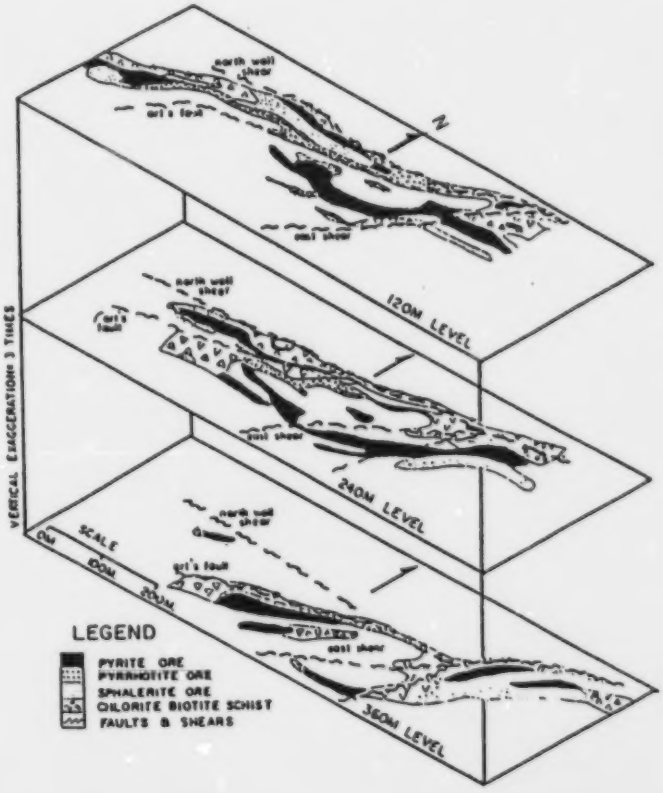

Figure 2.7: Isometric Diagram - Ruttan Deposit

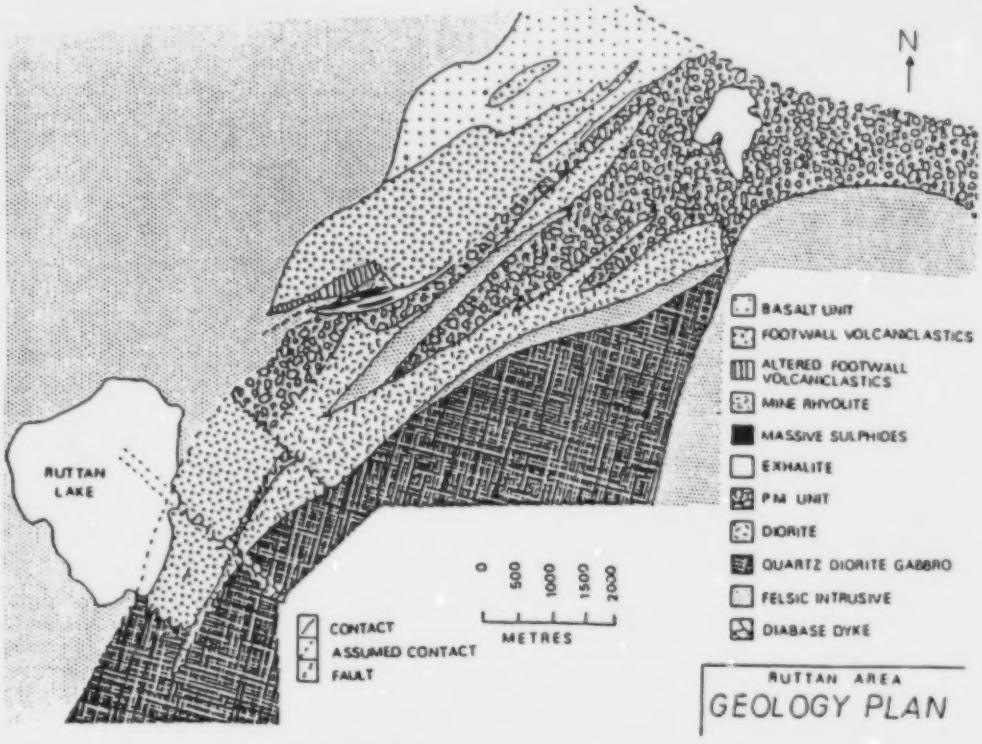

Figure 2.8: Local Geology

(Speakman et al, 1976)

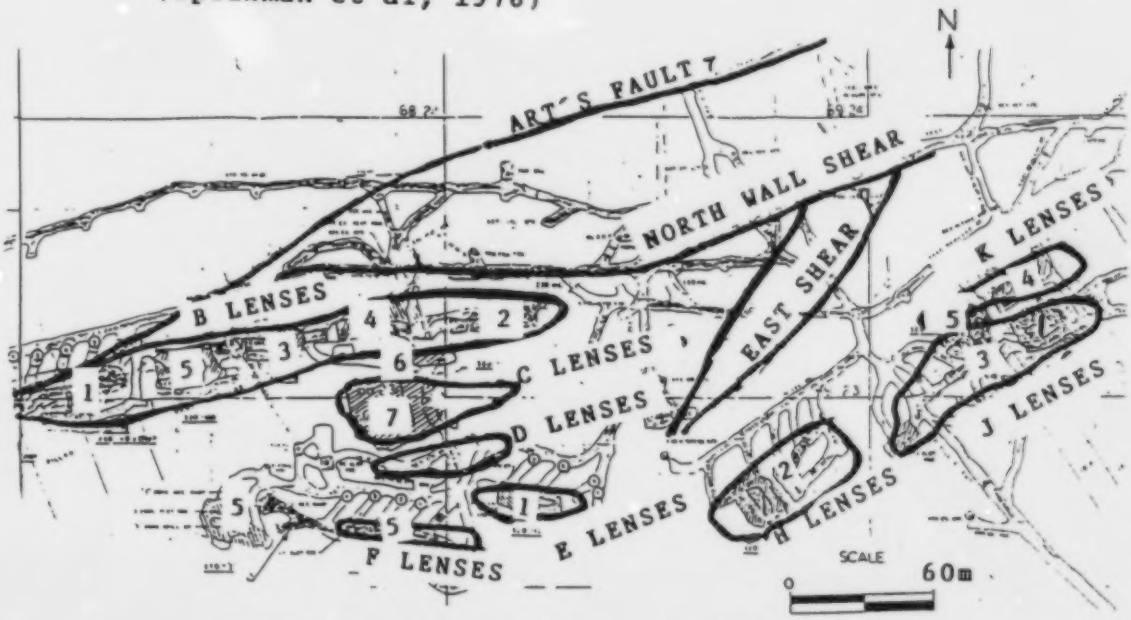

Figure 2.9: Plan of Ore Lenses - 260 m Level

- Numbers Refer to Sequence of Extraction

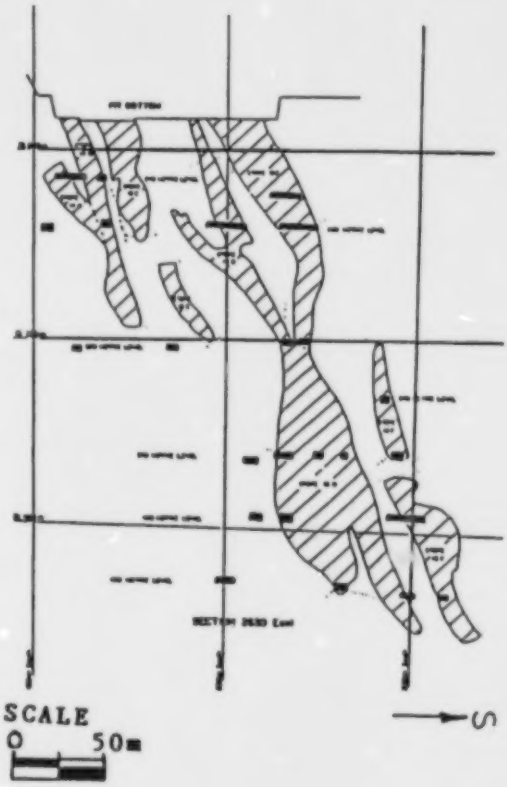

Figure 2.10: Typical Section - 2650E

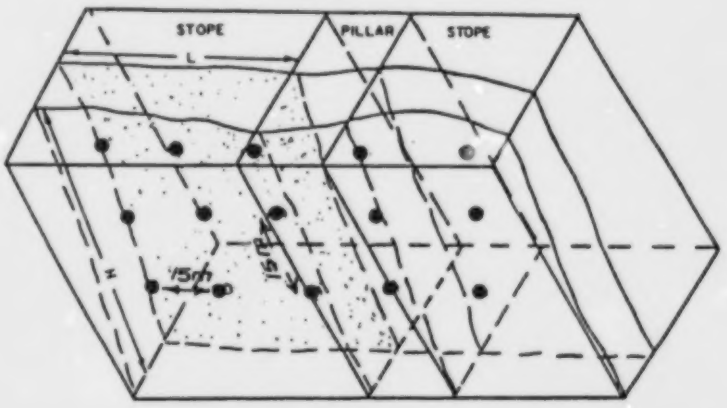

Figure 2.11: Ore Delineation Pattern

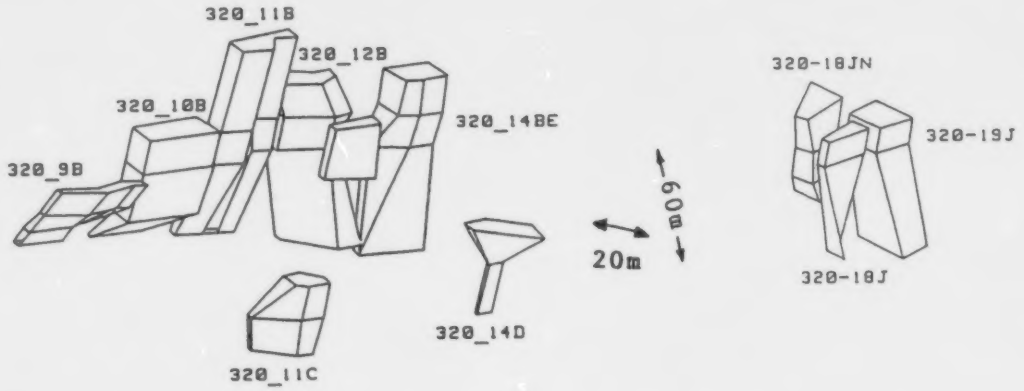

Figure 2.12: Isometric - 320 m Level

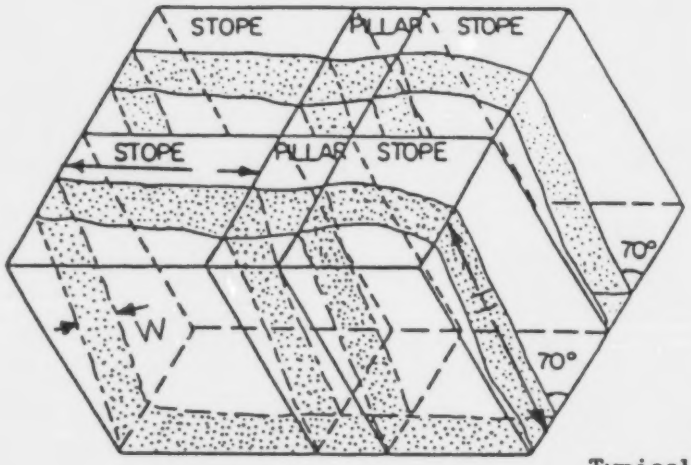

Typical Stope Dimensions

Stope Height (H) = 40-100 m
Stope Length (L) = 40-50 m
Stope Width (W) = 6-30 m
Rib Pillar Length = 6 m

Figure 2.13: Typical Stope Dimensions

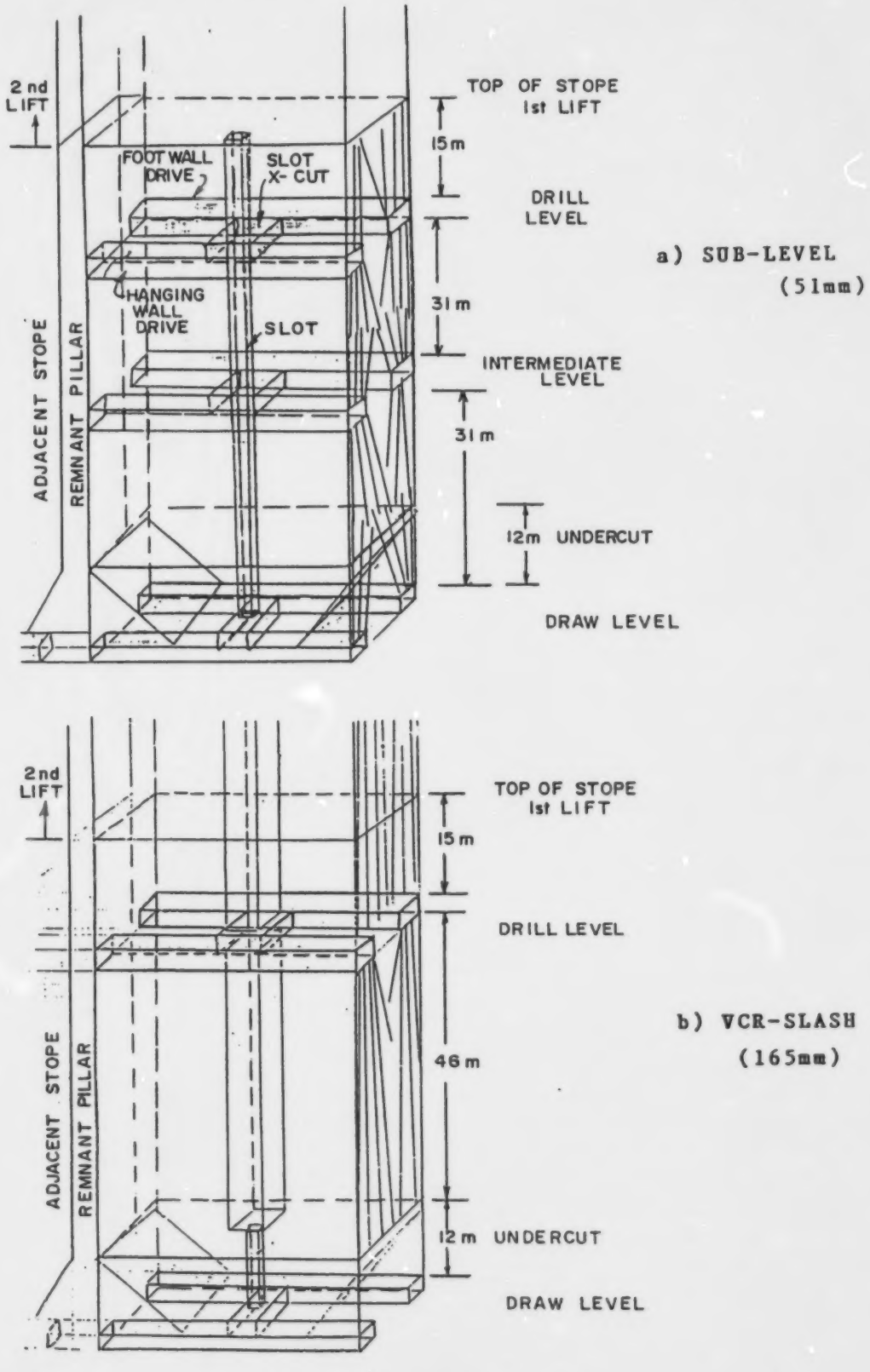

Figure 2.14: Stoping Method

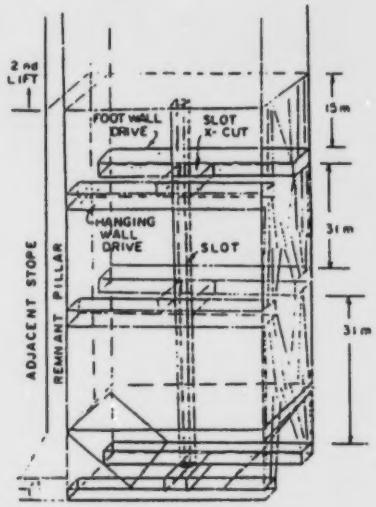

1) Initial Development
   - Drill Drives
   - Slot X-Cut
   - Slot Raise

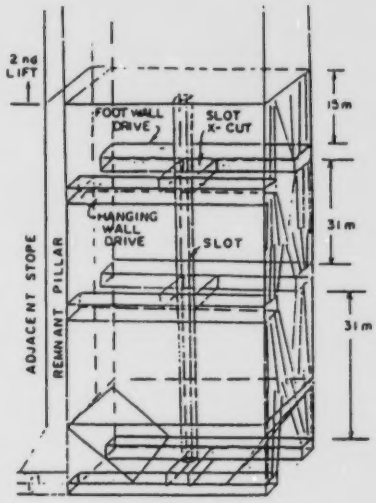

2) Stope Silled Out

Alternative

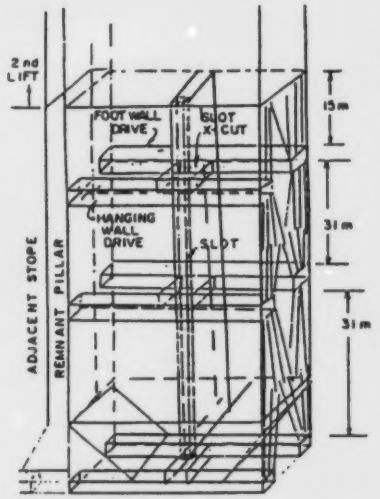

3) Slot Taken Full Stope Width (HW to FW). Rings Blasted on Either Side of Slot and Retreat to Pillar Access

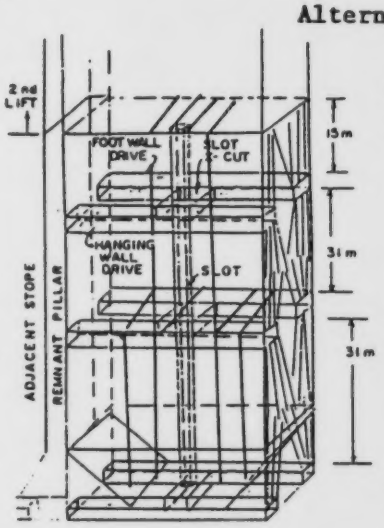

3a) Blasted Rings on Upper Levels Not Duplicated Below.

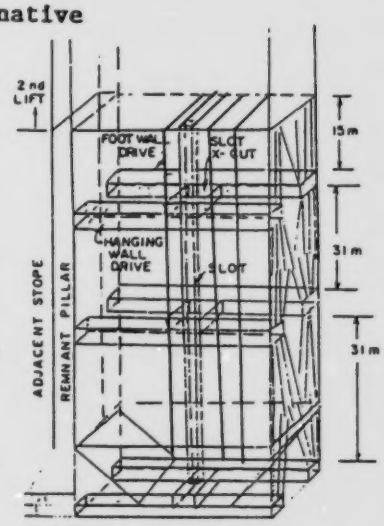

3b) Blasted Rings Coinciding on Each Level

Figure 2.15: Sequence of Extraction - Conventional

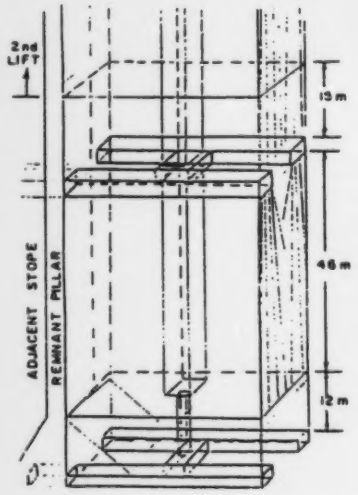

1) Initial Development

- Drill Drives
- Slot X-Cut
- Slot Raise

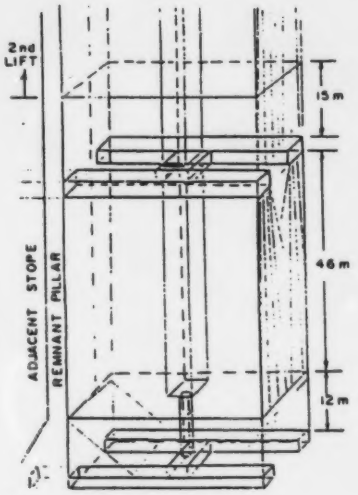

2) Stope Silled Out

Alternative

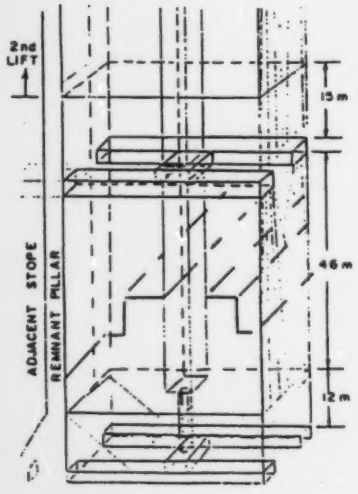

3) Slot Blasted and Stope Benched for Full Stope Width

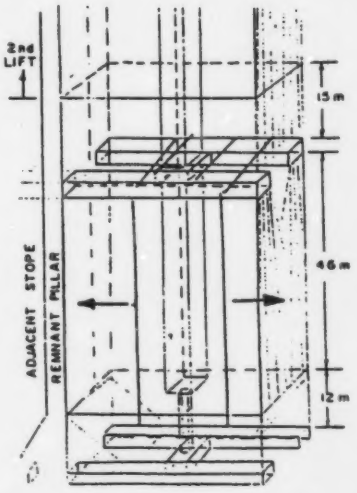

3a) Slot Taken Through to Upper Level and Slashed for the Full Stope Width. Production Slashing on Either Side of Slot.

Figure 2.16: Sequence of Extraction - VCR + Slash

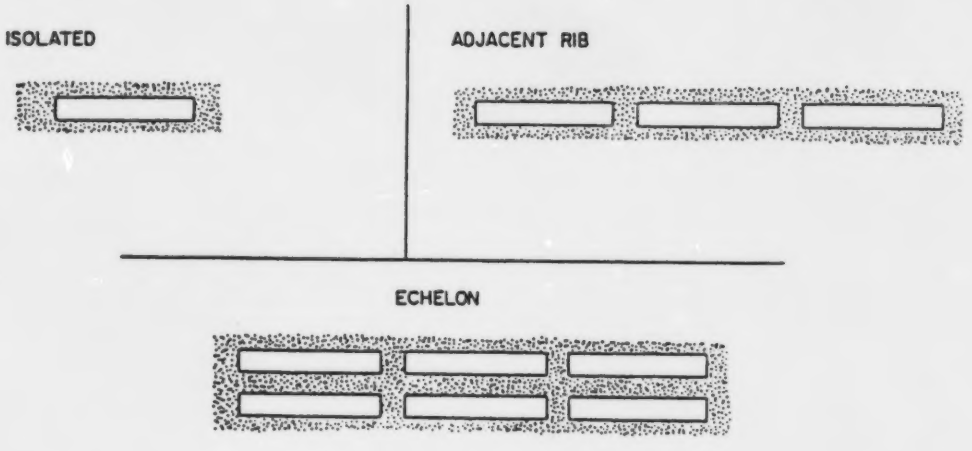

Figure 2.17: Categorization of Stopes - Plan View

The term "echelon" is synonomous with "parallel" for the context that it is employed in this thesis.

CHAPTER THREE
STOPE DESIGN METHODOLOGY

3.1 INTRODUCTION

The ultimate objective of this study is to develop design guidelines for the mining of a multi-lensed orebody.

3.2 LITERATURE REVIEW

There exists no accepted comprehensive design methods of predicting stope spans in jointed materials (Kersten, 1985). Beam theories, numerical models and empirical criteria have been employed in the past with some degree of success. The major drawback is that most of our classical design approaches have been based on assuming that homogeneous, isotropic elastic conditions exist.

Stope design practice has ranged from solutions involving trial and error, rule of thumb, beam theories, to numerical modelling. Rule of thumb approaches such as the stope span should equal one-half the stope height (Morrison, 1976), have evolved from field trials.

The elastic beam and plate solutions are based on concepts derived from solid mechanics (Evans, 1940). They assume that the rock above the excavation behaves as a series of elastic beams or plates loaded by self-weight and the roof span is designed on the tensile strength of the beam. A further modification (Beer and Meek, 1982) to beam theory is the "Voussoir" beam which recognized that cross joints may exist within the beam and consequently, may not allow any tensile stresses to develop. In addition, the Voussoir beam theory assumes that the beam carries its weight by arching, resulting in a confined situation. The basic assumptions common to beam and Voussoir theory are that:

* The ground above the hangingwall is completely distressed in the direction normal to the plate;

* The rock mass has parted along smooth bedding plane breaks, forming a series of beams or plates.

Horizontal confining stresses may also be incorporated in the above analysis. It is believed that the "Voussoir Beam" theory has definite possibilities in predicting stope spans at Ruttan. The major limitation may be the assumption of evenly distributed cross-joints, well defined bedding planes and the use of elastic,

homogeneous, isotropic theory. Possibly a combination of mass predicted strengths and "Voussoir theory" may result in a more realistic solution, Figures 3.1,3.2. This will be further evaluated in Chapter 9, "Applications".

Numerical modelling (Mathews et al, 1983) of mine openings would outline the state of stress present around the excavation. Relating the induced stress to the rock mass strength would outline possible failure areas. Figure 3.3 outlines typical failure modes that may result. A combination of structural and stress controlled failure is also a possible mode of instability.

This method of analysis requires accurate input into the model, in terms of the numerous parameters affecting the stability of the opening. The designer is offered an invaluable tool in comparing the stability of one opening relative to another configuration. In order to employ the results quantifiably, computer verification through field observation and measurements must be conducted. This, however, is not always a possibility especially in the preliminary design stages of a proposed operation. The use of analytical methods in stope design can best be summarized by Mathews et al (1981) whereby "in general, the number of variables to be considered is too high to permit other than empirical approaches to stope design. However, analytical methods are often used to identify excessive stress conditions or excessive deformations".

Input parameters, such as the rock mass moduli, are generally derived from performing a rock mass evaluation. Rock mass classification systems have evolved from the need to relate rock substance properties to those of the jointed rock mass. Rock mass classifications provide a common language and consequently, improve communications among all personnel concerned with the safe extraction of ore. It seems to overcome the problem caused by the complexity of the rock masses in terms of quantifying their properties.

Several rock mass classification systems have been developed since Terzaghi (1946) proposed his classification for the prediction of rock load on steel arch design. Several rock mass classification systems have been developed and the following are the most widely used:

Deere	(1971), RQD
Wickham	(1974), RSR
Barton	(1976), Q
Bieniawski	(1973), RMR

A summary of the comparison of the application of the rock mass classification systems reviewed is shown in Table 3.1, with limitations highlighted in Table 3.2.

A review of the critical parameters used for the major systems is outlined in Table 3.3.

Rock mass classifications have been successfully employed in the overall design of civil engineering structures since the late 1940's. It is only recently that this success is being transferred to mining related problems. Laubscher (1976) has devised a modified rock mass rating patterned after the Bieniawski system, which has been successfully employed in the design of bulk mining layouts. Nicholas (1981) employs a classification system in order to aid in the selection of an optimum mining method by characterizing the footwall, ore and hangingwall. Kendorski et al (1981) has proposed a method of classification for caving operations.

Recently, studies have been undertaken by Mathews et al (1981) whereby a modified NGI system has been employed to predict empirically the dimensions of isolated open stopes at depths below 1000 meters. Conclusions as stated by Mathews et al (1981), are as follows: "Results obtained from the limited data available were considered sufficient to develop the concepts presented, but insufficient to confirm them". The classification combines selected geotechnical factors into a "stability number" and plots, Figure 3.4, these values against a "shape factor" which accounts for the size and shape of the surface of the open stope to be investigated. These values are empirically calibrated against open stope data obtained from mine visits and literature (55 points) and assessed in terms of stable, potentially unstable, and potentially caving regions. The stability number used accounts for the rock mass quality (Q), the state of stress and the orientation of exposed surfaces. It is envisioned to incorporate the concepts and expand on the study since it strongly parallels the studies proposed to be conducted at Ruttan. The major criticism of this method is the limited number of case studies actually incorporating stope walls, since only seven (7) cases involved stope walls, the remainder were horizontal stope backs.

The method of stope design proposed in this study will incorporate, in addition to the factors found critical by Mathews, the following:

* relaxation effect on the hangingwall and footwall is not fully assessed;
* blasting effects;
* excavation rate;
* quantitative assessment of instability;
* stope configurations other than "isolated";.
* effects of fill.

The methods of design particularly relevant to the Ruttan orebody will be discussed in subsequent chapters on "Rock Mass Characterization", Chapter 5 and "Application", Chapter 9.

3.3 DESIGN PHILOSOPHY

Stope spans at Ruttan had been based on the assumption that the hangingwall acts as a simply supported beam that can bend only to the point that the strength of the intact rock will allow, Figure 3.5. The tensile stresses created at the centre of the beam, due to bending, must be less than the existing in-situ tangential compressive stress, in order to ensure that the beam is in confinement (Smith, 1976). Smith's design was based on experience and theory available at the time of the study. Subsequent research has shown that the resultant stress at mid-span is tensile under the prevailing stress regime. The balancing of bending stresses to the induced tangential stresses must take into account the three dimensional state of stress and resultant geometry of the opening.

The beam approach to analysis, as described above, recommended two stope lengths, the longer stope length being in areas having a higher in-situ tangential stress. Figure 2.13 outlines the typical stope and rib dimensions employed at Ruttan. The above method of design was employed in all rock types irrespective of the rock mass conditions. The above analysis was not able to explain local instabilities that occurred, which generally were due to the release of blocks along existing structures.

A different approach to stope design was incorporated in 1983 by the author whereby numerical modelling techniques were augmented by a large empirical database. This forms the basis for the development of a predictive stope design relationship.

Figure 3.6 is a plot of stress trajectories for the mined out stopes on the 320 meter level. Tensile zones are evident adjacent to most hangingwall and footwall contacts. The size of the zone is dependent upon the excavation geometry and the prevailing stresses. Visual observations at the mine indicated that the hangingwall and footwall contacts are more foliated in certain areas than others. The result was sloughing along preferential planes that were not restrained by a confining stress, Figure 3.7.

The absence of a confining stress, coupled with a foliated wall contact, enables one to arrive at a relationship showing that a higher dilution results in mining a stope having a poorer "Rock Mass Rating".

The Ruttan orebody is a multi-lensed en echelon type deposit which requires one to determine the influence of mining geometry. Sufficiently, large pillars separating individual stopes would limit this effort. Mathews (1981) suggests that pillar dimensions along strike should exceed the stope span by at least 25%. Pillars separating adjacent stopes at Ruttan are only 6 meters in length with stope spans varying from 40 to 50 meters. Employing tributary theory, it had been shown that the rib pillars would exhibit factors of safety much less that one. This indicates that the pillars are in a state of post-failure, Figure 3.8. The remnant pillar exhibits sufficient rock mass strength to remain standing. The pillar separating adjacent stopes may be considered as crushed, however, it will influence the stability of adjacent stopes by increasing the effective stope dimensions. Pillars at Ruttan were observed to fail in this manner rather than by an uncontrolled violent release of energy.

Other factors affecting stope span that must be investigated are:

* Blasting;
* Rate of Excavation;
* Geometrical Configuration of Stopes;
* Excavation Sequence;
* Depth Below Surface;

and, as previously discussed:

* Rock Quality; parameters as defined as in Table 3.3;
* Adverse Structure;
* Stress Regime; sequence of mining, fill.

Artificial support methods will not be addressed in this study, since Ruttan does not employ any method of stope support other than fill.

Groundwater is not considered to be a problem at this stage at Ruttan, since the deposit has been delineated on 15 meters x 15 meters centres, thus providing adequate depressurization, Figure 2.11. This will be further discussed in Chapter 5, "Rock Mass Characterization".

The above will be incorporated to determine empirical stope design guidelines based on a stability assessment for each individual volume of excavation.

Dilution at the Ruttan operation is recorded for each individual stope at various stages of excavation. It is envisioned to employ this value as an indicator of the stability of the opening. Dilution is an indirect indicator of the quantity of slough

originating from the stope walls. The database is comprised of forty-three (43) stopes at various stages of extraction, thereby yielding 432 stope geometries.

3.4 SURVEY OF OPEN STOPE OPERATORS

A questionnaire (Interim Report - Project 3) was distributed to thirty-eight (38) underground base metal mine operations throughout Canada. It was designed to assess the present state of knowledge with respect to stope design amongst mine operators. The selection criteria for this study were as follows:

* only Canadian underground base metal operations were surveyed;
* the extraction method had to include either open stoping and/or room and pillar;
* The daily production from underground had to exceed 1000 tonnes per day.

All underground operations satisfying the above requirements were contacted. The questionnaire was sent out in March, 1985. Twenty-two (22) operations had responded representing a 58% response rate.

The following areas were investigated by the questionnaire:

a) Mine Profile:

* Production rate
* Maximum depth of mining
* Ore dip, type
* Mining Method

b) Geomechanical database that is available at each operation:

* Rock strength parameters
* Stress investigations
* Rock mass parameters
* Monitoring
* Instrumentation

c) Stope and Pillar design, evaluated in terms of:

* Methods employed
* Success of design

- Stope characterization
- Resultant dilution

Parameters that are particularly relevant to the scope of this study are summarized within this section.

3.4.1 DILUTION ASSESSMENT

Dilution is a measure of external waste that has sloughed into the drawpoint. Stope dilution as estimated by the participating mine operators, is a quantitative parameter that enables the operator to evaluate the quality of his design. The following are the most common methods of estimating dilution as indicated by the questionnaire:

- % Dilution = (weight of external slough x 100)/(weight of ore reserves)
- Dilution = (undiluted in place grade (DDH))/(sample assay grade at drawpoint)
- Dilution = (undiluted in place grade reserves)/(mill head grades obtained for same tonnage)
- Dilution = (total waste tonnage)/(total tons mined)
- Dilution = (total waste mined)/(tons of ore reserves estimated)
- Difference between tonnage mucked and that blasted
- Difference between tonnage of backfill placed and that theoretically required to fill "ore reserves" void
- Dilution is visually observed and assessed
- "x" amount of feet in the footwall plus "y" amount of feet in the hangingwall divided by the stope width
- Historical average over past 10 years = actual tons drawn from stopes/calculated reserve tonnage

The level of acceptable dilution is highly dependent upon grade since a higher grade stope can be economical, whereas a lower grade stope with the same dilution will no longer be mineable.

It is proposed that the following thresholds be employed for comparative purposes:

* less than 10% dilution
* 10 - 19% dilution
* 20 - 35% dilution
* greater than 35% dilution

The non-entry methods of mining, such as open stoping, can accept a certain degree of wall slough without injury to the workers. The open stope dilution statistics reveal that 47% of all open stope operations have more than 20% dilution. It was generally stated by the operators that dilutions under 5% are acceptable and were classified as low. This is considered normal due to recording accuracy, blasting effects, and variability in the ore geometry and in the rock mass strengths.

3.5 CONCLUSIONS

The survey conducted indicated that dilution is of particular concern to open stope operators. The emphasis of this study will be in developing a method of design of optimum stope spans, since the observed dilution at Ruttan is solely a measure of the hangingwall and footwall slough. The deterioration of stope backs and pillars has caused only minor problems at Ruttan. It is realized that pillar stability is an important design requirement and will be addressed in Chapter Four (4).

The design methods that are available for assessing the stability of mine openings can be categorized as follows:

a) Analytical
b) Observational
c) Empirical

Analytical methods are based on the analyses of stresses and deformations around openings. Observational methods rely on the monitoring of ground movement during mining to detect measurable instability. Empirical methods assess the stability of mines by the use of statistical analyses of underground observations. Analytical methods are primarily employed for comparative design and parametric studies. The observational approach would require a large database and would have to be implemented in the initial stages of mine development in order to achieve some reliable measurement of opening stability. The Ruttan orebody is in an advanced stage of extraction and consequently, observational methods are of limited use in predicting hangingwall or footwall dimensions in various rock types and stope configurations. Bieniawski (1985) states that in order to meet the immediate needs of the mine practitioner, studies should be directed to the

development of empirical failure criteria. Jaeger and Cook (1979) suggest that a failure criteria has yet to be developed that describes the actual mechanism of fracture and that empirical equations fit the experimental results much better. Bieniawski suggests that such criteria can be selected by fitting a suitable equation to experimental data which do not necessarily require a theoretical basis. The empirical relation will serve to meet the requirements of adequate prediction, simplicity of use and speed of application. It is therefore proposed to employ an empirically based approach that evaluates the parameters that may have an influence on hangingwall and footwall stability design and ultimately develop a relation whereby:

$$Z = A + Bx + Cy + Du + ...$$

or

$$Z = A + Bx + Cy + Dx^2 + Ey^2 + Fxy + ...$$

where:

Z:	refers to the control variable which is quantifiable and will be for this study "Dilution"
A,B,C.....:	are constants determined by regression analysis performed on a linear hyper-surface or quadratic surface
x:	refers to the dimensions of the hangingwall of footwall
y,u,v.....:	refers to the variables that are critical to the evaluation

The "best fit" will be evaluated in terms of a statistical regression analysis performed on linear and quadratic equations. Statistics will determine the acceptance or rejection of the hypothesis. A rejection of the hypothesis would not enable an empirical equation to be estimated whereas an acceptance would suggest that an empirical formulation may be possible.

Table 3.1: Rock Mass Classification Systems - Applications

	APPLICATIONS \ CLASSIFICATION	TERZAGHI	LAUFFER-PACHER	DEERE	RSR	RMR	Q	KIRSTEN	LOUIS	FRANKLIN	COATES & PARSONS	BULICHEV	LAUBSCHER	KENDORSKI	McMAHON	MATHEWS	NICHOLAS	MULLER	COAL CLASSIFIC
MINING APPLICATIONS	MINING METHOD SELECTION												X	*X	*X		X		X
	MINE SEQUENCING												X						
	STAND-UP TIME		X			X	X												X
	MAX. UNSUPPORTED SPAN		X			X	X						X			X			X
	SUPPORT DESIGN				X	X	X	X					X	*X					X
	PILLAR DESIGN					X	X						X						X
	CAVABILITY												X	X	X				X
	CAVE ANGLE												X						
	ROOF STABILITY					X	X						X			X			X
	FLOOR STABILITY					X	X									X			X
	OPEN STOPE DESIGN					X	X						X			X			
	ROCK LOAD	X				X	X	X								X			
	RIPPABILITY					X		X											
ROCK MASS STRENGTH INDICES	COHESION					X	X	X										X	
	FRICTION ANGLE					X	X	X										X	
	DEFORMATION MODULUS			X		X	X	X											
	STRENGTH					X	X	X					X						
CIVIL APPLICATIONS	ROCK LOAD	X		X		X	X	X	X	X									
	STAND-UP TIME		X			X	X			X									
	MAX. UNSUPPORTED SPAN		X	X		X	X	X		X		X							
	SUPPORT DESIGN	X	X		X	X	X	X	X	X		X							
	FOUNDATION DESIGN					X	X	X											
	SLOPE DESIGN					X	X	X											

NOTE: In order for method to be classified as having a mining application, it must have been referenced in the literature.

Table 3.2: Limitations of the Major Rock Mass Classification Systems - Mining Applied

	LIMITATIONS \ CLASSIFICATION	TERZAGHI	DEERE	RSR	RMR	Q	KIRSTEN	LAUBSCHER	KENDORSKI	McMAHON	MATHEWS	NICHOLAS
CLASSIFICATION DOES NOT CONSIDER	STRESS FIELD		X	X	X					X		
	JOINT CONDITION		X							X		
	CONTINUITY		X							X		X
	JOINT ORIENTATION	X	X			X	X			X		X
	JOINT INFILLING		X	X						X		
	SWELLING MATERIAL		X		X			X		X		
	BLASTING EFFECT	X	X	X	X	X	X			X	X	X
	UNIAXIAL COMPRESSIVE STRENGTH	X	X	X						X		
	EXCAVATION METHOD	X	X		X					X	X	X
	GROUNDWATER		X							X		X
CLASSIFICATION REQUIRES	STRESS FIELD < 30MPA			X	X			X				
	EXTENSIVE EXPERIENCE					X	X	X				
	MORE FIELD EXPERIMENTATION						X	X	X	X	X	X

Table 3.3: Summary of Parameters Used in Rock Mass Classification Systems - Hard Rock Mining

	ROCK MASS PROPERTIES \ CLASSIFICATION	TERZAGHI	LAUFFER-PACHER	DEERE	RSR	RMR	Q	MODIFIED Q KIRSTEN	LOUIS	FRANKLIN	COATES AND PARSONS	BULICHEV	Mining: LAUBSCHER	KENDORSKI	McMAHON	MATHEWS	NICHOLAS	MULLER
ROCK MATERIAL	DEFORAMATIONAL CHARACTERISTICS										X							
	UNIAXIAL COMPRESSIVE STRENGTH					X	X	X	X	X	X		X	X		X	X	X
ROCK MASS JOINTING	ROCK QUALITY DESIGNATION			X		X	X	X	X	X			X	X	X	X	X	
	NUMBER OF SETS				X	X	X	X				X	X	X		X		
	SPACING				X	X				X	X		X	X			X	X
	CONTINUITY				X	X				X	X		X	X				
	CONDITION				X	X	X	X				X	X	X		X	X	
	ORIENTATION				X	X						X	X	X		X		
	OVERALL QUALITY	X	X															
ENVIRONMENT	VIRGIN STRESS						X	X		X			X	X		X	X	
	EXCAVATION STRESS	X					X						X	X				
	GROUNDWATER	X			X	X	X	X	X	X		X	X	X		X		
	EXCAVATION METHOD				X		X	X					X	X				
	OPENING GEOMETRY/ORIENTATION	X	X		X	X				X		X	X	X		X		
	STAND-UP TIME		X			X	X	X										
	LITHOLOGY			X		X				X	X							
	WEATHERING					X							X	X				

. To compensate for original assumptions, a factor of safety of six is generally employed. (Wright,1980)

Figure 3.1: Beam Theory

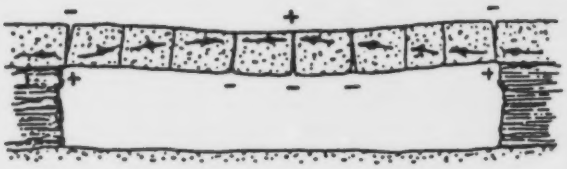

The beam is assumed to be supported by resultant arching action. Note shear stresses (interslice forces) must be overcome for a single block to fall out.

Figure 3.2: Voussoir Arch

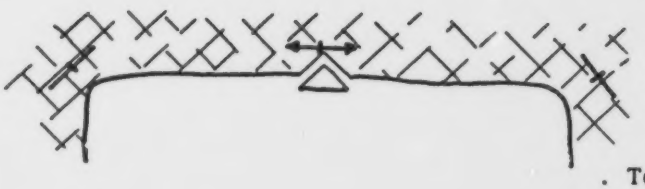

. Tensile stress in the back is an indicator that the region is in a state of relaxation and consequently, structural blocks may be released. If the back is a homogeneous beam, the tensile strength of the beam must be exceeded for failure to occur.

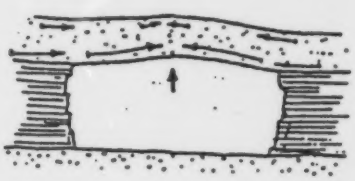

. High compression in the roof, coupled with low compressive forces normal to the roof may result in buckling failure. This is particularly true if structures paralleling the roof are present.

Figure 3.3: Numerical Solution

. Failure when the shear strength of the rock is exceeded.

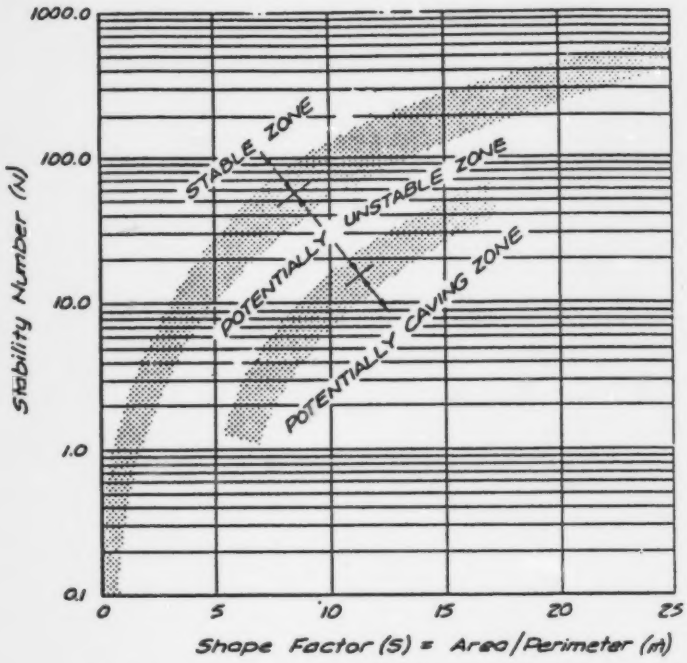

Figure 3.4: Mathews Method of Stope Design

(Mathews et al, 1981)

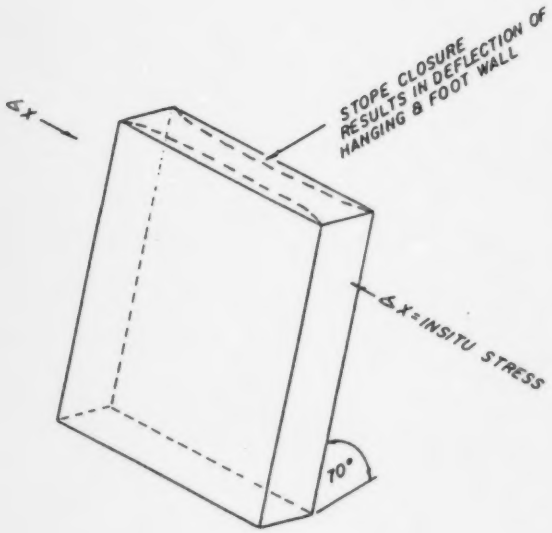

Figure 3.5: Hangingwall and Footwall Beam Deflection

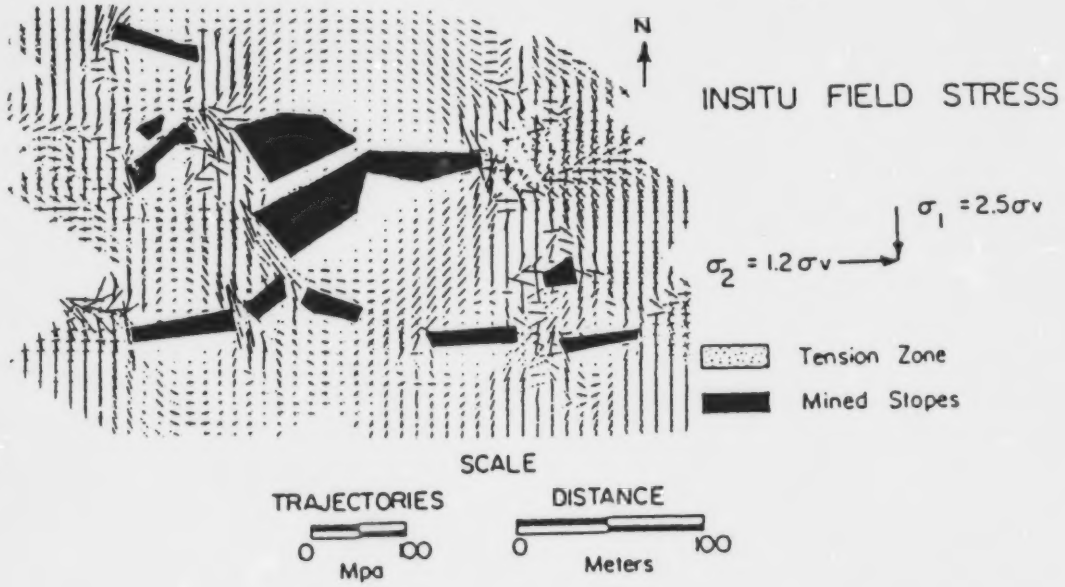

Figure 3.6: Stress Trajectories - 320 m Level, Plan View

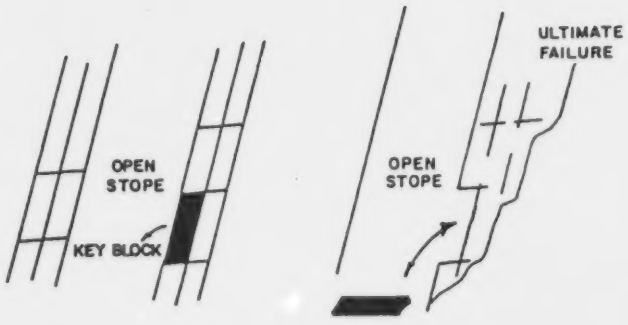

Figure 3.7: Structurally Controlled Failure - Section of Typical Stope

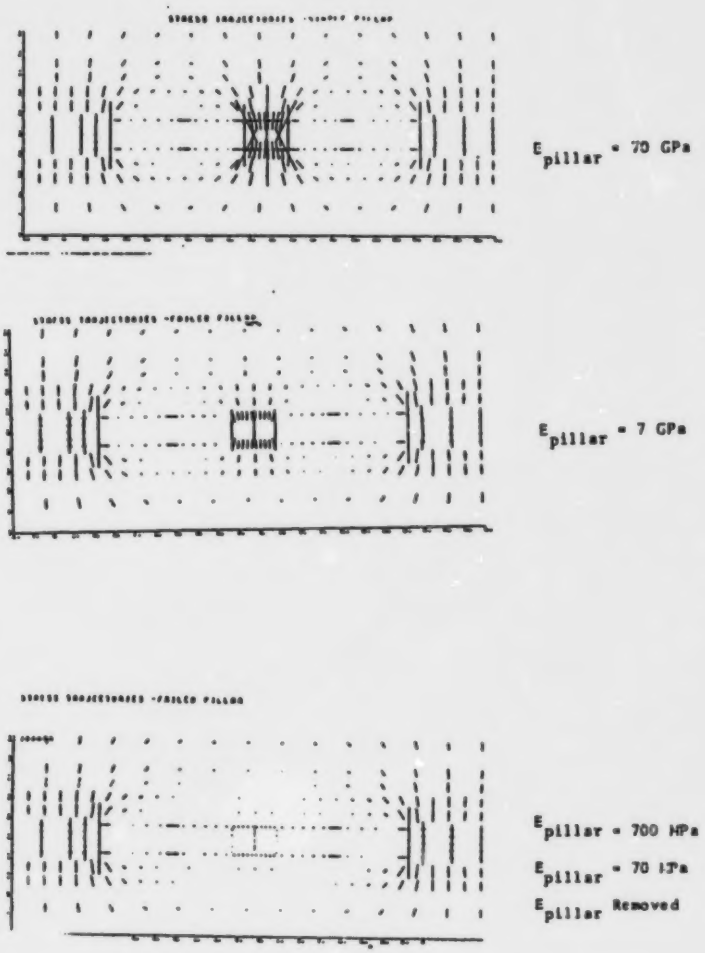

. Load is shed to adjacent areas as pillar is wrecked. This is simulated by reducing the pillar modulus.

Figure 3.8: Plan View of Two Adjacent Stopes

CHAPTER FOUR
STRESS

4.1 INTRODUCTION

This report attempts to delineate all parameters that contribute towards wall slough. Brady and Brown (1985) state that upon "identifying the feasible block collapse modes associated with joint attitudes and excavation surface geometry, it is necessary to determine the potential for block displacement under the ambient conditions which exist in the post-excavation state of the opening periphery". The contributing stress factors that would affect the stability of an individual block are gravitational, hydrostatic and confining stresses. This chapter will show that the hangingwall and footwall of stopes at Ruttan are in a state of relaxation. This dictates that all stresses (other than gravitational) acting on a particular wall segment are less than or equal to zero. Consequently, that particular segment is not confined, and coupled with a jointed material, would result in the block to slip out under its "own weight". This chapter will study the validity of the assumption that the hangingwall and footwall of the individual stopes are in a state of relaxation. The numerical analysis will be augmented by measurements recorded in the excavation of a test stope (800-26J), Chapter 9.

4.2 IN-SITU STRESSES AT RUTTAN

Prior to understanding the effect of stresses on openings at Ruttan, it is important to determine the magnitude and orientation of the in-situ rock stresses influencing the Ruttan operation. These stresses are related to the weight of the overlying strata and the geological history of the rock mass.

In-situ stress measurements were recorded at Ruttan at the 620, 660, and 800 meter levels (Interim Report - Project 213). The summary of results is shown in Figures 4.1, 4.2 and 4.3. Generally it can be concluded:

Vertical Stress	=	σV (mpA) = 0.027 X DEPTH (m)
Major Principal Stress	=	$\sigma 1 = 2.5 \ \sigma v$ (340°/-20°)
Intermediate Principal Stress	=	$\sigma 2 = 1.2 \ \sigma v$ (070°/0°)
Minor Principal Stress	=	$\sigma 3 = 0.8 \ \sigma v$ (160°/-70°)

(Based on 660 meter level)

4.3 STRESS CONFIGURATION

The stress magnitudes and orientations that were determined by in-situ stress measurement are summarized in Figure 4.3. These stresses were employed in order to determine the induced stresses that exist at the stope wall contacts using various numerical modelling techniques.

The objectives of the modelling was to:

1. Model as an isolated stope, 800-26J, and compare the results with in-situ rock mechanics instrumentation readings. This was evaluated employing two and three dimensional numerical codes.

2. Model various typical mining configurations and relate the results to instrumentation and observations recorded for similar stope geometries, thereby enabling one to delineate the extent and magnitude of the relaxed zone that encompasses an individual stope.

3. Model the effects of stope sequencing for various typical mining configurations encountered at Ruttan.

4. Compare various modelling techniques and assess their suitability for modelling stope geometries at Ruttan. Relate results obtained employing two and three dimensional codes.

5. Model the effects of backfill on an isolated stope.

4.3.1 NUMERICAL MODELS

The design of mine openings to achieve maximum productivity without endangering mine personnel or the mine operation in general is or major importance. Due to cost and safety considerations and the inherent variability of mining conditions, it is generally not possible to mine experimental stopes in order to determine the optimum opening design. The suitable application of numerical stress analysis models is one method in which proposed mining configurations can be simulated prior to their actual excavation.

To achieve this, the numerical model must be able to meet several basic requirements. These are:

1. It must be able to model complex geometries.

2. It must be able to model the initial in-situ tectonic stresses.

3. It must be capable of reproducing known deformations and stresses around existing openings.

4. It must be able to model elastic rocks.

5. The model must be cost effective.

6. The model itself must conform to certain mathematical and theoretical requirements such as solution convergence, numerical stability, etc.

It is also desirable to have the following additional features:

1. Ease of application, i.e. user friendly.

2. Extensive graphical output capabilities to simplify solution interpretation.

3. The capability of modelling non-linear rock properties and different constitutive equations and failure criteria.

4. The capability of modelling major faults and slip surfaces.

As with any modelling technique, empirical or numerical, a thorough understanding of the method's strengths, limitations and assumptions is essential. It is well known that the modelling of rock is inherently loaded with assumptions on strength, joint behaviour, effects of moisture, virgin stress levels and, of primary importance, the behaviour of rock mass. At the present time there is no satisfactory theory on the behaviour of the rock mass that can be applied to a numerical model. The use of two dimensional models to simulate three dimensional mine configurations adds a further assumption to the results. However, by understanding the methods used and combining them with in-situ measurements and experience, numerical modelling greatly assists in the design of mine openings.

For these reasons, it was decided to use several modelling methods and to compare these results.

4.3.1.1 Methods Available

Three major methods of numerical stress analysis modelling are generally available. These are the:

1. Finite element method (FE)
2. Boundary element methods - Boundary integral method (BI)
3. Finite differences (FD)

In addition, various hybrids of the finite element and boundary element methods have been developed. Naturally, all the methods have advantages and disadvantages.

In this study, the two most common boundary element methods have been utilized, the boundary integral method and the displacement discontinuity method. Two and three dimensional boundary element codes have been employed. Table 4.1 summarizes the models used.

The major advantages of the boundary element method is that it is relatively simple to set up the model geometry, although this is also a function of the pre-processor that is available. The finite element technique is still one of the most flexible methods available, allowing multiple material types, non-linearities, backfill and excavation sequence to be modelled. However, for complex geometries, the development of the mesh is time consuming. Primarily for this reason, the finite element method was not used in this project.

4.3.1.2 Two Dimensional Boundary Integral Model

The boundary integral method, BITEM, was used to model the typical stope geometries encountered, Figure 2.17. Developed by the CSIRO (Commonwealth Scientific and Industrial Research Organization), BITEM is capable of modelling up to five homogeneous regions. The program was modified by R. Pakalnis to run on an IBM-PC computer that employs a powerful post-processor (PCBEM, 1988).

In addition to displaying extensive graphical output, the post-processor also incorporates the following failure criteria:

* Mohr - Coulomb;
* No Tension;
* Hoek Rock Mass Failure Criterion.

These criteria may be used to identify zones of potential failure.

The major drawback of BITEM is that is cannot explicitly model the excavation sequence, although this can be done by using separate program runs.

4.3.1.3 Three Dimensional Boundary Integral Model

The three dimensional boundary integral program, 3DBELM, was developed by the CSIRO. The program models boundaries using linear strain triangular elements and can model multiple openings, but no excavation sequencing. Post-processing facilities are limited.

4.3.1.4 Three Dimensional Displacement Discontinuity Method

Three dimensional displacement discontinuity program BESOL/MS221, was developed by Crouch Research Inc. The method is designed to model excavations that are comparatively thin in one direction and fairly extensive in the other two. Typically, a thickness ratio (length/thickness) of three or more is considered to be acceptable. It is one of the sub-objectives of the displacement discontinuity method for modelling ore bodies similar to that of Ruttan.

BESOL is capable of modelling multiple openings, backfill, mining sequencing and the Mohr-Coulomb/Hoek and Brown failure criterion (Hoek and Brown, 1980).

Element density restrictions limits the output of data around complex geometries, such as en echelon stopes. These will be discussed subsequently.

4.3.2 MODEL INPUT PARAMETERS

A computer mine model must be based upon data obtained from laboratory and in-situ measurements, i.e. rock strength, rock mass rating, etc. In addition, the model must be validated against actual mine conditions. Both extensive laboratory testing and in-situ measurements have been carried out at the Ruttan mine by IMS and Ruttan mine personnel. These include rock strength testing, rock mass characterization and in-situ stress measurements.

In addition, rock mechanics instrumentation has been installed in an isolated test stope (800-26J) and the results have been used to validate the numerical models. Table 4.2 summarized the input parameters that have been used for modelling.

4.3.3 MODEL GEOMETRIES

Several geometries were modelled in order to achieve the objectives outlined in Section 4.3. These were:

* isolated stopes;
* rib stopes;
* echelon stopes.

These are summarized in Figure 4.4. Table 4.3 indicates which model was used with a given geometry and mining sequence. In addition to the various mining geometries and sequences, parametric studies were undertaken on the stress ratio "k" and the length/width ratio using BITEM.

The following sections outline the analyses results. In the subsequent discussions, the term "zone of relaxation" is taken to mean a zone that is unconfined, consequently enabling any structural blocks to be released under their own weight.

4.3.4 EFFECT OF LENGTH/WIDTH RATiO

An analysis of the effect of stope length/width ratio on the extent of the relaxed zone was carried out using BITEM. The objective of the study was to determine, for typical stope geometries encountered at Ruttan, whether a zone of relaxation occurs and its extent. The term length and/or span has been employed in this report to describe the strike length of a particular stope.

Parametric studies were conducted whereby the stope length/width ratios were altered under a constant stress regime, as shown in Figure 4.5. It was shown that for the isolated stope case, for stopes having length/width ratio exceeding 0.66:1, the hangingwall and footwall commence going into tension for a "k" equal to 2.1, Figure 4.6.

The stress configuration showing minor principal stresses (dashed) and major principal stress contours (solid) for the isolated cased analysed is shown in Figure 4.7. The extent of the tensile induced zone is shown by Figure 4.8 as a function of the stope geometry. Typical stope geometrics at Ruttan approach the 2:1 and 4:1 length/width ratios. This would ensure that the ore contacts will always be in a state of relaxation.

4.3.5 EFFECT OF DEPTH AND STRESS VARIATION

The initial data base for the study was derived from stopes mined between surface and the 430 meter level. In-situ stress measurements and historic data had indicated that the stress ratio "k" would decrease with depth ranging from 2:1 at 660 meters to 1:3 at 800 meters below surface. It was therefore important to model the effect of this changing stress ratio to determine whether the same failure mechanism would apply at depth.

The effect of stress variation was modelled using BITEM. Figures 4.9 and 4.10 summarize the results of the analysis. Although the lateral extent of the tensile zone does decrease with decreasing "k", as expected, the relaxed zone is still evident for the range of stresses encountered at Ruttan. It is therefore reasonable to expect the mode of stope wall failure to be the same throughout the mine.

4.3.6 EFFECT OF MINING GEOMETRY AND SEQUENCING

The effect of mining geometry/sequence on the induced stresses was modelled using BITEM and BESOL. This enables a comparison to be made between the two techniques and on the assumptions associated with the individual codes.

Figure 4.4 shows the different geometries and mining sequences modelled. Figures 4.11, 4.12 and 4.13 show results from isolated, rib and echelon configurations, modelled using BITEM with instantaneous excavation. Results of the BITEM analysis indicate that the extent of the relaxed zone increases with an increase in the number of rib stopes and decreases for echelon stopes, Figure 4.14. This trend is confirmed with the BESOL analysis, Figure 4.14, however the extent of the relaxed zone is greater.

In the case of rib stopes, the lateral extent of the zone of relaxation has not greatly increased beyond that of the isolated case. This is due to the integrity of the pillar that is modelled as a rigid element. In actual fact, due to the high compressive stresses in the rib pillars modelled, these pillars will ultimately crush. The final stress configuration will more closely resemble that of the isolated case with dimensions 8:1 and 12:1 (length/width).

The echelon configuration, as modelled by BITEM, reveals that the wall contact forming the longitudinal pillar is not in a state of relaxation, but in a state of confinement. The stope span that forms the abutment is in a lower state of tensile stress than that found for the base case, Figure 4.11. In addition, the lateral extent of the zone of relaxation has been reduced, Figure 4.14. The echelon configuration, Figure 4.13, commences to resemble the stress configuration for the 2:1 and 1.3:1 length/width ratios for the isolated stopes.

Mining sequences were modelled for both echelon and rib stopes, as shown in Table 4.3 and Figure 4.4. It is apparent from the modelling of the rib stopes that without accounting for the non-linearities of pillar failure or crushing, modelling mining sequences is of limited value. Figures 4.15, 4.16 and 4.17 show the stresses perpendicular to the hangingwall of the stopes for "Case 2" of Figure 4.4. There is minimal variation in the local stresses between Cases 2, 3 and 4. Two mining sequences were modelled for echelon stopes, footwall to hangingwall and

hangingwall to footwall. Results of the sequential excavation are shown in Figures 4.18 and 4.19. It can be compared to the instantaneous excavation modelled by BITEM, Figure 4.20.

The most significant difference between the models is that BESOL predicts tension in the centre of the longitudinal pillars unlike BITEM. This is probably a closer reflection of reality since the pillars are generally unconfined. The mining sequence makes a very minor difference on the stress regime and, apart from the minor variation caused by the dip of the orebody, the analyses are essentially the same.

4.3.7 COMPARISON OF MODELLING METHODS

Two models have been used extensively for the analysis of stresses at Ruttan, BITEM, a two dimensional boundary integral program, and BESOL, a three dimensional displacement discontinuity program. In addition, a three dimensional boundary integral program, 3DBELM, was used in certain cases. The results of an analysis of a single isolated stope using the three programs is given in Figure 4.21. It can be seen that there are major differences between the modelling techniques. These can be attributed to the:

1. inherent assumptions in the model itself;
2. number of dimensions modelled;
3. element size used for modelling.

The large element size used for the 3DBELM analysis are attributed to causing the extremely low stresses at the stope wall contact, approximately -5 * σv.

The use of smaller boundary elements would improve the results, but would also greatly increase the time and cost of program execution.

It appears from Figure 4.21 and the BESOL analysis predicts a significant stress perpendicular to the stope wall. This is not the case. As the stope wall contact is approached, the orientation of the major principal stress changes from the virgin stress state of being perpendicular to the orebody to being parallel to the strike of the orebody. The intermediate principal stress behaves in a similar manner. The intermediate principle stress at the stope wall contact is perpendicular to the stope and is zero in magnitude.

The differences between the analyses results must therefore be attributed to the different modelling techniques used and to a lesser extent on the assumptions of an infinite extent of the orebody perpendicular to the model in two dimensions.

Further work is required in this area to study which modelling techniques are the most applicable to different mining configurations and geometries.

4.3.8 STOPE 800-26J

A sequential excavation analysis of stope 800-26J was undertaken using the three dimensional BESOL program. Figure 4.22 shows the modelled excavation sequence. The results are summarized in Figures 4.23, 4.24 and 4.25. These results can be compared to the deformation and induced stress measurements recorded for stope 800-26J. Figure 4.25 shows that the stress changes associated with mining steps 2 to 5 at the 760 meter level result in a drop of in-situ stress at the H/W and F/W and an increase within the pillars. This is similar to that observed through stressmeters located on the 730 meter level.

Extensometer X7301-Anchor 3(15 m) in the slot area of the stope recorded a maximum displacement of 0.018 m, Figure 9.11a. The displacement modelled (BESOL) at this location was 0.022 M. Anchors 1 and 2 (X7301) were lost due to wall slough prior to complete excavation of 800-26J (Step 5). It was concluded that the magnitudes modelled and observed were similar and enabled verification of subsequent studies through parametric analysis.

A simple fill analysis was undertaken, simulating the instantaneous filling of stope 800-26J after mining. It was observed that the fill had no discernible effect on displacements or stress regime when compared to the results previously modelled for the no-fill option.

4.4 CONCLUSION

The purpose of this chapter was to prove an important assumption in order to employ the data base under the premise that failure is kinematically controlled. Subsequent chapters will show that adversely oriented discontinuities exist and are primarily responsible for the resultant dilution. The degree of dilution will then be related to parameters that will have the greatest impact on its magnitude, stress not being one of those factors.

The relaxed zone was concluded in this chapter to encompass all isolated, rib, and en echelon stopes having configurations resembling those of Ruttan. The resultant dilutions are well within the zones of relaxation and consequently are not considered to be greatly affected by geometry. This will be discussed further in Chapter 6, "Dilution".

TABLE 4.1 NUMERICAL CODES

TITLE:	**BOUNDARY INTEGRAL TECHNIQUE FOR MULTIPLE MATERIALS**
PROGRAM:	BITEM
CAPACITY:	Solves two-dimensional elasticity problems for a piecewise homogeneous, isotropic elastic solid using the boundary integral equation method with linear variation of displacements and tractions along the boundary seqments, and allowing mixed displacement and traction boundary conditions. The solid may be composed of at most five homogensous regions with differing elastic constants. Problem symmetry can be taken into account. Facilities for automatic data generation are available.
ORIGIN:	BITEM was written at the CSIRO division of Applied Geomechan. and is based on program BITE which analyses homogeneous solids only. Refer Crotty and Wardle (1977) and Riccardella (1973).
TITLE:	**THREE DIMENSIONAL BOUNDARY INTEGRAL PROGRAM FOR MINING APPLICATIONS**
PROGRAM:	3DBELM
CAPACITY:	Program models a three-dimensional boundary by piecewise flat triangles over which the displacements and tractions vary linearly. The boundary may be composed of multiple openings within a single homogeneous region. Problem symmetry can be taken into account.
ORIGIN:	3DBELM was written at the CSIRO Division of Applied Geomechanics and is based on program BITE which analyses homogeneous solids. Refer Crotty and Wardle (1977) and Riccardella (1973).
TITLE:	**THREE DIMENSIONAL DISPLACEMENT DISCONTINUITY METHOD FOR MULTIPLE SEAM PLANES**
PROGRAM:	BESOL/MS221
CAPACITY:	Models three dimensional multiple seam planes in a semi-infinite isotropic region. Both on seam and off seam stresses are determined on 30 x 30 grids or windows. Models mining sequences, backfill and is capable of employing user input failure criterion.
ORIGIN:	BESOL was developed by Dr. C. R. Crouch of Crouch Research Inc.

TABLE 4.2 NUMERICAL MODEL - INPUT PARAMETERS

a) In-Situ Stress (MPa)

σv = .027 x Depth (m)		
$\sigma 1$ = 2.5 σv	340°/-20°	(azimuth/dip)
$\sigma 2$ = 1.2 σv	70°/0°	
$\sigma 3$ = 0.8 σv	160°/-70°	

b) Material Properties Test Stope 800-26J

Laboratory	E ore = 88 GPa, ν = 0.2			
	E host = 77 GPa, ν = 0.2			
In-Situ	E ore = 51 GPa, ν = 0.2	RQD = 80%	Em/El = .6*	
	E host = 23 GPa, ν = 0.2	RQD = 75%	Em/El = .3	

(* as derived using modulus reduction ratio after Bieniawski, 1978)

TABLE 4.3 SUMMARY OF NUMERICAL ANALYSIS PERFORMED

Model/Case*	1	2	3	4	5	6
BITEM	X	X			X	
3DBELM	X					
BESOL	X	X	X	X	X	X

* Refer Figure 4.4

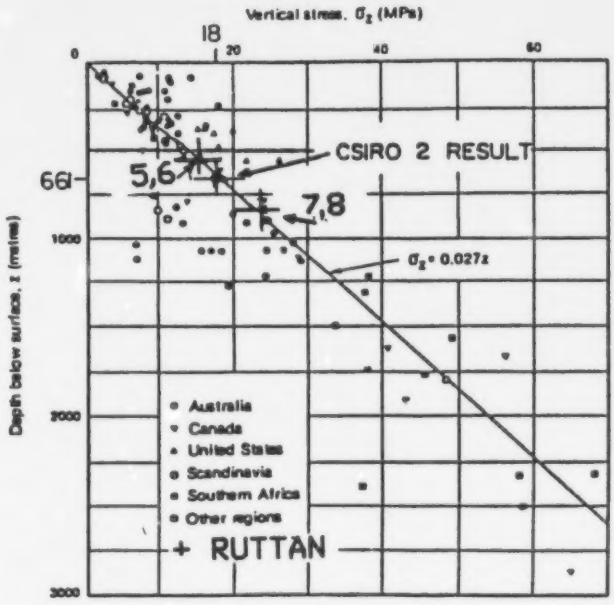

Figure 4.1: Vertical Stress vs Depth (Hoek, 1983)

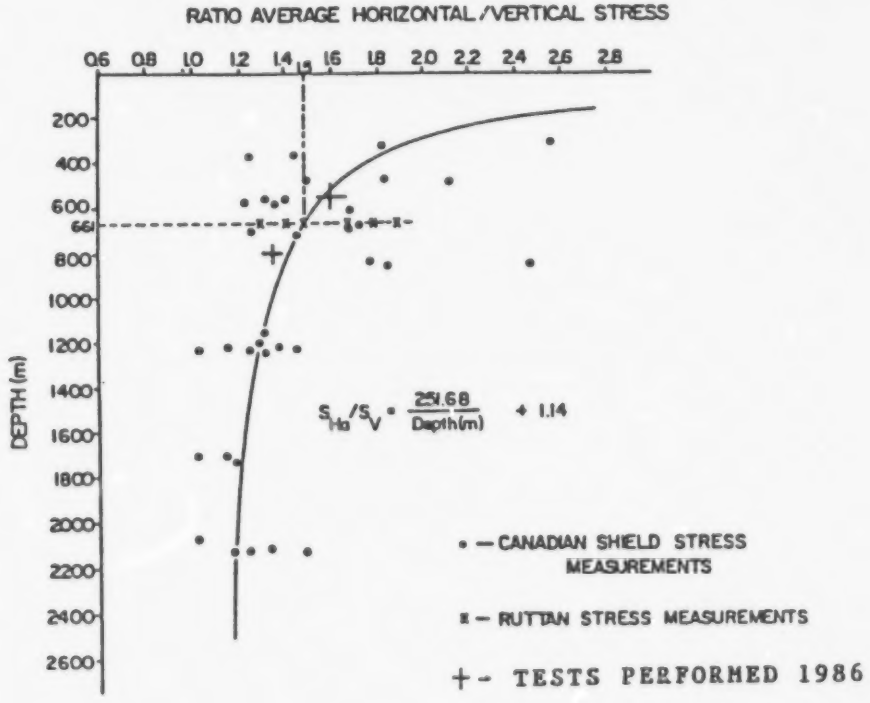

Figure 4.2: Horizontal Stress vs Depth (Herget, 1980)

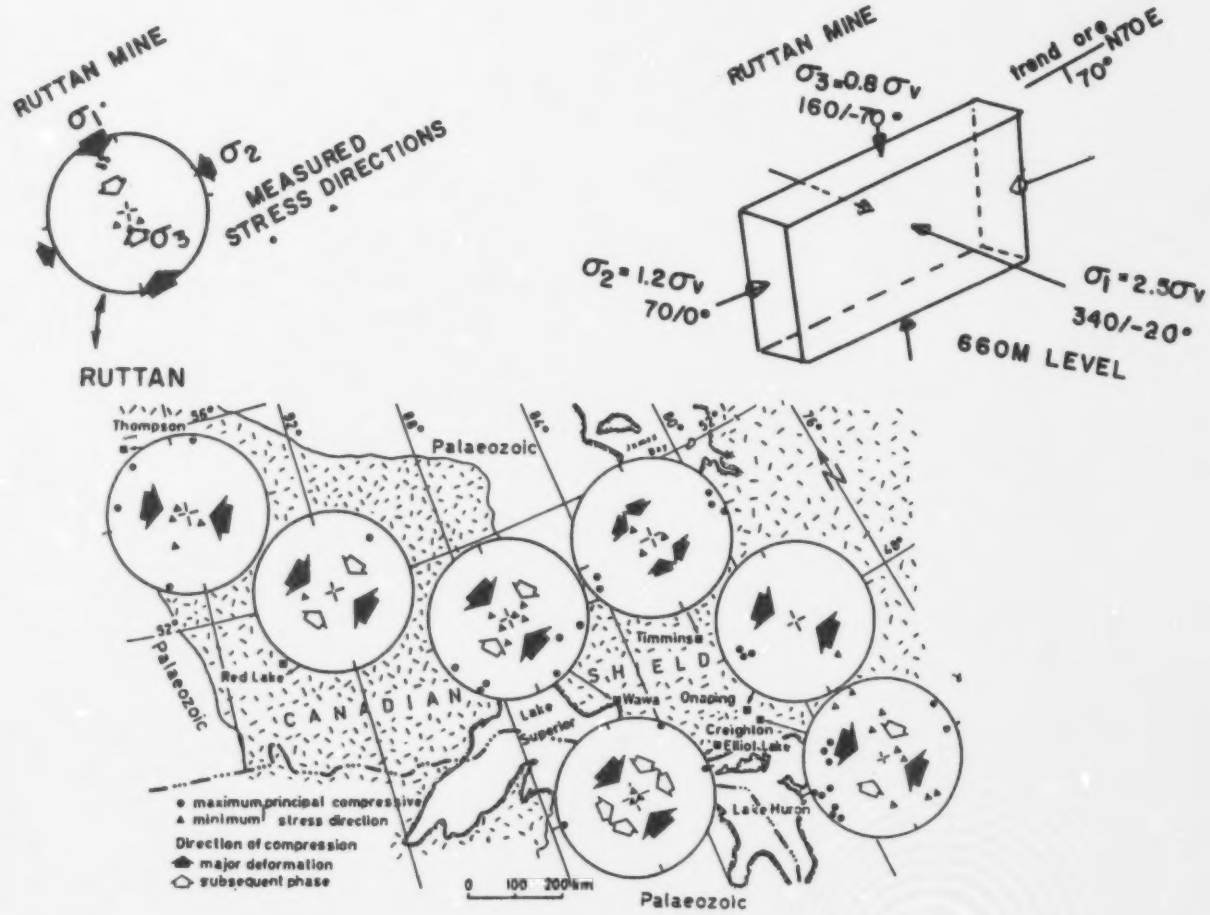

Figure 4.3: Suggested Direction of Compression During Tectonic Deformation and Measured Principal Stresses from Overcoring Plotted in Lower Hemisphere of Equal Area Net

From: In-situ Stress Determination at Ruttan Mine, Sherritt Gordon Mines Limited, Miller, Pakalnis, Madill, CIM Bul., Dec. 1985.

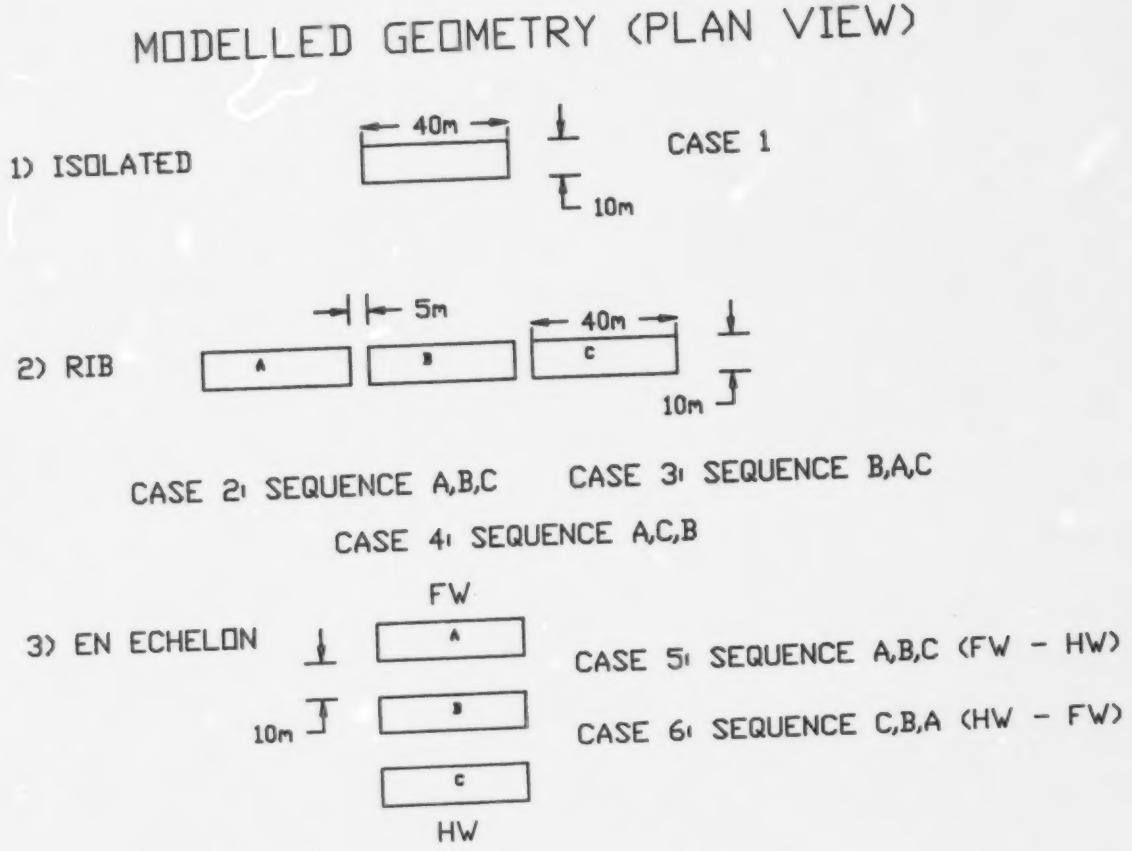

Figure 4.4: Modelled Stope Configuration/Sequences - Plan View
(Stope Height = 60 m)

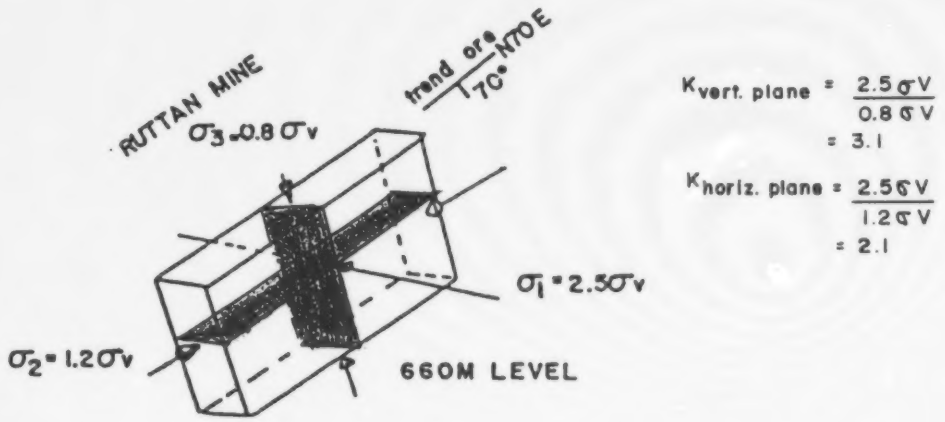

Figure 4.5: Horizontal/Vertical Stress Ratio (k)

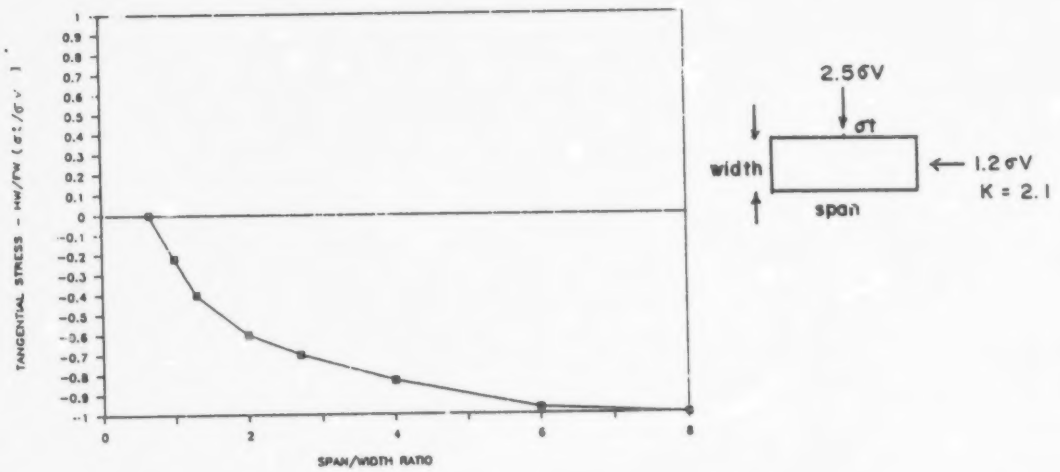

Figure 4.6: Tangential HW/FW Stress vs Span/Width

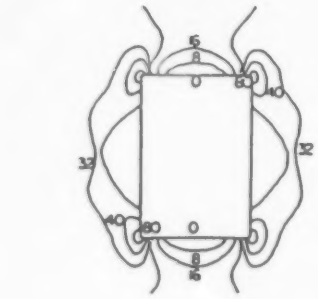

Length/Width = 0.66:1

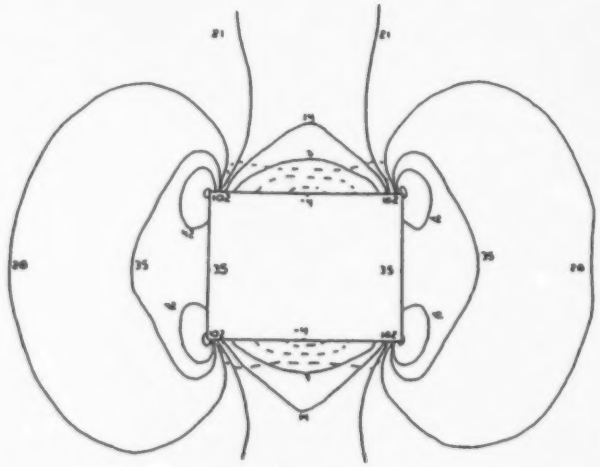

Length/Width = 1.3:1

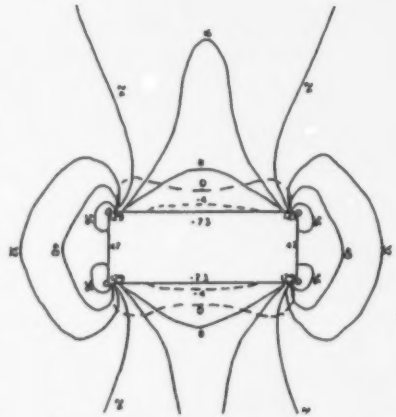

Length/Width = 2.7:1

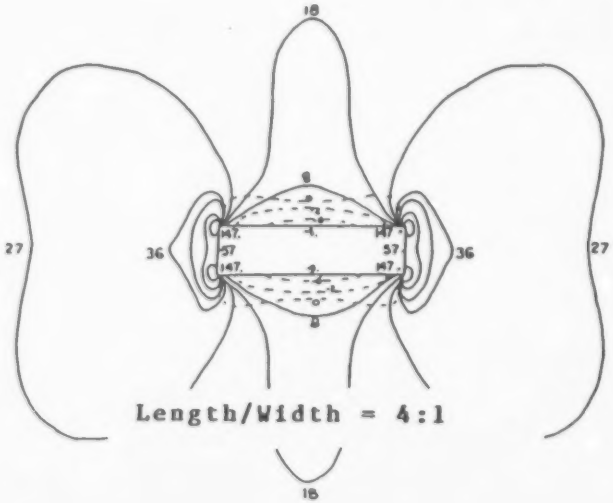

Length/Width = 4:1

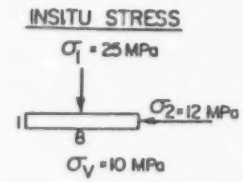

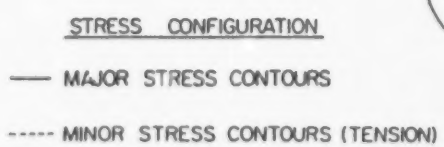

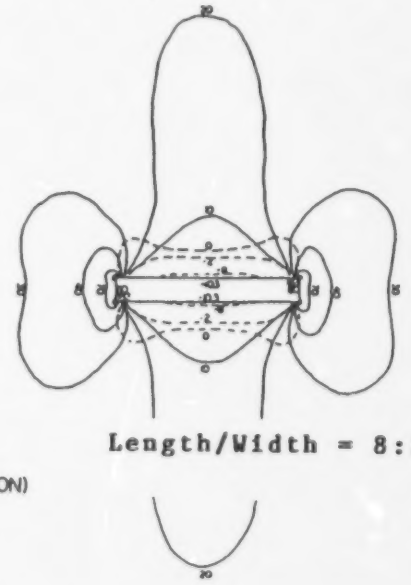

Length/Width = 8:1

Figure 4.7: Stress Configuration - Parametric Study "k" - 2.1

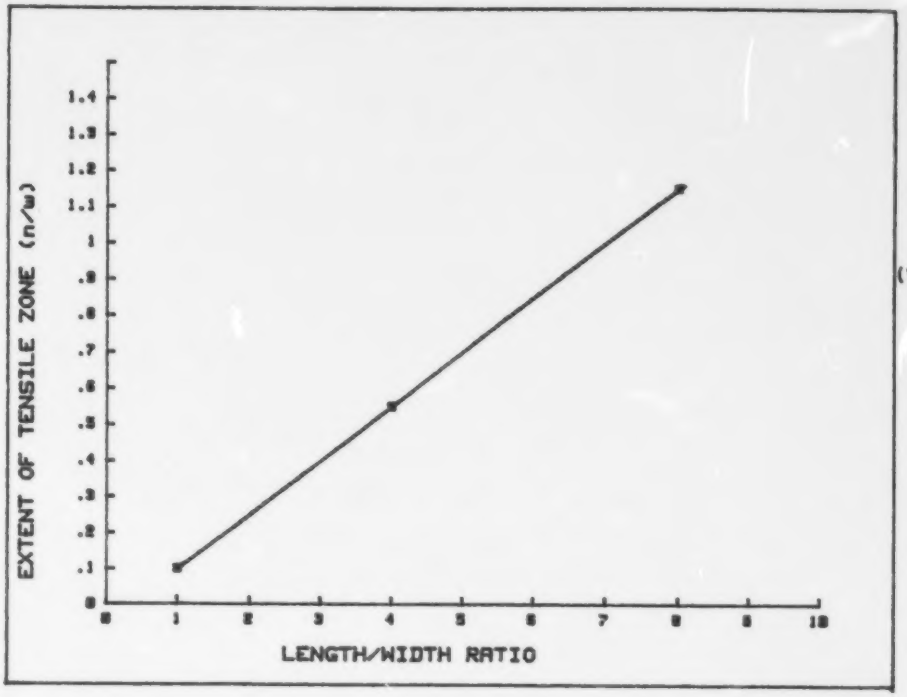

Figure 4.8: Lateral Extent of Tensile Zone

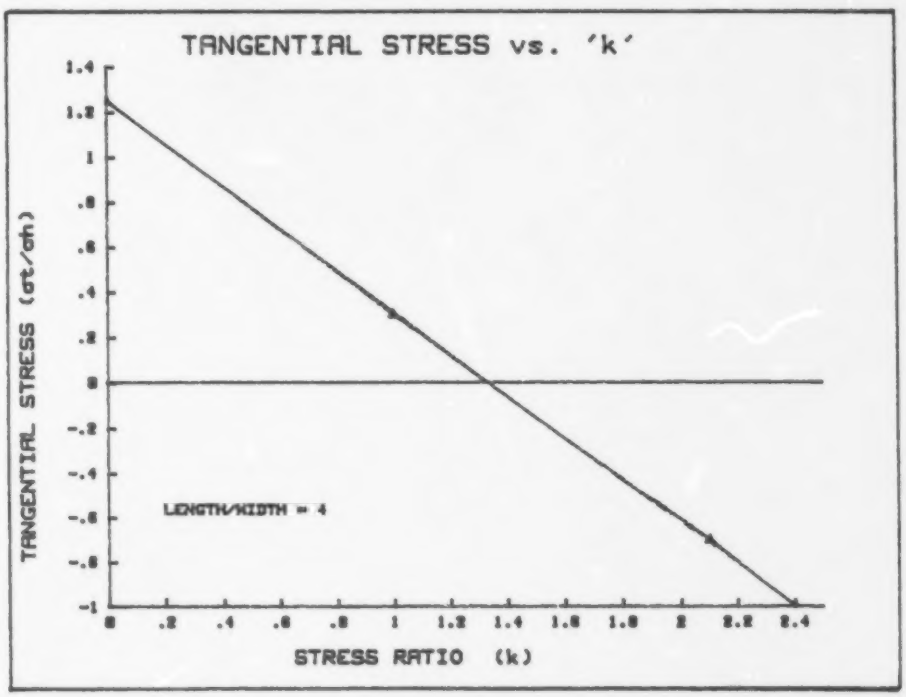

Figure 4.9: Effect of "k" on Tangential Stress in the FW/HW

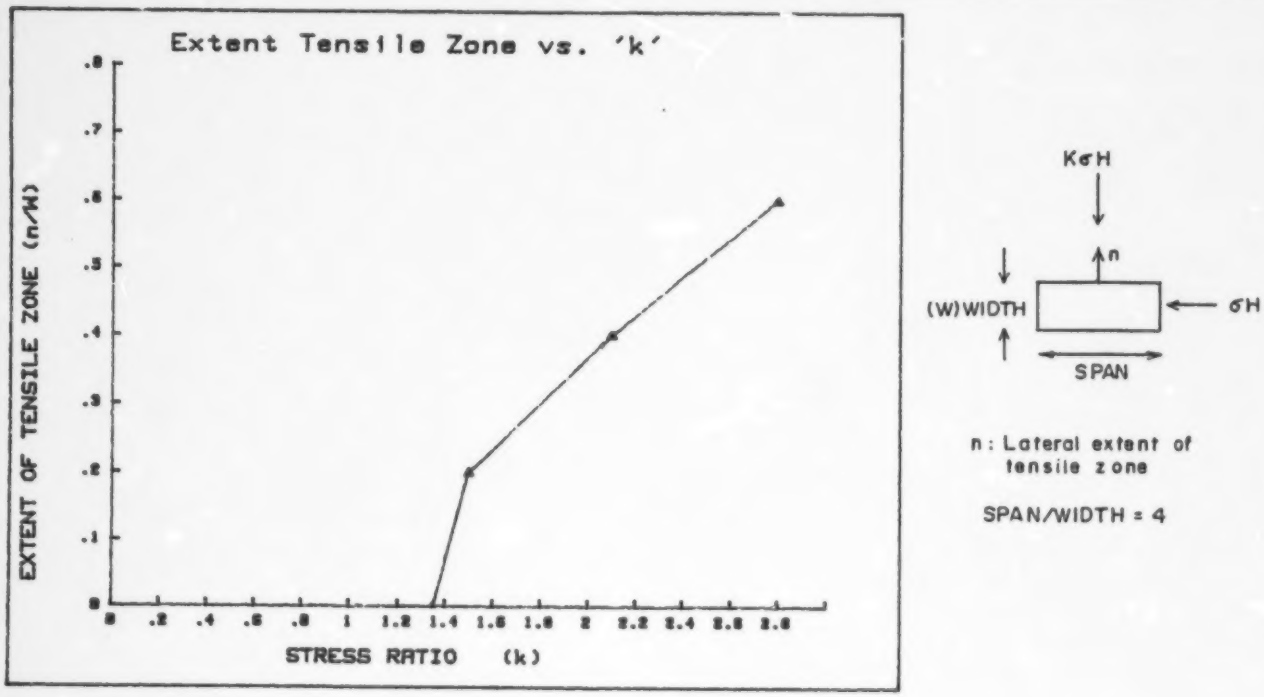

Figure 4.10: Extent of Lateral Tensile Zone with Variance in "k"

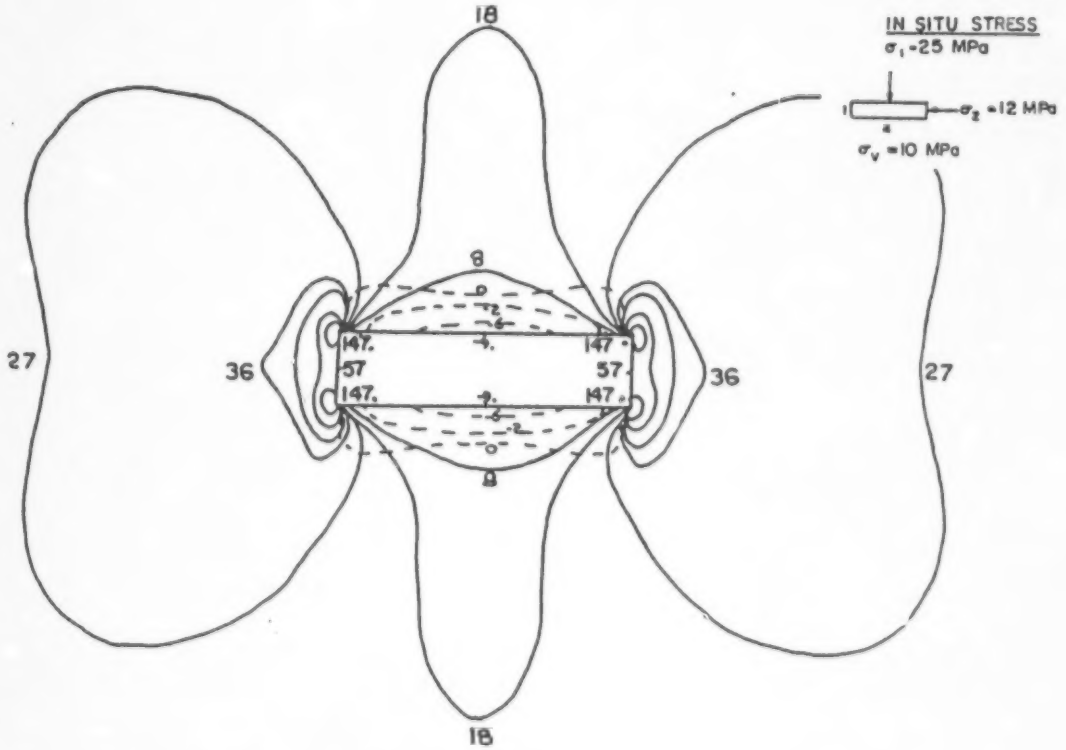

Figure 4.11: Base Case - Stress Configuration

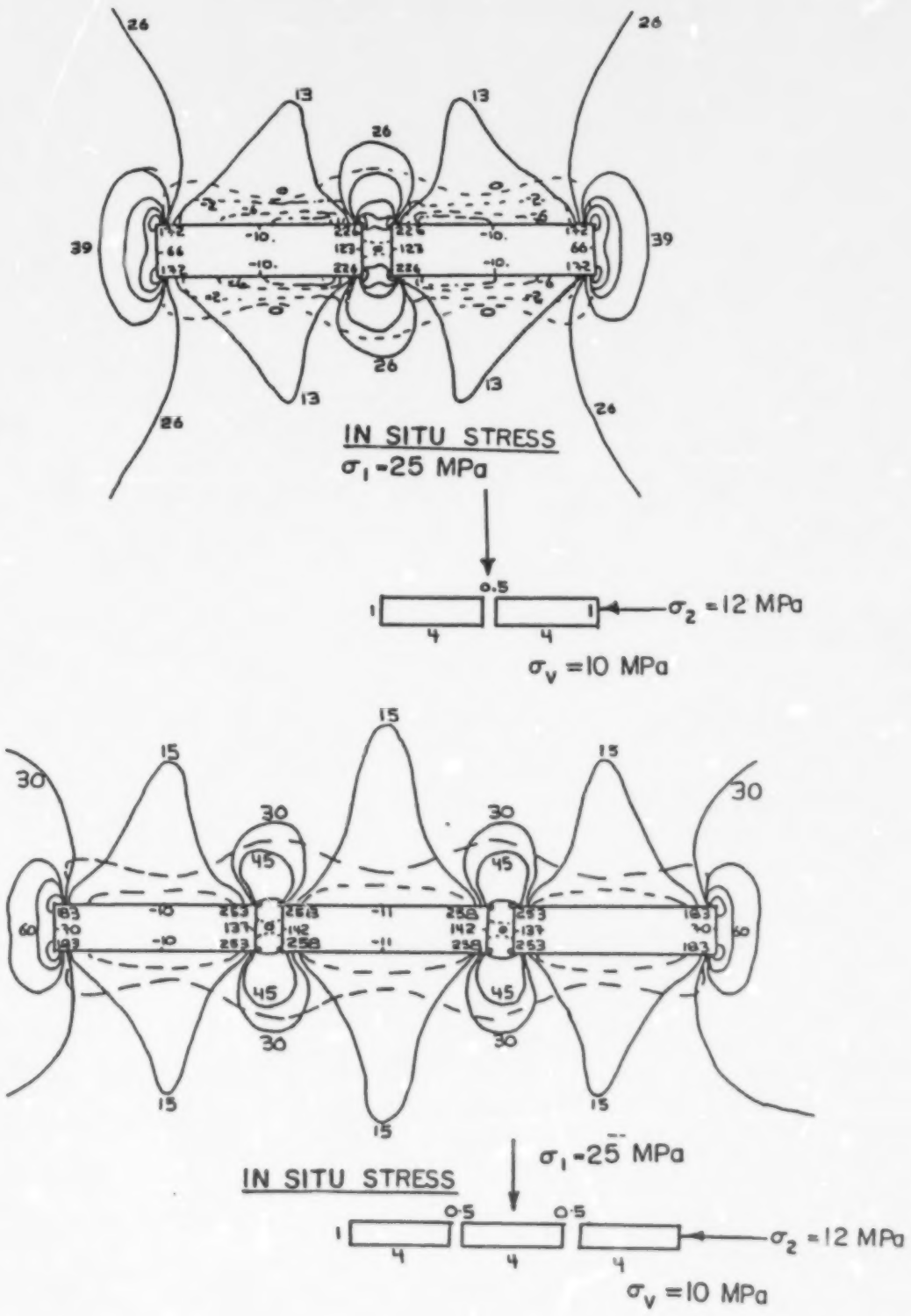

Figure 4.12: Stress Configuration - Rib Stopes
(Instantaneous Excavation)

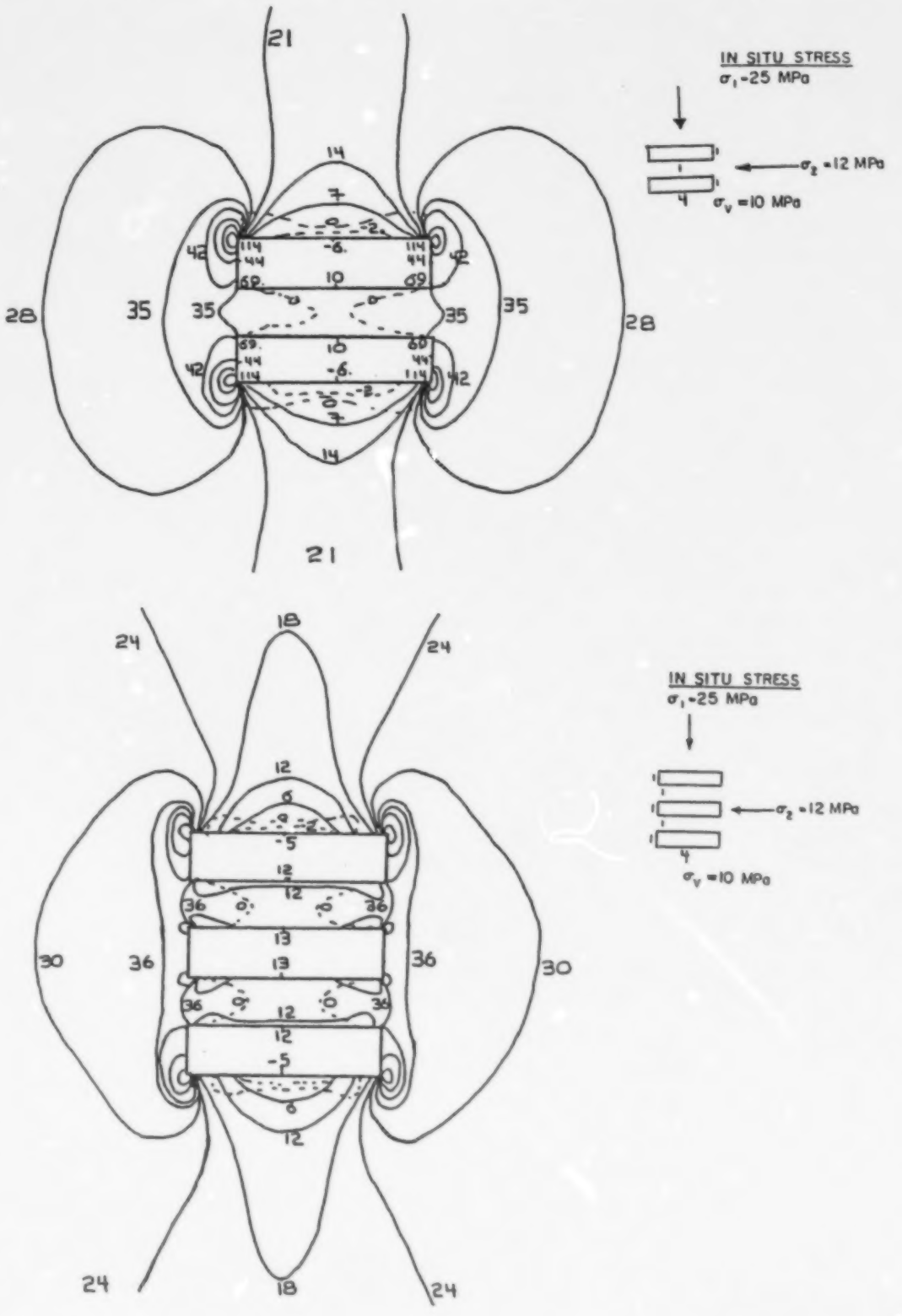

Figure 4.13: Stress Configuration - Echelon Stopes

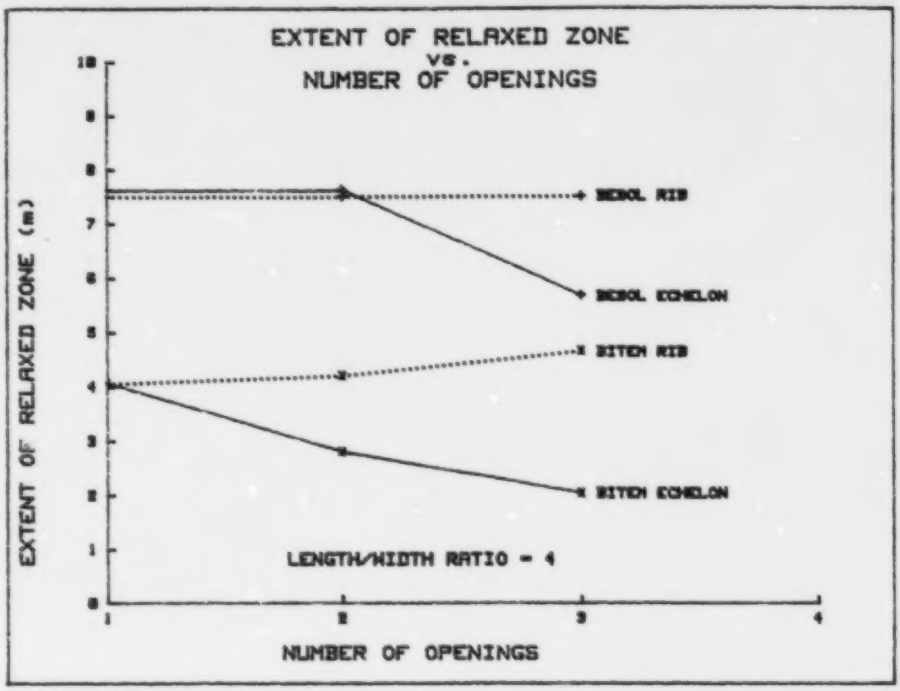

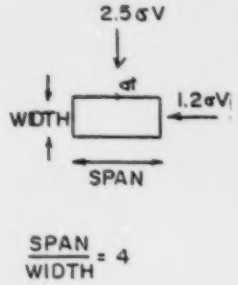

Figure 4.14: Variation of Lateral Extent of Tensile Extent with Number of Openings (W = 10 m)
(Span = 40 m)
(Ht. = 60 m)

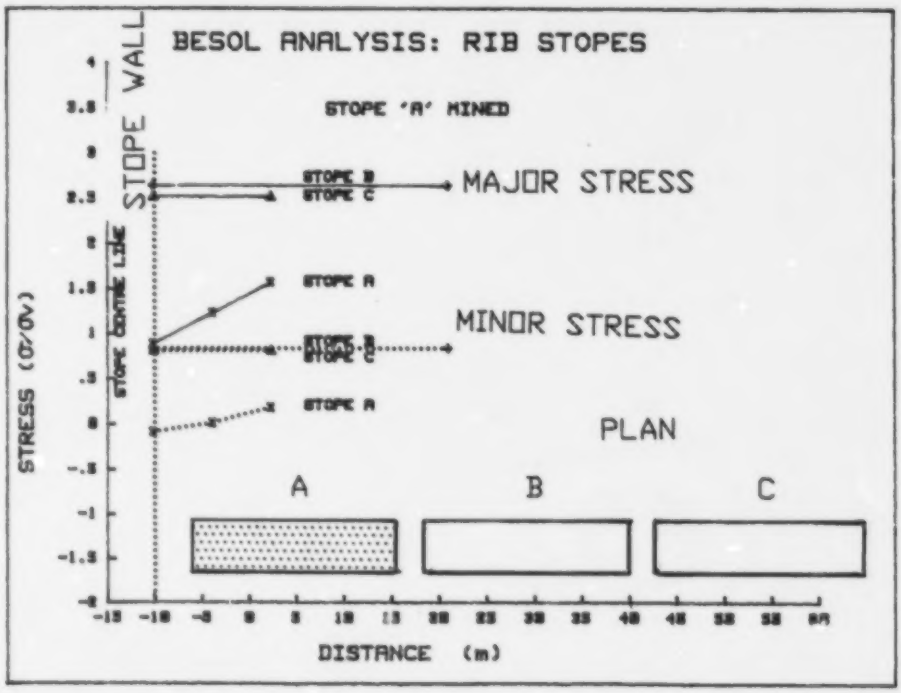

Figure 4.15: BESOL - Rib Stope Analysis - Stope "A" Mined (Major/Minor Stress Magnitudes)

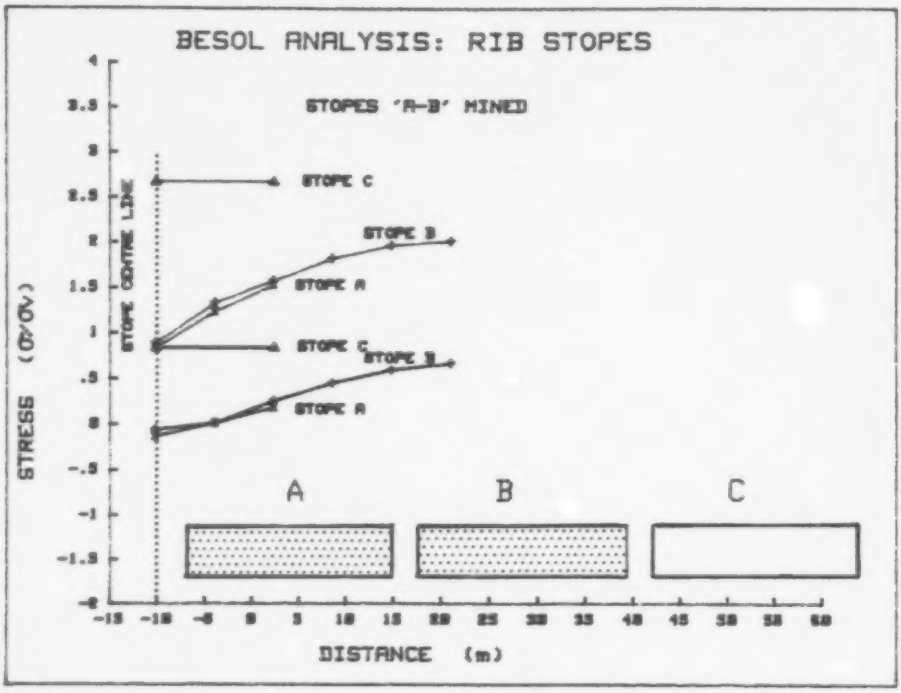

Figure 4.16: BESOL - Rib Stope Analysis - Stope "A & B" Mined (Major/Minor Stress Magnitudes)

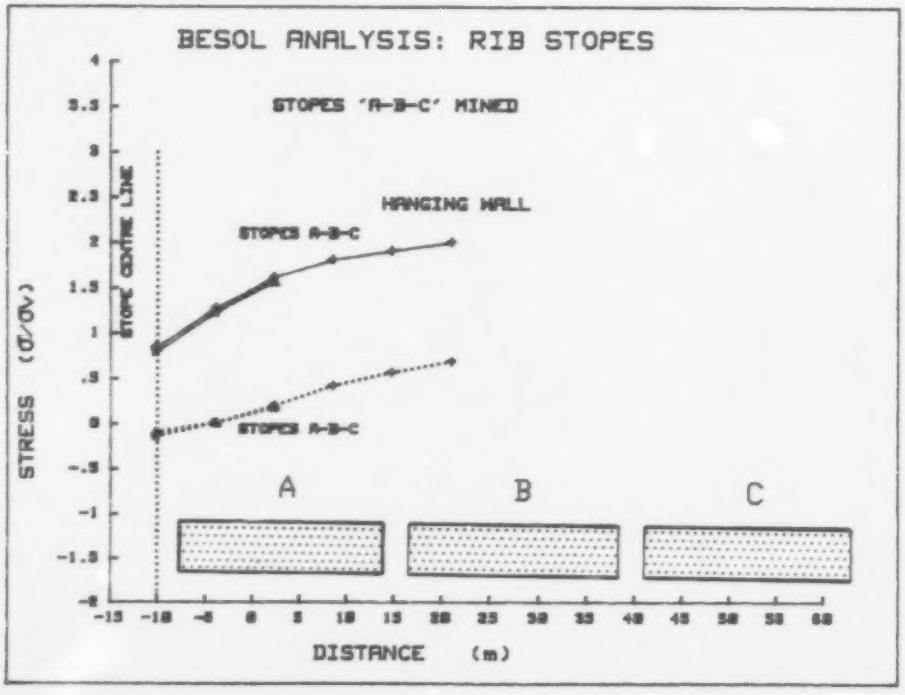

Figure 4.17: BESOL - Rib Stope Analysis - Stope "A, B, C," Mined (Major/Minor Stress Magnitudes)

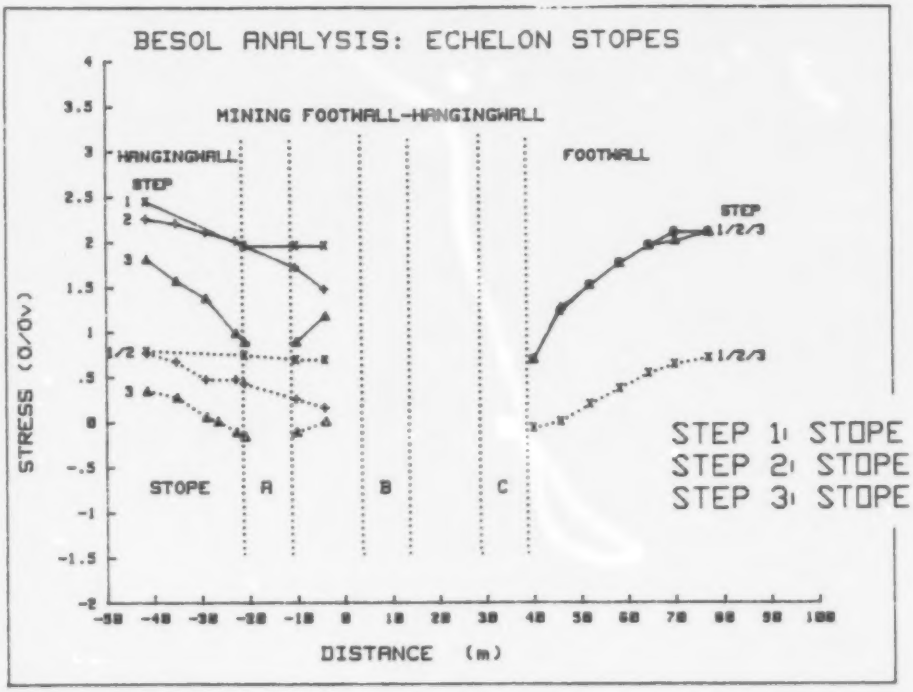

Figure 4.18: BESOL - Echelon Analysis FW/HW Cases
(Major/Minor Stress Magnitudes)

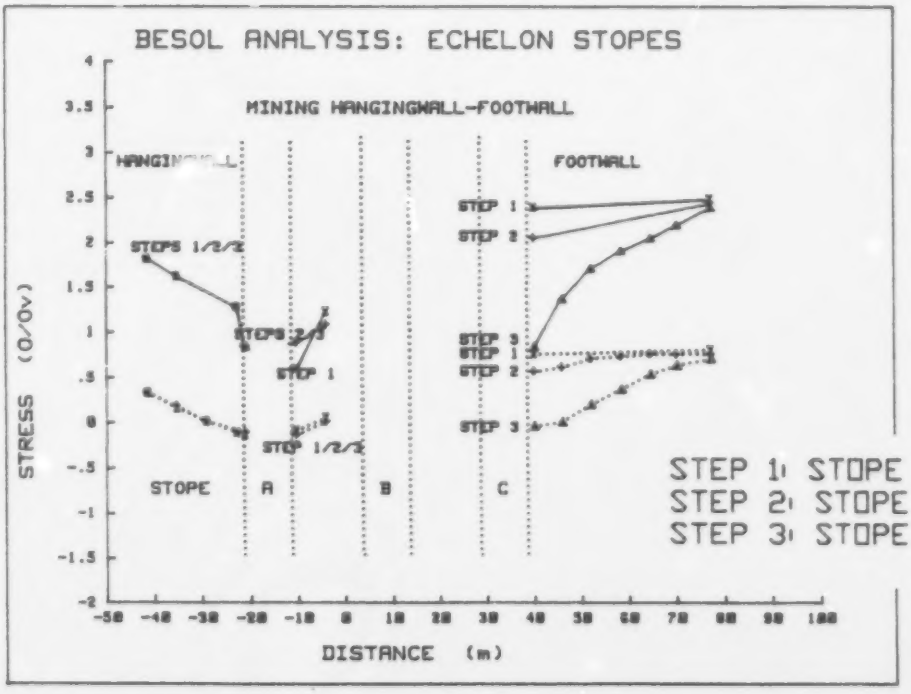

Figure 4.19: BESOL - Echelon Analysis HW/FW Cases
(Major/Minor Stress Magnitudes)

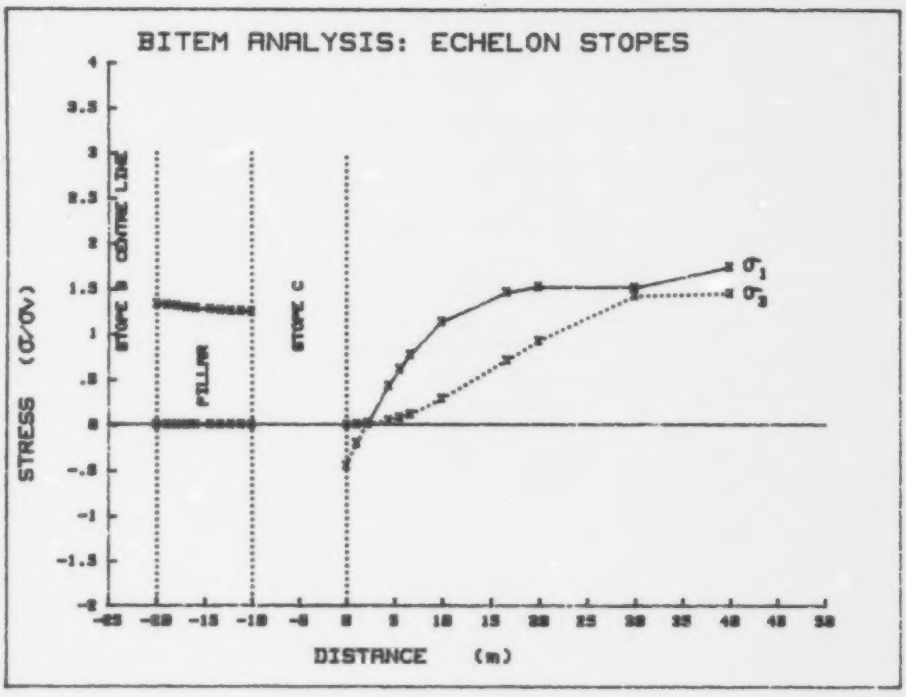

Figure 4.20: BITEM - Echelon Analysis - Instantaneous Excavation (Case 6)

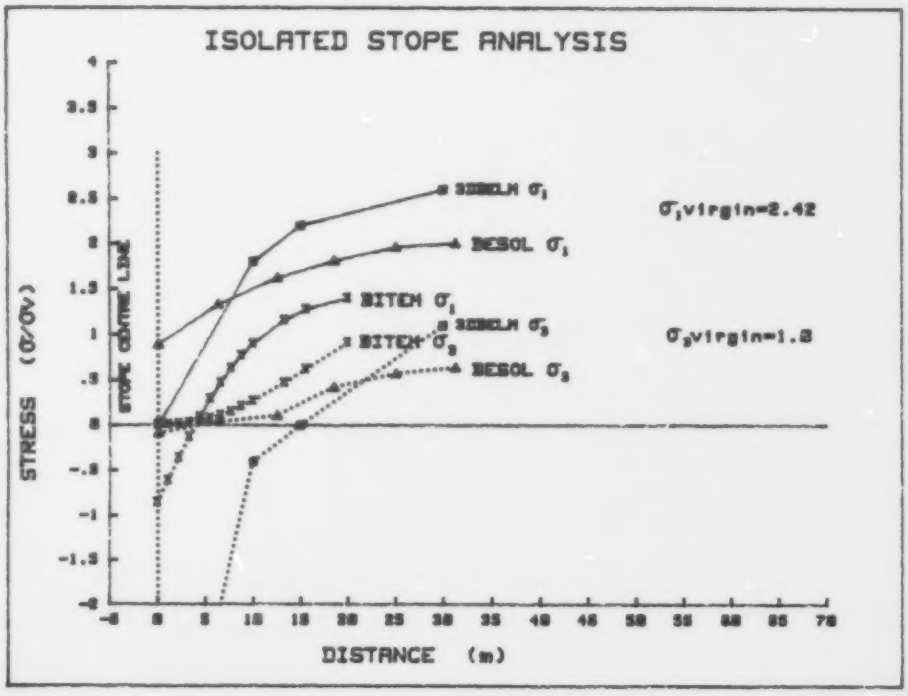

Figure 4.21: Isolated Stope Analysis - Comparison of Case 1 Modelling Methods (Major/Minor Stress Magnitudes)

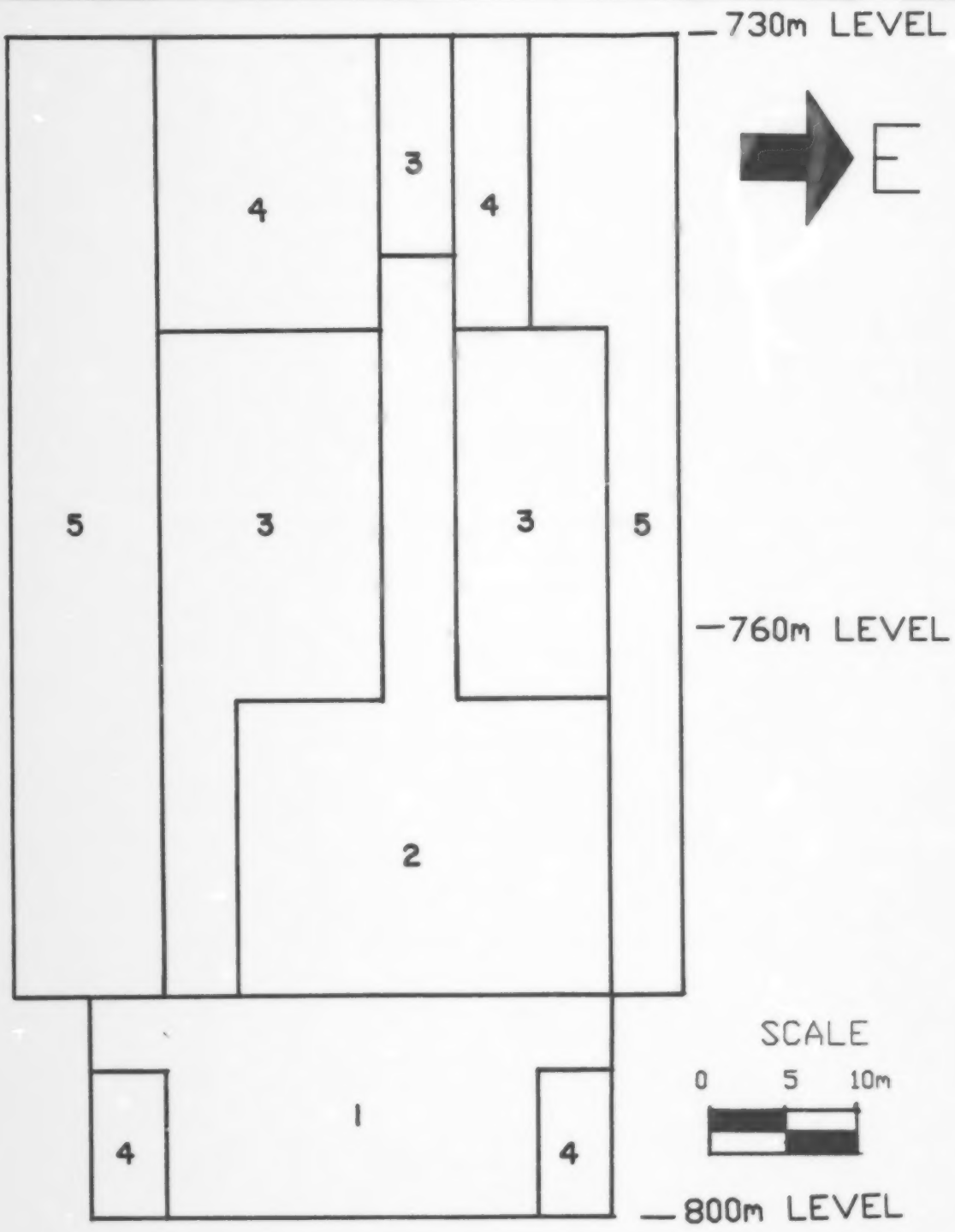

Figure 4.22: Longitudinal (Parallel to Strike) Presentation of Test Stope 800-26J
BESOL Analysis - Modelled Excavation Sequence
(Stope Width = 20 m inclined at 70°)
(Stope Length = 44 m)

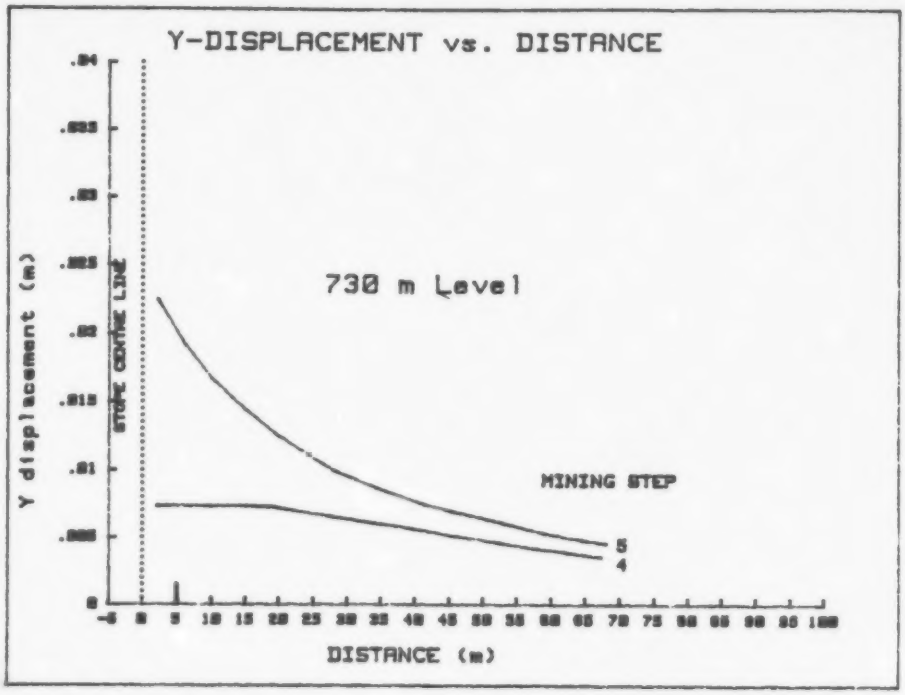

Figure 4.23: BESOL Analysis - Hangingwall Displacement on 730 m L of 800-26J. Displacement "y" Refers Movement Towards Opening.

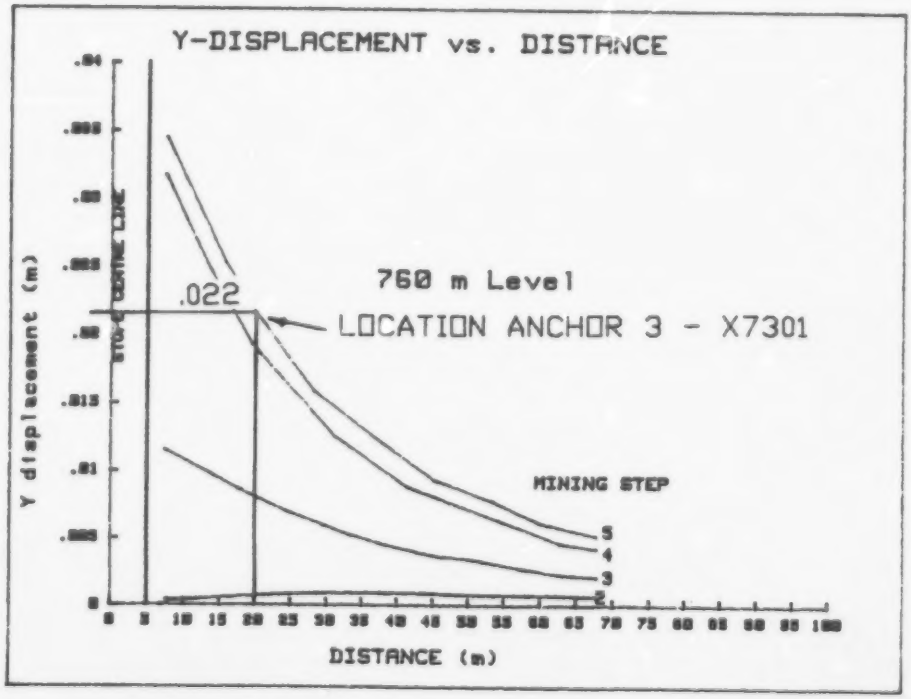

Figure 4.24: BESOL Analysis - Hangingwall Displacement on 760 m L of 800-26J

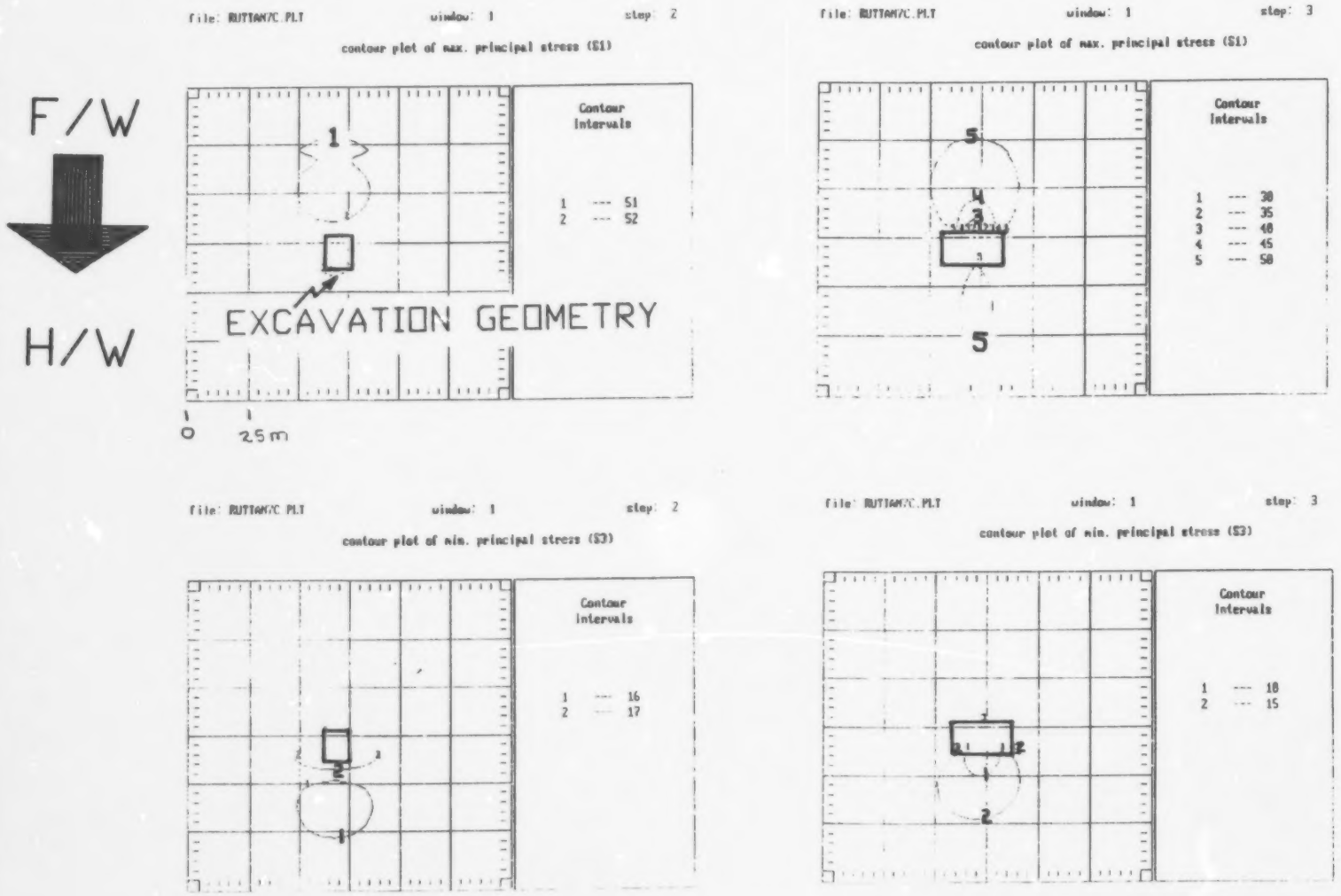

Figure 4.25a: BESOL Analysis - Horizontal Cross-Section Stress Configuration on 760 m Level, 800-26J. Contour Intervals in MPa.

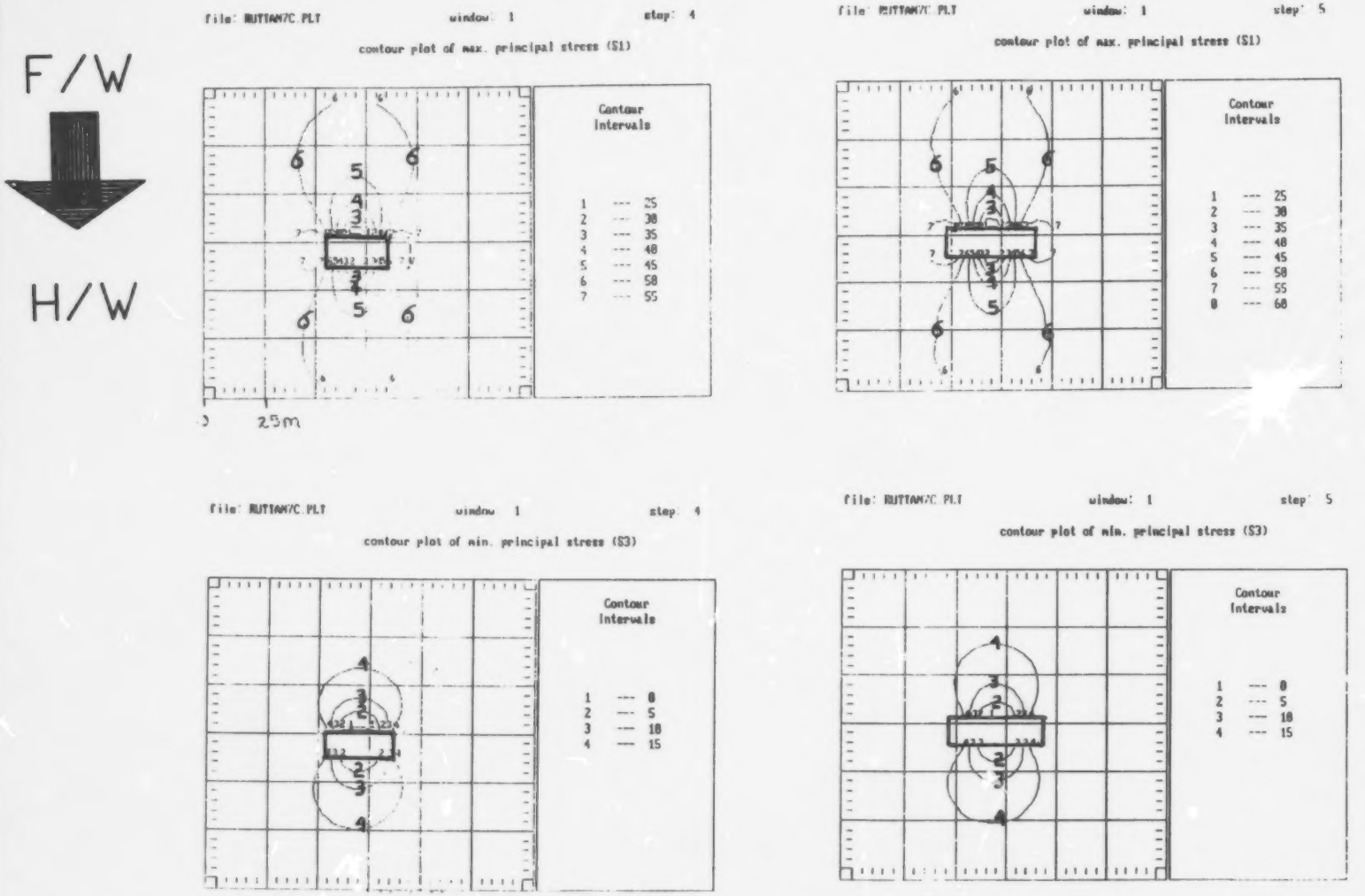

Figure 4.25b: BESOL Analysis - Horizontal Cross-Section Stress Configuration on 760 m Level, 800-26J.

CHAPTER FIVE
ROCK MASS CHARACTERIZATION

5.1 INTRODUCTION

This chapter identifies the parameters describing the rock mass that have the greatest influence upon stope dilution. It begins with a critical evaluation of existing rock mass classification systems. A particular system was selected in order to relate the rock quality of individual stopes at Ruttan to a much larger database that has been derived throughout the literature. This enables the rock quality to be evaluated quantifiably in terms of existing relationships that have been developed by other investigators. The significance of the parameters incorporated into the classification are subsequently analysed in order to assess their relative importance in terms of stope design at Ruttan, Chapter 7. A structural assessment, in terms of delineating potential failure modes of individual stope hangingwall and footwall contacts, is presented. A kinematic analysis identifies structure as being a principal factor affecting dilution.

5.2 ROCK MASS CLASSIFICATION

Rock mass classification systems have been developed primarily to assist in recommending support for underground civil projects.

Generally, civil structures are normally isolated from any nearby openings, do not account for the extraction process, are at moderate to shallow depth, and expose a minimum of open ground. These deficiencies do not enable them to be directly applied to the design of underground mining structures. The classifications, although on their own are not adequate to predict mine design requirements, do provide a procedure for investigation. The rock mass classification systems of particular relevance to underground mining applications are the:

* Geomechanical Classification System (RMR) (1973);
* Q System (1974).

These systems have empirically evolved from a large database. In addition, they not only reflect the experiences of the developers, but also the preceding investigators such as Terzaghi (1946), Lauffer (1958), Stini (1950), Deere (1964), Wickham et al (1972, among others. The systems were primarily derived for the design of civil engineered tunnels. However, they provide the basis for subsequent modifications that enable them to be applied to mining. Laubscher (1976), Mathews

et al (1981), Kendorski (1983), and Hoek (1983) have applied adjustments to the existing systems to aid in the design of mining structures.

An ideal mine classification system must have the flexibility that allows it to be used for various mine applications, and it must be simple so that it can be easily assessed and understood. It is only in this manner that it can function as an important tool in the design and operation of a mine. The RMR and Q Systems satisfy the above criteria. Deficiencies do exist with the two classifications, but through adjustments one is able to overcome the criticisms. In particular, the Q System is said to be too rigorous (Kendorski, 1983), has a poorly defined factor that accounts for stress, and does not account for structural orientation. These criticisms are incorporated into adjustments by Mathews (1981) and Kirsten (1983). The RMR system is said to be too simple; it does not account for stress and the input parameters are too qualitative. These limitations are incorporated into adjustments by Laubscher (1976), Kendorski (1983).

A classification system for the Ruttan operation should be patterned after the "Q or RMR" systems with the relevant geotechnical parameters associated with each mining method identified. This requires the generation of a large empirical database specifically categorized in terms of similarities of applications for open stope design. This database was equally sparse when Terzaghi proposed his system in 1946. This database has since expanded and grown, and the systems have been refined due to its acceptance among the civil engineering community. This was largely due to the continued success achieved in tunnel support prediction.

One of the major differences between the civil and mining disciplines is the requirement of mines to generally operate within a rock mass of which the peak strength has been exceeded. In addition, controlled and predicted failure is acceptable in mining which is not the case in civil construction. The temporary requirements of mine openings are generally not reflected within the confines of civil engineering. These factors, plus the geometrical and excavation considerations, require one to modify the existing system through the collection of empirical data relevant to open stope design.

The majority of the classification systems include, either directly or indirectly, an assessment of the following parameters, Table 3.3:

* Intact rock strengths (unconfined compressive strength). It is a necessary parameter since it forms the upper strength limit of a rock mass which is subsequently reduced due to rock defects.

* Rock quality designation (RQD). The parameter is an indirect measure of fracture frequency. It is a quantitative index based on a modified core recovery procedure.

* Spacing of discontinuities.

* Condition of discontinuities. This includes roughness, continuity, separation, joint wall weathering and in-filling.

* Orientation of discontinuities.

* Groundwater conditions. This is a measure of inflow rates and water pressures.

* Stress field. This refers to the prevailing in-situ stress environment.

The RMR system was selected as the vehicle for stope wall characterization due to its incorporation of the many variables that are considered to influence the behaviour of a rock mass. The interrelationship between the variables and the constitutive equations linking the different variables to the rock mass behaviour are complex. Therefore, an approach was selected that could be empirically calibrated to the optimum stope design through observed resultant dilution measurements. The RMR system was selected since:

* It incorporates key parameters affecting the rock mass behaviour as defined by the literature.

* The system is simple to employ and is readily applicable to existing methods of core logging and mapping techniques as practised at Ruttan, Table 5.1. This is particularly important in relating historic core logs in terms of a rock mass number, since the logs generally form the only available descriptor for a particular stope. This is due to either limited stope wall access and/or the unavailability of drill core due to sampling.

The RMR system was employed in isolated areas of the mine and was found to be a good predictor of mine behaviour. Areas having a low RMR rating were found to have problems with:

* drawpoint plugs due to falls of ground from the FW/HW and from the exposed benched bask, Figure 2.15;
* excessive dilution from the FW/HW;
* large amounts of re-drills.

This study will be particularly concerned with quantifying the RMR parameter in terms of its effect on dilution. Not all the parameters shown in Table 3.3 are incorporated into the RMR rating and these will be discussed individually in Chapter 7, "Database". The individual parameters incorporated into the RMR number will be assessed in terms of their influence on stope design.

5.3 STRUCTURAL ASSESSMENT

The database for this study is comprised of 66 stopes and is distributed as follows:

* 48 stopes mined at the time of completion of this phase of the study, of which 43 were suitable for subsequent analysis;
* 20 additional stopes mined subsequent to the completion of the phase will be employed to reinforce or disprove the design methodology as derived through observation and analytical assessment.

A detailed structural investigation of the Ruttan operation was conducted by the author in order to identify domains with potentially similar ground behaviour. In terms of mine design, it is important to identify areas that would exhibit similar rock mass behaviour upon extraction. These would enable a mine plan to be implemented. The concepts of domain analysis were employed (Brady, 1985), however individual stopes were attributed rock mass characteristics and analysed individually, and subsequently related to the observed dilution upon extraction. Volume II, "Database", presents in detail the structural analysis of the rock fabric comprising the Ruttan orebody. Tables 5.2 and 5.3 summarize the observed rock mass characteristics observed at Ruttan.

The values have been derived for each rock type that forms the individual contact zones. The rock mass information has been compiled from core logs information and has been augmented by structural mapping. The diamond drill core was AQ size (27 mm). Figure 5.1 is a stope characterization procedure employed for all stopes at Ruttan. A stope is characterized by two drill holes per section and two sections per stop, Figure 2.11. In essence, four holes are analysed which are representative of the footwall, ore and hangingwall for a particular stope. Three meters of the immediate hangingwall and footwall were evaluated in addition to the full length of the ore for a particular drill hole. However, the rock quality of the drill core within two stop diameters was studied, but in less detail. Major structures are recorded in addition to the geometry of the proposed stope and its configuration (open ground) at the time of mining. The rock mass rating is further grouped into the following classes:

Class	Rock Mass Rating
A	81 - 100%
B	61 - 80%
C	41 - 60%
D	21 - 40%
E	0 - 20%

Through visual estimates and historic observation, it is generally accepted that wall slough at Ruttan is primarily confined to the hangingwall. This has been determined primarily through visual observation at the drawpoints and the drill levels. It is for this reason that the rock quality in the vicinity of the hangingwall will be employed in characterizing an individual stope. In certain instances, however, it was found that an assessment of the footwall was more critical when:

* a major fault intercepts the footwall;
* the rock mass rating of the footwall was much lower than that of the hangingwall (one class or more difference).

A further practice was reducing the rock mass rating by a single class when a major structure intercepted either of the wall contacts. The RMR system classifies the mean rock mass parameters. A major structure must be treated separately from the adjacent bounding units. This modification was shown to empirically be a good estimator of dilution, Chapter 7. It is realized that kinematically each major structure should be analysed in greater detail. However, for purposes of this investigation, it was found that by reducing the RMR values by a class, resulted in statistically higher correlations between the modified RMR and dilution. The orientation of the individual structures at Ruttan are generally oriented parallel to the stope contact. The major difference is found in the frequency and strength of the individual jointing. This is described in detail in subsequent chapters. Groundwater was not incorporated into the characterization, Figure 5.1. This is primarily due to the absence of water as evidenced by falling head tests conducted on the 430 meter, 370 meter and 260 meter levels (Interim Report - Project 213). The close diamond drill pattern generally ensures that any trapped groundwater has an access to drain.

The rock unit can be generalized as follows:

Hangingwall and Footwall Units:

Chlorite Talc Schist (CTC)
Quartzite (QTZ)
Acid Sediments (AS)
Basic Dyke (BD)
Massive Sulphides (MS)

Ore Units:

Semi-massive Sulphide with Basic Dyke (SMS-BD)
Semi-massive Sulphide with Quartzite (SMS-QTZ)
Semi-massive Sulphide with Chlorite Talc Schist (SMS-CTC)
Semi-massive Sulphide with Chlorite Schist (SMS-SC)
Massive Sulphides (MS)

Figure 5.2 shows the distribution of RMR for the hangingwall of all stopes at Ruttan. The east lenses generally exhibit higher RMR values and are normally associated with lower stope dilutions.

A detailed line mapping survey was conducted in the vicinity of the individual lenses. This was supplemented by geologic mapping conducted by Ruttan Geologists. The information was compiled onto lower hemisphere stereoplots which are documented in Appendix I. Figure 5.3 is a photograph identifying the major design sets which are summarized below:

SET 1:	Most Dominant - N 50 - 80° E/75° SE
SET 2:	Moderate Occurrence - Flat Structure 0 - 20° Dip
SET 3:	Minor Occurrence - N 0 - 30° E/80 - 90° SE

The continuity of the structure was observed as exceeding 200 meters and 100 meters respectively for design sets, one and two. Design set three was disjointed and cut by set one; it is estimated to be less than 15 meters in length. The continuity was primarily recorded from pit mapping, Figure 5.4.

5.3.1 KINETIC ANALYSIS

Residual friction angles on saw-cut joints were performed by Smith (1975), employing direct shear tests on samples of quartz-biotite-chlorite gneiss. The results indicated a residual friction angle of 29° based upon six staged shear tests. Figure 5.5 shows an isometric outlining the potential for failure along the design sets. Employing a simplified analysis, as outlined by Hoek and Bray (1977) and

reproduced in Figure 5.6, it is shown that toppling failure of the hangingwall is possible. This is derived from employing a base (b) to block height (h) ratio equivalent to a joint spacing of 3 meters and a height of 60 meters. The maximum joint spacing according to Table 5.3 should not exceed three meters. The footwall is generally more stable than the hangingwall, however a combination of planar and toppling failure is a possibility. A more rigorous solution is possible, but in the author's opinion, not warranted, since it is the purpose of this section to outline that instability due to structure is a possible failure mechanism.

Stereonets of individual stopes indicate that structures exist which would generally yield failure in the footwall as shown in Figure 5.7. Joint set 3 is considered to be a lateral release plane for the failure modes indicated in Figure 5.7. This was also the observed method of slough for the majority of stopes at Ruttan.

Toppling or slabbing from the hangingwall is generally the observed method of instability at Ruttan. The parting is along a foliation of joint surface that parallels the ore lens. The observed failure mode is simulated by Figure 5.8. This is a base friction model of which the dimensions and failure geometry typifies the observed conditions for stopes at Ruttan.

5.4 OBSERVATIONS/CONCLUSIONS

This chapter summarized the characteristics of the rock fabric identifying the possible failure modes. Structural instability is evident through toppling on joints sets paralleling the stope contact and resting on flat cross-cutting joints. Further investigations will be based upon the conclusion that:

* the hangingwall and footwall for a particular stope is in a relaxed state;
* failure due to structural instability is a possible mechanism.

Table 5.1: Core Logging Format - Ruttan

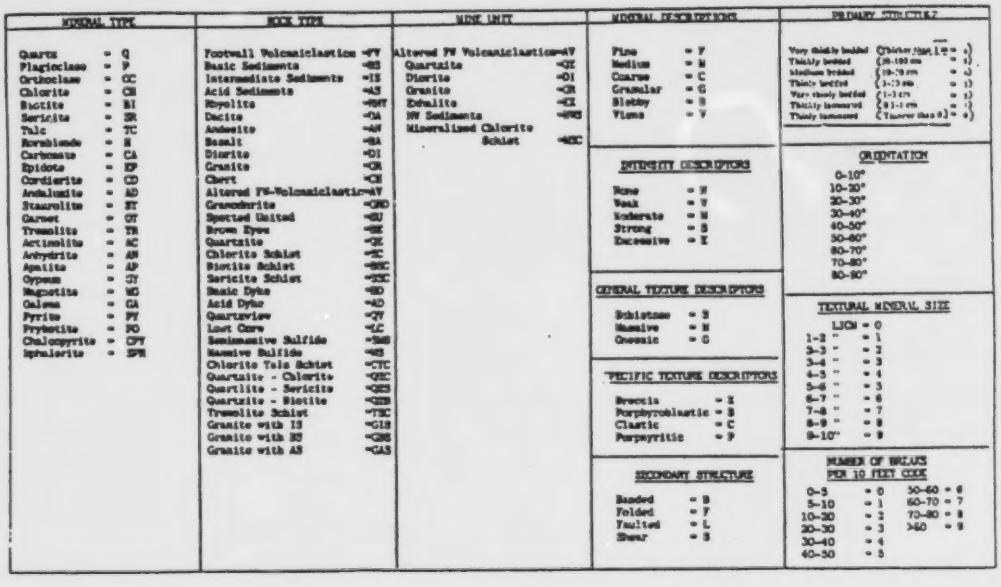

Old Format (Prior 1983)

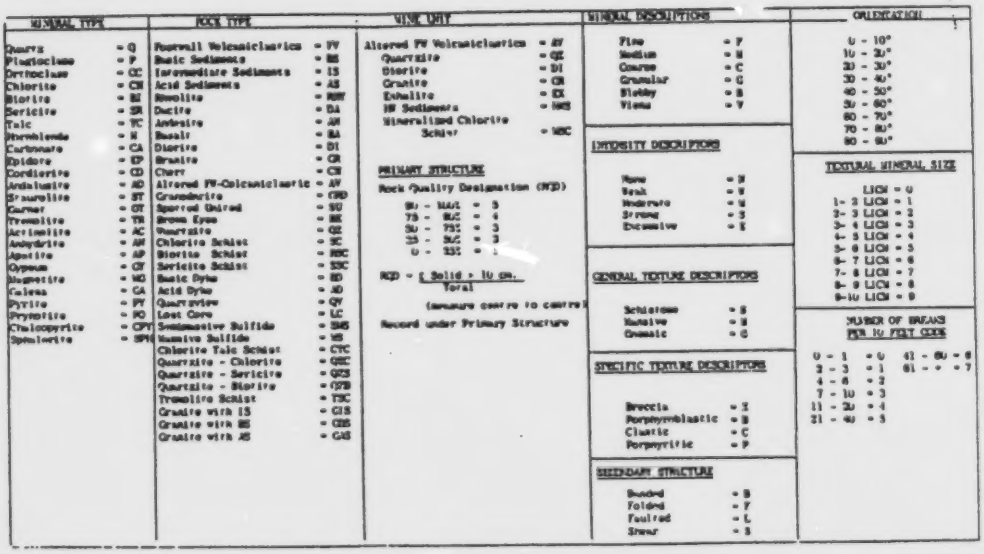

New Format (Post 1983)

Point Load Strength Values Recorded on Both Formats

Table 5.2: Intact Rock Strength Parameters

Rock Type	Uniaxial Compressive Strength (MPa)	Poisson's Ratio	Modulus of Deformation (GPa)	Number of Samples
Semi-Massive Sulphide-Chlorite	70 ± 24	0.23 ± 0.05	66 ± 19	13
Massive Sulphide	89 ± 37	0.2 ± 0.08	88 ± 37	39
Basic Dyke	202 ± 66	0.2 ± 0.07	81 ± 14	10
Acid Seds.	135 ± 43	0.19 ± 0.07	77 ± 19	6
Quartzites	113 ± 49	0.12 ± 0.06	54 ± 23	4
Chlorite Schists	49 ± 11	0.34 ± 0.12	50 ± 17	14
Chlorite Talc Schists	25 ± 14	0.33 ± 0.09	39 ± 9	13

Table 5.3: Summary of Rock Mass Parameters

ROCK TYPE	OBSERVATIONS			Is_{50}*	RQD(%)	SPACING (m)
	FW	Ore	HW**			
CTC(7)	5	-	2	<1	25 ± 8	.16 ± .2
SC(31)	17	-	14	2.1 ± 1.1	47 ± 19	.97 ± .7
QTZ(34)	16	-	18	4.8 ± 1.9	69 ± 18	1.4 ± .8
AS(8)	1	-	7	3.9 ± 1.8	68 ± 22	1.2 ± .7
BD(6)	3	-	3	5.3 ± 2.6	70 ± 20	1.1 ± .7
MS(63)	12	41	10	2.9 ± .9	82 ± 10	1.7 ± .8
SMS-SC(9)	-	9	-	1.6 ± .6	48 ± 13	.88 ± .7
SMS-BD(1)	-	1	-	6.0	68	1.3
SMS-QTZ(1)	-	1	-	3.0	70	1.6
SMS-CTC(2)	-	2	-	1.5 ± 1.	44 ± 24	.3 ± .3
	(54)	(54)	(54)			

* Unconfined Compressive Strength Is_{50} x 24 (Smith, 1981)

** Refers to Number of Stope Walls Affected

( ) Sample Size

STOPE: _____

CLASSIFICATION PARAMETERS AND THEIR RATINGS

PARAMETER			RANGE OF VALUES				
1	strength of intact rock material	point load strength index	> 8 MPa	4-8 MPa	2-4 MPa	1-2 MPa	for low range, ucs test preferred
		uniaxial compressive strength	> 200 MPa	100-200 MPa	50-100 MPa	25-50 MPa	10-25 | 3-10 | 1-3 MPa
	rating		15	12	7	4	2 | 1 | 0
2	drill core quality, RQD		90-100 %	75-90 %	50-75 %	25-50 %	< 25 %
	rating		20	17	13	8	3
3	spacing of joints		> 3m	1-3 m	0.3-1m	50-300 mm	< 50 mm
	rating		30	25	20	10	5
4	condition of joints		v rough, not cont. no separ. hrd. jn. wall rock	slt. rough surf. separ. < 1mm hrd jn. wall rock	slt rough surf. separ. < 1mm slft jn. wall rock	slk. surf. gauge < 5mm, jn open 1-5 mm, cont jn	slf gauge > 5mm jn open > 5mm cont jn
	rating		25	20	12	6	0

ROCK MASS RATING

	FOOTWALL	ORE	HANGING WALL
STRENGTH			
R.Q.D.			
SPACING			
CONDITION			
TOTAL			
MAJOR STRUC. COMMENT			
ROCK TYPE			
HOLE NUMBER			
SECTION			

CLASSIFY
ISOLATED ___
RIB ___
ECHELON ___

DIMENSIONS

LEVEL	SPAN	WIDTH

HEIGHT: _____

BLASTING: _____

OPEN GROUND
(sketch/fill)

VOLUME, m^3

EXCAV. RATE (x1000 m^3/mth)	5,000	10,000	20,000	30,000

RATING

F.W.	ORE	H.W.
___	___	___

Figure 5.1: Stope Characterization

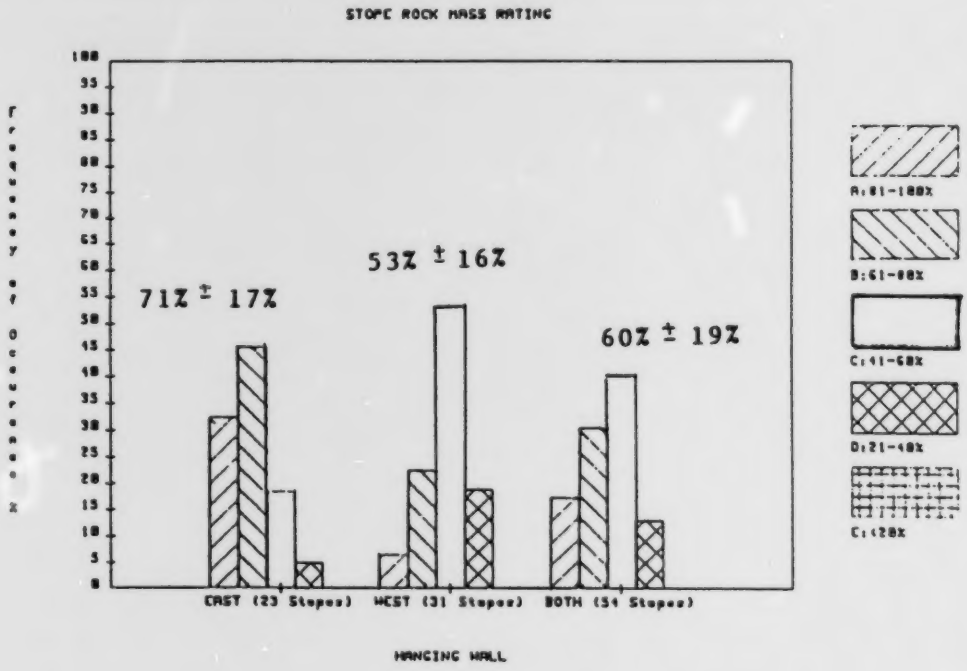

Figure 5.2: Rock Mass Distribution

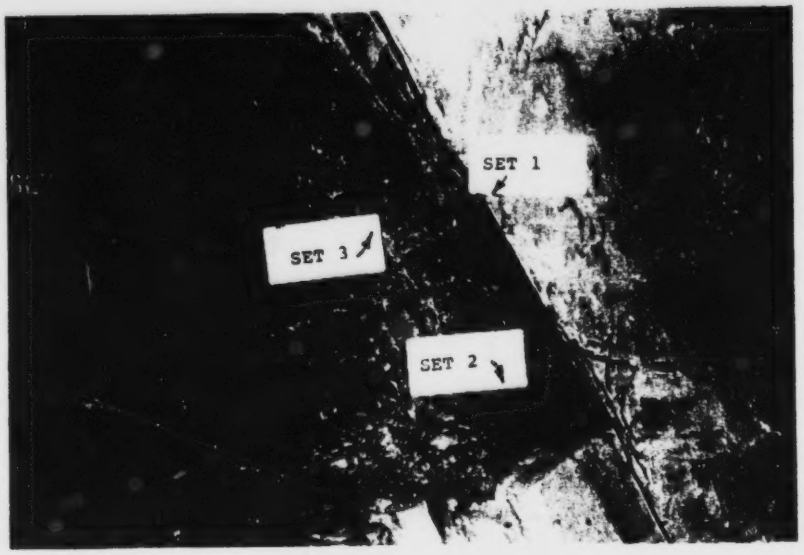

HANGING WALL

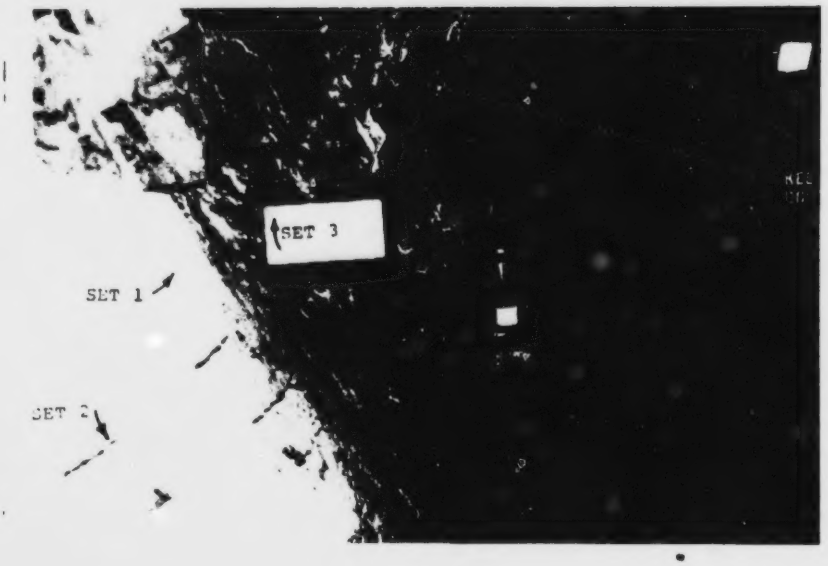

FOOTWALL

Figure 5.3: Photographs Identifying the Major Sets at Ruttan

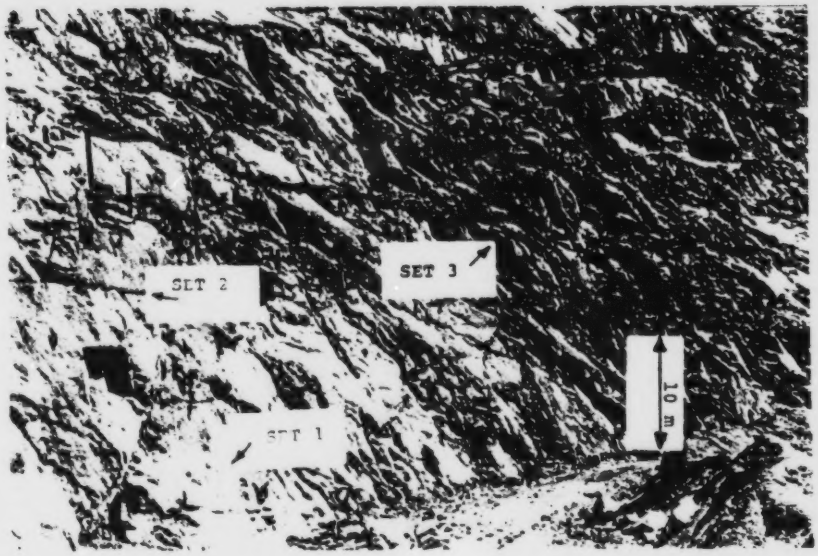

Figure 5.4: Photograph Showing the Continuity of Structure

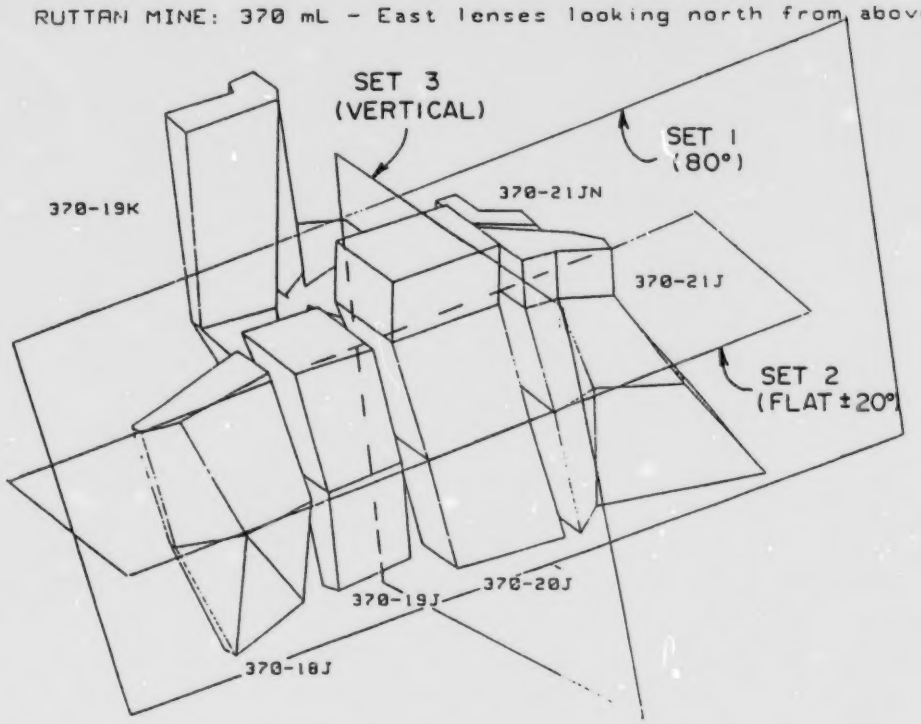

Figure 5.5: Design Sets

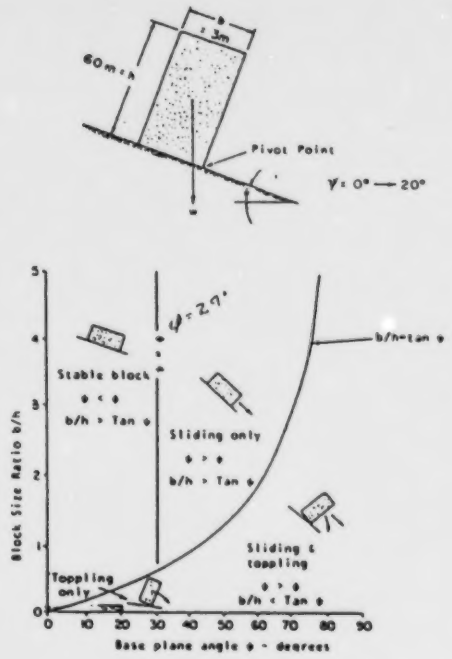

Figure 5.6: Conditions for Sliding and Toppling of a Block on an Inclined Plane **(Hoek and Bray, 1977)**

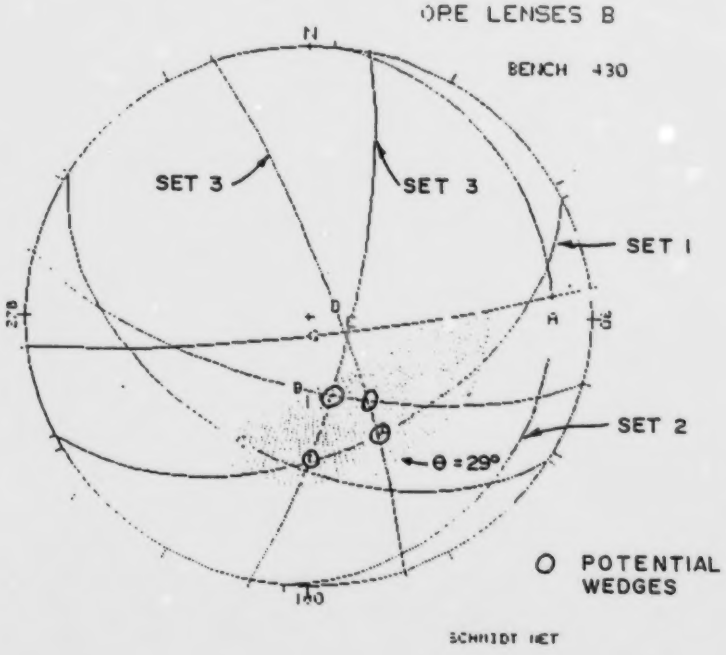

Figure 5.7: Stereonet Showing the Potential for Failure in the FW of the "B Lenses" on the 430 m Level

Figure 5.8: Base Friction Model

CHAPTER SIX
DILUTION

6.1 INTRODUCTION

This parameter is a measure of the quality of the stope design. Various definitions exist, however, it is a parameter recorded by most open stope operators. Chapter 3.4. Dilution will be considered as the dependent control variable. The significance of the individual stope characteristics will be evaluated empirically in terms of dilution. Dilution figures from forty-three stopes will be analysed at various stages of extraction yielding 432 dilution values. These values are subsequently averaged into 133 observations.

6.2 DEFINITION

Various definitions exist as indicated in Chapter 3.4. Dilution has a direct affect on profitability (Kersten, 1983) and stope scheduling. The calculation of a diluted geological ore reserve at Ruttan has been historically determined in the following manner. As each mining block is defined, a certain amount of dilution is attributed to the block, this being one meter of the footwall and 1.8 meters in the hangingwall (historic method). These numbers have no theoretical basis, but reflect the fact that because of the 70 degree dip of the orebody, most of the dilution is attributed to the hangingwall. This width of dilution divided by the width of the ore reserve block gives a volume percentage of dilution. This value is then converted to tonnes dilution which when divided by in-situ tonnes of ore for the block, gives a weight percentage of dilution. This weight percent external dilution is then combined with other blocks forming the reserve for a given stope and an average weight percent dilution is then determined. Consequently, prior to mining, one has an estimated dilution attributed to each stope. At the end of the stope life, an actual dilution figure based on the history of mining of that stope is required in order to properly reconcile it back to the original ore reserve. This is achieved by visual observation of each producing stope on a daily basis by grade control geologists.

A visual interpretation of the volume percentage of massive sulphide, semi-massive sulphide, disseminated material and dilution based on iron content is made for each producing drawpoint. Dilution is classified as anything with less than 10% iron or less than 1% copper. It can be classified as either internal or external to the ore reserve. Based on prior knowledge of the rock types inherent to a particular stope, the size of muck and/or the presence of blast holes within the muck, the geologist can estimate what percentage of the dilution is internal or external. These visual estimations are compiled at the end of each month and a total average

dilution figure for internal and external dilution is derived. The external dilution is converted to a weight percent as follows:

> Dilution Weight % = (Dilution Volume % x Tonnage Factor for Ore/Tonnage Factor for Waste)/(100-Dilution Volume % x Tonnage Factor for Ore/Tonnage Factor for Waste)

An average weight percent for the external dilution is determined for a particular stope life. This enables the geologist to reconcile back to the original ore reserve estimation and therefore determine subsequent mining losses. This method has been employed at Ruttan since 1979.

The "rule of thumb" quantity of 1 meter and 1.8 meters of wall slough is employed irrespective of depth, rock quality, stope configuration or stope width. The dilution, as estimated in terms of ore reserve weight, enables the operator to quickly assess the amount of material mined external to the ore. It is a more meaningful value than a volume dilution in that the variability of ore density is incorporated into the definition. This definition will be employed for the purpose of this study.

It is important to comment on the accuracy of the procedure. Dilution is an observed parameter that has been recorded in most instances on a daily basis for each drawpoint. The frequency of observation and the consistency of measurement has produced a figure that is a reliable measure of the waste tonnage that comes from a particular stope. In addition to the dilution being observed, the copper and zinc grades are estimated on a monthly basis for each producing stope. They are determined from grab samples, drill hole assays and from the observed dilution. The observed grades were found to be historically within 3% of milled grade (1979 - present). Dilution evaluated solely on a grade basis would yield:

$$\text{Dilution } (\%) = (Go - Gm)/(Gm - Gd)$$

where: Go - is the grade of undiluted ore
Gm - is the grade of tonnage milled
Gd - is the grade of dilution

The problem associated with this method is in determining the value "Go and Gd". Presently, work is being conducted in better estimating the two grades on a monthly basis and relating the value to the observed dilution. In addition, sonic probes are being developed by Ruttan/UBC in enabling the operator to profile the void created. It is assumed that the accuracy of grade observation extends to that of dilution estimation since one has an effect on the other. However, the dilution

approach at Ruttan is valid for Ruttan and the absolute values must be calibrated for other operations intending to employ this methodology towards stope design.

6.3 OBSERVED DILUTION

The following outlines the method employed in determining the resultant dilution at various stages of stope extraction. As mentioned, the observed dilution is a measure of the external waste for a particular stope and can be defined as shown in Figure 6.1. Dilution measurements are recorded daily and tabulated monthly as indicated previously. This is subsequently converted by the author into a given volume of stope excavation exhibiting a particular level of dilution. Monthly tabulations are made and plotted as shown in Figure 6.2 for a particular stope. The cumulative dilution is recorded versus the volume extracted. This volume excavated is determined through recording the trammed tonnes for a particular stope.

The volume drawn is related to the volume excavated since it is general practice at Ruttan to:

* Muck evenly from all drawpoints. This is required in order to ensure that the dilution is evenly distributed, i.e. the dilution values recorded are representative for the void mined. By shutting down a drawpoint, one would bias the dilution estimates.

* Muck all stopes until empty, thereby ensuring a free-face for the subsequent blast. Normally a maximum lag time between tonnes blasted and mucked is two months. The undercut may be full, therefore the blasted reserves may not exactly be related to the dilutions determined for the tonnes trammed.

The volume associated with the resultant dilution was estimated in this manner rather than employing blasted reserves, in that the dilution estimate is directly related to the tonnes drawn and/or the void created. It is not necessarily related to the tonnes blasted especially if not all the blasted reserves have been trammed.

The incremental dilution (%) is a measure of the amount of wall slough over an increment of excavated volume. Figure 6.2 depicts the resultant incremental dilution for successive mining intervals that are equivalent to 10% of the total stope reserve volume. It graphically shows that as the stope is initially excavated, i.e. first 10% of ore volume removed, the dilution is low. However, when the stope is almost completely excavated (80%), for an additional 10% of stope volume removal, the dilution associated with that 10% volume has increased to 16%.

This incremental dilution will be employed subsequently in estimating blast induced damage, error in estimation and other factors that are difficult to quantify.

6.3.1 VOLUME TRAMMED VERSUS STOPE DIMENSIONS MINED

Stope span was determined by employing either of two methods:

* Method 1: Average span recorded from stope longitudinal, Figure 6.4.

* Method 2: Average span back calculated from the volume trammed, Figure 6.5, whereby:

  Inferred Span = (Volume Trammed)/(Vertical Stope Height x Apparent Stope Width), Figure 6.5.

Generally, when intermediate levels are employed, the stope was blasted for the full stope height and width, Figure 2.15. Prior to January, 1983, ITH stopes were benched, Figure 2.16, where after they were blasted for the full stope height. Method 2 would be a poor approximation for benched stopes. It is true that the benched stopes were blasted for the full stope width, however the stope height was variable. In employing method 2, calculation of the span would be underestimating the true span by employing the final stope height. This affected eight (8) stopes in our database of forty-three (43). The stope extraction profile could be reproduced for these stopes prior to 1983. These stopes were included within the database by recording solely the final stope geometry and the resultant overall dilution.

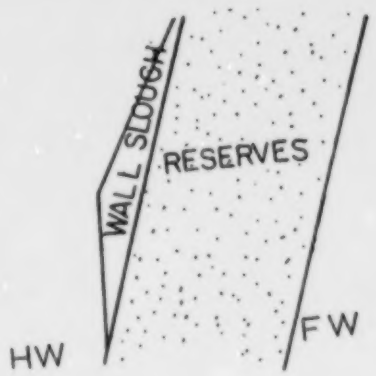

$$\text{Dilution} = \frac{\text{Wt. wall slough}}{\text{Wt. reserves}} \times 100$$

Figure 6.1: Definition of Dilution

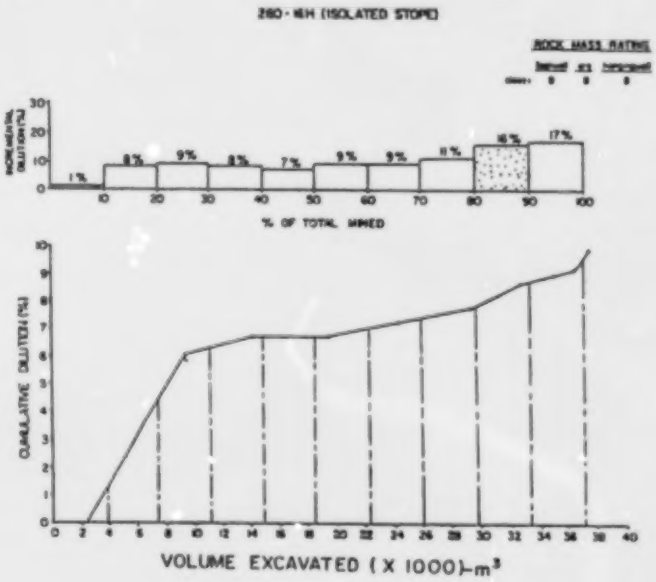

Figure 6.2: Cumulative Dilution vs Volume Excavated

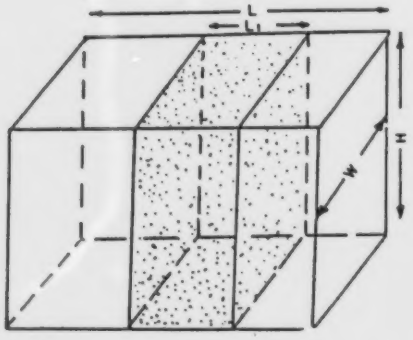

Figure 6.3: Volume Trammed = L1 x W x H

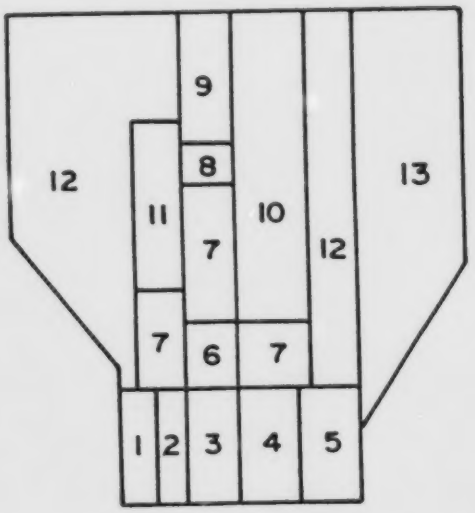

Figure 6.4: Longitudinal Showing a Typical Extraction Sequence

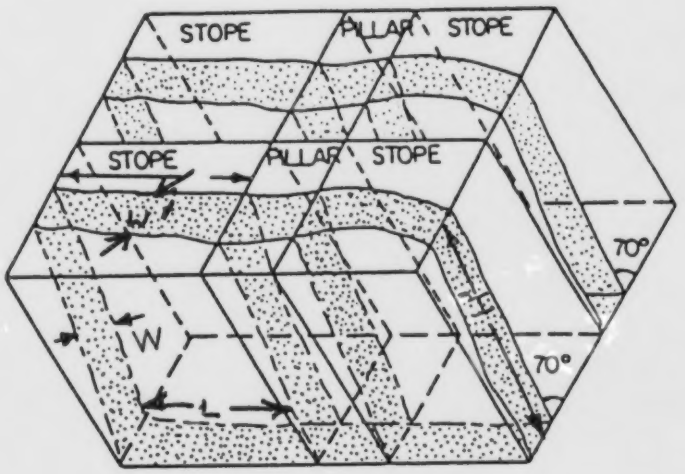

Figure 6.5: Inferred Measurement of Stope Span

$$\text{Stope Volume} = H \times W' \times L$$
$$\text{Stope Volume} = H' \times W \times L$$

where:

H' = Apparent Stope Height in Plane of Hanging Wall
W = True Stope Width
L = Stope Span
W' = Apparent Stope Width Measured in Horizontal Plan
H = Vertical Stope Height

CHAPTER SEVEN
DATABASE

7.1 INTRODUCTION

This chapter identifies the most critical parameters as determined through single and multivariate statistical analysis. Trend surface analysis has been used to summarize data that is too numerous to be grasped readily by eye. Linear correlations between variables as defined by Spiegel, 1972 were employed initially to determine the relationship between the most critical parameters in order to formulate a governing empirical relationship. A section describing the statistical technique is briefly presented which will outline the general concept employed in arriving at a statistically significant relationship.

The identification of the parameters formulating the database are reproduced, which will be subsequently analysed in determining the most critical parameters in terms of their effect on dilution. The blast correction factor will be discussed in detail since it forms an all encompassing term which will partly compensate for recording error and any blast induced damage. The critical parameters will subsequently incorporated into a governing equation in Chapter 8 which will analyse further the significance of stope configuration.

7.2 STATISTICS

In order to assess the suitability of individual sample populations to be described by an appropriate function, multivariate statistical methods were employed. This analysis has been used to describe data that is too numerous to be visually analysed. This allows values to be predicted along with a quantitative appraisal of the reliability of the prediction.

Koch (1980) suggests that selecting a suitable model depends on "taste, judgement and luck". It is also suggested that the predictive model be chosen in relation to the database available. A simple model such as a linear or quadratic polynomial or fourier series may be useful if the database is well defined and local variability is low and well controlled. A sufficiently complicated function will fit any given set of data, however, this function is not unique (Koch, 1980). Therefore, one should not employ multivariate statistical analysis with the hope of generating increasingly more complicated functions with the goal of identifying a "correct predictive relationship".

This chapter employs multivariate linear correlations between the control parameter "dilution" and the parameters influencing the control parameter. Initially linear correlations between two parameters, i.e. Dilution and Area, will be assessed and subsequently a curve to a plane will be fitted and extended to a linear hyper-surface. This form of expression exhibits a linear variance between the dependent and independent variables employed. They may be reproduced as follows:

$$\text{Dilution } (\%) = A + B(x) \text{ line}$$
$$\text{Dilution } (\%) = A + B(x) + C(y) \text{ plane}$$
$$\text{Dilution } (\%) = A + B(x) + C(y) + D(w) + \ldots \text{ linear hyper-surface}$$

where:

Dilution - Independent parameter
A,B,C,D, - Constants
x,y,w - Dependent parameters

The next most complicated expression will be attempted, Chapter 8, which is a quadratic surface. It is expressed as follows:

$$\text{Dilution } (\%) = A + B(x) + C(x^2) \text{ quadratic line}$$
$$\text{Dilution } (\%) = A + B(x) + C(x^2) + D(y) + E(y^2) + F(xy) \text{ quadratic surface}$$

This section will briefly outline the statistical concepts employed. The reader is referred to Koch (1980) for a more detailed treatise on this topic.

7.2.1 DEFINITION OF STATISTICAL TERMS

Multivariate analysis attempts to relate independent parameters to the dependent parameters, in terms of a relationship expressed in mathematical form, by determining an equation connecting the variables. A first step is the collection of data showing corresponding values of the variables. Figure 7.1 shows how a curve is fitted to a "scatter diagram". In order to avoid individual judgment in constructing lines, parabolas, or other approximating curves, it is necessary to agree on a definition of a "best-fitting curve". In Figure 7.1 the independent parameter is "x" and the dependent is "y" (dilution). The goodness of fit is determined by the deviation of the "y predicted" from the "y observed" parameter (yl). Consequently, where the following relation is a minimum, one arrives at the best fit curve defining the relationship between the variables:

$$d1^2 + d2^2 + \ldots + dn^2 = \text{a minimum}$$

where:

$$dn = (\text{y predicted}) - (\text{y observed})$$

A curve approximating the data in Figure 7.1 is said to fit the data in the least-squares sense and is called a least-squares line, curve or surface. The dependent parameter, in the context of this study, is defined as dilution and is also the control parameter.

The independent parameters, among others, are areas, rock quality, exposure rate and stope configuration. The least-squares line approximating the set of points (xl,yl), ..., (xn,yn) has the equation "y = A + Bx" where the constants "A" and "B" are determined by simultaneously solving the equations:

Least Squares Line

$$\begin{aligned} y &= A + B(x) \\ \Sigma y &= An + B\Sigma x \\ \Sigma xy &= A\Sigma x + B\Sigma x^2 \\ (n &= \text{number of observations}) \end{aligned}$$

Similarly, the least squares plane, hyper-surface and quadratic surfaces are also determined from the "normal" equations represented below:

Least Squares Plane

$$\begin{aligned} z &= A + Bx + Cy \\ \Sigma z &= nA + B\Sigma x + C\Sigma y \\ \Sigma xz &= A\Sigma x + B\Sigma x + C\Sigma xy \\ \Sigma yz &= A\Sigma y + B\Sigma xy + C\Sigma y^2 \end{aligned}$$

Least Squares Quadratic Line

$$\begin{aligned} z &= A + Bx + Cx^2 \\ \Sigma z &= nA + B\Sigma x + C\Sigma x^2 \\ \Sigma xy &= A\Sigma x + B\Sigma x^2 + C\Sigma x^3 \\ \Sigma x^2y &= A\Sigma x^2 + B\Sigma x^3 + C\Sigma x^4 \end{aligned}$$

Least Squares Hyper-Surface

$$
\begin{aligned}
z &= A + Bx + Cy + Dw + Et \\
\Sigma z &= nA + B\Sigma x + C\Sigma y + D\Sigma w + E\Sigma t \\
\Sigma xz &= A\Sigma x + B\Sigma x^2 + C\Sigma yx + D\Sigma wx + E\Sigma tx \\
\Sigma yz &= A\Sigma y + B\Sigma xy + C\Sigma y^2 + D\Sigma wy + E\Sigma ty \\
\Sigma wz &= A\Sigma w + B\Sigma xw + C\Sigma yw + D\Sigma w^2 + E\Sigma tw \\
\Sigma tz &= A\Sigma t + B\Sigma xt + C\Sigma yt + D\Sigma wt + E\Sigma t^2
\end{aligned}
$$

Least Squares Quadratic Surface

$$
\begin{aligned}
z &= A + Bx + Cy + Dx^2 + Fxy \\
\Sigma z &= nA + B\Sigma x + C\Sigma y + D\Sigma x + E\Sigma y + F\Sigma xy \\
\Sigma xz &= A\Sigma x + B\Sigma x^2 + C\Sigma xy + D\Sigma x^3 + E\Sigma y^2x + F\Sigma x^2y \\
\Sigma x^2z &= A\Sigma x^2 + C\Sigma x^2y + D\Sigma x^4 + E\Sigma y^2x^2 + F\Sigma x^3y \\
\Sigma yz &= A\Sigma y + B\Sigma xy + C\Sigma y^2 + D\Sigma x^2y + E\Sigma y^3 + F\Sigma xy^2 \\
\Sigma zy^2 &= A\Sigma y^2 + B\Sigma xy^2 + C\Sigma y^3 + D\Sigma x^2y^2 + E\Sigma y^4 + F\Sigma y^3x \\
\Sigma zxy &= A\Sigma xy + B\Sigma x^2xy + D\Sigma x^3y + E\Sigma xy^3 + F\Sigma x^2y^2
\end{aligned}
$$

A correlation coefficient measures how well a predicted surface will fit the sample data. It is calculated as follows:

$$
r^2 = \frac{\Sigma(y\ est - \bar{y}\ obs)}{\Sigma(y\ obs - \bar{y}\ obs)} = \frac{\text{Explained Variation}}{\text{Total Variation}}
$$

where:

$$
\begin{aligned}
y\ est &= \text{predicted value of independent parameter} \\
\bar{y}\ obs &= \text{mean value of the observed independent parameter} \\
y\ obs &= \text{value of the observed independent parameter}
\end{aligned}
$$

The value r^2 can be interpreted as the fraction of the total variation which is explained by the least-squares regression line. "R" measures how well the least-squares regression line fits the sample data. If the total variation is entirely explained by the regression line, i.e. $r = +1$, it is said that there is perfect correlation. If the total variation is entirely unexplained, then the explained variation is zero and so "$r = 0$". In practice, the quantity of "r" lies between "0 and 1". A correlation coefficient of -0.81 indicates that 66% (110 x)-.81)) of the variability of the control (dilution) parameter is explained by the fitted relationship.

A correlation of -.27 indicates that only 7% of the variability is explained by the fitted relationship. The deviations "y est - y obs" follow a definite and predictable pattern.

The above concepts can be generalized to more variables. Since the multiple correlation coefficient, as defined previously, is not evaluated in terms of the independent parameters but only by the control and estimated control parameter.

A further important parameter describing the best fit curve or estimate of the dilution parameter is determining the "confidence levels" for the regression curve. A measure of the scatter of the estimated dilution parameter (y est) for a given value of x1, x2, ... xn is determined as follows:

Unbiased Standard Error of Estimate of y on x

$$Sy.x = \sqrt{\frac{\Sigma(y\ obs - y\ est)^2}{N}}$$

where:

n = number of sets of observations
N = number of degrees of freedom
i.e. y.x. then N = n - 2
y.x.t then N = n - 3

This value is called the standard error of estimate of the predicted dilution given the independent variables from which it was calculated. It is inherent of the definition of the least squares regression curve that the difference between the observed and predicted (z - z est) dilution be a minimum. This will result in the smallest standard error of estimate than for any other possible regression curve.

The standard error of estimate has properties analogous to those of standard deviation. Constructing a pair of lines parallel to the regression line of y on x at respective vertical distance Syx, 2Syx and 3Syx from it, and if "n" is large enough, then there would be included between these pairs of lines about 68%, 95% and 99.7% of the sample points respectively, Figure 7.2. This assumes that the sample population is large and does not require one to estimate the normal distribution of the population by means of the "t" statistic. For Sample sizes exceeding thirty (30), it is called a large sample, and can be approximated by a normal distribution and the approximation will improve with increasing "n". For samples of size "n" less than thirty (30), called small samples, this approximation is not as desirable and worsens with decreasing "n". This requires that "small sampling theory" be employed. The above definition for unbiased standard error of estimate for the population is

satisfactory for sample sizes exceeding thirty (Spiegel, 1972). This is the situation for the Ruttan database.

A further statistical test must be introduced - the "level of significance". This test is required in order to determine that the correlation values that have been calculated, have not done so by chance. This involves hypothesis testing, whereby one is able to determine whether the value of the correlation coefficient found for a sample has arisen from a normal universe. A normal universe is characterized by having a correlation coefficient of zero. Associated with a sample correlation coefficient is distribution. It is therefore important to determine whether achieving a population correlation coefficient of zero is entirely possible, given the spread of the sample results. This requires that the sample correlation distribution be approximated by a "t" distribution. The probability must then be determined that the standardized distribution, which represents the population correlation coefficient, exceeds zero at a given significance level. Values of correlation coefficients for different levels of significance and degrees of freedom are shown in Table 7.1. This table shows the probability if error in accepting a sample correlation as significant when it should have been rejected. Generally statisticians adopt the terminology results that are: (Spiegel, (1972).

* significant at the 0.01 level are "highly significant";
* significant at the 0.05 level but not the 0.01 level are "probably significant";
* significant at levels larger than 0.05 are "not significant".

7.3 DISTRIBUTION OF DATABASE

Figure 7.3 shows the distribution of the data formulating the Ruttan database. Forty-three (43) stopes were assessed from a total of forty-six (46) since the commencement of mining. It was intended to incorporate all stopes at Ruttan and not to bias the results by a selection procedure. The stopes that were not selected were:

* 320-19B, a shrinkage-type of stope. i.e. entire stope blasted then tramming commenced. Consequently, trammed dilution is not related to void created.
* 370-14D, a shrink stope.
* 370-11D, a mine development problem caused premature stope shutdown.

Tables 7.2a,b,c, identify the individual parameters for each isolated, en echelon and rib stope configuration. An observation consists of the following:

1) Number of Observation

2) Stope Name

This is defined by the draw level, the stope number and a lens describer (letter).

3) Rock Mass Rating [RMR(%)]

This is defined for the critical wall contact. It normally refers to the hangingwall classification.

4) Stope Height [ht. (m)]

This is a measure of the apparent stope height (H') as defined in Figure 6.5.

5) Stope Width [Wdth. (m)]

This is a measure of the true stope width (W) as defined in Figure 6.5.

6) Stope Volume [Vol. (m^3)]

This is a measure of the volume of reserves mined. Observation points were selected at intervals of volume yielding 5000m^3, 10000m^3 and subsequently in 10000m^3 intervals.

7) Dilution [Dil. (%)]

This parameter was calculated as described in Chapter 6. It was interpolated from plots of "cumulative dilution" versus "volume extracted", Figure 6.2. The interpolation procedure is actually a summary of monthly observations recorded throughout the stope excavation history. For example, the isolated stope database consists of twenty-two (22) stopes, yielding sixty-one (61) observations which are based upon 200 recordings. This value is recorded as the total cumulative dilution for the stope volume extracted. It has been corrected for the dilution that is recorded at the time of "slot blasting". This will be described subsequently, however, the control parameter has been corrected by subtracting the "blast correction factor "4" from the observed cumulative dilution. The value recorded in Table 7.2 represents the dilution for a particular volume of mine reserves. The total dilution, however, is actually the recorded value plus the wall slough attributed to slot excavation.

8) Span [m]

This represents the stope span for the volume of reserves removed. It has been determined as outlined in Chapter 6.3.1.

9) Hydraulic Radius [m]

This value has been employed throughout the literature by authors who have conducted work in the field of empirical stope design, Laubscher (1976), Mathews et al (1981). It was employed to determine if it would be a critical parameter in relating the exposed surface area to the control parameter. It is a fluid mechanics term (Vennard and Street, 1975) that has been extended to describing the ratio between the exposed surface area/exposed surface perimeter. Mathews has coined this term as the "shape factor" and it is reproduced in Figure 7.4. It is employed to distinguish between one way spanning situations where one dimension is particularly large with respect to the other. It is shown by this figure that when the long to short span exceeds approximately 4:1, the change in the hydraulic radius is minimal. It is for these geometries that Mathews and Laubscher were particularly trying to distinguish. The initial premise was that a one way spanning situation (i.e. tunnel having an exposed surface area of 1000m^2 or 100 meters long by 10 meters high) is more stable than a stope wall of which long and short dimensions are similar (32 meters long by 32 meters high). This was shown empirically, by both Laubscher and Mathews, to be true. Narrower openings would tend to add a degree to confinement and/or inhibit the occurrence of exposed structures. The hydraulic radius was determined for the Ruttan study in an attempt to relate the results to a wider database as compile by previous researchers. It is generally the case for open stoping operations that the hangingwall and footwall surfaces are two-way spanning. It is unlikely that the span ratios would exceed 4:1. This was the case at Ruttan where average span ratios ranged from 1:1 to 3:1. The exposed surface area was also calculated from the span and stope height and correlated to the control parameter.

10) Exposure Rate [m^2/mth]

This value refers to the rate of excavation for a particular stope. It is expressed, initially, as the volume excavated per month, Figure 6.3. The exposure rate is subsequently calculated as the rate at which the hangingwall or footwall area is exposed. It is expressed as the surface area exposed per month. An example is shown in Figure 6.3 whereby, for the first three

months of mining, the shaded area shown in Figure 6.3 has been extracted, consequently:

Rate of Excavation = L1 x h x W/(3 mths.) = Volume/3 mths.
Exposure Rate = L1 x H/(3 mths.) = Exposed Surface Area/3 mths.

or alternatively:

Exposure Rate = Rate of Excavation/Width

where:

Width (W) is measured perpendicular to strike and refers to the true stope width.

11) Blast Correction Factor [BCF, % Dilution]

It was found that an initial dilution was present at lower volumes of excavation. This value was higher for stopes exhibiting a lower rock mass quality. Figure 7.5 shows the effect of stope configuration on the extent of the zone of relaxation. A slot is initially excavated from footwall to hangingwall which has the dimensions shown in Figure 7.5. The slot excavated exposes a minimal wall contact under the most favourable confining conditions. Generally the slot is 3.7 meters x 3.7 meters for sub-level stopes and 6.1 meters x 6.1 meters for ITH stopes, extends for the full stope height and is subsequently slashed for the full stope width. This initial dilution was analysed separately from the dilutions observed subsequently. It is generally assumed by Ruttan that dilution in the slot area is negligible and if present, is due to blasting. This dilution is then assumed to be constant over the remainder of the stope life, since the blast practice does not change. Subsequent sections will evaluate the significance of incorporating this correction to the database. This initial value was subtracted from the subsequent dilution figures recorded to result in a corrected dilution reading. This factor would also tend to compensate for observation error in estimating dilution, since this value should also remain constant for a given stope.

Figure 7.6 shows that the incremental dilution is fairly constant until 30% of the stope has been excavated. The slot generally encompasses a volume of 2500m^3 - 3000m^3. The incremental dilution shows that 7% is constant for the first 3000m^3, after which, it increased and will be subsequently shown to be directly correlated to the enlarged surface area exposed due to mining. Blast

damage for 270 Z-Zone is assessed at 7%. This value is generally between 0 - 3%. It has been systematically recorded for the stopes in the calibrated database as the dilution resulting from the slot area. The slot dilution was calculated as shown above employing incremental dilution estimates and relating the value to the slot area exposed. Figures 7.7, 7.8, 7.9 summarize the parameter distribution that forms the Ruttan Database for the isolated, en echelon and rib configurations respectively. A statistical evaluation for the relevant parameters analysed for each individual configuration and for the total database is shown in Table 7.3. A mean and a standard deviation is recorded for each parameter outlined in Figure 7.7, 7.8, 7.9 and Table 7.3. The average dilution for the forty-three (43) isolated stopes is 10%, whereas the average dilution as derived from the intermediate geometries (133 observations) is only 6%. In order to describe the database, one has to look at the individual observations for the final and intermediate stope geometries. It is important to know the limitations of any empirically derived formulation, since it is only as accurate as its database. Extrapolating the observations beyond the observed quantities may have a poorer chance of prediction.

7.4 IDENTIFICATION OF CRITICAL PARAMETERS

The observations recorded in Tables 7.2 a,b,c, form the basis for the selection of the parameters which have the greatest effect on the control variable "dilution". Initially, dilution was correlated by applying a linear regression analysis to the parameters outlined in Figure 7.10. The dilution sensitive parameters were evaluated with respect to the isolated database, thereby ensuring that stope configuration would not bias the resulting correlations. The mutual correlations were as follows:

a) Rock Mass Rating

The individual parameters which combine to form the "Rock Mass Rating" were analysed with respect to the control parameter for the isolated database. The database is shown in Table 7.4. A statistically significant correlation coefficient must exceed 0.295 given "n-2" degrees of freedom (61-2=59). Individually, each coefficient is not statistically significant, Figure 7.11. The highest correlation was obtained between the RQD and dilution (r=.24). The statistical test is true in the same sense that it would select or rank the most critical parameters assuming that the other parameters would not overly bias the correlation. In order to isolate the effect of the other parameters, such as the exposed surface area, multivariate analysis must be employed. This would enable the resultant marginal increase in the overall "best fit" expression to be assessed, Figure 7.10. Grouping all the parameters that

combine to form the "Rock Mass Rating" results in a multiple correlation of 0.3. Relating the RMR value with dilution results in an increased significant correlation of +0.36, Figure 7.10. Consequently, the RMR is selected as a parameter that will reflect the importance of rock quality on dilution. This is not to imply that the NGI system will not be an equal or even better correlative parameter. The RMR was chosen due to its compatibility to the method of data gathering employed at Ruttan. Incorporating "Exposed Surface Area" with the individual RMR parameters indicates that they would all improve the mutual correlation that exists with dilution and area alone. A third criteria for selection of critical parameters is described. The difference between a correlation of 0.71 and 0.73 is not statistically different at the 95% significance level (Koch, 1983) and should be treated jointly, however, in order for the difference to be statistically significant, the correlations would have to generally differ by 0.20 for the isolated database. The approach taken by the author is to define the most significant parameters "Primary Parameters" and to group the remaining into a linear or quadratic equation that would yield the highest correlation coefficient. A second criteria was the "Criteria for Sensitivity". In order for a parameter to be classified as being dilution sensitive, it must pass the test outlined in Figure 7.12. The governing equation will incorporate the most dilution sensitive and correlative parameters.

b) Stope Dimensions

The best fit parameters were that of exposed surface area, hydraulic radius and span. A mutual correlation between area exposed and hydraulic radius yielded a correlation of +0.96 and the following expression:

$$\text{Area}(m^2) = 460 + 250[\text{Hydraulic Radius}(m)]$$
$$r = +.96 \quad s = \pm m^2$$

Among the three parameters investigated, hydraulic radius and area resulted in higher correlations, Figure 7.10. The primary parameter "Area" will be employed rather than hydraulic radius, due to the high correlation that exists between the two. However, a governing equation in terms of hydraulic radius will also be generated in order for the author to enable comparison of results to other researchers. Figure 7.13 shows the resultant multiple correlations upon combining RMR and stope geometry with that of dilution.

Historically, mine operators associated dilution with that of increased span. It was found that for the isolated database that:

Dil.(%) = 0.45 + 0.27 (span in meters)
r = ± 0.68 s + ± 3.8%
The governing equation will also be generated in terms of span.

c) Stress

The significance of depth on dilution was assessed in Figure 7.10. It did not yield a statistically significant correlation on its own. Upon combining RMR and "Area", as shown in Figure 7.13, it only marginally increased the combined correlation (.76 to .77). It however, was not sensitive as per the original definition, Figure 7.12.

The use of fill and no fill was correlated to the "en echelon" database since fill in adjacent stopes would only affect the en echelon and rib configurations. Upon closer examination of the mining sequence and filling cycles, it was concluded that fill was only used as a working platform and not as a means of stabilizing adjacent areas as initially planned. Only five stopes had benefited from having fill in the adjacent stopes, all of them being of the en echelon configuration:

320-18J
370-20KN
370-19K
430-12D
430-13D H/W
(19 obs.)

Employing multivariate analysis on the en echelon database does not result in an improvement in either correlation or sensitivity, Figure 7.14. The results were significant at the 99% confidence level, however, it is of the author's opinion that the database is not sufficiently large to be a reliable estimator.

d) Mining Method

The excavation and exposure rate were mutually correlated to dilution as shown in Figure 7.10. Upon combining RMR and Area, this resulted in multiple correlations as shown in Figure 7.13. The exposure rate was subsequently employed as augmenting the primary parameters since it yielded an overall higher correlation and sensitivity.

A further analysis was conducted on stopes employing 51 mm (conventional) and 165mm (ITH) drilling and their resultant effect on dilution. The 51 mm stopes are as follows, refer Table 7.2a:

370-10B
370-15C
370-19J
370-12/13F
430-13D F/W
430-14D
430-12F
(29 obs.)

Multivariate analysis showed that this parameter was not statistically significant, Figure 7.13.

Mine sequence, which refers to the direction of mining, i.e. footwall to hangingwall lenses or vice versa, was correlated to the expression shown in Figure 7.14 for the en echelon configuration. The following en echelon stopes were mined from hangingwall to footwall:

320-18J
370-20KN
370-19K
370-21J
370-21KN
430-21J F/W
(21 obs.)

Figure 7.14 indicates that the correlation coefficient improved upon incorporating mine sequence into the empirical equation and was marginally sensitive. This was further assessed by introducing the "mine sequence parameter" as an option. A mining direction from hangingwall to footwall would dictate that the parameter "opt. = 0" otherwise, it would be set to "opt. = 1". The following equation was derived:

$$Dil(\%) = 7.1 - .12(RMR) + .003(Area) + 1.4(Opt.)$$
$$r = \pm .81 \quad s = \pm 3\%$$

Upon combining the secondary parameter "Exposure Rate" with the existing governing equation, Figure 7.14, it is determined that the mine sequence does

not marginally improve the overall correlation/sensitivity. In addition the partial correlation coefficient (Section 7.4.1) for "mine sequence" was found to not be statistically significant, Figure 7.16

The "Blast Correction Factor" was correlated to the RMR and was shown to be statistically significant at the 99% confidence level. It showed that as the Rock Mass Rating increased, the BCF decreased. Other parameters affecting the BCF were not studied since the factors that would contribute to the BCF were not recorded in the original database, Chapter 7.3. These factors would be difficult to quantify (other than RMR) since they should include a detailed assessment of blasting/drilling practices, sampling error in dilution estimate and a study of possible stress induced failure that may exist within the slot area. These, among other factors, should be studied in greater detail in determining the extent of the BCF. Present practice at Ruttan is to reduce the BCF to where the governing equation is able to account for all the dilution that is attributed to a stope.

The governing equation is a combination of the primary parameters:

Area
Rock Mass Rating

and the secondary parameter:

Exposure Rate

A sensitivity analysis was performed on the best fit equation incorporating the relevant parameters for the "total stope" database (131 obs.), Figure 7.15.

An alternate method of analysing the above relevant parameters is described in the following section employing "partial correlation coefficients". This was employed in order to determine the secondary parameters critical to the governing equation.

7.4.1 PARTIAL CORRELATION (rp)

It is often required to measure the correlation between the dependent variable (dilution) and one independent variable when all other variables involved are kept constant. This can be obtained by defining a coefficient of partial correlation (Spiegel, 1973). It is derived as follows:

$$r12.3 = \frac{r12 - r13 \times r23}{\sqrt{(1-r^2 13) \times (1-r^2 23)}}$$

$$r12.34 = \frac{r12 - r13.4 \times r23.4}{\sqrt{(1 - r^2 13.4) \times (1 - r^2 23.4)}}$$

given: dil (%) = A + B(Area) - C(RMR - D(Exp. Rate)
Parameter [1] : [3] [4] [2]

r12.3 = correlation coefficient between parameter [1] and [2] while parameter [3] is constant. In obtaining this coefficient other parameters are not considered.

r12 = correlation coefficient between parameter [1] and [2]

r12.34 = represents correlation coefficient between parameter [1] and [2] while parameters [3] and [4] are constant and others are not considered.

Figure 7.16 shows the partial correlation coefficient (rp) between the secondary parameters and the control parameter keeping "RMR and Area" constant. Similar results to that of Figures 7.13, 7.14 are obtained. The only statistically significant secondary parameter being that of "Exposure Rate". Figure 7.10 shows that dilution is largely insensitive to the "stope span/width" ratio when area and rock mass rating are held constant.

7.5 QUADRATIC/LINEAR INTERPRETATION

The above analysis was based upon a linear interpretation of variance between parameters. A quadratic expression was also attempted as shown in Figure 7.17. Figure 7.18 compares the correlations as derived between the primary parameters. The quadratic equation yields a mean sample difference between the observed and predicted dilution of 2.1%, whereas the linear expression resulted in 2.5%. It is true that the quadratic correlation results in a statistically more significant coefficient than the linear expression and therefore would produce a better fit.

Given "n" observations, a curve having "n" number of parameters would yield a perfect correlation. This of course could be theoretically possible, but practically difficult to employ and understand. Consequently, the additional quadratic surface that would incorporate all the significant primary and secondary parameters would have to be of the form of expression shown in Figure 7.17 (3). The marginal increase in predictive accuracy does not warrant the additional complexity inherent

to the quadratic equation. Consequently, linear interpretation will be employed since it has produced significant correlations comprised of simply defined relationships.

7.6 OBSERVATIONS/CONCLUSIONS

This chapter summarizes the parameters that were found to be particularly significant and sensitive to the control parameter "Dilution". The governing equation will incorporate "Area, Rock Mass Rating and the Exposure Rate" which statistically are significant at a 99% confidence level. It is concluded that:

DILUTION IS DIRECTLY RELATED TO THE ROCK QUALITY, THE EXPOSED SURFACE AREA AND THE RATE OF MINING GIVEN THE CONDITIONS PREVAILING FOR THE RUTTAN OREBODY.

Table 7.1: Values of Correlation Coefficient for Different Levels of Significance

DEGREES OF FREEDOM	PROBABILITY	
	.05	.01
1	.988	1.00
2	.900	.980
3	.805	.934
4	.729	.882
5	.669	.883
6	.621	.789
7	.582	.750
8	.549	.715
9	.521	.685
10	.497	.658
11	.476	.634
12	.457	.612
13	.441	.592
14	.426	.574
15	.412	.558

DEGREES OF FREEDOM	PROBABILITY	
	.05	.01
16	.4	.542
17	.389	.528
18	.378	.515
19	.369	.503
20	.360	.492
25	.323	.445
30	.296	.409
35	.275	.381
40	.257	.358
45	.243	.338
50	.231	.322
60	.211	.295
70	.195	.274
80	.183	.256
90	.173	.242
100	.164	.230

Table 7.2a Isolated Stopes Data Base

ISOLATED STOPES DATA BASE — NUMBER OF STOPES = 22

No.	Stope	RMR(%)	Ht.(m)	Wdth.(m)	Vol.(m^3)	Dil.(%)	Span(m)	H.R.(m)	E.R.(m^2/mth)	B.C.F.(%)
1	260 11 F	60	45	8	5000	5	15	6	0.19	3
2	260 11 F	60	45	8	10000	10	53	12	0.23	3
3	260 18 J	51	84	10	5000	3	6	3	0.30	5
4	260 18 J	51	84	10	10000	6	12	5	0.40	5
5	260 18 J	51	84	10	20000	6	24	9	0.40	5
6	260 18 J	51	84	10	30000	9	34	12	0.30	5
7	260 16 H	80	95	13	5000	2	6	3	0.25	0
8	260 16 H	80	95	13	10000	6	15	7	0.36	0
9	260 16 H	80	95	13	20000	7	20	8	0.37	0
10	260 16 H	80	95	13	30000	8	29	11	0.38	0
11	260 16 H	80	95	13	40000	9	46	16	0.21	0
12	270 0 Z	46	48	8	5000	6	13	5	0.15	7
13	270 0 Z	46	48	8	10000	11	26	8	0.09	7
14	320 14 BE	25	105	10	5000	20	44	16	0.21	3
15	320 13 E	79	80	10	5000	6	16	7	0.13	-1
16	320 15 H	66	75	17	5000	0	4	2	0.10	5
17	320 15 H	66	75	17	10000	1	9	4	0.14	5
18	320 15 H	66	75	17	20000	2	17	7	0.22	5
19	320 15 H	66	75	17	30000	3	25	9	0.23	5
20	320 15 H	66	75	17	40000	3	32	11	0.22	5
21	320 18 JN	81	75	13	5000	9	12	5	0.22	-1
22	320 19 J	84	75	25	5000	0	8	3	0.15	0
23	320 19 J	84	75	25	10000	4	16	7	0.18	0
24	320 19 J	84	75	25	20000	6	32	11	0.16	0
25	320 11 B	41	77	9	5000	22	45	14	0.20	-1
26	340 11 C	43	40	8	5000	5	16	6	0.13	10
27	340 11 C	43	40	8	10000	9	42	10	0.14	10
28	370 21 JN	3	52	10	5000	14	37	11	0.32	-1
29	370 15 H	80	76	23	5000	6	23	9	0.09	-1
30	370 10 B	51	63	11	5000	2	8	3	0.12	10
31	370 10 B	51	63	11	10000	3	16	6	0.11	10
32	370 15 C	51	63	9	5000	0	9	4	0.21	29
33	370 15 C	51	63	9	10000	7	19	7	0.19	29
34	370 15 C	51	63	9	20000	11	43	13	0.17	29
35	370 19 J	43	60	23	5000	0	4	2	0.16	2
36	370 19 J	43	60	23	10000	0	8	4	0.19	2
37	370 19 J	43	60	23	20000	5	15	6	0.20	2
38	370 19 J	43	60	23	30000	13	29	10	0.13	2
39	370 16 H	80	76	20	5000	7	27	10	0.12	-1
40	370 12 13F	70	60	10	5000	0	8	4	0.11	0
41	370 12 13F	70	60	10	10000	3	21	8	0.13	0
42	430 13 D F/W	80	60	32	5000	2	3	1	0.08	0
43	430 13 D F/W	80	60	32	10000	4	5	2	0.13	0
44	430 13 D F/W	80	60	32	20000	5	10	4	0.16	0
45	430 13 D F/W	80	60	32	30000	5	16	6	0.16	0
46	430 13 D F/W	80	60	32	40000	5	21	8	0.16	0
47	430 13 D F/W	80	60	32	50000	6	26	9	0.16	0
48	430 13 D F/W	80	60	32	60000	6	31	10	0.16	0
49	430 13 D F/W	80	60	32	70000	7	36	11	0.15	0
50	430 13 D F/W	80	60	32	80000	10	42	12	0.13	0
51	430 14 D	80	60	30	5000	1	3	1	0.06	0
52	430 14 D	80	60	30	10000	3	6	3	0.09	0
53	430 14 D	80	60	30	20000	6	11	5	0.11	0
54	430 14 D	80	60	30	30000	8	17	7	0.03	0
55	430 14 D	80	60	30	40000	9	22	8	0.03	0
56	430 14 D	80	60	30	50000	12	40	12	0.03	0
57	430 21 K	70	52	10	5000	1	10	4	0.21	0
58	430 21 K	70	52	10	10000	1	20	7	0.26	0
59	430 21 K	70	52	10	20000	2	40	11	0.25	0
60	430 12 F	32	85	10	5000	1	6	3	0.11	0
61	430 12 F	32	85	10	10000	25	30	11	0.10	0

BCF = -1 Refers to Benched Stope

Table 7.2b: Echelon Stopes Data Base

ECHELON STOPES DATA BASE — NUMBER OF STOPES = 12

No.	Stope	RMR(%)	Ht.(m)	Width.(m)	Vol.(m^3)	Dil.(%)	Span(m)	H.R.(m)	E.R.(m^2/mth)	B.C.F.(%)
1	320 12 HE	47	80	7	5000	11	9	4	0.10	4
2	320 12 HE	47	80	7	10000	12	27	10	0.14	4
3	320 18 J	56	73	9	5000	4	15	6	0.21	9
4	320 18 J	56	73	9	10000	10	35	12	0.10	9
5	370 20 KH	45	64	15	5000	1	6	3	0.09	2
6	370 20 KH	45	64	15	10000	3	11	5	0.12	2
7	370 20 KH	45	64	15	20000	9	22	8	0.15	2
8	370 20 KH	45	64	15	30000	12	46	13	0.13	2
9	370 20 KH	45	64	15	40000	13	49	14	0.13	2
10	370 13 D	49	50	25	5000	1	4	2	0.18	3
11	370 13 D	49	50	25	10000	3	8	3	0.24	3
12	370 13 D	49	50	25	20000	3	16	6	0.20	3
13	370 13 D	49	50	25	30000	7	24	8	0.11	3
14	370 13 D	49	50	25	40000	10	35	10	0.10	3
15	370 19 K	62	115	13	5000	0	3	2	0.18	0
16	370 19 K	62	115	13	10000	1	7	3	0.22	0
17	370 19 K	62	115	13	20000	3	14	6	0.21	0
18	370 19 K	62	115	13	30000	4	21	9	0.22	0
19	370 19 K	62	115	13	40000	5	28	11	0.25	0
20	370 19 K	62	115	13	50000	8	35	13	0.22	0
21	370 21 J	60	65	15	5000	0	5	2	0.23	2
22	370 21 J	60	65	15	10000	1	10	4	0.23	2
23	370 21 J	60	65	15	20000	3	20	8	0.21	2
24	370 21 J	60	65	15	30000	4	30	10	0.19	2
25	370 21 KH	23	44	8	5000	2	16	6	0.28	7
26	370 21 KH	23	44	8	10000	12	30	9	0.28	7
27	370 12 D	26	85	24	5000	2	3	1	0.04	3
28	370 12 D	26	85	24	10000	7	5	2	0.07	3
29	370 12 D	26	85	24	20000	11	10	4	0.08	3
30	370 12 D	26	85	24	30000	15	38	13	0.08	3
31	430 13 F	33	42	10	5000	1	16	6	0.19	8
32	430 13 F	33	42	10	10000	9	35	10	0.28	8
33	430 12 D	26	85	24	5000	2	3	1	0.04	3
34	430 12 D	26	85	24	10000	7	5	2	0.07	3
35	430 12 D	26	85	24	20000	11	10	4	0.08	3
36	430 12 D	26	85	24	30000	15	38	13	0.08	3
37	430 21 J F/W	65	53	24	5000	4	4	2	0.05	2
38	430 21 J F/W	65	53	24	10000	5	18	7	0.04	2
39	430 13 D H/W	52	64	18	5000	2	5	2	0.10	0
40	430 13 D H/W	52	64	18	10000	4	9	4	0.14	0
41	430 13 D H/W	52	64	18	20000	6	19	7	0.16	0
42	430 13 D H/W	52	64	18	30000	7	28	10	0.17	0
43	430 13 D H/W	52	64	18	40000	8	37	11	0.13	0
44	430 13 D H/W	52	64	18	50000	8	40	12	0.11	0

BCF = -1 Refers to Benched Stope

Table 7.2c: Rib Stopes Data Base

RIB STOPES DATA BASE — NUMBER OF STOPES = 9

No.	Stope	RMR(%)	Ht.(m)	Width.(m)	Vol.(m^3)	Dil.(%)	Span(m)	H.R.(m)	E.R.(m^2/mth)	B.C.F.(%)
1	320 10 B	34	112	12	5000	0	4	2	0.22	0
2	320 10 B	34	112	12	10000	8	7	3	0.22	0
3	320 10 B	34	112	12	20000	13	15	7	0.25	0
4	320 10 B	34	112	12	30000	16	22	9	0.27	0
5	320 10 B	34	112	12	40000	16	30	12	0.29	0
6	320 10 B	34	112	12	50000	16	37	14	0.30	0
7	320 10 B	34	112	12	60000	16	44	16	0.31	0
8	320 10 B	34	112	12	70000	16	46	16	0.28	0
9	320 12 B	23	106	10	5000	27	20	8	0.24	-1
10	340 12 C	30	40	20	5000	8	6	3	0.12	5
11	340 12 C	30	40	20	10000	10	13	5	0.16	5
12	370 20 J	69	75	22	5000	5	3	1	0.04	1
13	370 20 J	69	75	22	10000	7	6	3	0.08	1
14	370 14 C	47	65	7	5000	8	12	5	0.16	22
15	370 14 C	47	65	7	10000	13	32	11	0.20	22
16	370 18 J	54	75	10	5000	2	7	3	0.20	2
17	370 18 J	54	75	10	10000	9	14	6	0.30	2
18	370 18 J	54	75	10	20000	14	29	11	0.37	2
19	370 18 J	54	75	10	30000	14	43	14	0.31	2
20	370 11 F	57	50	10	5000	9	10	4	0.04	15
21	430 15 D	51	64	15	5000	2	6	3	0.19	0
22	430 15 D	51	64	15	10000	6	11	5	0.23	0
23	430 15 D	51	64	15	20000	9	22	8	0.23	0
24	430 15 D	51	64	15	30000	11	33	11	0.24	0
25	430 15 D	51	64	15	40000	14	47	13	0.15	0
26	430 20 K	74	46	10	5000	1	11	4	0.28	0
27	430 20 K	74	46	10	10000	1	22	7	0.18	0
28	430 20 K	74	46	10	20000	2	38	10	0.21	0

BCF = -1 Refers to Benched Stope

Table 7.3: Data Base - Statistical Summary

PARAMETER	TOTAL	ISOLATED	ECHELON	RIB
No. OF STOPES	43	22	12	9
No. OF OBSERVATIONS	133	61	44	28
Rock Mass Rating (%)	55 ± 19	64 ± 19	47 ± 14	48 ± 16
	(56 ± 20)	(59 ± 22)	(45 ± 15)	(49 ± 17)
EXP. RATE ("1000m^2/mth)	.18 ± .09	.18 ± .09	.15 ± .07	.22 ± .09
	(.18 ± .08)	(.17 ± .07)	(.15 ± .08)	(.18 ± .09)
HYD. RADIUS (m)	7 ± 4	7 ± 4	7 ± 4	8 ± 5
	(11 ± 3)	(11 ± 3)	(11 ± 2)	(10 ± 4)
SPAN (m)	20 ± 14	21 ± 14	19 ± 14	21 ± 15
	(31 ± 13)	(32 ± 13)	(34 ± 8)	(24 ± 16)
SURFACE AREA (m^2)	1450 ± 1120	1420 ± 1020	1360 ± 1085	1705 ± 1545
	(2250 ± 1120)	(2254 ± 970)	(2360 ± 924)	(2090 ± 1550)
SPAN/WIDTH RATIO	1.6 ± 1.3	1.6 ± 1.5		
	(3.4 ± 1.7)	(3.2 ± 1.8)		
STOPE HEIGHT (m)	71 ± 21	68 ± 15	72 ± 23	78 ± 28
	(68 ± 20)	(68 ± 16)	(68 ± 21)	(70 ± 25)
BCF (%)	3 ± 6	3 ± 9	3 ± 3	3 ± 7
DILUTION (%)	7 ± 6	6 ± 5	6 ± 4	10 ± 7
	(10 ± 6)	(10 ± 6)	(10 ± 4)	(12 ± 7)
STOPE DEPTH (m)	368 ± 54	356 ± 65	385 ± 36	369 ± 47
	(360 ± 48)	(346 ± 55)	(382 ± 40)	(369 ± 40)
STOPE INCLINATION (°)		67 ± 9		
		(68 ± 9)		
STOPE WIDTH (m)		18 ± 9		
		(15 ± 8)		
LONG SPAN/SHORT SPAN		5.1 ± 5		
		(2.1 ± 1.1)		
( ) Refers to Final Stope Configuration				

Table 7.4: Isolated Stopes Data Base

- Typical RMR Classification

ISOLATED STOPES DATA BASE - TYPICAL RMR CLASSIFICATION

No.	Stope	Bd(%)	Strgn.	RQD	Spac.	Condit
1	260 11 F	5	7	8	20	12
2	260 11 F	10	7	8	20	12
3	260 10 J	3	4	8	10	20
4	260 10 J	6	4	8	10	20
5	260 10 J	6	4	8	10	20
6	260 10 J	9	4	8	10	20
7	260 16 H	2	7	17	25	20
8	260 16 H	6	7	17	25	20
9	260 16 H	7	7	17	25	20
10	260 16 H	8	7	17	25	20
11	260 16 H	9	7	17	25	20
12	270 9 J	6	4	10	15	12
13	270 9 J	11	4	10	15	12
14	320 14 HW	20	4	2	10	6
15	320 13 E	6	7	17	25	20
16	320 15 H	0	7	10	21	12
17	320 15 H	1	7	10	21	12
18	320 15 H	2	7	10	21	12
19	320 15 H	3	7	10	21	12
20	320 15 H	3	7	10	21	12
21	320 18 FW	9	12	17	25	20
22	320 19 J	0	12	17	25	20
23	320 19 J	4	12	17	25	20
24	320 19 J	6	12	17	25	20
25	320 11 B	42	7	8	20	6
26	340 11 C	5	2	8	20	6
27	340 11 C	9	2	8	20	6
28	370 21 FW	14	2	2	5	3
29	370 15 H	6	8	17	25	20
30	370 10 B	2	4	8	20	6
31	370 10 B	3	4	8	20	6
32	370 15 C	0	7	8	20	20
33	370 15 C	7	7	8	20	20
34	370 15 C	11	7	8	20	20
35	370 19 J	0	7	8	10	8
36	370 19 J	3	7	8	10	8
37	370 19 J	5	7	8	10	8
38	370 19 J	13	7	8	10	8
39	370 16 H	7	8	17	25	20
40	370 12 HW	0	7	13	20	20
41	370 12 HW	3	7	13	20	20
42	430 13 B F/W	2	7	18	25	20
43	430 13 B F/W	4	7	18	25	20
44	430 13 B F/W	5	7	18	25	20
45	430 13 B F/W	5	7	18	25	20
46	430 13 B F/W	5	7	18	25	20
47	430 13 B F/W	6	7	18	25	20
48	430 13 B F/W	6	7	18	25	20
49	430 13 B F/W	7	7	18	25	20
50	430 13 B F/W	10	7	18	25	20
51	430 14 B	1	7	17	25	20
52	430 14 B	3	7	17	25	20
53	430 14 B	6	7	17	25	20
54	430 14 B	8	7	17	25	20
55	430 14 B	9	7	17	25	20
56	430 14 B	12	7	17	25	20
57	430 21 E	1	4	17	13	6
58	430 21 E	1	4	17	13	6
59	430 21 E	2	4	17	13	6
60	436 12 F	1	5	8	20	3
61	436 12 F	25	5	8	20	3

Table 7.5: Isolated Stopes Data Base

- Comparison Quadratic and Planar Surface Empirical Equations

ISOLATED STOPES DATA BASE - COMPARISON QUADRATIC AND PLANAR SURFACE EMPIRICAL EQUATIONS

$$\underline{Dil(\%) = 6 - 8(RMR) + 3.5(AREA)}$$
$$\underline{r = .76 \quad S_e = 3.4\%}$$

$$\underline{Dil(\%) = 1.1 + 10.3(AREA) - 11.2(RMR) - .7(AREA)^2 + 13.2(RMR)^2 - 7.1(AREA)(RMR)}$$
$$\underline{r = .82 \quad S_e = 2.9}$$

No.	RMR(%)	AREA (m^2)	Res. Dil(%)	Quad. Dil(%)	Diff.(%)	Lin. Dil(%)	Diff. (%)
1	60	675	5	3	2	4	1
2	60	2385	10	10	0	10	0
3	51	504	3	2	1	4	1
4	51	1008	6	5	1	5	1
5	51	2016	6	9	3	9	3
6	51	2856	9	12	3	12	3
7	80	570	2	3	1	2	0
8	80	1425	6	6	0	5	1
9	80	1900	7	7	0	6	1
10	80	2755	8	8	0	9	1
11	80	4370	9	7	2	15	6
12	46	624	6	3	3	5	1
13	46	1248	11	6	5	7	4
14	25	4620	20	24	4	20	0
15	79	1280	6	5	1	4	2
16	66	300	0	1	1	2	2
17	66	675	1	3	2	3	2
18	66	1275	2	5	3	5	3
19	66	1875	3	8	5	7	4
20	66	2400	3	9	6	9	6
21	81	900	9	4	5	3	6
22	84	600	0	3	3	1	1
23	84	1200	4	5	1	3	1
24	84	2400	6	7	1	8	2
25	41	3465	22	16	6	15	7
26	43	640	5	3	2	5	0
27	43	1680	9	9	0	8	1
28	3	1924	14	18	4	12	2
29	80	1748	6	7	1	6	0
30	51	504	2	2	0	4	2
31	51	1008	3	5	2	5	2
32	51	567	0	2	2	4	4
33	51	1197	7	6	1	6	1
34	51	2709	11	12	1	11	0
35	43	240	0	0	0	3	3
36	43	480	0	2	2	4	4
37	43	900	5	5	0	6	1
38	43	1740	13	9	4	9	4
39	80	2052	7	7	0	7	0
40	70	480	0	2	2	2	2
41	70	1260	3	5	2	5	2
42	80	180	2	1	1	0	2
43	80	300	4	2	2	1	3
44	80	900	5	3	2	2	3
45	80	960	5	4	1	3	2
46	80	1260	5	5	0	4	1
47	80	1560	6	6	0	5	1
48	80	1860	6	7	1	6	0
49	80	2160	7	7	0	7	0
50	80	2520	10	8	2	8	2
51	80	180	1	1	0	0	1
52	80	360	3	2	1	1	2
53	80	660	6	3	3	2	4
54	80	1020	8	5	3	3	5
55	80	1320	9	5	4	4	5
56	80	2400	12	8	4	8	4
57	70	520	1	2	1	2	1
58	70	1040	1	5	4	4	3
59	70	2080	2	8	6	8	6
60	32	510	1	3	2	5	4
61	32	2550	25	15	10	12	13

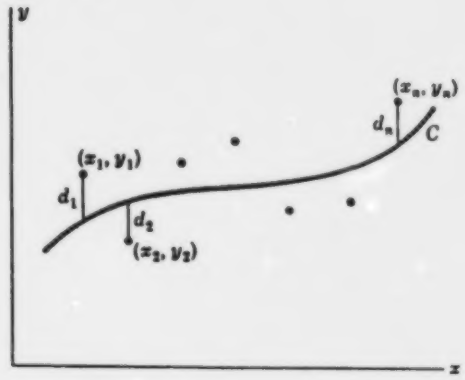

Figure 7.1: Scatter Diagram

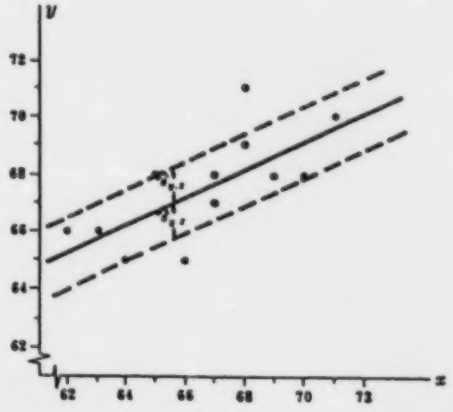

Figure 7.2: Example of Standard Error of Estimate

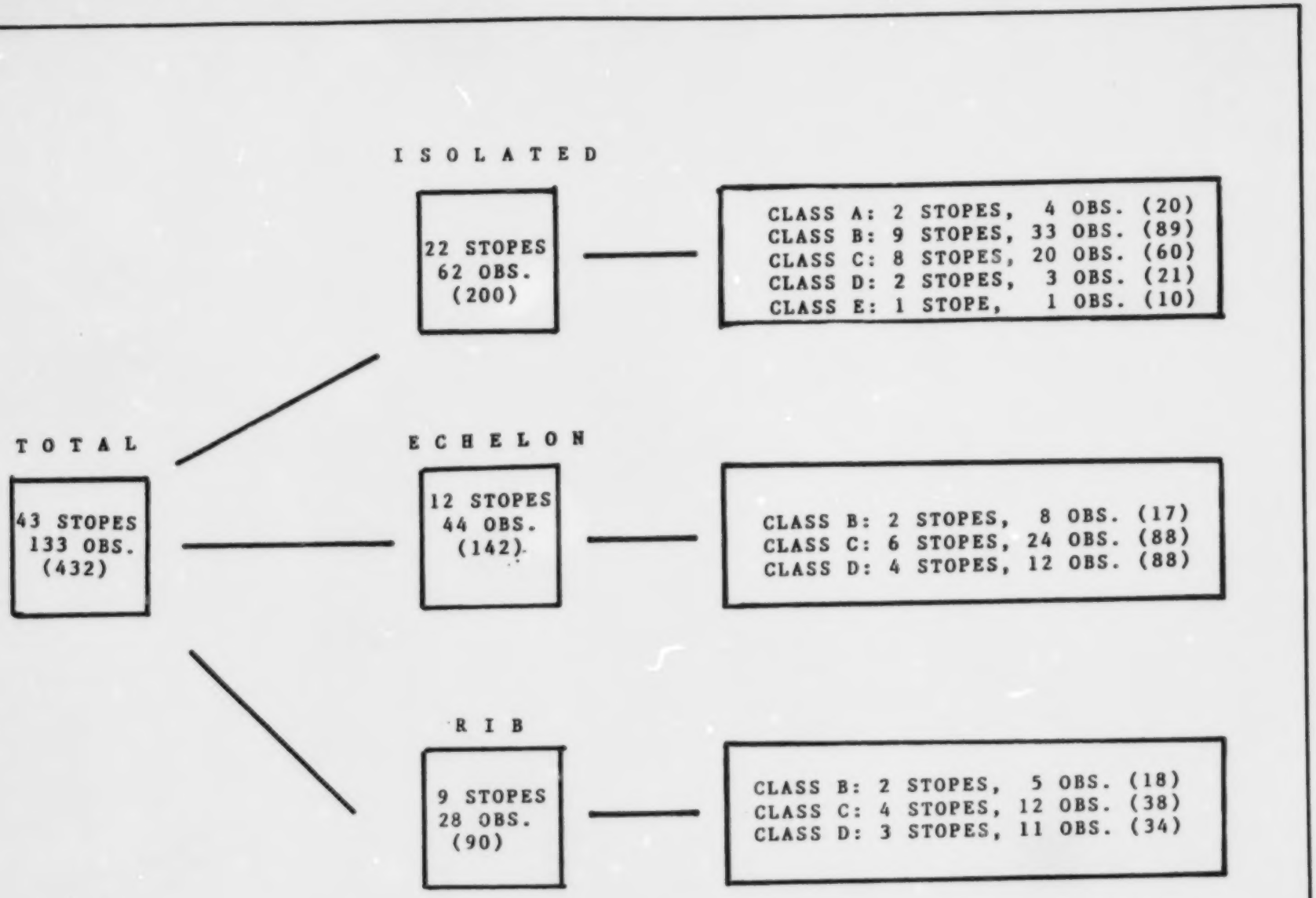

Figure 7.3: Distribution of Stopes - Data Base

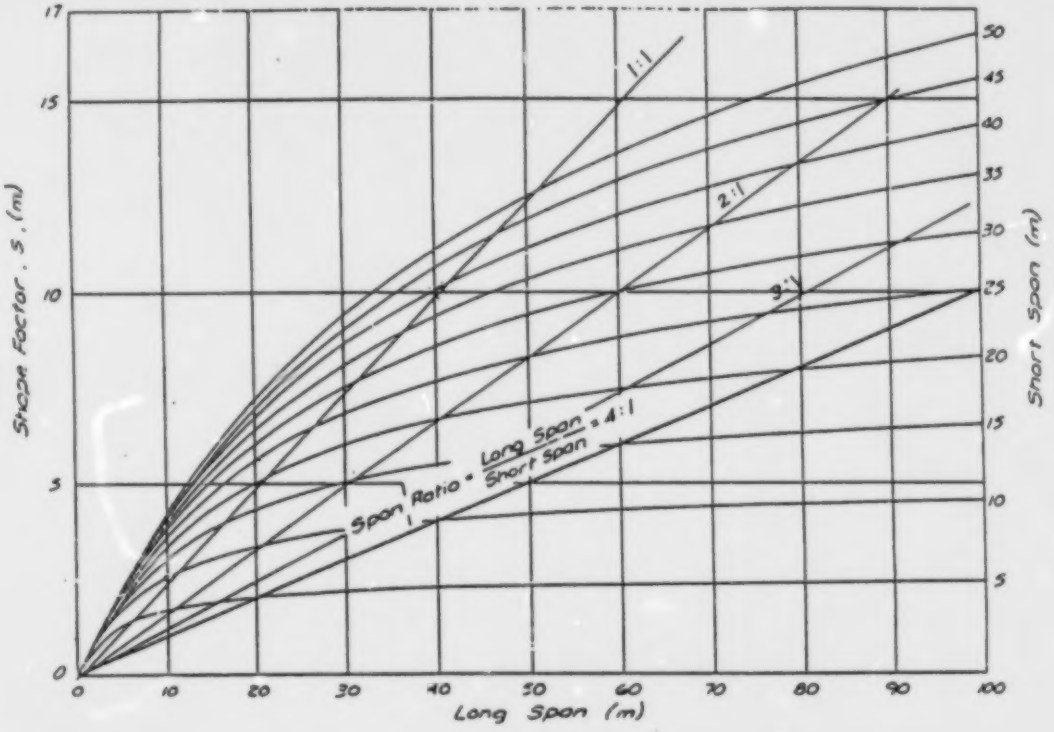

Figure 7.4: Shape Factor (Hydraulic Radius)

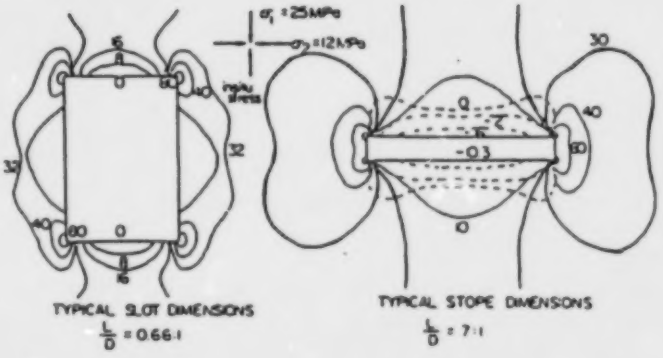

Figure 7.5: Minor (Dashed) and Major (Solid) Stress Contours Surrounding Stopes at Ruttan - Plan View

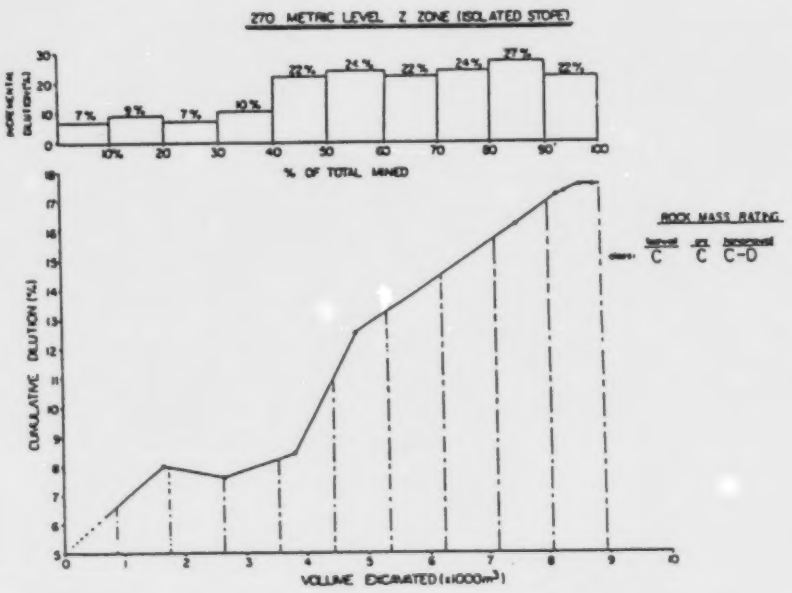

Figure 7.6: Stope Dilution - Blasting

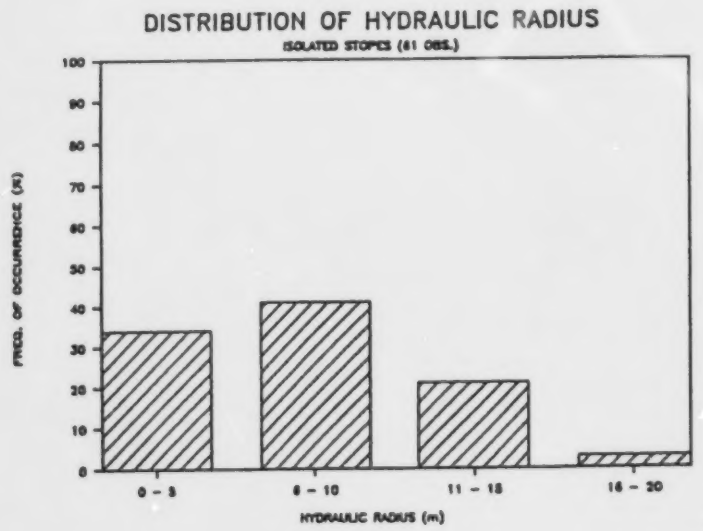

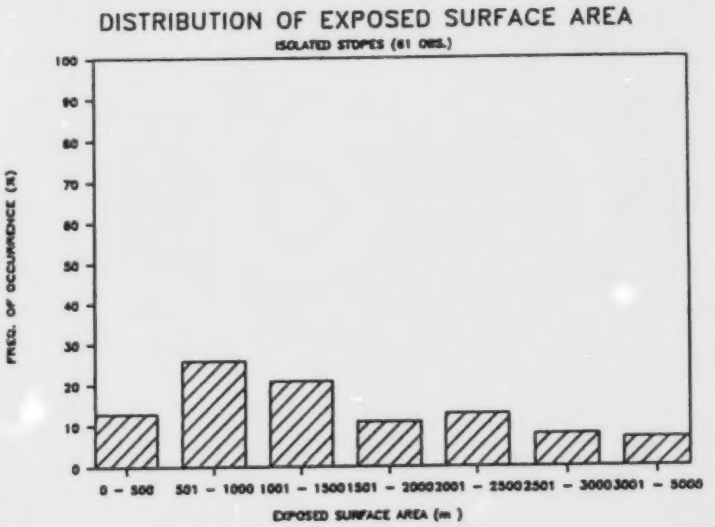

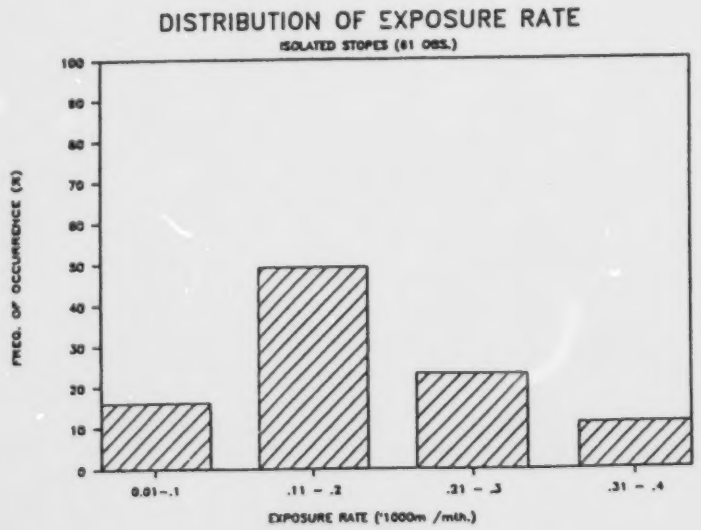

Figure 7.7a: Distribution of Parameters Comprising Isolated Data Base

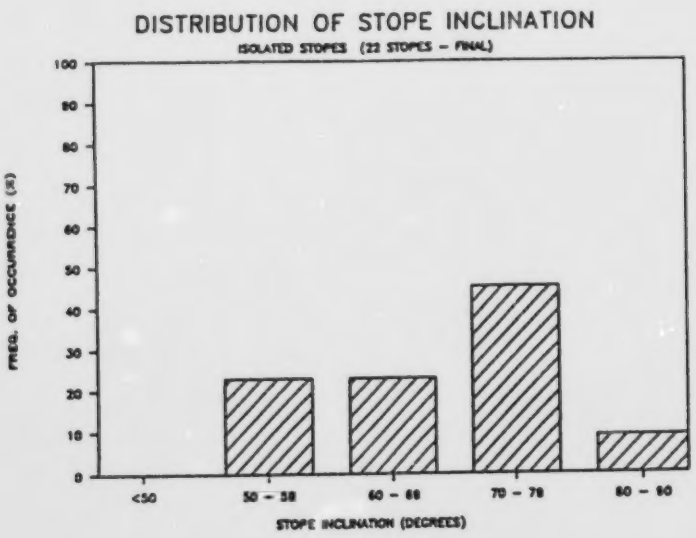

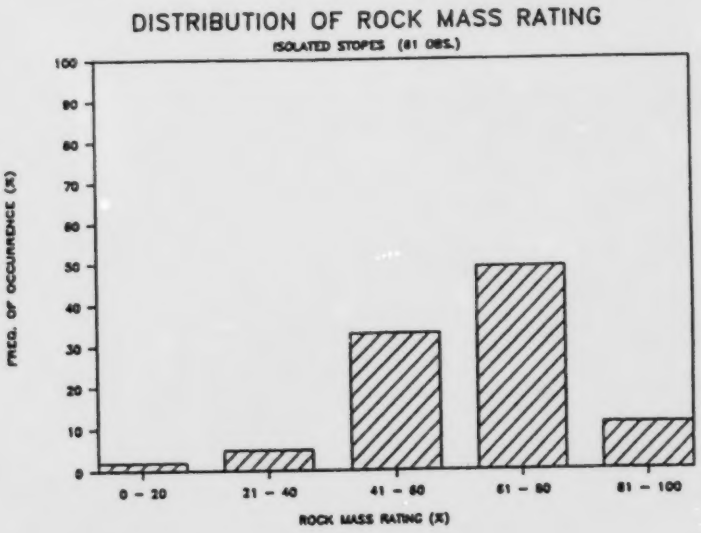

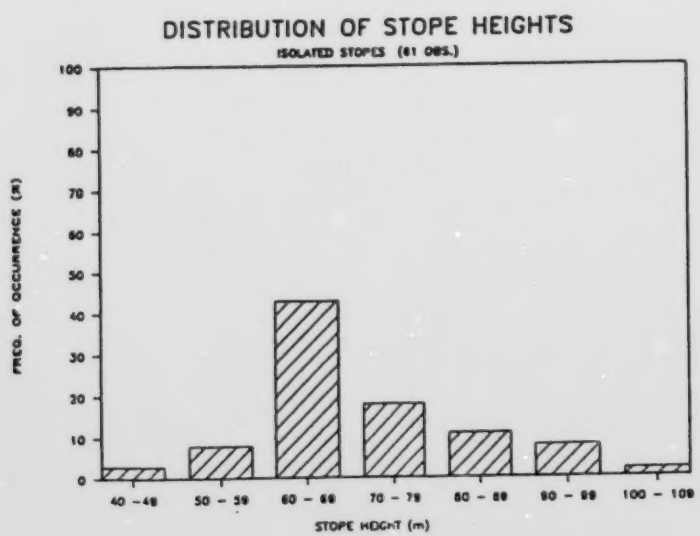

Figure 7.7b: Distribution of Parameters Comprising Isolated Data Base

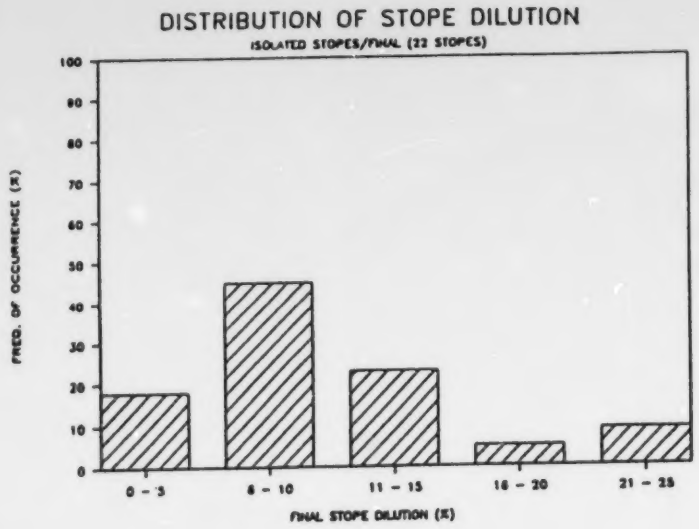

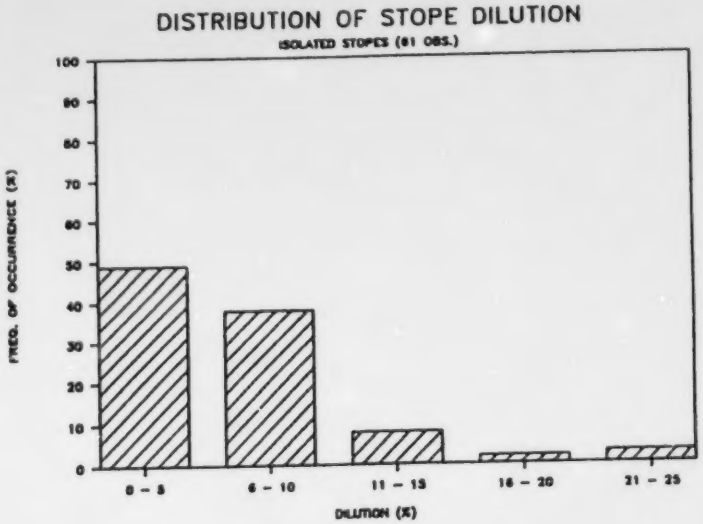

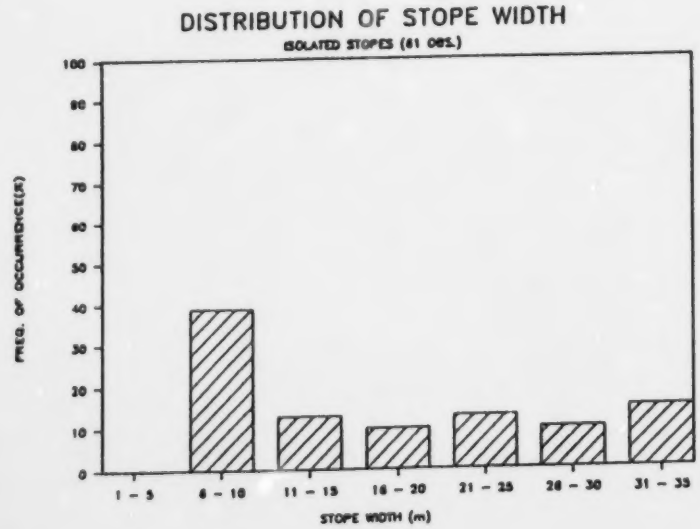

Figure 7.7c: Distribution of Parameters Comprising Isolated Data Base

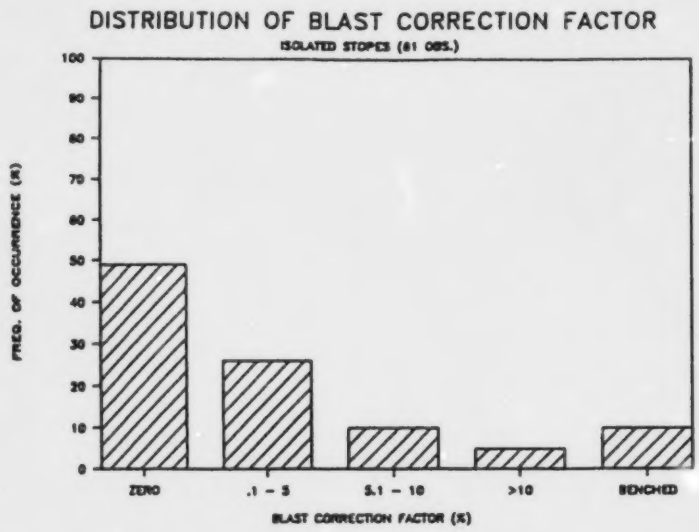

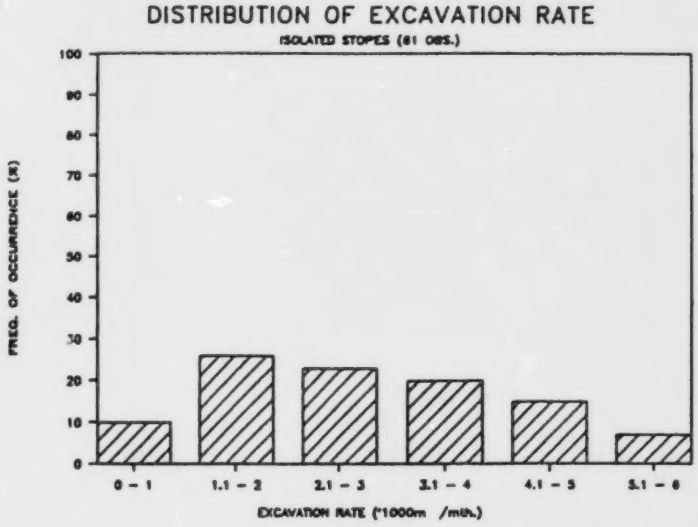

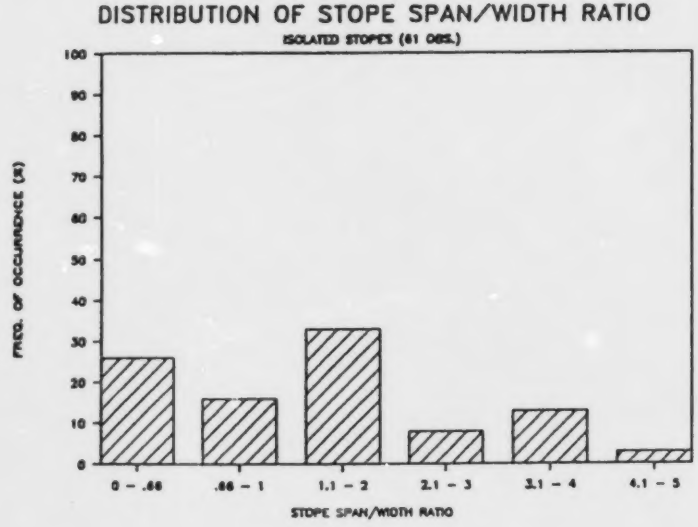

Figure 7.7d: Distribution of Parameters Comprising Isolated Data Base

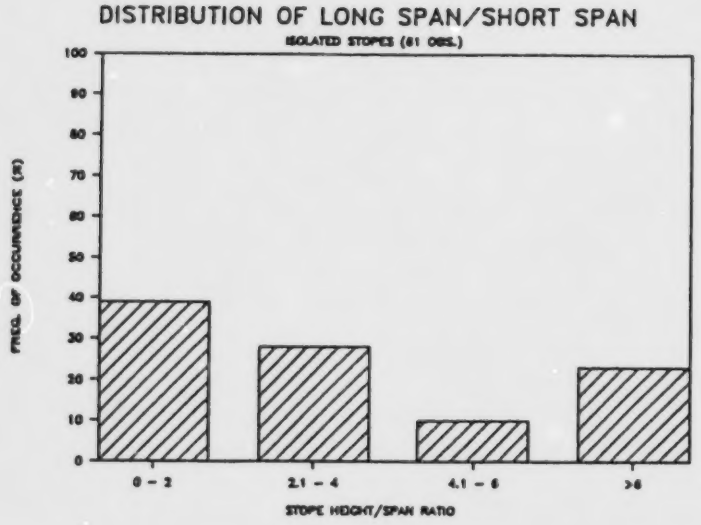

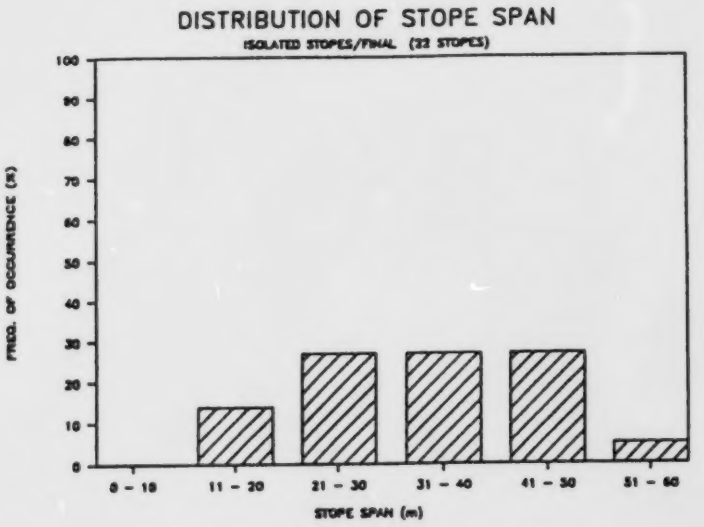

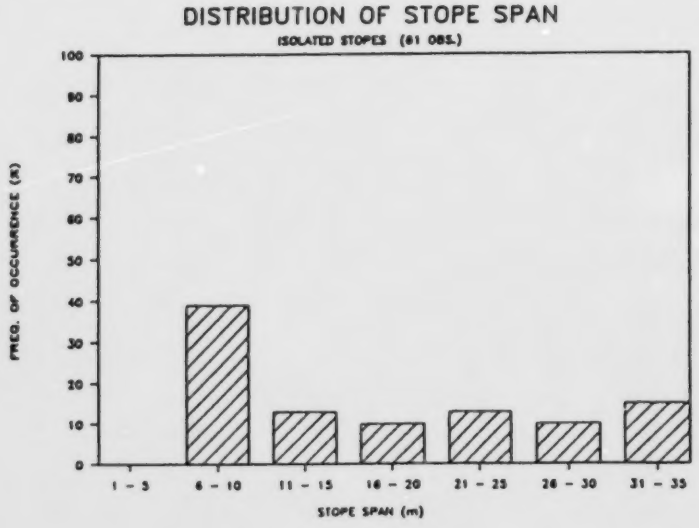

Figure 7.7e: Distribution of Parameters Comprising Isolated Data Base

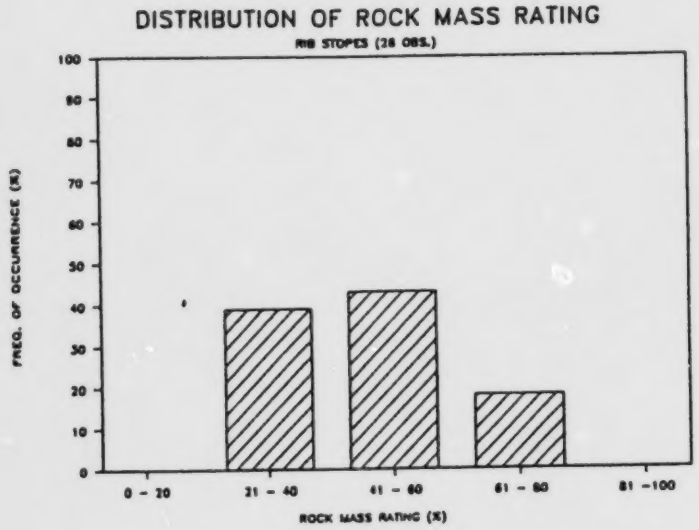

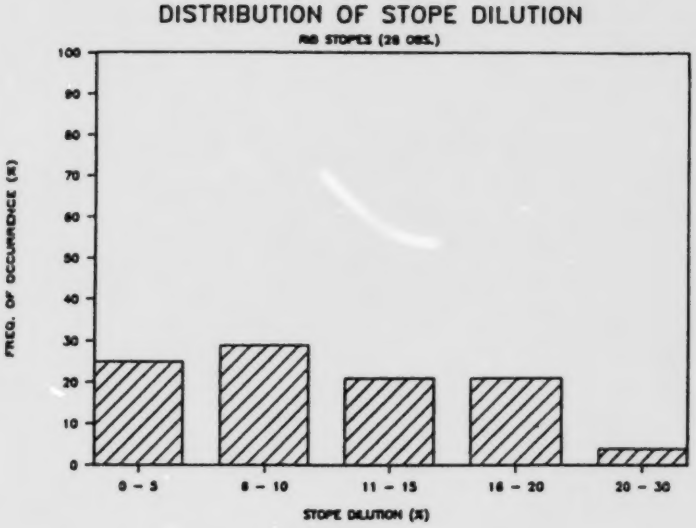

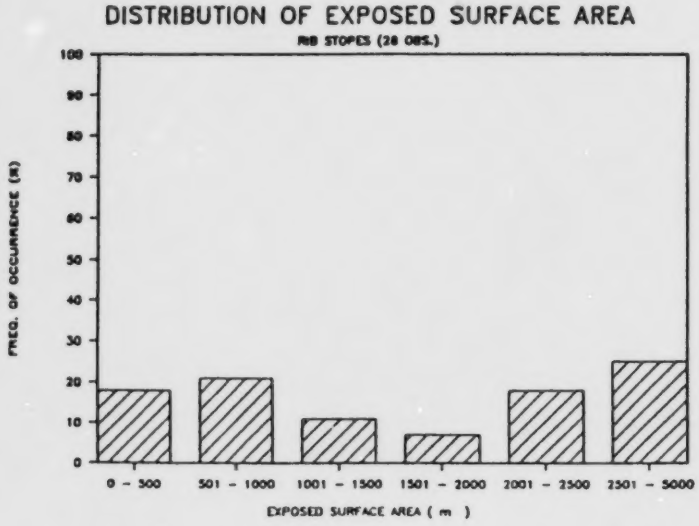

Figure 7.8a: Distribution of Parameters Comprising Rib Data Base

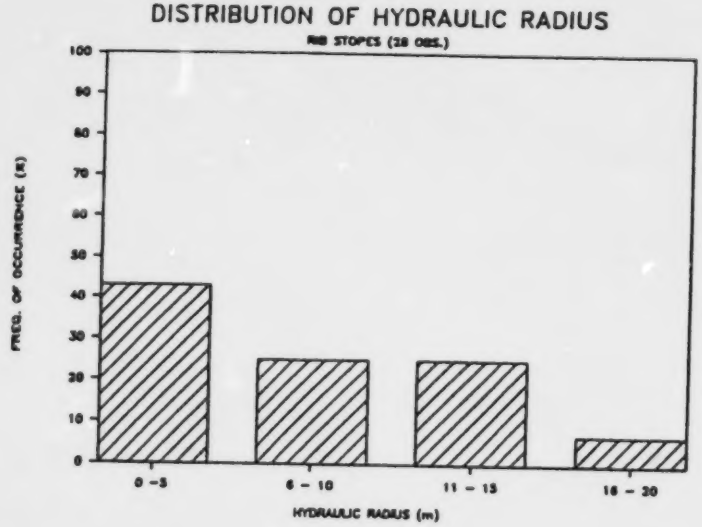

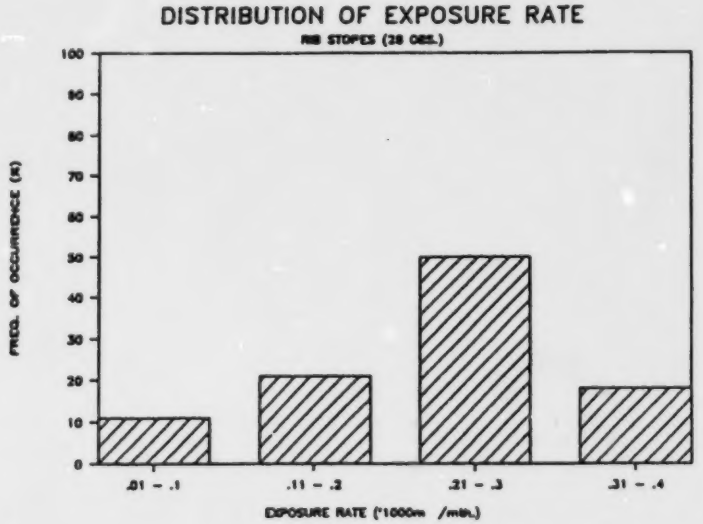

Figure 7.8b: Distribution of Parameters Comprising Rib Data Base

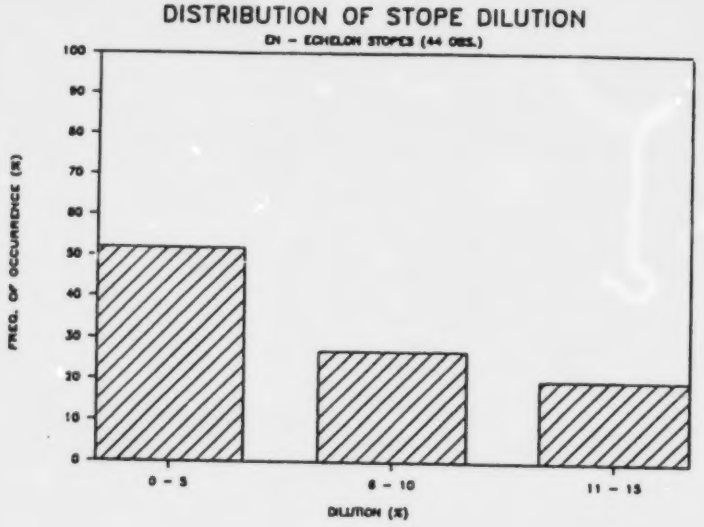

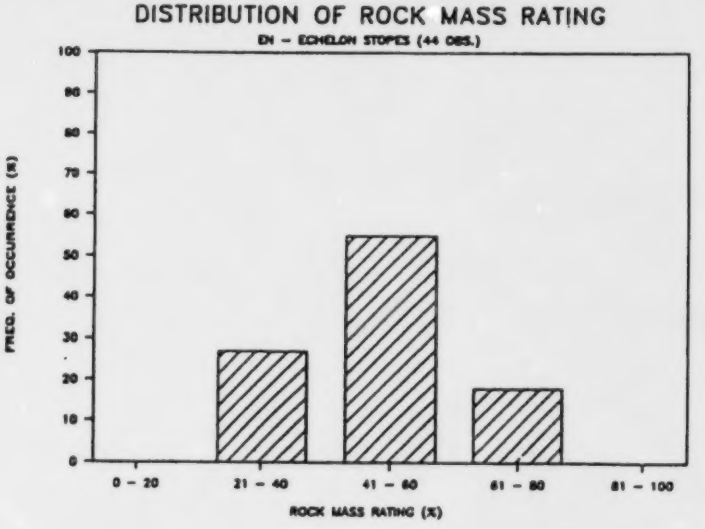

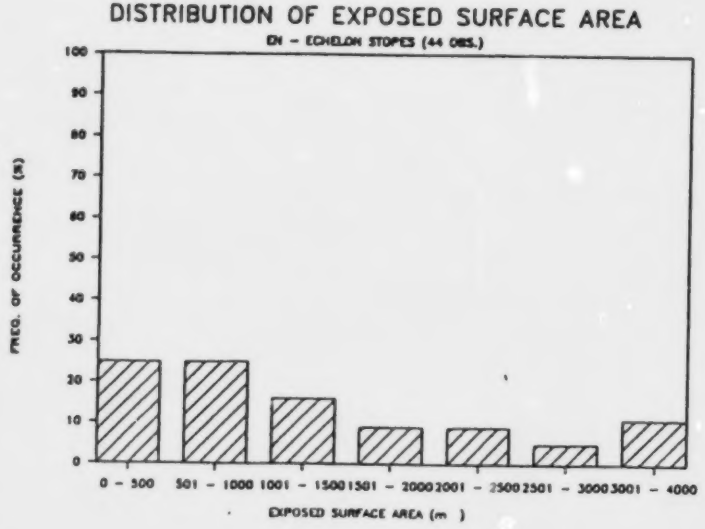

Figure 7.9a: Distribution of Parameters Comprising Echelon Data Base

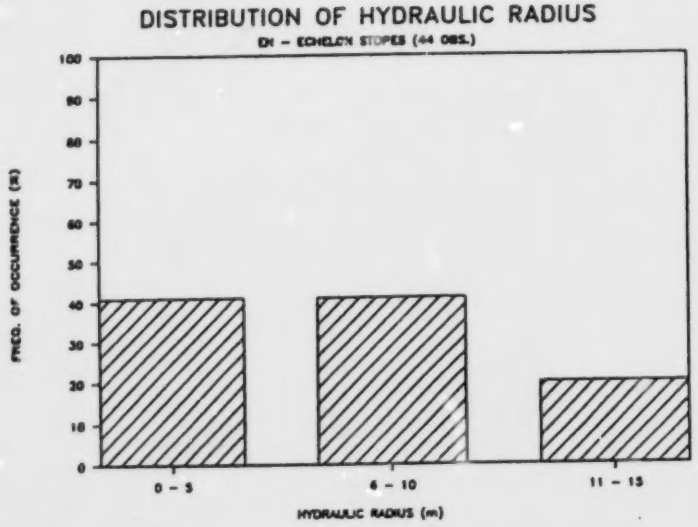

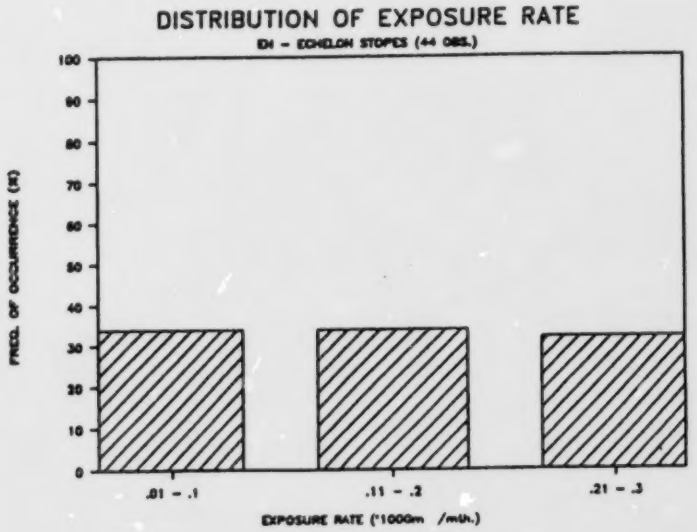

Figure 7.9b: Distribution of Parameters
Comprising Echelon Data Base

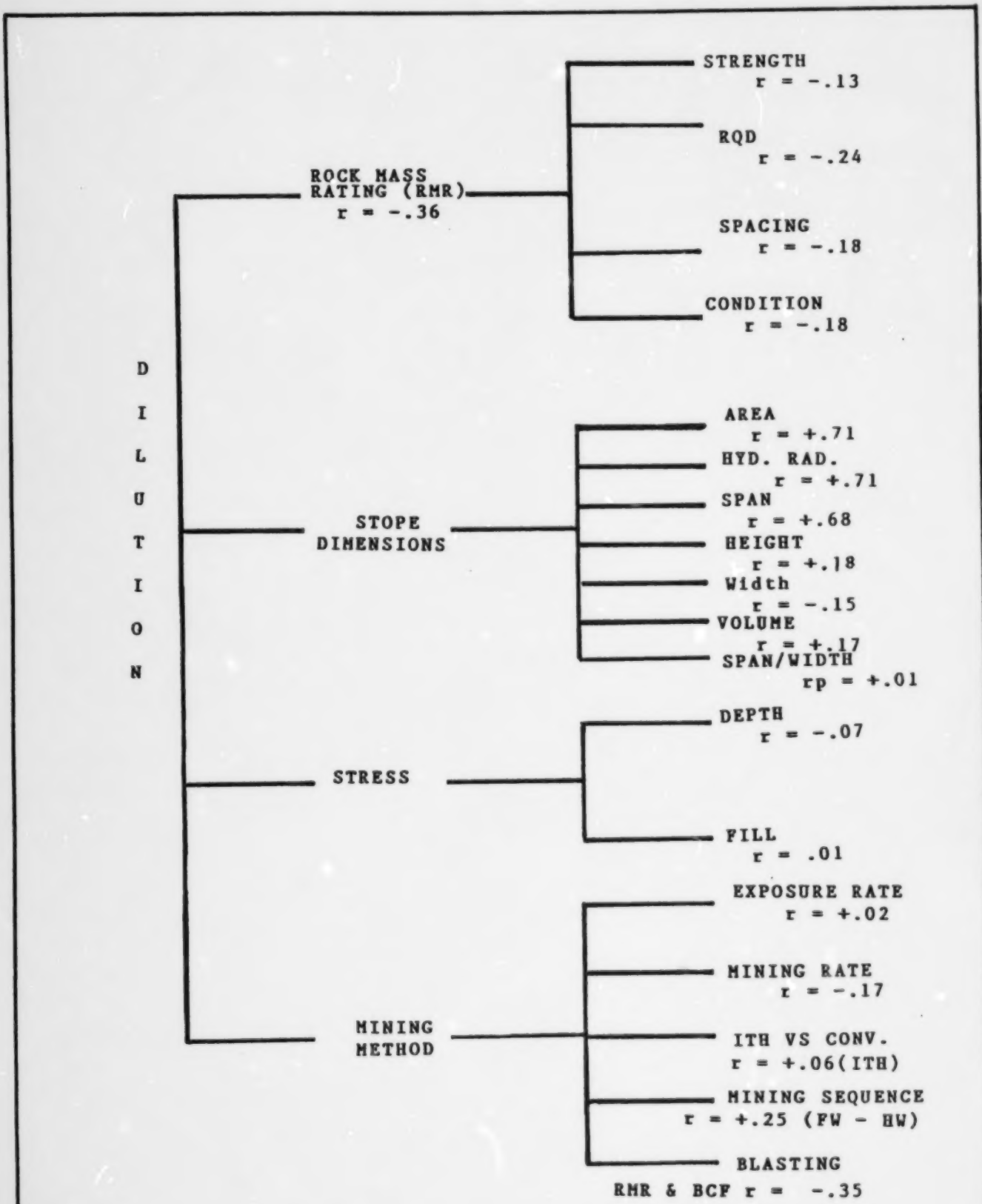
DILUTION
ROCK MASS RATING (RMR) r = -.36
STRENGTH r = -.13
RQD r = -.24
SPACING r = -.18
CONDITION r = -.18
STOPE DIMENSIONS
AREA r = +.71
HYD. RAD. r = +.71
SPAN r = +.68
HEIGHT r = +.18
Width r = -.15
VOLUME r = +.17
SPAN/WIDTH rp = +.01
STRESS
DEPTH r = -.07
FILL r = .01
MINING METHOD
EXPOSURE RATE r = +.02
MINING RATE r = -.17
ITH VS CONV. r = +.06(ITH)
MINING SEQUENCE r = +.25 (FW - HW)
BLASTING
RMR & BCF r = -.35

Figure 7.10: Critical Parameters

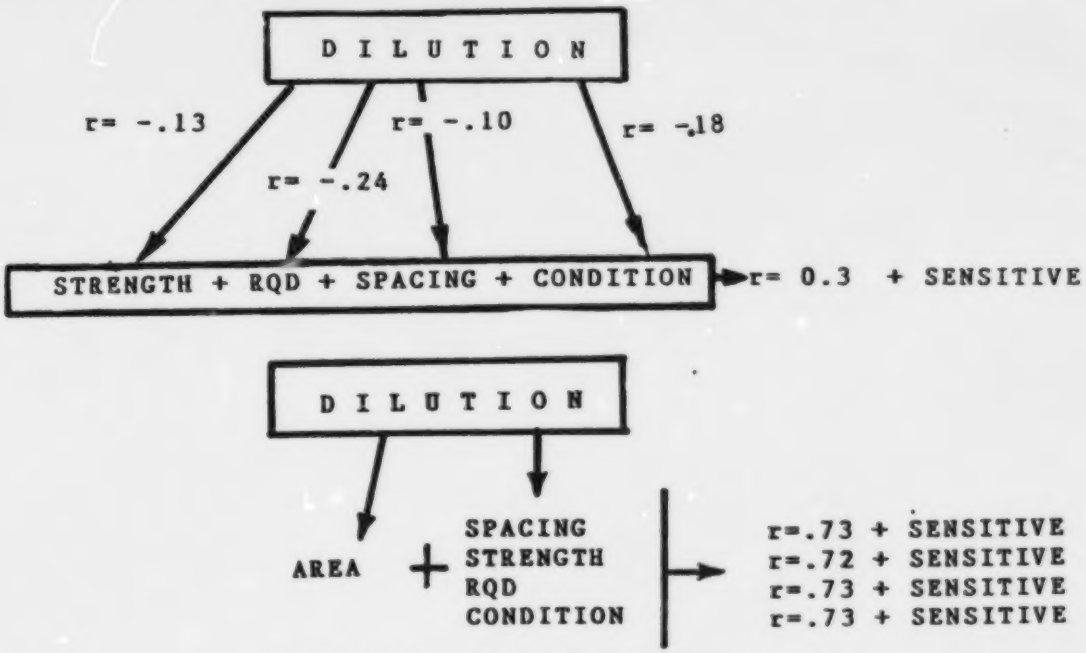

Figure 7.11: Rock Mass Analysis

ACCEPTANCE

100% INCREASE IN THE MEAN VALUE OF A PARAMETER HAS GREATER THAN A 1% (ABSOLUTE) AFFECT ON THE CHANGE IN DILUTION.

EXAMPLE

DILUTION (%) = 1.8 - .08(RMR) + .0037(AREA) + .002(DEPTH)

MEAN AREA = $1418m^2$

MEAN DEPTH = 368m

A) TEST: DEPTH

BASE = |.002*368| = 0.7% DILUTION

SENSITIVITY = |.002*(368*2)| = 1.5% DILUTION

|BASE - SENSITIVITY| < 1% "REJECTED"

B) TEST: AREA

BASE = |.0037*1418| = 5.2% DILUTION

SENSITIVITY = |.0037*(1418*2)| = 10.5% DILUTION

|BASE - SENSITIVITY| > 1% "ACCEPTED"

Figure 7.12: Criteria for Sensitivity

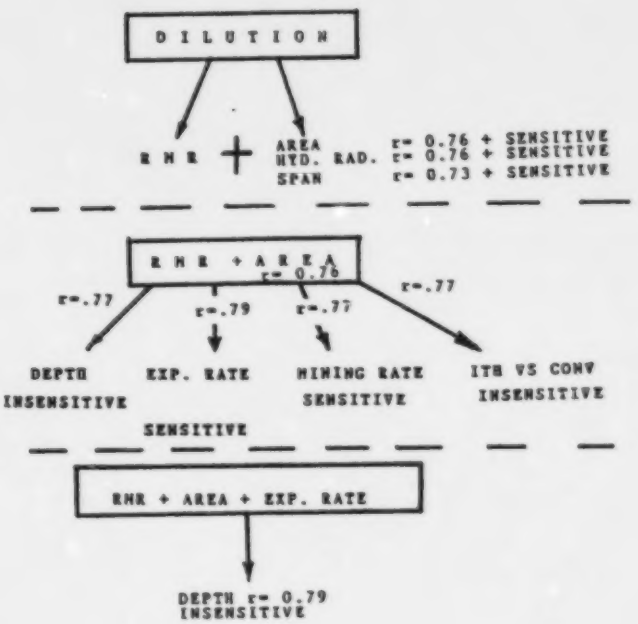

Figure 7.13: Governing Equations
- Derivation for Isolated Stopes

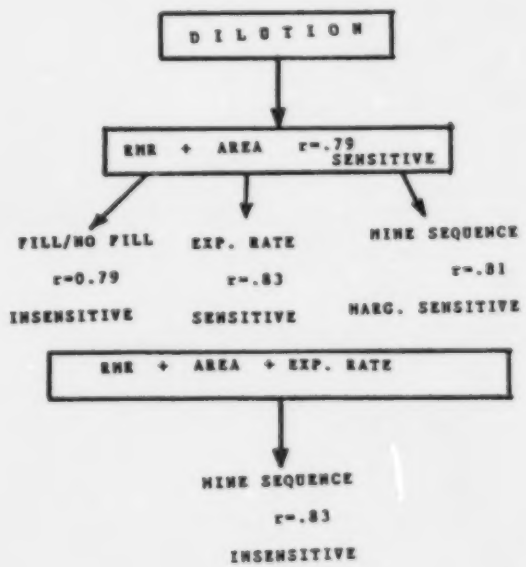

Figure 7.14: Governing Equations - Derivation for Echelon Stopes

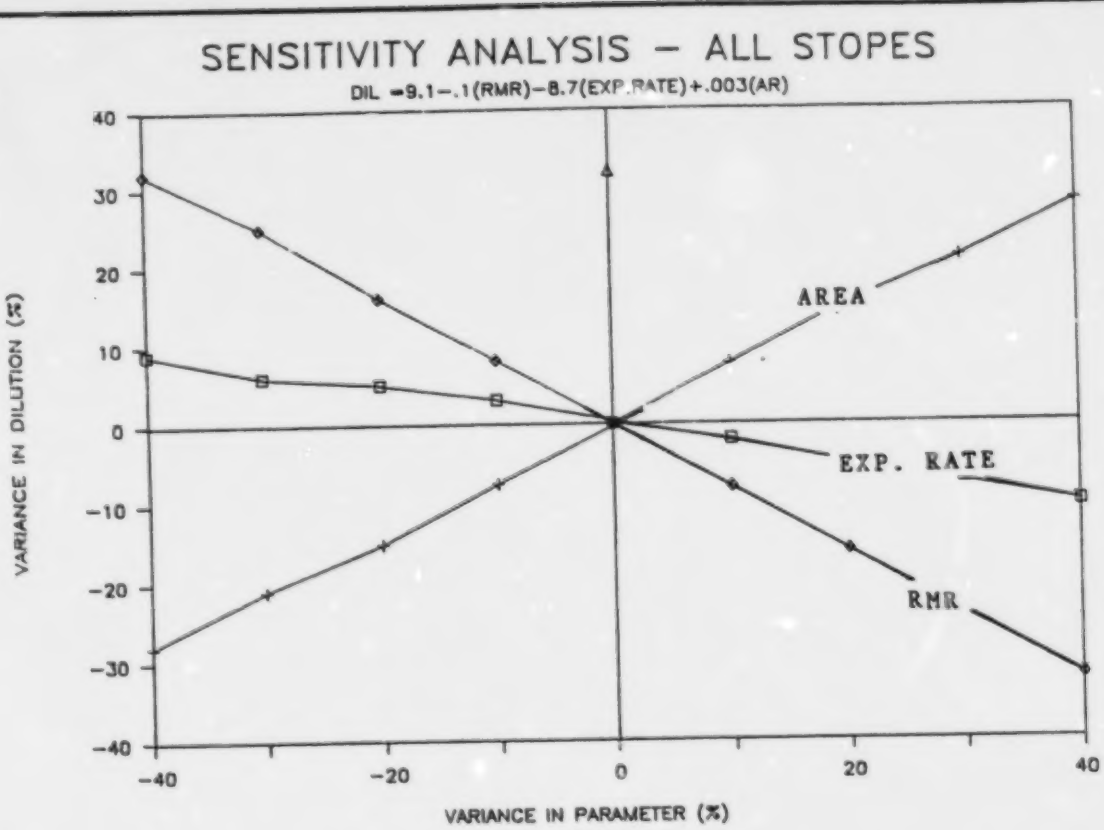

Figure 7.15: Sensitivity Analysis - Data Base = All Stopes

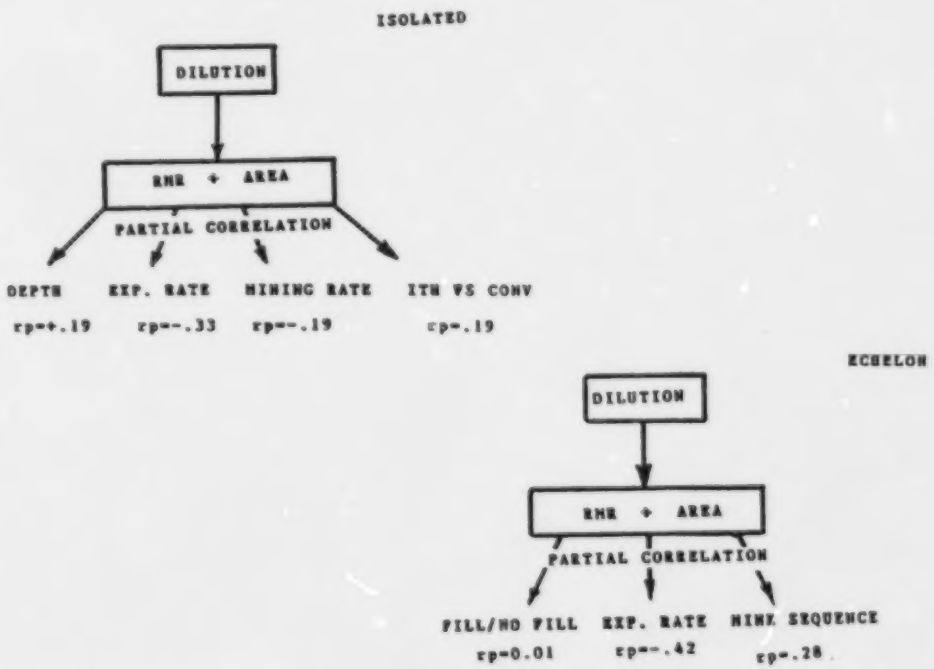

Figure 7.16: Partial Correlation

$$\text{LINEAR} : Z = a + b(X) + c(Y) + d(W) + \ldots\ldots$$

$$\text{QUADRATIC} : Z = a + b(X^2) + c(X)$$

$$Z = a + b(X) + c(Y) + d(X^2) + e(Y^2) + f(X)(Y)$$

$$Z = A + b(X) + c(Y) + d(W) + e(X^2) + f(Y^2) + g(W^2) + h(X)(Y) + i(X)(Z) + j(Y)(W) + k(X)(Y)(W)$$

Figure 7.17: Comparison - Type of Equation (Linear/Quadratic)

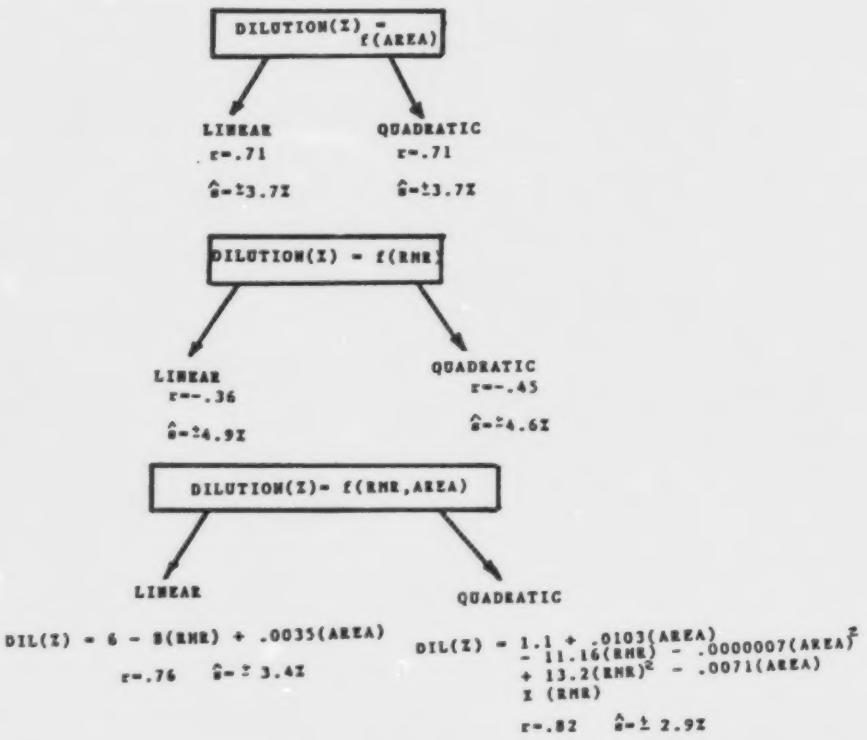

Figure 7.18: Quadratic/Linear Correlation - Isolated Stopes

CHAPTER EIGHT
STOPE DESIGN

8.1 INTRODUCTION

This chapter employs the critical parameters "Rock Mass Rating, Area and Exposure Rate" and incorporates them into a governing equation for each individual stope configuration. The influence of stope configuration on the predicted dilution is estimated and the blast correction factor is quantified statistically. This is shown to be important parameter in establishing an empirical set of equations that would be a reliable predictor of dilution.

8.2 STOPE CONFIGURATION

The governing equations for the Ruttan database are shown in Figure 8.1. The hydraulic radius and area method are presented since both derivations will result in similar predicted dilutions. Generally the hydraulic radius dilution is employed at Ruttan, however, the area method is used as a check in situations where the two may differ. They have been determined from a least squares regression analysis and are based upon the observations established in the preceding chapter.

In order to determine the significance of stope configuration, the following analysis was employed:

a) Isolated + Echelon + Rib

A database incorporating all 133 observations was employed in generating a best fit hyper-surface. This empirical equation does not distinguish between the different stope configurations. The governing equation is as shown in Figure 8.2. Employing this equation and the observations for the isolated database results in a correlation coefficient of 0.78. Equally for the en echelon and rib observations, the predictive equation would result in correlations of .71 and .72 respectively. In all three situations the correlations and therefore the best fit is lower than that outlined in Figure 8.1. In addition, a further analysis was performed whereby the isolated stope were designated a value "opt. = 0" and the remaining observations assess a value of "opt = 1". This resulted in a multiple correlation as shown in Figure 8.2 of 0.77, and a partial correlation of 0.01. In addition the sensitivity of the option parameter is less than 1%. However, the remaining configurations result in significant correlations and sensitivities. This implies that the en

echelon and rib configurations cannot be incorporated with the remainder to the database since configuration is a critical parameter.

b) Grouped Stopes

A similar analysis was conducted on the grouped configurations. The isolated and en echelon combination, as shown in Figure 8.3, results in a multiple correlation of 0.79 and a partial correlation of 0.3. Similarly, isolated/rib and en echelon/rib combinations indicated that the configuration is significant and sensitive. The grouped empirical equation gave lower correlations for an individual configuration than if a single equation describing that same database was employed, Figure 8.1. The above indicates that the individual stope configurations are statistically significant and their effect on dilution particularly sensitive. They cannot, therefore, be grouped without employing some parameter (opt.) which would account for configuration. Individual governing equations will be employed in relating dilution to the critical parameters for a particular stope configuration. The governing design equations are summarized Figure 8.1. The equivalent and span formulation is shown in Figure 8.4. It is interesting to note that a relative comparison of generated dilution can be made from the previous analysis, Figure 8.2. The isolated option would yield approximately 2% more dilution than the en echelon and 1.5% less dilution than the rib configuration. The rib would yield approximately 4% more than the en echelon. Consequently, the en echelon yields the lowest dilution followed by the isolated and rib geometries. This observation has been partly explained by Chapter 4.3.

8.3 BLAST CORRECTION FACTOR

This has been previously discussed and will be analysed in a statistical contest in this section.

Figure 8.5 shows the option of incorporating the "BCF" factor for individual stope geometries. The isolated database would result in the multiple correlation for the governing equation to be reduced to 0.64 from 0.79. This represents a partial correlation of 0.6. Similarly, significant results are shown for the en echelon and rib configurations. Figure 8.6 shows the resultant correlation for a database, whereby stopes having a BCF value greater than zero are omitted. This would greatly reduce the number of observations, however, they are statistically significant at the 99% confidence level. Obviously, they may pass the test of statistics, but not the test of practical acceptance that is inherent to the study through the experienced observations made by the author.

8.4 PREDICTIVE EQUATIONS (GOVERNING EQUATIONS)

Figure 8.1 shows the governing equations that have been derived from this study and will be subsequently employed in estimating optimum exposed design dimensions. Tables 8.1, 8.2, 8.3 show the critical parameters for the individual stope configurations as identified in the preceding chapters. The governing equations are employed to predict the dilution. These equations are subsequently compared to the observed dilution. The average absolute difference in estimation is 2.4% for the isolated, 1.8% for the en echelon and 2.7% for the rib configurations. These errors of estimation are determined for the sample and for the population estimate, Figure 8.1. Figure 8.7 graphically depicts the predicted versus observed dilution for the individual stope databases. The upper and lower bounding lines, figure 8.7, represent a 68% (one standard deviation) confidence that the observed value will fall within the ranges delineated. A further observation is that one is 84% confident that the observed dilution would be less than the mean estimated dilution plus one standard deviation. The above is only true if the sample population can be approximated by a normal distribution. Probability graph paper is employed which plots the cumulative relative frequency of the differences between the estimated and observed dilutions for the isolated case, Figure 8.8. The sample is "normally distributed" since a linear plot is achieved (Spiegel, 1973). This is generally the case since it is inherent to the definition of correlation that the predicted dilution is the mean estimate of the best fit expression.

Table 8.1: Comparison Predicted/Observed - Isolated

ISOLATED STOPES DATA BASE — NUMBER OF STOPES=22

EMPIRICAL EQUATION : DILUTION(%) = 8.6 - 0.05(RMR) - 12.2(E.R.) + 0.0032(AREA)

r = 0.79 , r^2=0.62

No.	Stope	RMR(%)	E.R.(m^2/ath)	Area(m^2)	Obs. Dil(%)	Pred. Dil(%)	Diff.(%)
1	260 11 F	66	0.19	675	5	3	2
2	260 11 F	66	0.22	2385	10	9	1
3	260 18 J	51	0.30	504	3	2	1
4	260 18 J	51	0.40	1008	6	3	3
5	260 18 J	51	0.40	2016	6	6	-0
6	260 18 J	51	0.30	2856	9	11	-2
7	260 16 M	80	0.25	570	2	0	2
8	260 16 M	80	0.36	1425	6	2	4
9	260 16 M	80	0.37	1900	7	4	3
10	260 16 M	80	0.38	2755	8	7	1
11	260 16 M	80	0.21	4270	9	15	-6
12	270 9 J	46	0.15	624	6	5	1
13	270 9 J	46	0.09	1248	11	8	3
14	320 14 NE	25	0.21	4620	20	21	-1
15	320 13 E	79	0.13	1280	6	5	1
16	320 15 M	66	0.10	200	0	2	-2
17	320 15 M	66	0.14	675	1	3	-2
18	320 15 M	66	0.22	1275	2	5	-3
19	320 15 M	66	0.22	1875	3	7	-4
20	320 15 M	66	0.22	2400	3	9	-6
21	320 18 JN	81	0.22	900	9	2	7
22	320 19 J	84	0.15	600	0	1	-1
23	320 19 J	84	0.18	1200	4	3	1
24	320 19 J	84	0.16	2400	6	8	-2
25	320 11 B	41	0.20	3465	22	15	7
26	340 11 C	43	0.13	640	5	5	-0
27	340 11 C	43	0.14	1680	9	9	-0
28	370 21 JN	3	0.32	1924	14	11	3
29	370 15 M	80	0.09	1748	6	7	-1
30	370 10 B	51	0.12	504	2	4	-2
31	370 10 B	51	0.11	1008	3	6	-3
32	370 15 C	51	0.21	567	0	3	-3
33	370 15 C	51	0.19	1197	7	6	1
34	370 15 C	51	0.17	2709	11	12	-1
35	370 19 J	43	0.16	240	0	4	-4
36	370 19 J	43	0.19	480	0	4	-4
37	370 19 J	43	0.20	900	5	6	-1
38	370 19 J	43	0.13	1740	13	10	3
39	370 16 M	80	0.12	2052	7	8	-1
40	370 12 13F	70	0.11	480	0	3	-3
41	370 12 13F	70	0.13	1260	3	5	-2
42	430 13 B F/W	80	0.08	180	2	1	1
43	430 13 B F/W	80	0.13	300	4	1	3
44	430 13 B F/W	80	0.16	600	5	2	3
45	430 13 B F/W	80	0.16	960	5	3	2
46	430 13 B F/W	80	0.16	1260	5	4	1
47	430 13 B F/W	80	0.16	1560	6	5	1
48	430 13 B F/W	80	0.16	1860	6	6	-0
49	430 13 B F/W	80	0.15	2160	7	8	-1
50	430 13 B F/W	80	0.13	2520	10	9	1
51	430 14 B	80	0.06	180	1	1	-0
52	430 14 B	80	0.09	360	3	2	1
53	430 14 B	80	0.11	660	6	2	4
54	430 14 B	80	0.02	1020	8	5	3
55	430 14 B	80	0.03	1320	9	6	3
56	430 14 B	80	0.03	2400	12	10	2
57	430 21 K	70	0.21	520	1	2	-1
58	430 21 K	70	0.26	1040	1	3	-2
59	430 21 K	70	0.25	2080	2	7	-5
60	430 12 F	32	0.11	510	1	6	-5
61	430 12 F	32	0.10	2550	25	14	11

Table 8.2: Comparison Predicted/Observed - Echelon

ECHELON STOPES DATA BASE — NUMBER OF STOPES = 12

EMPIRICAL EQUATION : DILUTION(%) = 10.2 −0.13(RMR) − 14.8(E.R.) + 0.003(AREA)

$r = 0.83$, $r^2 = 2.61$

No.	Stope	RMR(%)	E.R.(10^{-6}/psi)	Area(ft^2)	Res. Dil(%)	Pred.Dil(%)	Diff.(%)
1	370 12 HE	47	0.10	720	11	5	6
2	370 12 HE	47	0.14	2160	12	9	3
3	370 10 J	56	0.21	1955	4	3	1
4	370 10 J	56	0.13	2525	10	9	1
5	370 20 KH	45	0.09	384	1	4	-3
6	370 20 KH	45	0.12	704	3	5	-2
7	370 20 KH	45	0.15	1408	9	6	3
8	370 20 KH	45	0.13	2944	12	11	1
9	370 20 KH	45	0.13	2336	12	12	1
10	370 12 D	49	0.18	200	1	2	-1
11	370 12 D	49	0.24	400	3	2	1
12	370 12 D	49	0.29	800	3	3	-0
13	370 12 D	49	0.11	1290	7	6	1
14	370 12 D	49	0.10	1750	10	8	2
15	370 15 K	62	0.18	345	0	1	-1
16	370 15 K	62	0.22	805	1	1	-0
17	370 15 K	62	0.21	1610	3	4	-1
18	370 15 K	62	0.22	2415	4	6	-2
19	370 15 K	62	0.25	3222	5	8	-3
20	370 15 K	62	0.32	4025	8	11	-3
21	370 21 J	60	0.23	325	0	0	-0
22	370 21 J	60	0.23	650	1	1	-0
23	370 21 J	60	0.21	1300	3	3	-0
24	370 21 J	60	0.19	1950	4	6	-2
25	370 21 KH	53	0.23	704	2	5	-3
26	370 21 KH	53	0.26	1320	12	7	5
27	370 12 D	26	0.04	255	2	7	-5
28	370 12 D	26	0.07	425	7	7	-0
29	370 12 D	26	0.08	850	11	8	3
30	370 12 D	26	0.08	3230	15	15	-0
31	430 12 F	23	0.19	672	1	5	-4
32	430 12 F	23	0.29	1470	9	6	2
33	430 12 D	26	0.04	255	2	7	-5
34	430 12 D	26	0.07	425	7	7	-0
35	430 12 D	26	0.08	850	11	8	3
36	430 12 D	26	0.08	3230	15	15	-0
37	430 21 J F/W	65	0.05	212	4	2	2
38	430 21 J F/W	65	0.04	954	5	4	1
39	430 13 D H/W	52	0.13	320	2	3	-1
40	430 13 D H/W	52	0.14	576	4	3	1
41	430 13 D H/W	52	0.16	1216	5	5	1
42	430 13 D H/W	52	0.17	1792	7	6	1
43	430 13 D H/W	52	0.12	2368	8	9	-1
44	430 13 D H/W	52	0.11	2560	8	10	-2

Table 8.3: Comparison Predicted/Observed - Rib

RIB STOPES DATA BASE — NUMBER OF STOPES = 9

EMPIRICAL EQUATION : DILUTION(%) = 15.8 − 0.18(RMR) − 7.7(E.R.) + 0.00[illegible]AREA)

$r = 0.89$, $r^2 = 4.3$

No.	Stope	RMR(%)	E.R.(10^{-6}/psi)	Area(ft^2)	Res. Dil(%)	Pred.Dil(%)	Diff.(%)
1	370 10 B	34	0.22	448	0	5	-5
2	370 10 B	34	0.22	784	8	10	-2
3	370 10 B	34	0.25	1680	12	12	1
4	370 10 B	34	0.27	2464	16	14	2
5	370 10 B	34	0.29	3360	16	15	-0
6	370 10 B	34	0.30	4144	16	18	-2
7	370 10 B	34	0.31	4928	16	20	-4
8	370 10 B	34	0.28	5152	16	21	-5
9	370 12 B	23	0.24	2120	27	15	12
10	340 12 C	30	0.12	240	8	10	-2
11	340 12 C	30	0.16	520	10	11	-1
12	370 20 J	69	0.04	225	5	4	1
13	370 20 J	69	0.08	450	7	4	3
14	370 14 C	47	0.16	780	8	8	-0
15	370 14 C	47	0.20	2080	13	11	2
16	370 18 J	54	0.20	525	2	6	-4
17	370 18 J	54	0.30	1050	9	7	2
18	370 18 J	54	0.27	2175	14	9	5
19	370 18 J	54	0.31	3225	14	12	2
20	370 11 F	57	0.04	500	9	7	2
21	430 15 B	51	0.15	384	2	6	-4
22	430 15 B	51	0.23	704	6	7	-1
23	430 15 B	51	0.23	1408	9	9	0
24	430 15 B	51	0.24	2112	11	10	1
25	430 15 B	51	0.15	2908	14	13	1
26	430 20 K	74	0.28	505	1	2	-1
27	430 20 K	74	0.18	1012	1	4	-3
28	430 20 K	74	0.21	1748	2	5	-3

ISOLATED STOPES (61 OBS)

DIL(%) = 8.6 - 0.09(RMR) - 13.2(EXP.RATE) + .0038(AREA)

r = ± 0.79 s = ± 3%

DIL(%) = 5.9 - 0.08(RMR) - 10.1(EXP.RATE) + .08(HYD.RAD)

r = ± 0.78 s = ± 3%

EN ECHELON STOPES (44 OBS)

DIL(%) = 10.3 - 0.13(RMR) - 14.8(EXP.RATE) + 0.0030(AREA)

r = ± 0.83 s = ± 2%

DIL(%) = 8.8 - .12(RMR) - 18.2(EXP.RATE) + .8(HYD.RAD)

r = ± .83 s = ± 2%

RIB STOPES (28 OBS)

DIL(%) = 15.8 = 0.18(RMR) - 7.7(EXP.RATE) + 0.0026(AREA)

r = ± 0.8 s = ± 4%

DIL(%) = 16.2 - .22(RMR) - 11.4(EXP.RATE) + .9(HYD.RAD)

r = ± 0.81 s = ± 4%

where:

DIL(%) - DILUTION(%), i.e. 16%, DIL = 16
RMR - ROCK MASS RATING (%), i.e. 40%, RMR = 40
EXP.RATE - EXPOSURE RATE (x1000 m^2/mth)
AREA - EXPOSED SURFACE AREA (m^2)
HYD.RAD - HYDRAULIC RADIUS (m)

Figure 8.1: Governing Equations

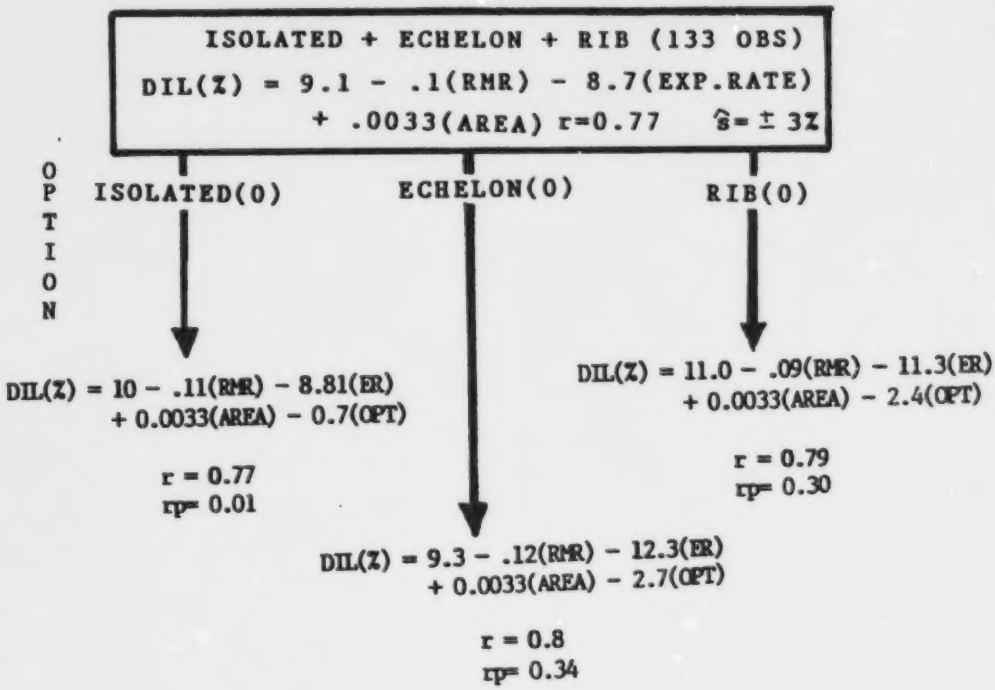

Figure 8.2: Stope Configuration - All Stopes

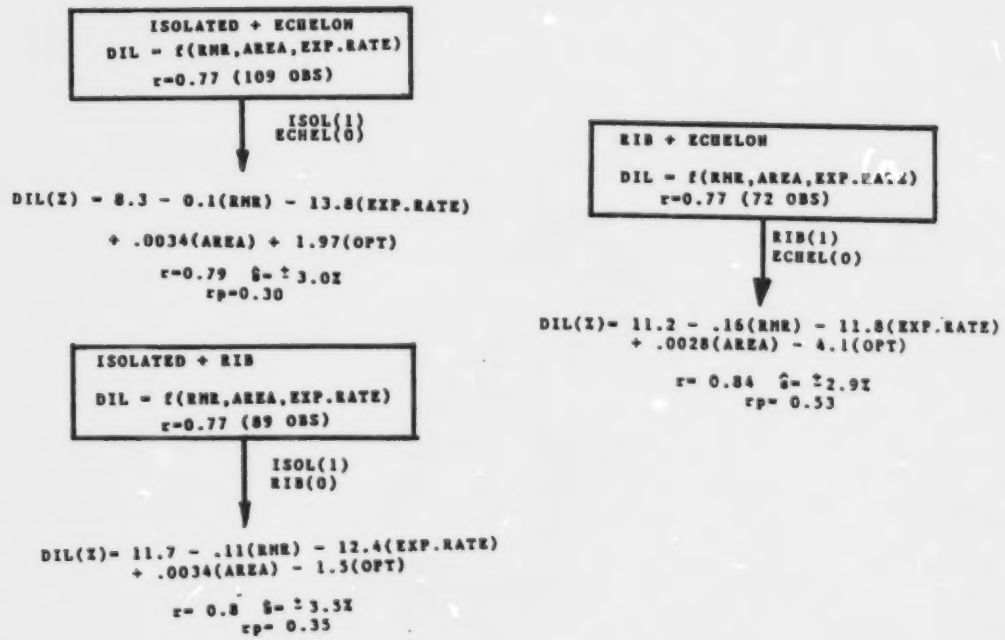

Figure 8.3: Stope Configuration - Combined

ISOLATED STOPES (61 OBS)

DIL(%) = 7.0 - .08(RMR) - 7.4(EXP.RATE) + .26(SPAN)
$r \pm = 0.74$ $\hat{s} = \pm 3.6\%$

ECHELON STOPES (41 OBS)

DIL(%) = 8.8 - .10(RMR) - 17.1(EXP.RATE) + .23(SPAN)
$r \pm = 0.83$ $\hat{s} = \pm 2.4\%$

RIB STOPES (28 OBS)

DIL(%) = 17.6 - .25(RMR) - 3.7(EXP.RATE) + .22(SPAN)
$r \pm = 0.79$ $\hat{s} = \pm 4.1\%$

where:

RMR = ROCK MASS RATING (%)
EXP.RATE = EXPOSURE RATE (x1000m²/mth)
SPAN = SPAN (m)

Figure 8.4: Span Derivation

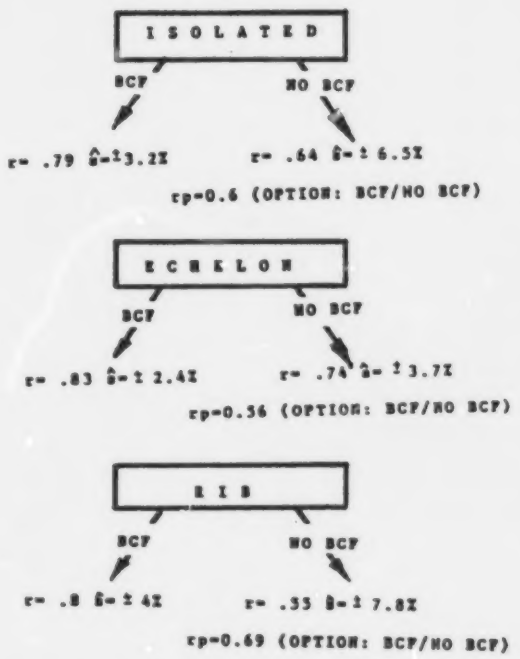

Figure 8.5: Incorporating Blast Correction Factor

I S O L A T E D (13 STOPES, 36 OBS.) →	DIL(%) = 11.9 - .12(RMR) - 12.8(EXP.RATE) + 0.0035(AREA) r=0.78 $\hat{s}$=±3.4%
E C H E L O N (2 STOPES, 12 OBS.) →	r= 0.98 $\hat{s}$=±0.69%
R I B (4 STOPES, 16 OBS.) →	r=0.84 $\hat{s}$=±4.4%

Figure 8.6: Stopes with "BCF > 0" Omitted From Data Base

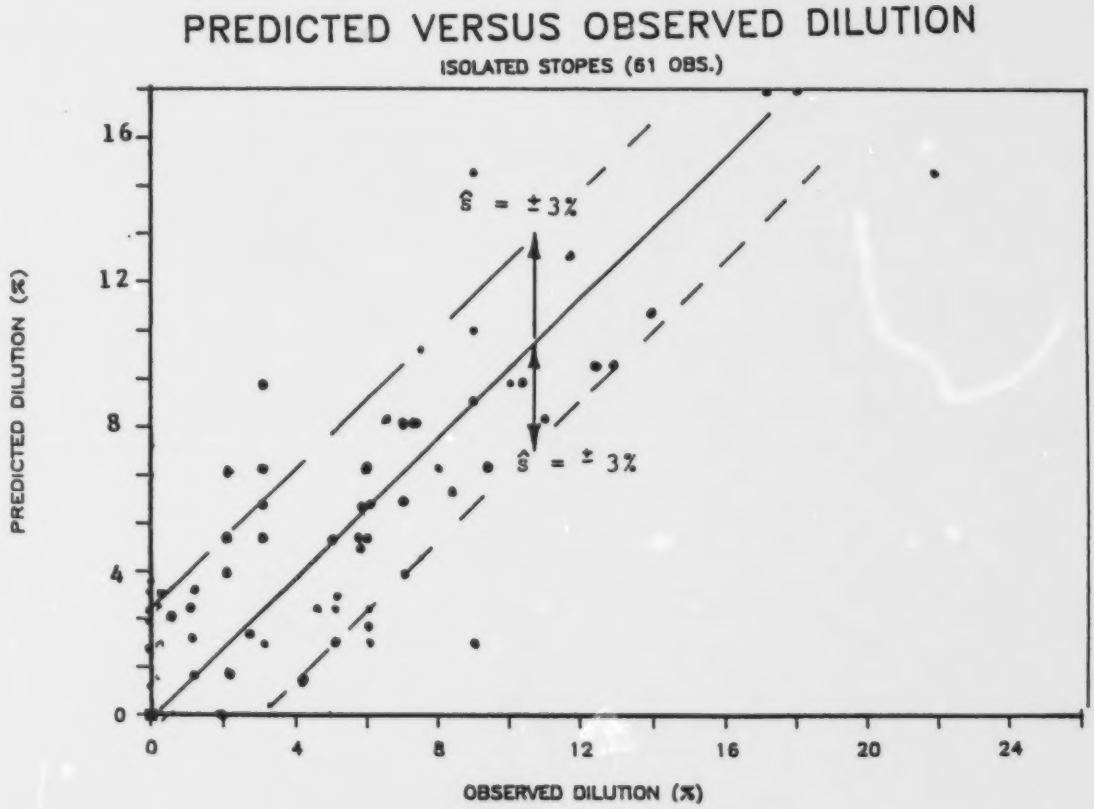

Figure 8.7: Predicted vs Recorded Dilution

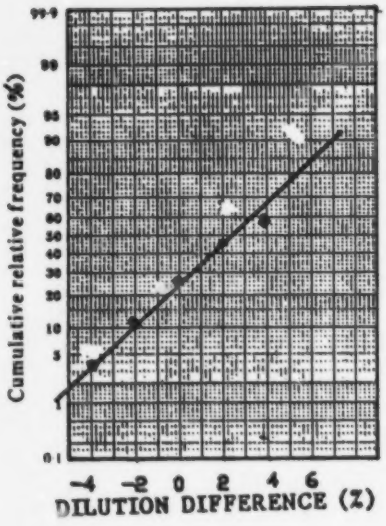

Figure 8.8: Cumulative Relative Frequency vs Dilution Difference

CHAPTER NINE
APPLICATION

9.1 INTRODUCTION

The governing equations, Figure 8.1, were employed to estimate dilutions for twenty (20) stopes that were mined subsequent to the study. A brief comparison between the most promising methods is also summarized.

9.2 CALIBRATED DATABASE

The stopes that comprise the calibrated database are shown in Table 9.1. They consist of:

Three isolated stopes (2 observations)
Two en echelon stopes (7 observations)
Fifteen rib stopes (19 observations)

The governing equations (hydraulic radius derivations), Figure 8.1, were employed to arrive at an estimated total dilution. An average BCF = 3% was employed, Table 7.3. These results are shown in Table 9.2. An average error of estimate of 3% was obtained. The values were tabulated by the Ruttan Mine personnel and the "BCF" values were recorded as dilution attributed to the slot removal. The results were subsequently added to the original database to arrive at the empirical equations shown in Figure 9.1. The coefficients for the augmented database are similar to the original governing equations.

The calibrated stopes are in close approximation to the predictive dilutions yielded by the governing equations outlined in Figure 8.1.

9.3 OTHER METHODS

The isolated database was compared to the empirical methods of Mathews et al (1981), Laubscher (1976), Barton (1974) and Bieniawski (1972). It is intended to introduce the methods and to relate them to that observed at Ruttan. Figure 9.2 shows the relationship that exists between that of Mathews and the observed database at Ruttan. It incorporates the following four parameters, Figure 9.2 into a stability number:

* Barton's Q rating. This value can be derived from the "Rock Mass Rating".

* Stress Factor (A). This factor empirically relates the strength of the intact rock to the induced stress. This value is equated to "1.0" where tensile zones are observed (Ruttan).

* Structure Defect Parameter. This factor relates empirically the orientation of structure with respect to the stope. This factor is equated to "0.5" for structure paralleling the stope walls (Ruttan).

* Stope Inclination Parameter. This factor accounts for the stope inclination. This value is equated to "5.6" for stopes inclined at 70 degrees (Ruttan).

Figure 9.2 shows that the stability number (N), once plotted against the shape factor (hydraulic radius), can be categorized into stable, potentially unstable or potentially caving regions. Observations were plotted within zones of instability, whereas lower dilutions were associated with more stable areas.

Figure 9.3a relates RMR to the critical hydraulic radius that would cause instability for an open stope operation as defined by Laubscher. For rock mass ratings similar to that of Ruttan, Laubscher suggested that the hydraulic radius should not exceed 24 meters. A stope height of 60 meters would dictate a maximum stope span of 240 meters. This method of design is not based upon observations from open stoping, but from caving operations. The exposed surface area in caving operations is gently sloping, whereas in open stope operations, the hangingwall is generally inclined. The author would like to note that the definition as originally stated by Laubscher in describing hydraulic radius for an open stope, is vague since it was derived for caving operations where flat backs are the norm. The hydraulic radius, as defined in Chapter 7 was employed in the author's interpretation of critical span.

Figure 9.3b shows that Barton would design unsupported spans between 10 to 20 meters for the average rock mass ratings recorded at Ruttan. Bieniawski would predict unsupported spans of between 4 to 9 meters, Figure 9.3c. This shows the conservatism associated with the individual databases which were derived primarily from civil projects.

Figure 9.4 shows the method as proposed by Beer and Meek (1982) in terms of predicting stope spans employing Voussoir arch theory. It is particularly applicable in the design of excavations in well-bedded formations where the direction of the bedding planes parallel the long dimension of the opening. It is assumed that the ground above the hangingwall is completely distressed in the direction normal to bedding. In addition, it assumes that the rock mass has parted along smooth bedding plane breaks, thereby forming a series of "no-tension" beam members.

Failure could be "flexural" or "shear" failure, as indicated in Figure 9.4a. Figure 9.4c shows the suggested critical span given the:

* strata thickness (0.3m - 1m);
* modulus of deformation for the rock mass (8000MPa);
* stope inclination (65°);
* uniaxial compressive strength (100MPa).

Curve "A" in Figure 9.4c describes the plan strain situation, whereas curve "E" describes that of a square hangingwall. The intermediate curves relate the critical design for the rectangular configurations, Figure 9.4b.

The following parameters are required for input into Figure 9.4c:

* The average joint spacing at Ruttan for the isolated database is 0.3 meters to 1 meter, Table 7.4.

* The in-situ modulus of deformation for an "RMR=64%" is 22GPa. According to Brown (1985), the value should be halved, thereby employing a factor of safety of two. Consequently, the in-situ modulus is 11GPa for the Ruttan database.

* The unconfined compressive strength is 50 - 100MPa, Table 7.4.

Employing the curves shown in Figure 9.4 would approximate the critical suggested span given the above input parameters. This analysis suggests that the critical span should not exceed 20 meters to 45 meters. The similarity in the predicted and actual observed spans employed at Ruttan indicate that the Voussoir method does have application for stope design. The difficulty arises in estimating the strata thickness and in calibrating the strength parameters to that of the mine database.

The alternative methods were introduced to show that workable solutions can be obtained with the increased application of the individual methods and the subsequent calibration to actual observations. This would result in a more comprehensive method for the design of open stope spans.

9.4 TEST STOPE

9.4.1 INTRODUCTION

Instrumentation in terms of wire extensometers, stress meters and shear strips were installed in 800-26J. This stope was the first to be mined in the Lower Mine (below

430mL). It also was the largest to be excavated since the commencement of mining. The following questions were required to be answered by monitoring this test stope:

1. Does the empirical approach to design as developed from stope data in the Upper Mine valid at depth?

   This has various consequence towards design in that the empirical approach has shown that dilution will not increase with depth since it is controlled primarily by the exposed surface area.

2. How valid are the assumptions made in the empirical design approach?

   Various assumptions were made concerning the suitability of the empirical model, the most critical being that the hangingwall and footwall contacts are in a state of relaxation. In addition, this state of relaxation extends beyond the zone encompassing the resultant wall slough.

3. Can a numerical model be calibrated to quantifiably predict stresses and displacements surrounding an individual stope?

   This is particularly important for the design of rib pillars and in the estimation of how development openings will respond in the vicinity of large stopes.

4. How does the hangingwall respond upon extraction of the stope?

   This refers to the failure model. Does wall slough occur immediately upon critical excavation or requires a certain degree of strain relief prior to failure?

9.4.2 TEST STOPE 800-26J

9.4.2.1 Stope Geometry

Figure 9.5 shows an isometric view of 800-26J and the surrounding instrumentation. Figure 9.6 represents the final stope longitudinal showing the individual cuts extracted. Figure 9.7 is a plan of the 730mL (top of first lift) outlining the stope and the respective locations of the extensometers and stress meters that were installed (Appendix I).

The individual sections are represented in Figure 9.8a,b,c. The stope is 42 meters in strike length, having a stope height of 75 meters and an apparent width of 23 meters. The stope is inclined at 70 degrees, Figure 9.5.

9.4.2.2 Production History

Figure 9.6 shows the individual blast sequence as the stope was extracted. The stope was extracted employing large diameter (165mm) drilling and the "VCR + Slash" method. The upper drill drive for the first lift was located at the 730mL whereas the draw level was at 800mL.

The production record is summarized in Table 9.3 and graphically displayed in Figure 9.9.

The undercut was removed in October, 1985, and stope blasting continued until July 21, 1986. The stope was emptied on December 12, 1986 and prepared for filling for subsequent removal of the 2nd lift (660-730mL's).

The observed dilution is shown in Table 9.4 and Figure 9.10 as a function of total undiluted reserves excavated.

9.4.2.3 Instrumentation

Test stope instrumentation is comprised of wire extensometers, stress meters and shear strips. The instrumentation was installed in the footwall were lost soon after due to damage resulting from vehicle traffic.

Each wire extensometers consisted of five (5) anchors and all instrumentation were monitored weekly.

9.4.2.3.1 Extensometers

Extensometers X7301 were installed in the slot area of the test stope. It's purpose was to monitor the deflection of the hangingwall. A shear strip was installed adjacent to anchor 1, Figure 9.8b. The history of X7301 is shown in Figure 9.11. The plots represent cumulative displacement with respect to an initial arbitrary value. The absolute displacement is determined by subtracting the initial reading. The initial observations indicate that minor displacement occurred prior to January 24, 1986, considering that the accuracy of the extensometers are generally within μ241 0.025cm. The extensometer anchors only commenced to react when the slot was excavated in the vicinity of the anchor, Figure 9.6. This occurred after "cut 20X" whereafter a sharp rise occurred after the removal of "cut 22X". The observations were modelled in section 4.3.8. Anchor 1 was lost between March 11 and 20, 1986, due to a wall slough as shown in Figure 9.8B. This was verified by the shear strip which recorded that a 6 meter slough of ground occurred. This

coincides with the loss of anchor 1. Consequently, Ruttan is confident that the shear strips are a reliable warning devices when a ground fall is involved.

The anchors were all inoperable after July 23 where it was noticed that a slough of ground resulted in the anchors to become wedged into the drill hole. The extent of this slough is not known.

All anchors reacted at some stage converging towards the stope, therefore indicating a relaxed zone existing in the direction measured. This was verified by BESOL (Chapter 4.3.8).

X7302 was installed along the west extremity of the test stope. It traversed the hangingwall into the footwall, Figure 9.8a. Figure 9.11b and Table 9.5 show the history accompanying this extensometer. It was installed in order to monitor the behaviour of the footwall, hangingwall and pillar as the stope is extracted. Generally anchors 1 & 2 which were located in the footwall showed convergence towards the stope (i.e. anchor moved towards collar). Anchor 3 which was located in the centre of the pillar showed slippage but generally minimal movement. Anchors 4 & 5 showed that the hangingwall converged towards the void. This was to be expected as shown in Figure 9.8a. Loss of the anchors occurred after June 14, 1986, due to blasting of ground in which the anchors were installed. All anchors showed stope closure and consequently ground relaxation in the plan of the closure. The shear strip paralleling anchor 4 had indicated that a wall slough of five (5) meters occurred after June 13, 1986. Again it verified the loss of anchor 4.

X7303 was installed along the east extremity of the test stope. It traversed the hangingwall into the footwall, Figure 9.8c. Figure 9.11c and Table 9.5 show the history accompanying this extensometer. It was installed in order to monitor the behaviour of the hangingwall and footwall similar to that of X7302.

Similar observations to X7302 were made and, in particular, anchor 4 indicated minimal movement, as it should have been observed, since it was at the centre of the pillar.

The extensometers were reviewed qualitatively and have functioned in a consistent and predictive manner. They showed similar displacements to that modelled in section 4.3.8. The extensometers have showed that the stope walls are in a state of relaxation in the plane of the measurement. The shear strips have proved to be reliable warning devices.

9.4.2.3.2 Stress Meters

The stress meter locations are shown in Figure 9.7. Figures 9.12a,b,c show the North-South, East-West, and Vertical stress meter results. The hangingwall was generally in a state of relaxation as shown by the reduction in the measured stress in both the NS and EW direction (i.e. gauge 2NS and 2EW).

The zone, however, is limited as shown by gauge 5EW, 1EW and 3NS (approximately one stope width). The pillar is generally in a state of confinement as shown by the NS stress increase in gauge 2NS. Stope blasting was completed by July 21, 1986.

It is generally concluded from the observations and modelling (Chapter 4.3.8) of the test stope that the zone encompassing the stope footwall and hangingwall is in a state of relaxation. A stress drop of 12 MPa was observed with BESOL in the H/W of 800-26J, Figure 4.25, at the location where S7302E was installed. The actual stress drop as recorded by S7302E was 9.7 MPa, Figure 9.12b. The differences are most likely due to not being able to install the stress meters at the mid stope height due to access. Figure 4.25 indications correspond to stresses at the 760 m L, whereas the stress meters were located at the 730 m L.

9.4.3 EMPIRICAL DESIGN

The method of stope design adopted by Ruttan is based upon an empirically derived expression that relates the resultant dilution to the exposed surface area, the rock mass rating and the exposure rate. These parameters have been determined upon analysing the variables that would yield the greatest observed dilution. It is based upon the Ruttan database whereby forty-three stopes were analysed at various stages of extraction. A multivariate analysis yielded the following statistically significant design equation for an isolated stope:

Dil(%) =	5.9 - .08(RMR) - 10.1 (EXP.RATE) + .98 (HR) eqn. 1
Dil(%):	External dilution measured as tonnes waste/ore
RMR(%):	Rock Mass Rating of the hangingwall
ER(1000m²/mth):	Exposure Rate measured as mining rate/stope width
HR(m):	Hydraulic Radius measured as exposed surface $\frac{\text{area}}{\text{perimeter}}$

A stope characterization was performed upon 800-26J which yielded the following:

FOOTWALL

Rock Type:	Massive Sulphide
RMR:	70%
Strength:	110 MPa
Joint Spacing:	1 meter
RQD:	75%
Joint Condition:	Slightly rough surfaces, separation <1mm, hard joint wall rock

ORE

Rock Type:	Massive Sulphide
RMR:	82%
Strength:	90 MPa
Joint Spacing:	2 meters
RQD:	80%
Joint Condition:	Slightly rough surfaces, separation <1mm, hard joint wall rock

HANGINGWALL

Rock Type:	Acid Sediments and Semi-Massive Sulphide
RMR:	75%
Strength:	75 MPa
Joint Spacing:	1.3 meters
RQD:	85%
Joint Condition:	Slightly rough surfaces, separation <1mm, hard joint wall rock

9.4.3.1 Design Parameters

The following input parameters are required to evaluate the predicted dilution equation.

Stope Length:	42 meters
Stope Width:	23 meters
Stope Height:	75 meters
Tonnage Factor:	0.254 m^3/tonne
RMR:	75% (H/W)
Excavation Rate:	20000 tonnes/mth or 4938 m^3/mth
Stope Type:	Isolated

Exposure Rate: 215m²/mth (design): 213m²/mth (actual)
Hydraulic Radius: 13.5m (42 x 75)/(42 x 2 + 75 x 2)

This would yield:

RMR = 75% (Note F/W RMR is lower)
Exposure Rate = .215 x 1000 m²/mth
Hydraulic Radius = 13.5m (42 x 75)/ (84 + 150)

Dil(5) = 5.9 - 0.08(75) - 10.1(.215) + .98(13.5) + 3

The above would yield a predicted dilution of 14% assuming an average blast correction factor of 3% (eqn. 1).

The predicted versus actual dilution observed is shown in Figure 9.10 and Table 9.4. Note that in Table 9.4 that the cumulative dilution is calculated as cumulative slough conveyed divided by cumulative reserves conveyed. Cumulative reserves conveyed = tonnes trammed/(1 + Dil (%)) whereas the cumulative slough conveyed = tonnes trammed - cumulative reserves conveyed. The expression employed in the past whereby tonnes waste = Dil (%) x tonnes trammed is not consistent with the definition for external dilution which is calculated as tonnes external waste/tonnes ore reserves. Note that the tonnes trammed represents the diluted ore reserves.

The empirical expression approximates accurately the observed dilution as shown by Figure 9.10. The total cumulative reserves conveyed, Table 9.4, of 75040m³ represents a volume of 75 meters (ht.) x 23 meters (wdth.) x 43.5 meters (length). The actual stope span is 43 meters which indicates that the cumulative reserves volume evaluated based upon the observed dilution closely parallels the final stope dimensions actually recorded. The zero dilution recorded for the first 2500 m³ indicates that the BCF = 0%. The actual recorded is 10%. The incremental dilution which evaluates the dilution observed for each 10% cut of stope excavation is shown in Figure 9.13. It indicates that the dilution upon excavation is 0%, which according to definition indicates that the Blast Correction Factor (BCF) is equal to 0% and not an average as calculated from previous stopes of 3%. Associated with mining the last 10% of the stope volume, is a dilution of 31% observed or 18% predicted. The predicted versus observed dilutions closely approximate each other and for purposes of design it is recommended based on the test stope that:

1. The empirical stope dilution method be employed for estimating cumulative dilution based upon a given set of stope characteristics.

2. The incremental stope dilution approach be employed to give the operator a more realistic picture of what the dilution can be expected for particular intervals. Larger dilutions are expected at the end of the stope life which are more readily observed when an incremental approach is employed. This may result in modifying scheduling of stopes in particular for the mining of second lifts which require the complete removal of the first lift prior to drawing the muck from the second lift.

9.4.4 CONCLUSIONS

The above analysis of the instrumentation indicated that the hangingwall and footwall of the test stope is in a state of relaxation with the boundary pillars exhibiting compression. The extent of the relaxed zone approximates one stope diameter (width). A quantitative analysis was performed in section 4.3 which involves numerical calibration through modelling. The empirical approach is an accurate tool for the estimation of how the stope behaves during mining. This behaviour being translated into observed dilution.

The design equations that have been developed are presently being applied employing hydraulic radius. Similar equations have been developed using exposed surface area as an input parameter. The deviation in predicted dilutions are insignificant when area or hydraulic radius is used for single lifts. Since most of the database that comprised the input for the derivation of the governing equations is based upon a single lift one must proceed with caution when extrapolating the above to two double lift stopes. The deviation between area and hydraulic radius derived dilution is large when double lifts are involved. This difference is being evaluated.

TABLE 9:1

STOPES MINED SUBSEQUENT TO STUDY

CALIBRATED DATABASE - STOPES MINED SUBSEQUENT TO STUDY (20 STOPES)

NO.	STOPE	RMR %	HT. (m)	WDTH (m)	VOL. (m^3)	DIL %	SPAN (m)	H.R. (m)	ER (m^2/MTH)	BCF %	CONFIGURATION
1	320-I	80	125	7	10,000	5	13	5.9	.24	0	ISOLATED
2	260-15H	75	55	15	20,000	6	36	10.9	.18	0	ISOLATED
3	800-26J	75	75	23	75,000	12	42	13.5	.21	0	ISOLATED
4	490-1D	49	45	23	40,000	10	40	10.6	.16	3	ECHELON
5	370-14CR	47	50	7	5,400	8	25	8.3	.15	3	ECHELON
6	260-14B	74	50	17	27,000	12	32	9.8	.39	3	RIB
7	290-11C	53	62	16	31,000	12	30	10.1	.13	0	RIB
8	340-10C	26	40	23	9,000	10	23	7.3	.31	7	RIB
9	260-11F	60	37	12	18,000	6	63	11.7	.45	0	RIB
10	320-9B	44	65	13	30,000	9	36	11.6	.33	4	RIB
11	660-4D	56	60	15	22,000	15	45	12.9	.16	0	RIB
12	260-19J	70	60	17	12,000	11	25	8.8	.18	3	RIB
13	260-17JN	75	75	11	21,000	10	54	15.7	.30	3	RIB
14	550-2D	57	24	25	51,000	7	42	7.6	.21	0	RIB
15	430-19J	63	55	12	20,000	16	43	12.1	.33	0	RIB
16	260-17J	53	60	13	36,000	16	50	13.6	.33	4	RIB
17	260-4/5CR	67	75	13	44,000	9	50	15	.36	3	RIB
18	260-15H	78	78	12	13,600	3	32	11.3	.57	0	RIB
19	340-9C	26	28	6	7,100	20	50	9.0	.35	6	RIB
20	430-20J	71	48	17	32,800	8	40	10.9	.21	0	RIB

* TOTAL DILUTION OBSERVE = DIL % + BCF

TABLE 9.2

CALIBRATED DATABASE - PREDICTED DILUTION

CALIBRATED DATABASE - STOPE MINED SUBSEQUENT TO STUDY (20 STOPES)

TYPE	NO.	STOPE	RMR %	E.R(m^2/MTH) X 1000	HR (m)	RES. DIL %	PRED. DIL %	DIFF. %	
ISOL	1	320-I	80	.24	5.9	5	6	+1	
	2	260-15H	75	.18	10.9	6	12	+6	
	3	800-26J	75	.21	13.5	12	14	+2	
ECHELON	4	490-1D	49	.16	10.6	10	11	+1	
	5	370-14CR	47	.15	8.3	8	10	+2	
	6	260-14B	60	.39	9.8	12	10	+2	
RIB	7	290-11C	53	.13	10.1	12	15	+3	
	8	340-10C	26	.31	7.3	10	17	+7	*
	9	260-11F	60	.45	11.7	6	11	+5	*
	10	320-9B	44	.33	11.6	9	16	+7	*
	11	660-4D	56	.16	12.9	15	17	+2	
	12	260-19J	70	.18	8.8	11	10	-1	
	13	260-17JN	75	.30	15.7	10	13	+3	
	14	550-2D	57	.21	7.6	7	11	+4	
	15	430-19J	63	.33	12.1	16	13	-3	
	16	260-17J	53	.33	13.6	16	16	0	
	17	260-4/5CR	67	.36	15	9	14	+5	
	18	260-15H	78	.57	11.3	3	6	+3	
	19	340-9C	26	.35	9.0	20	18	-2	
	20	430-20J	71	.21	10.0	8	11	+3	

* STOPE CHOKE BLASTED

ISOLATED DIL(%) = 5.9 - .08 (RMR) - 10.1 (ER) + .98(HR) + 3%
RIB DIL(%) = 16.2 - .22 (RMR) - 11.4 (ER) + .9 (HR) + 3%
ECHELON DIL(%) = 8.8 - .12 (RMR) - 18.2 (ER) + .8 (HR) + 3%

TABLE 9.3

BLAST PRODUCTION RECORD - 800-26J

Date Blasted	Tonnes	Cumulative Tonnes	
29-Oct-85	100,569	100,569	Undercut removed - Month of October
13-Nov-85	2,000	102,569	11X Removed
15-Nov-85	1,750	104,319	12X Removed
25-Nov-85	5,515	109,834	13X Removed
27-Nov-85	2,727	112,561	14X Removed
02-Dec-85	4,240	116,801	15X Removed
06-Dec-85	7,250	124,051	16X Removed
13-Dec-85	4,255	128,306	17X Removed
03-Jan-86	15,103	143,409	18X Removed
17-Jan-86	4,090	147,499	19X Removed
31-Jan-86	36,000	183,499	20X Removed
07-Feb-86	4,000	187,499	21X Removed
05-Mar-86	46,068	233,567	22X Removed
16-Apr-86	3,176	236,743	23X Removed
04-Jun-86	6,272	243,015	A24 Undercut
09-Jan-86	6,239	249,254	A25 Undercut
14-Jun-86	25,000	274,254	26X Removed
05-Jul-86	8,242	282,496	27X Removed
21-Jul-86	43,065	325,561	28X Removed

TABLE 9.4

STOPE WORKSHEET - EMPIRICAL APPROACH TO DESIGN

STOPE: 800-26J

MONTH	CREDITED %	DIL (%)	CONVEYED RESERV(t)	CUM RESERV CONVEYED(t)	CUM RESERV VOL. (m^3)	SLOUGH CONVEYED(t)	CUM. SLOUGH CONVEYED(t)	CUM. DIL (%)	PRED. DIL (%)
Oct/85	19,295	0	19,295	19,295	4,764	0	0	0	0
Nov/85	6,000	0	6,000	25,295	6,245	0	0	0	0
Dec/85	32,132	3	31,196	56,491	13,948	936	936	2	2
Jan/86	33,660	5	32,057	88,548	21,863	1,603	2,539	3	4
Feb/86	29,541	4	28,405	116,953	28,876	1,136	3,675	3	5
Mar/86	26,884	10	24,220	141,393	34,910	2,444	6,119	4	6
Apr/86	26,148	8	24,211	165,604	40,888	1,937	8,056	5	7
May/86	34,301	7	32,057	197,661	48,803	2,244	10,300	5	8
Jun/86	30,512	11	27,488	225,149	55,589	3,024	13,324	6	9
Jul/86	17,130	11	15,432	240,582	59,400	1,698	15,021	6	9
Aug/86	12,300	12	10,982	251,564	62,111	1,318	16,339	6	10
Sep/86	21,312	17	18,215	269,779	66,609	3,097	19,436	7	10
Oct/86	23,255	20	19,379	289,159	71,393	3,876	23,311	8	11
Nov/86	20,975	42	14,771	303,930	75,040	6,204	29,515	10	11

ISOLATED STOPES (64 OBS., 25 STOPES)

DIL(%) = 6.5 - .09(RMR) - 10.1(EXP.RATE) + .94(HYD.RAD)

$r = \pm .7$ $\hat{s} = \pm 3.3\%$

ECHELON STOPES (46 OBS., 14 STOPES)

DIL(%) = 8.8 - .12(RMR) - 18.0(EXP.RATE) + .8(HYD.RAD)

$r = \pm 0.85$ $\hat{s} = \pm 2.3\%$

RIB STOPES (43 OBS., 14 STOPES)

DIL(%) = 17.1 - .23(RMR) - 13.9(EXP.RATE) + .8(HYD.RAD)

$r = \pm 0.76$ $\hat{s} = \pm 4\%$

Figure 9.1: Augmented Data Base

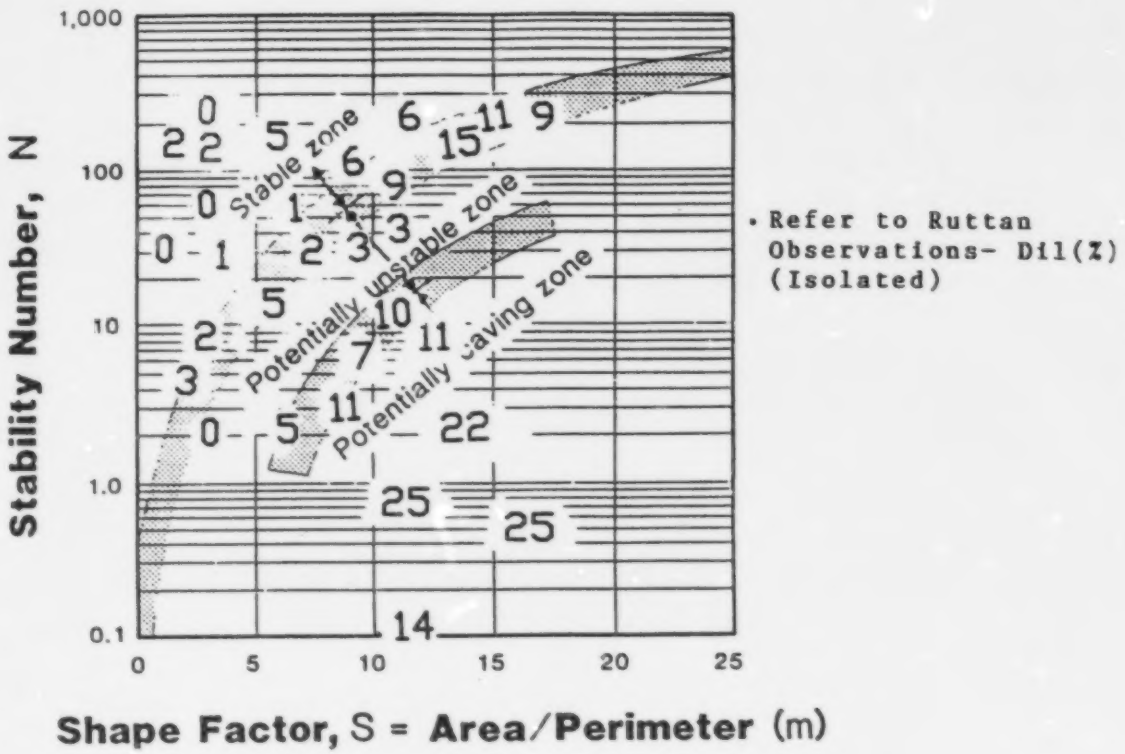

STABILITY NUMBER "N"

The stability number N is determined from the following equation:

$$N = Q' \times A \times B \times C$$

where
- Q' = modified NGI rock mass rating
- A = rock stress factor
- B = rock defect orientation factor
- C = orientation of design surface factor

Figure 9.2: Mathews Method of Span Determination (Mathews et al, 1981)

ADJUSTED CLASS RMR %	100 - 80	80 - 60	60 - 40	40 - 20	20 - 0
HYDRAULIC RADIUS		24	24 - 16	16 - 6	< 6

Figure 9.3a: Laubsher Approach to Span Design (Laubsher, 1976)

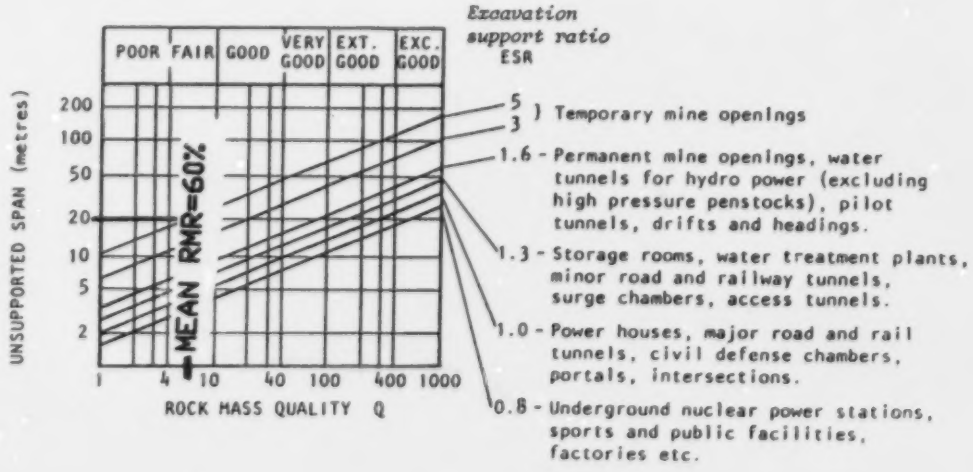

Figure 9.3b: Barton Approach to Span Design (Barton, 1974)

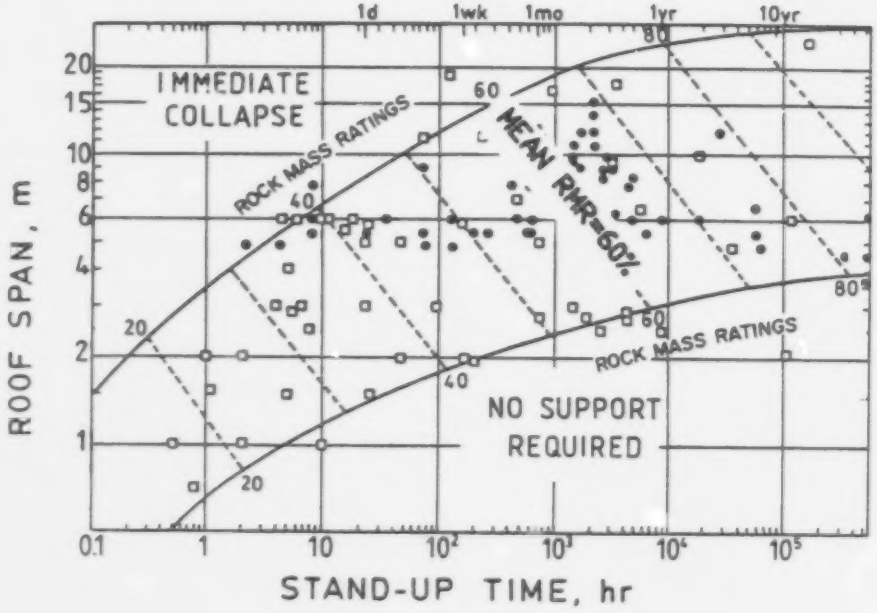

Figure 9.3c: RMR Method of Span Determination
(Bianiawski, 1984)

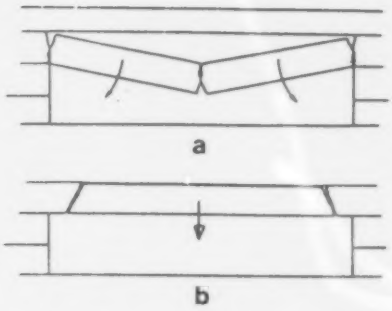

Two Basic Modes of Roof Failure: a) Snap through and b) Shear Failure

Diagram Showing Yield Lines for Rectangular Panel

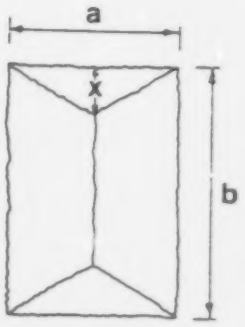

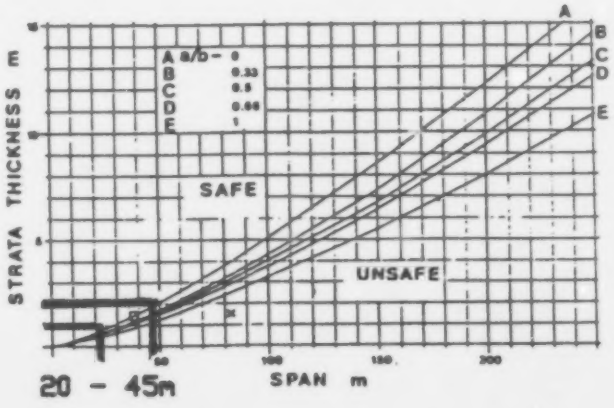

Design Curves for Rectangular Hanging Wall Panel
for Different Values of a/b (E=8000MPa, Dip = 65°)

Figure 9.4: Voussoir Beam Method of Span Determination
(Beer et al, 1982)

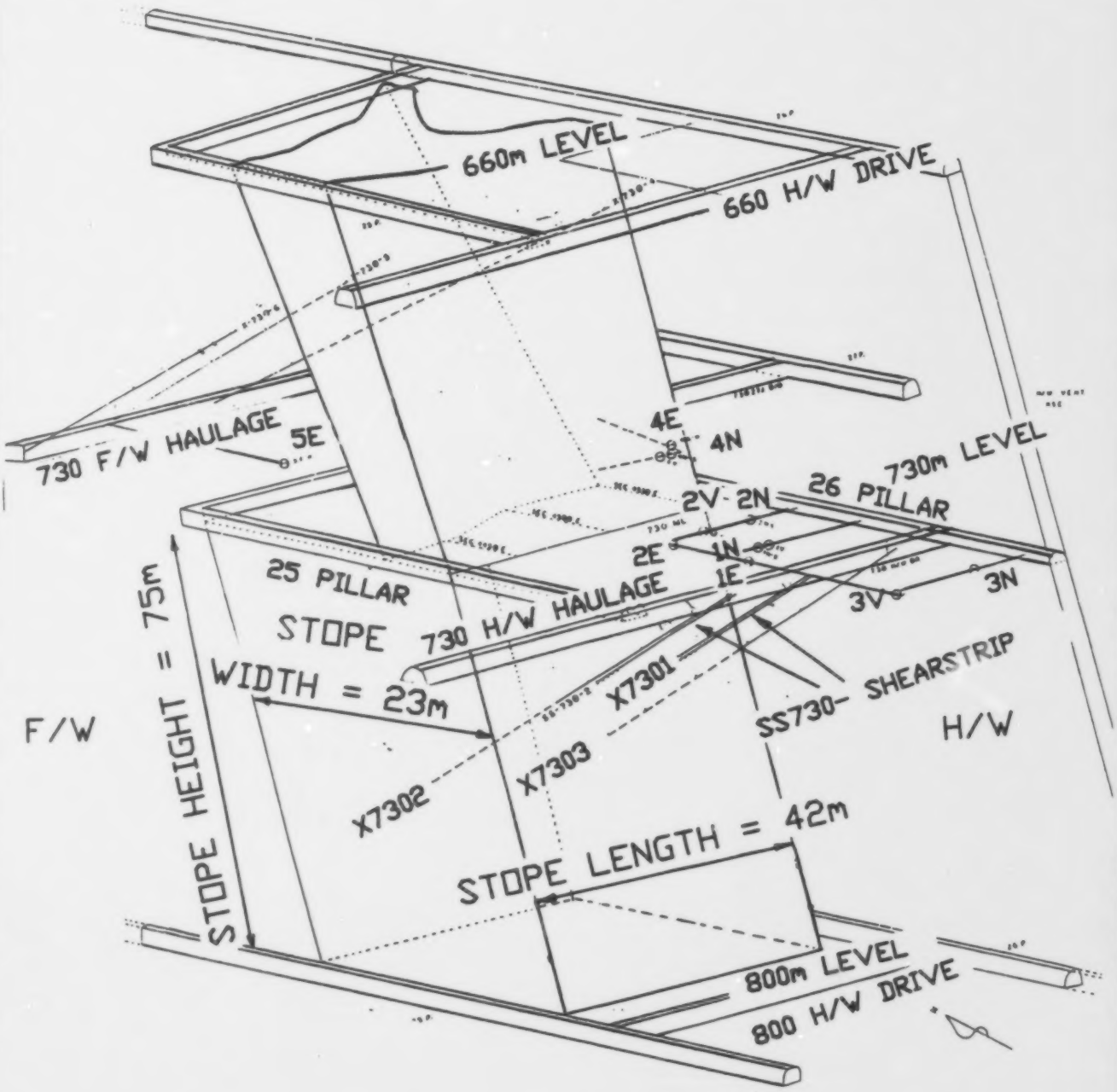

800-26J

LEGEND

X-730- EXTENSOMETER

8 1N-S STRESSMETER

Figure 9.5: Isometric Test Stope 800-26J

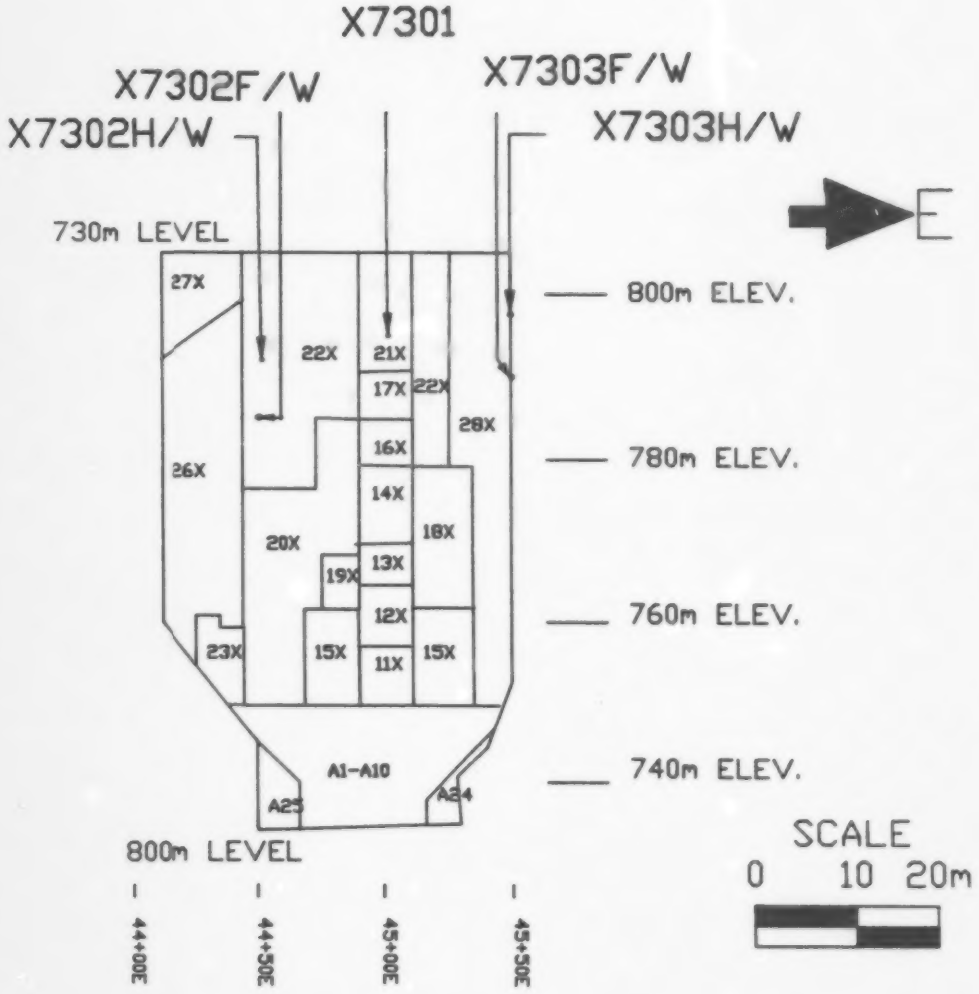

Figure 9.6: Longitudinal 800-26J (Blast Sequence)

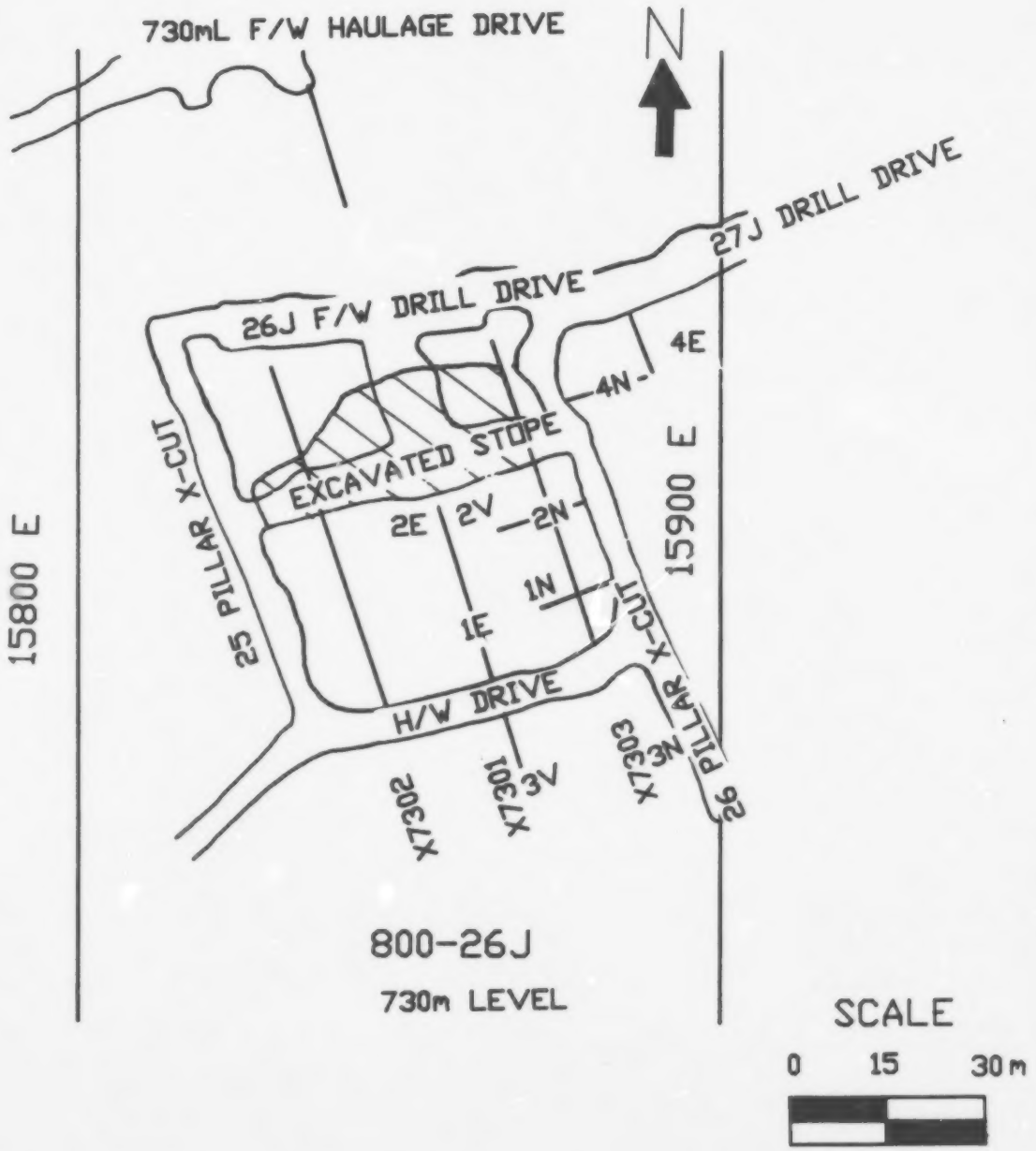

Figure 9.7: Plan 730 m L Location
800-26J Stope

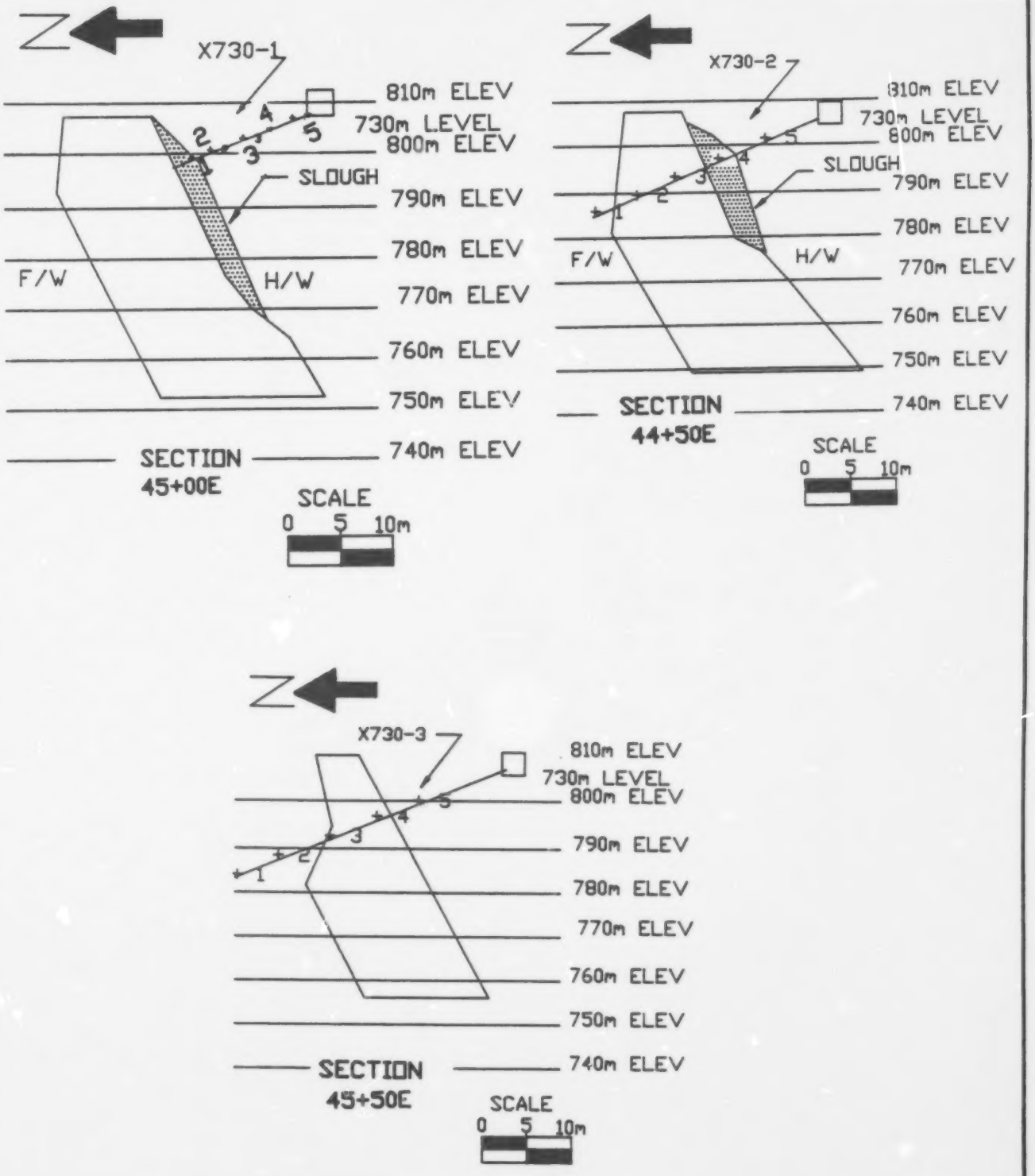

Figure 9.8: Sections Instrumented

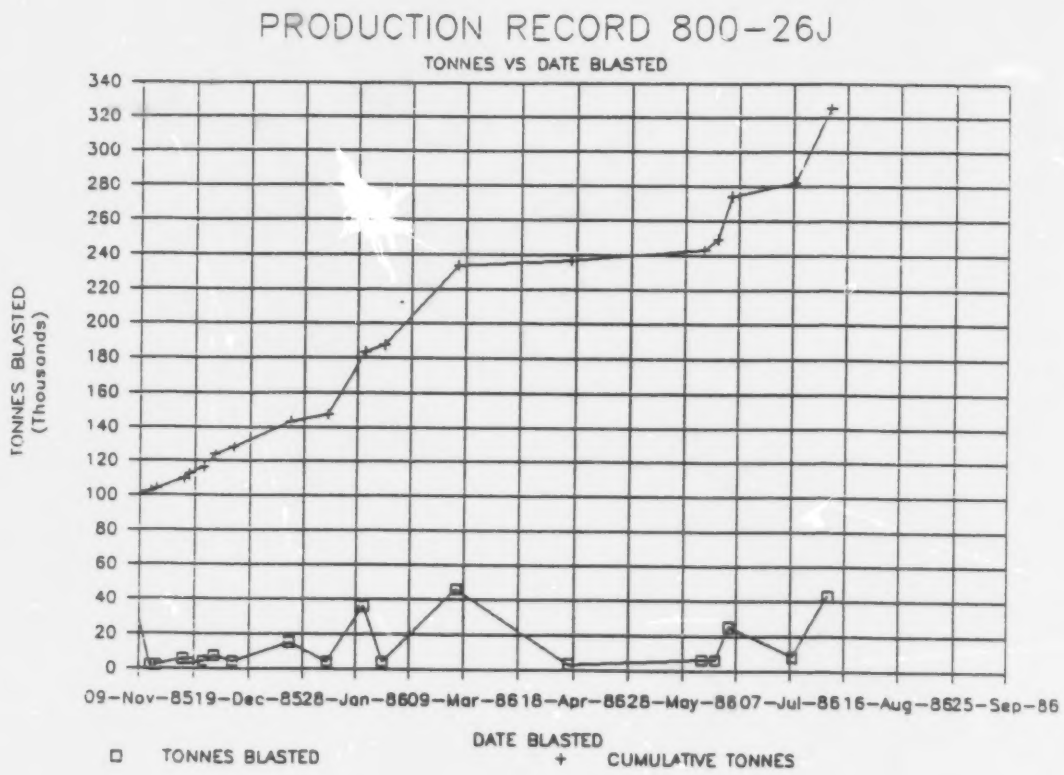

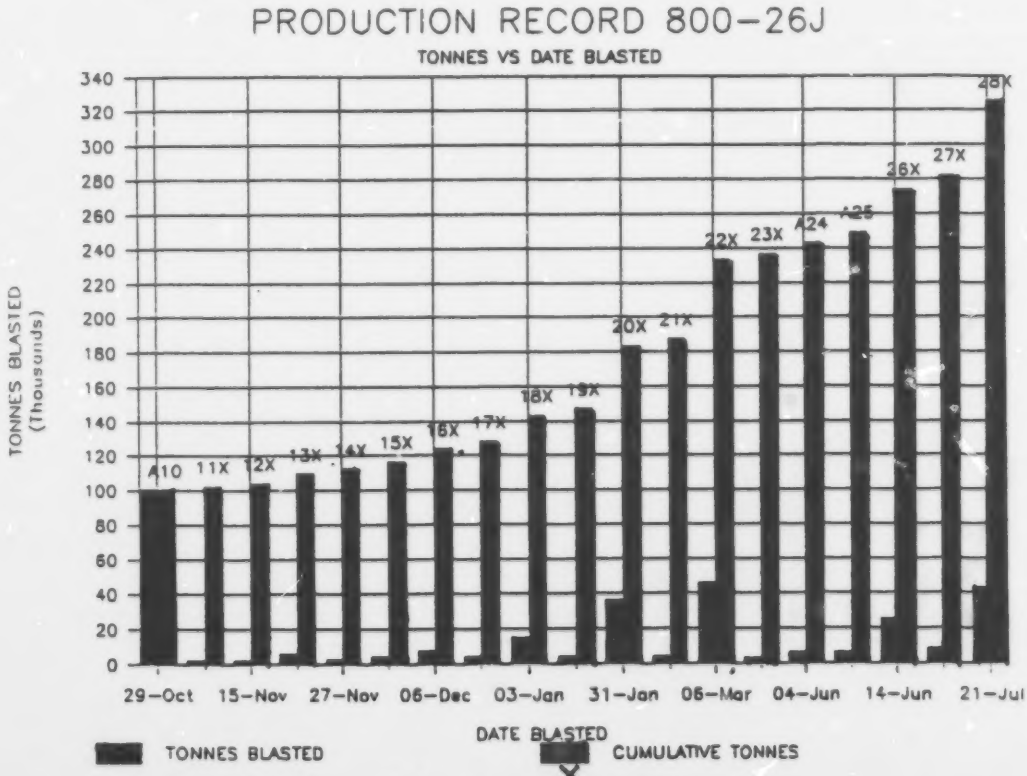

Figure 9.9: Longitudinal Record

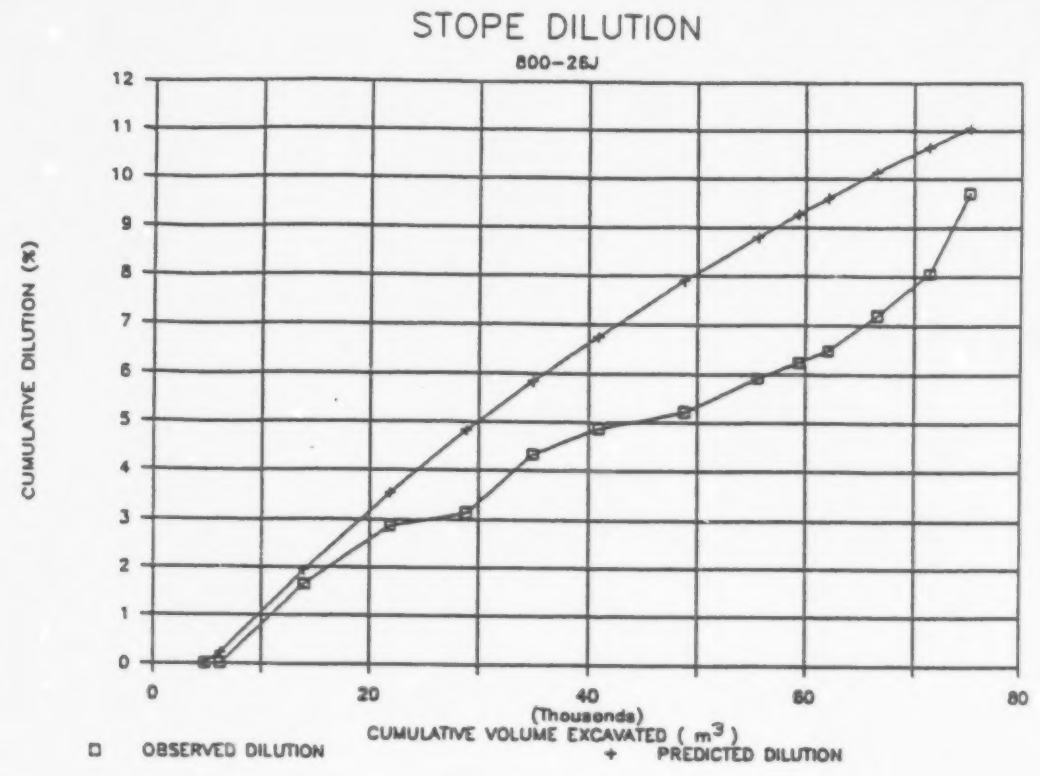

Figure 9.10: Stope Dilution

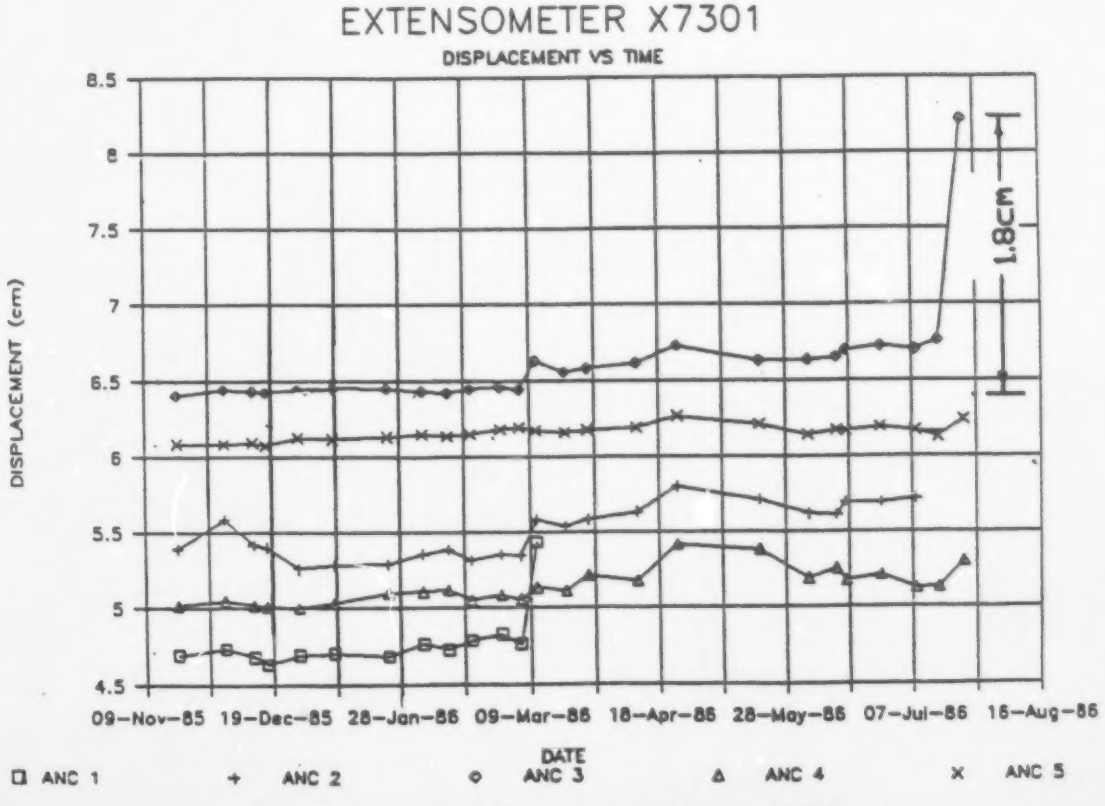

Figure 9.11a: Displacement vs Time - X7301

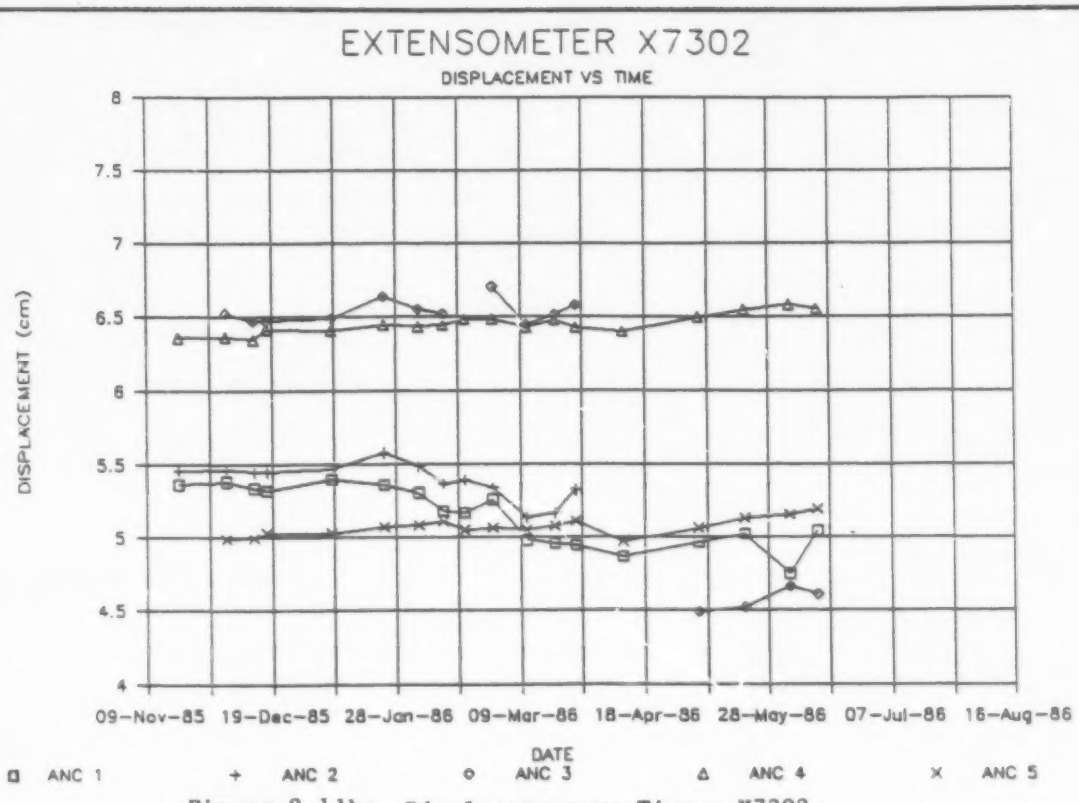

Figure 9.11b: Displacement vs Time - X7302

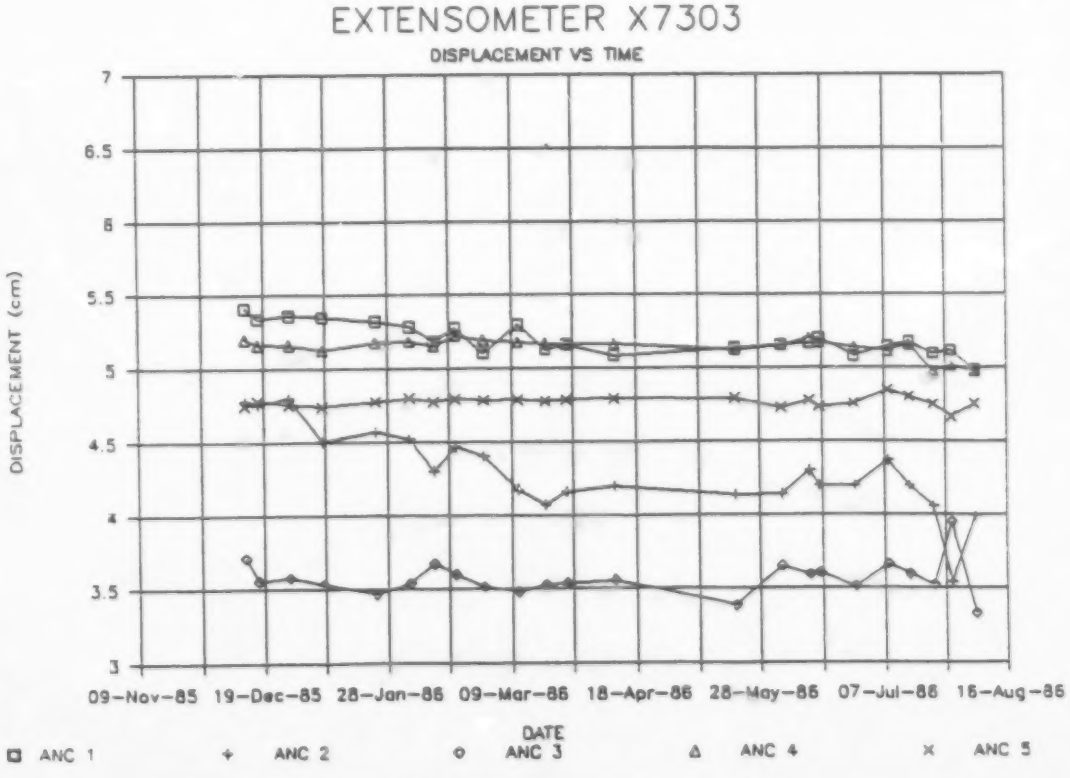

Figure 9.11c: Displacement vs Time - X7303

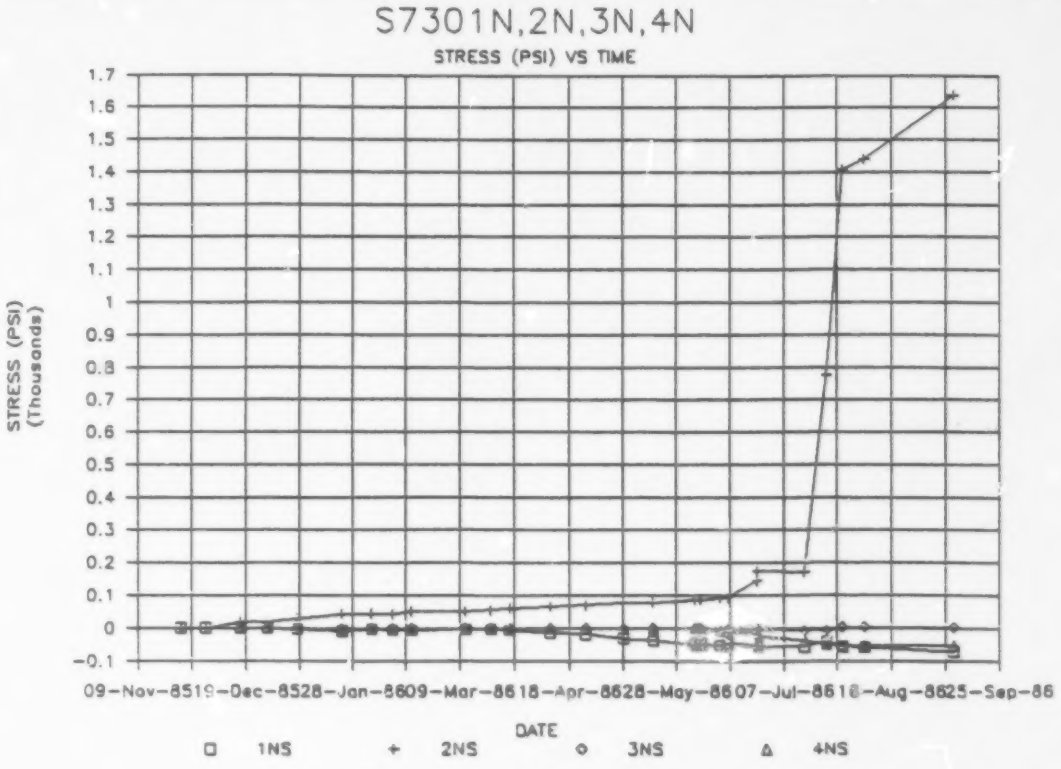

Figure 9.12a: NS Stress Meters

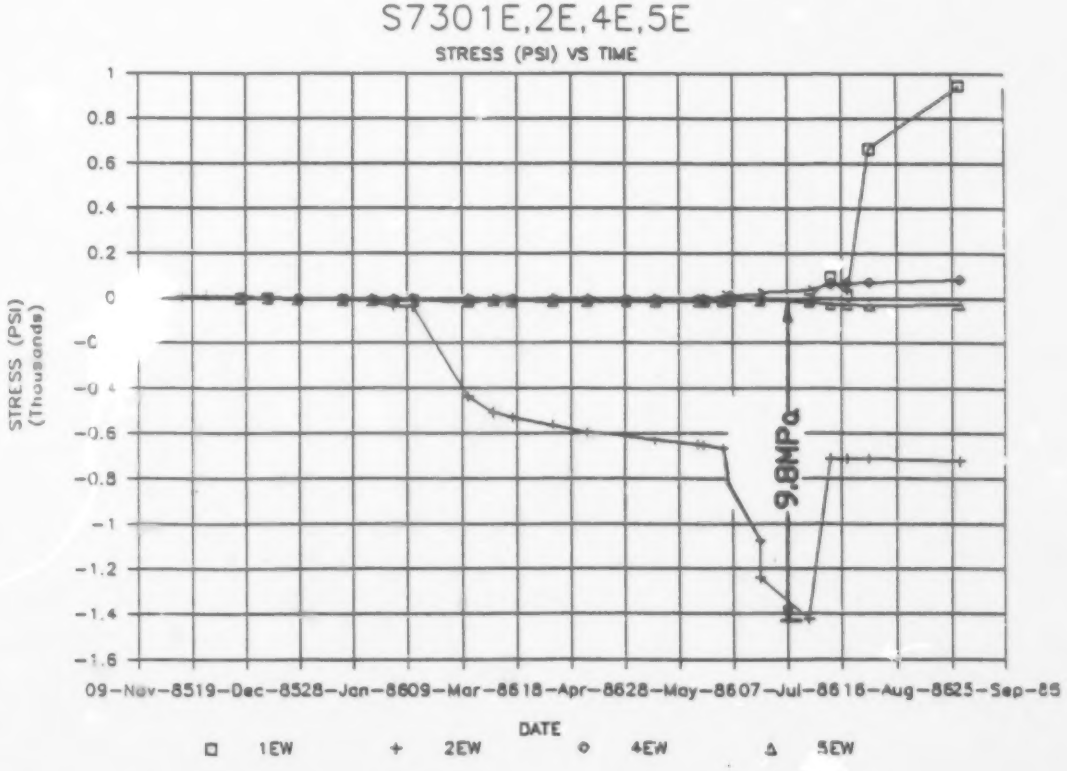

Figure 9.12b: EW Stress Meters

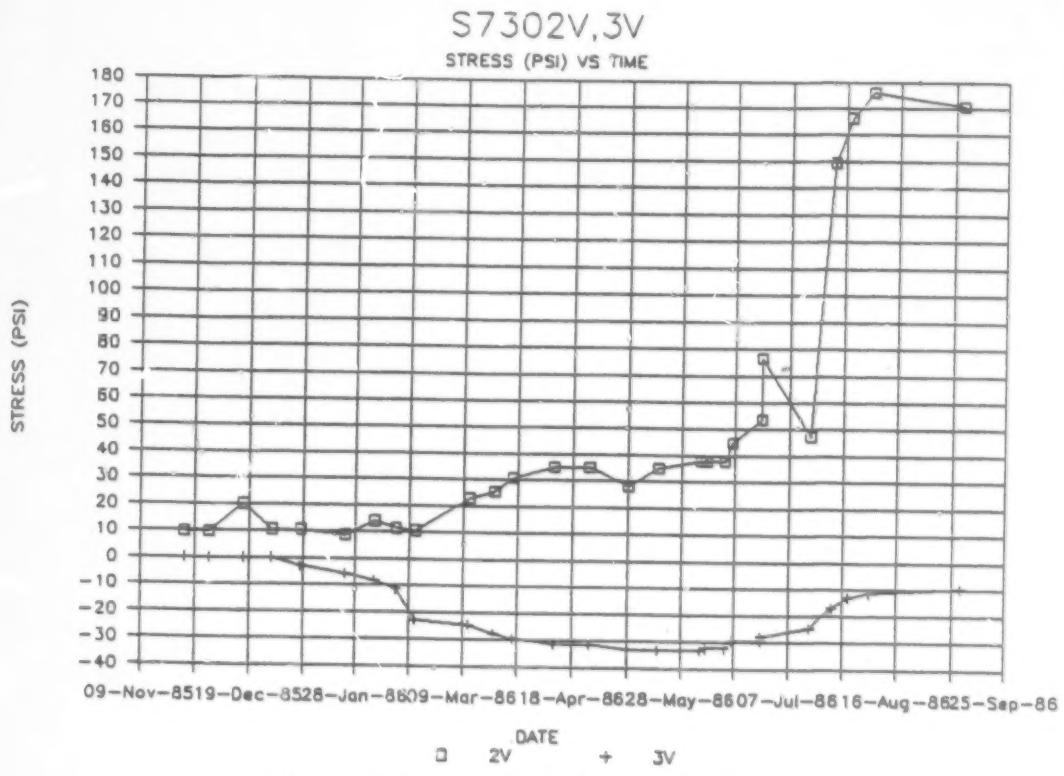

Figure 9.12c: Vertical Stress Meters

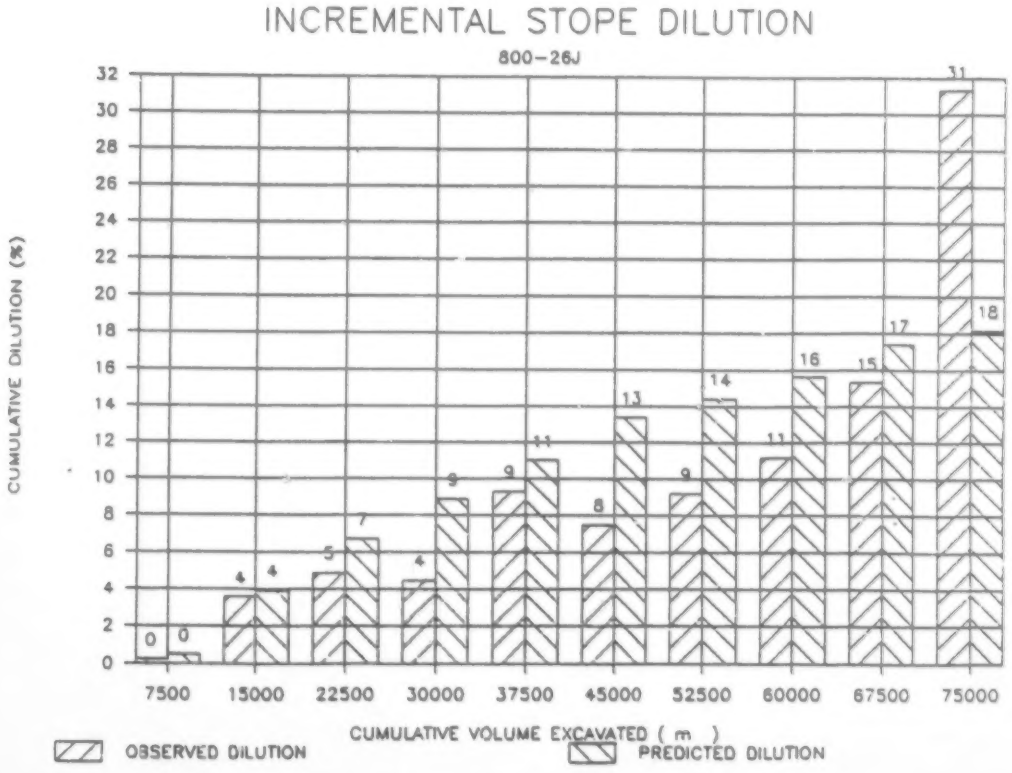

Figure 9.13: Incremental Dilution

CHAPTER TEN
MINE DESIGN GUIDELINES

10.1 INTRODUCTION

This chapter summarizes the practice of implementing rock mechanics data obtained through observation, measurement or through modelling into the design of mine openings at Ruttan. The previous chapters enable the engineer to develop an understanding of the factors affecting the stability of mine structures. The purpose was to define the critical parameters and to incorporate them into a quantitative tool in enabling one to predict optimum stope spans for the Ruttan operation. The concepts that have been derived from this study have been applied to determining an optimum mining sequence, support recommendation and the extraction of the crown pillar at Ruttan. The failure mode associated with the mining of jointed materials in a relaxed zone has resulted in the implementation of displacement monitoring devices rather than stress meters as a warning and design tool.

10.2 STOPE AND PILLAR DESIGN

10.2.1 STOPE DESIGN

The empirical design equations that have been derived are shown in Figure 8.1. They have been used successfully at Ruttan in estimating the degree of wall slough that can be expected for a given stope geometry. It was determined that the quantity of wall slough is a function of the rock mass rating, the surface area exposed and the rate of extraction. The design of stope spans in a jointed rock mass has formed the basis of this study and the reader is referred to Chapter 8 for a full treatise on the subject.

10.2.2 PILLAR DESIGN

Rib pillars at Ruttan initially are excavated to 15m in strike lengths and subsequently cut to a rib dimension of 6m. The induced stresses exceed the rock mass strength of the pillar as calculated employing "m and s" failure criterion as defined by Hoek and Bray (1982). This is generally the case in all pillars at Ruttan, however, the integrity of the pillar is maintained after failure due to the associated post-failure strength.

The "failed pillar" concept that is proposed and has been observed at Ruttan upon excavation in the immediate vicinity is shown in Figure 10.1a. Failure of the rib pillar was modelled by reducing the modulus of the pillar in stages from 70GPa

(laboratory) to 7GPa to 70MPa. A modulus of 70GPa corresponds to an 85% RMR, Figure 10.1b. The modulus is reduced to a lower rock mass rating which is analogous to a failed pillar. BITEM was employed to generate the stress trajectories shown in Figure 10.2. The average pillar stress for the 70GPa stage is approximately 75MPa which exceeds the rock mass strength for most rock types at Ruttan as determined by employing the "m and s" failure criterion.

This has been measured in isolated areas through the use of Irad gauges that were installed in 1979. The gauges were installed for purposes other than for monitoring of pillar failure and consequently the placement was poor. However, the pattern of readings had showed that a stress drop was associated with a visible deterioration within the pillar cross-cut. It was attempted to verify this in the test stope of 800-26J. However, the stress gauges were destroyed as the pillar crosscut for the adjacent rib stope was being developed (800-27J). Also sloughing of portions of the rib pillar into 800-26J caused the gauges to be lost.

This approach to mining assumes that all rib pillars at Ruttan will fail but in a controlled manner resulting in a reduction of RMR from in-situ to a much lower rock quality as adjacent mining commences. The poor rock quality still enables access through the individual pillar but requires conditioning and monitoring to forewarn of slough.

It is concluded the that rib pillars at Ruttan serve the purpose of limiting a stope span in terms of isolating the dilution that is derived from one stope from the adjacent stope. This enables one to control the expected amount of wall slough by limiting the span. The intervening rib pillar can be subsequently extracted once stope mining has been completed thereby resulting in a similar recovery but mined in a manner that would minimize the overall dilution.

10.3 MINE SEQUENCE

Due to the en echelon nature of the deposit, the most optimum direction for mining must be determined. That being the footwall stopes mined first progressing to the hangingwall or vice versa, Figure 10.3.

Modelling of the above with BESOL (Chapter 4.3.6) had shown that both sequences would generate similar results. This is based upon an elastic solution. This requires that the longitudinal pillar separating the two be intact. In addition, the backfilled stopes employing HW to FW mining would dictate that the producing stope will always have fill above the workings. The integrity of the longitudinal must be maintained. The FW to HW option would result in the least risk option based on the following assessment:

a) The HW of the producing stope will always be in virgin rock. The longitudinal which will be potentially damaged from mining the previous stope will be the FW of the present stope. This is generally the more stable wall.

b) Filling of previously mined en echelon stope would result in fill below the present workings which is generally a safer situation. Also the longitudinal will be resting on top of the fill and one would not have the full weight of the fill lying on top of the longitudinal as would be the case if mining was from HW to FW.

Chapter 8 had shown that no marginal change in dilution was found when either method was employed. Once an echelon lense has been mined a change in mining sequence will result in ground control problems if the sequence is not adhered to whether it be FW or HW or the opposite.

10.4 SUPPORT

10.4.1 FILL

Fill at Ruttan is used as a working platform for successive lifts, Chapter 2. In addition it is used to limit the exposed span through ensuring that caving will not progress from one stope to an adjacent stope. Mining of the intervening rib pillar is only undertaken after it has been determined that a major structure is not continuous enough to cause a large collapse of ground. Generally this has not been observed at Ruttan. The jointed nature of the ground results in wall slough to be comprised of blocks of ground of dimensions much less that the ultimate stope span. Modelling has shown that the change in the observed state of stress before and after filling is generally the same. Benefits in terms of filling was not observed to be statistically significant when the Ruttan database was evaluated.

The major problem in terms of fill at Ruttan is in not being able to get the hydraulic fill to the stope. One of the reasons is the low percolation rates associated with certain stopes/pours. It was attempted to increase the percolation rate by:

a) applying a vacuum to the exit drain and
b) installing a filter fabric down the length of the stope to increase the flow and to act as a decant tower.

A 50 cfm electric vacuum pump was employed on the exit drain on stope 430-19J. An average vacuum pressure of 46cm (18") was obtained which resulted in doubling

the rate of flow over that obtained with gravity alone. The results of the tests are tabulated below:

DATE		VACUUM/GRAVITY	FLOW
Dec.	20 (8 am)	Gravity	50.3. GPM
	21 (8 am)	Gravity	21.7
	22 (8 am)	Gravity	21.7
	23 (8 pm)	Vacuum on	50.3
	24 (8 pm)	Vacuum remains on	50.3
	25 (8 pm)*	Vacuum remains on	34.2
	26 (8 am)	Gravity	3.8
	27 (8 am)	Gravity	3.8
	28 (8 am)	Gravity	3.8
	29 (8 am)	Gravity	12.0
	30 (8 am)	Gravity	12.0
	30 (8 pm)	Vacuum on	34.0
	31 (8 pm)*	Vacuum on	34.0

* refers to vacuum being turned off after reading taken.

The vacuum test was successful in that is showed that a vacuum can be maintained in a backfilled stope and also that it would assist in drainage. The rate of backfill pour was variable for this stope due to problems with the backfill plant and consequently it was difficult to conduct the test under control conditions. A water balance for the stope had indicated that the saturation level of the backfill exceeded 80%. The main problem with the vacuum pump was the large amount of fines that it exhausted along with the water. This would require a modification to the pump if it was to be implemented over a long duration of time. Figure 10.4 shows the vacuum/water pump assembly employed at Ruttan.

10.4.2 MECHANICAL SUPPORT

Ruttan employees three classes of support which are as follows:

Class A

Spot bolting employing mechanical bolts 2.4m long.

This support is used for areas where the RMR exceeds 80% and where the area will not undergo major stress changes due to mining in the vicinity. An example is an access ramp removed from the mine workings.

Class B

Swellex/grouted bolts spaced on a 1.2m x 1.2m pattern. The length should be equal to 1/2 the span to a minimum of 2.4m.

This support is used in areas such as pillar cross-cuts where stress changes will result upon mining of adjacent stopes and consequently a reduction in RMR. An in-situ RMR of 60 - 80% is required.

Class C

Swellex/grouted bolts spaced on a 1.2m x 1.2m pattern. The length should be equal to 1/2 the span to a minimum of 2.4m. In addition, 5.1cm x 5.1cm weld mesh should be employed.

The above support is placed in drifts and other access ways The use of crib-sets and straps is employed in areas where the RMR is generally under 50% and requires re-conditioning.

10.5 CROWN PILLAR EXTRACTION

The procedure at Ruttan in order to determine a plan of extraction of the echelon lenses to surface was to model the crown pillar employing BITEM. The extraction of stopes at Ruttan had showed that pillar failure occurs but in a nonviolent manner. The crushed pillar still maintains post failure strength sufficient to retain its geometry. This has been observed, monitored and modelled and has resulted in the following method of crown excavation.

It was shown through modelling that the crown will fail at some point but it will retain its configuration with the only result being in the transfer of stress to other areas of the mine. The result is that the excavation will occur in a relaxed medium. This is partly shown in Figure 10.2 which shows how changing the modulus of the rib pillar results in a redistribution of stress. The following section describes the method of extraction proposed and practised for the crown pillar at Ruttan.

10.5.1 CASE HISTORY - WEST LENSES

Open pit production ceased during the winter of 1980 as underground production rates were being increased to 6000 tpd. The open pit had been mined to a depth of 210m in the West Lenses. At this point, a mining plan was to be adopted to ensure future recovery of the west lens crown pillar. Due to the en echelon nature

of the orebody, Figure 10.5, the crown pillar retrieval consisted of four main ore zones, "B/BE,C,D and F lenses".

The first stope in the mining sequence was the "F" zone. It was isolated from the adjacent lenses. The stope was mined from the 260mL, and blasted to pit bottom (210mL) in two lifts.

The first lift was initially blasted in June, 1983, and mined until December, 1983, to a height of 35m. The second lift was started in September, 1985, to February, 1986, and was mined through to pit bottom. The final stope dimensions were as follows:

Strike Length (Span)	- 63m
Stope Width	- 12m
Stope Height	- 60m (260mL to Pit Bottom)

The predicted stope dilution as per Figure 8.1 was 12%, though the observed dilution was only 6%. A ten meter crown was left behind for ventilation purposes and is presently still in place.

Prior modelling of this stope indicated major stress concentrations would occur at the toe of the stope as the opening was increased. This was the case as the ground in the drawpoints deteriorated during mining of the second lift. Rock mechanics monitoring of this stope was limited and no major problems were incurred while mining proceeded.

The second crown planned was the 12B-14BE stopes, the first major crown excavation, located in the footwall of the en echelon lenses. Both stopes had been mined previously from the 320mL to an overcut on the 260mL, with delayed backfilling to the 260mL prior to mining the crown.

A series of prisms were placed along a line on the pit bottom and in the vicinity of the 12B-14BE stope prior to mining. Monitoring of the prisms from monuments along the crest of the pit were taken prior and during blasting operations. Initial readings indicated minimal crown movement during initial blasting, however, eventually all stations were destroyed by fly rock as the crown was excavated in the vicinity. This proved to be an ineffective and unreliable method of monitoring the crown movements.

Initial blasting of 12B/14BE began in the spring of 1986 and is scheduled for completion in 1989. Final stope dimensions were:

Strike Length (Span)	- 72m
Stope Width	- 17m
Stope Height	- 50m (260mL to Pit Bottom)

The predicted stope dilution was 15% as per Figure 8.1, while the observed to date is 16%. Again no major ground problems were encountered through mining of this stope.

The mining sequence (footwall to hangingwall) dictated that the next stope in sequence was the 12C crown. It was decided to mine the longitudinal pillar between "B" and "C" zones with the 12C stope, Figure 10.5. This would create a void from the footwall of 12B-14BE to the hangingwall of 12C (approx. 60m).

The first and second lifts of 12C were not filled, and therefore would be mined from the 340mL while blasting was being conducted between the 210 and 240 meter levels.

Diamond drill core results indicated that the 12C zone was a highly sheared and jointed rock mass exhibiting a low RMR and RQD. This emphasized the need for a detailed ground monitoring program to safely excavate this area. The jointed nature of the ground indicated that failure and relaxation had occurred due to mining in the vicinity and therefore required conditioning.

Prior to development, a series of test holes were drilled to determine the approximate location of the back of the 12C - second lift stope at the 240mL. Test hole information revealed that the back had not sloughed, and was still intact. Geologic mapping from development drifts on the 220mL indicated the presence of several large shear zones. The drifts were conditioned with rockbolts, swellex and strapping. Convergence rod stations were set up in the 220mL drill drift to monitor back movement (pit bottom at 210mL). Extensometers were placed in the test holes and monitored by flashing lights.

On May 14, 1987, the flashing light extensometer had successfully indicated rock sloughing along a shear on the hangingwall of the ore zone. Initial blasting began on May 15, 1987. Sloughing along the hangingwall shear zone accelerated as the slot opening was increased.

This was confirmed by extensometers in the hangingwall along the length of the stope. On June 2, 1987, approximately 44,500 tonnes were blasted at 8:00 p.m.,

during the same evening approximately 110,000 tonnes had failed, sloughing into the 12C stope. The actual failure of this area was predictable given the availability of the rock mechanics information and conditions, although the time of the failure was not. This emphasized the importance for a detailed ground monitoring program in high risk mining areas, such as the crown pillar extraction. The final stope dimensions were as follows:

Strike Length- 50m
Stope Width - 60m
Stope Height - 140m (340mL to pit bottom)

10.6 INSTRUMENTATION

Wire extensometers are employed for the monitoring of stope wall movement. They have been found to be easy to install, inexpensive, and reliable. They have been augmented with a limit switch which triggers a flashing light once movement is detected, Figure 10.6a. This instrumentation is used in drill drifts in the vicinity of open stopes to forewarn of any movement. They have been successfully used in the extraction of the crown. Employing the reasoning that the hangingwall and footwall of an individual stope is in relaxation, these instruments enable the operator to quantify the displacements.

Vibrating wire flat jacks, Figure 10.6b, were installed at the base of the test stope 800-26J prior to the commencement of filling. The purpose was to determine the amount of stress that the fill would exhibit onto the underlying sill pillar. This is important in trying to determine the sill pillar dimensions required in order to retain the overlying fill. The gauge was placed at the base of the open stope underneath the brow. The practise at Ruttan is to pour dry fill into the stope first to a height of 10m whereafter hydraulic fill would be placed. The maximum pressure recorded in the fill was 4 psi at a fill height of 40m. Employing the following equation as derived by Askew et al (based upon Terzaghi) would indicate that the fill pressure should be in the range of 80psi. Similar values were obtained employing Coates (1965) and Laubsher (1981) approaches to estimation of stress due to overlying fill.

Equation (1) After ASKEW et al (1981)

$$\delta z = \frac{B\alpha - C}{K \tan\phi}\left(1-e^{\left(-\frac{kz \tan\phi}{B}\right)}\right)$$

where:

δz = vertical stress at any depth in a fill mass

B = stope width (23m)
α = fill density (1922 kg/m^3)
ϕ = friction angle of fill (38 deg.)
k = vertical/horizonal stress ratio = $\frac{1}{1 + 2 \tan^2 \phi}$ (Coates, 1972)

z = depth of fill
c = cohesion of fill (0MPa)

The reason for the difference may be:

* that the gauge would have given an erroneous reading since large blocks overlaid the immediate brow and may have resulted in arching over the instrument;
* that arching had occurred due to the pour of dry fill which supported the bulk of the hydraulic fill on the sides of the stope walls.

Another gauge was lowered on top of the dry fill from the upper drill drive. It, however, was damaged by a fall of loose fill.

The use of instrumentation at Ruttan is employed to forewarn of ground slough and to verify the assumptions made throughout the study.

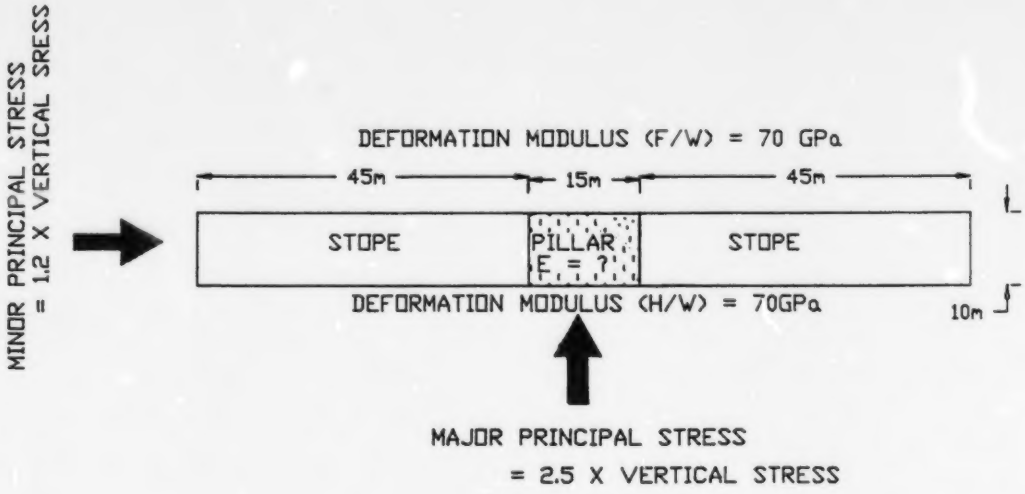

Figure 10.1a: Modelled Geometry - Plan View

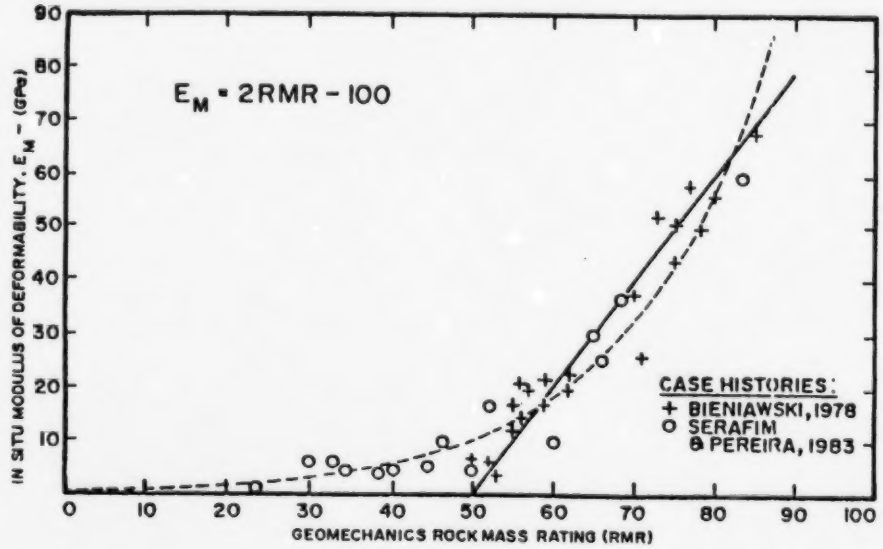

Figure 10.1b: Modulus of Deformation vs RMR - Bieniawski (1983)

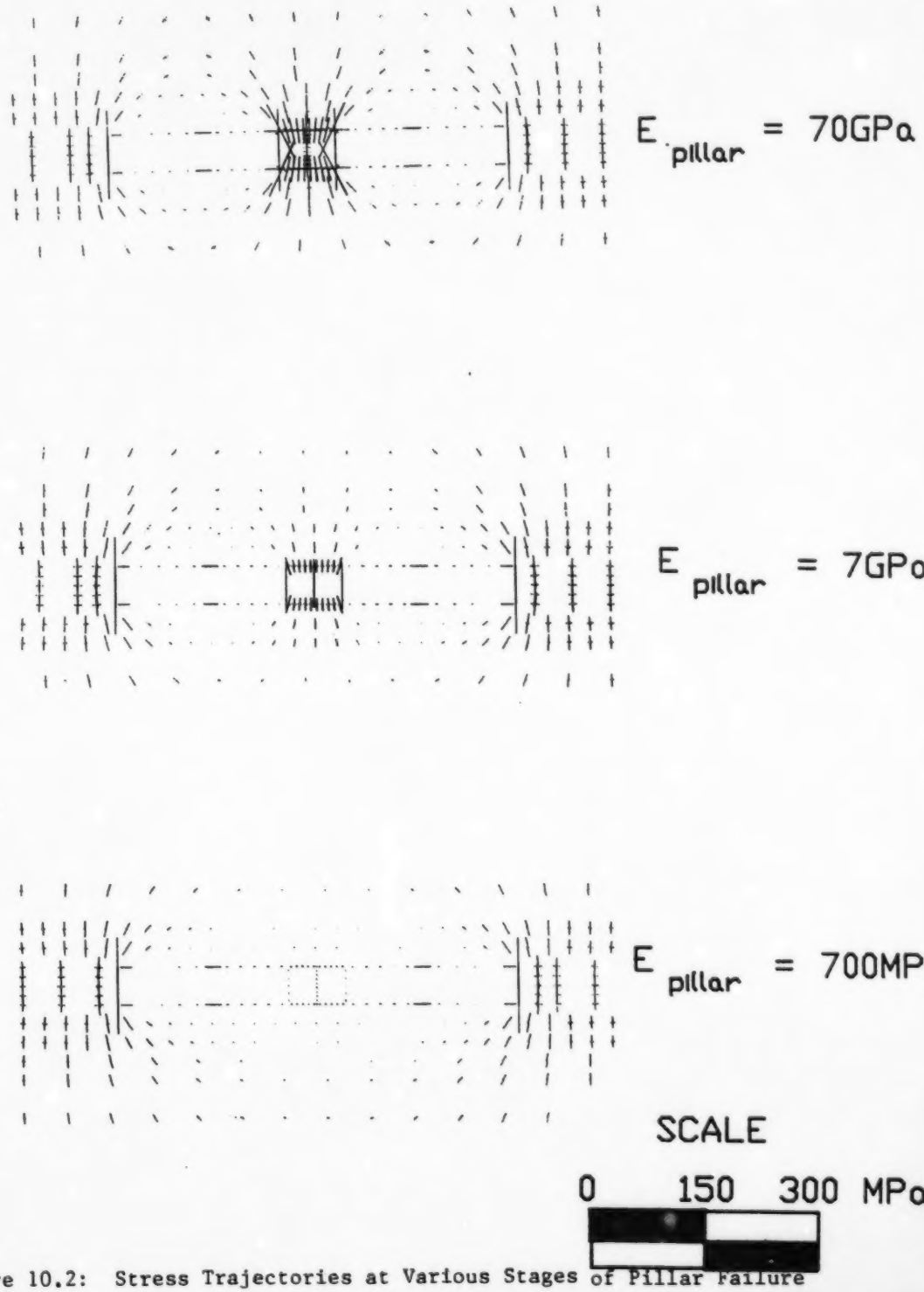

Figure 10.2: Stress Trajectories at Various Stages of Pillar Failure

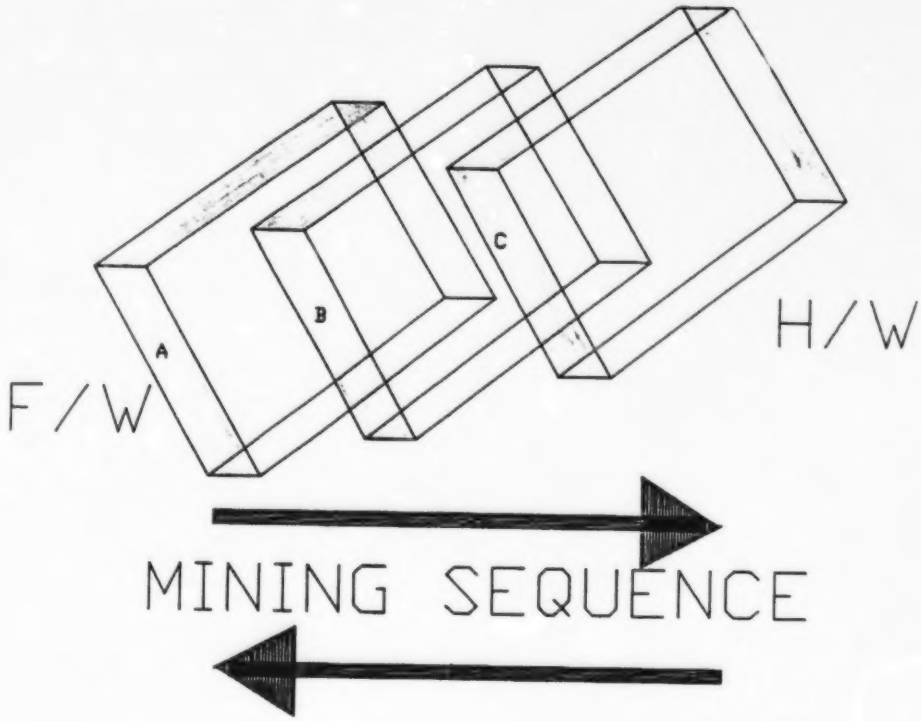

Figure 10.3: Mining Sequence

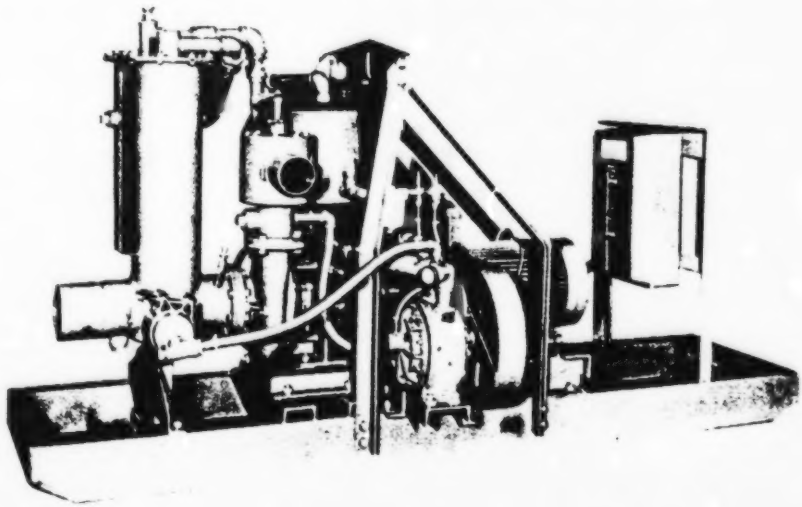

Figure 10.4: Vacuum Pump Employed at Ruttan

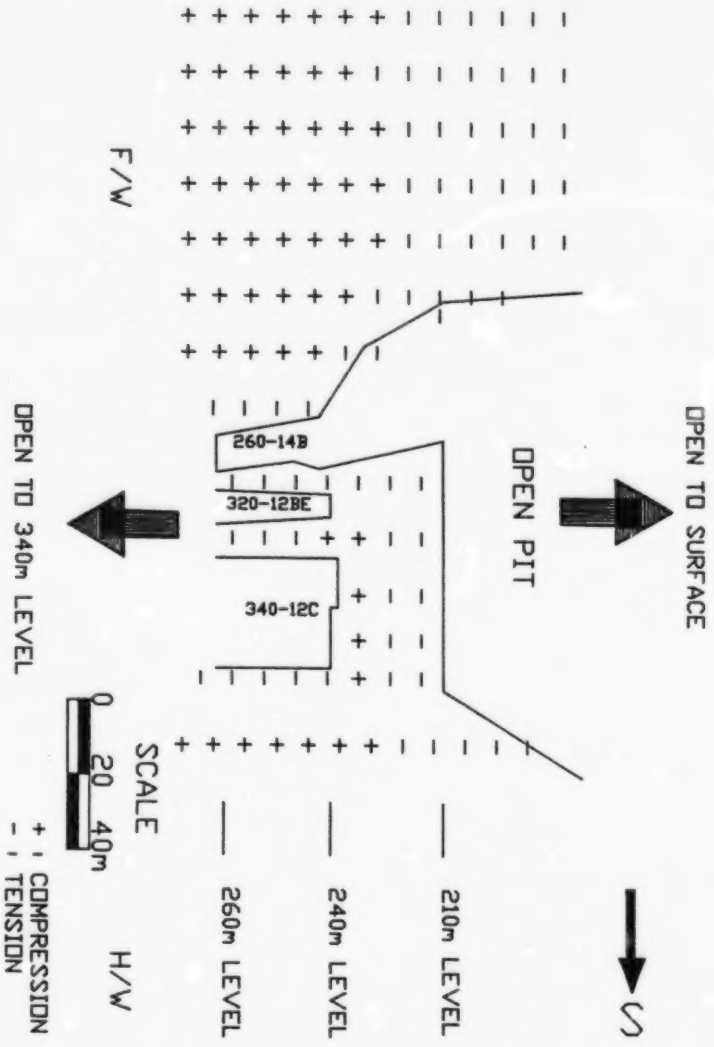

Figure 10.5: Numerically Modelled Crown - Section

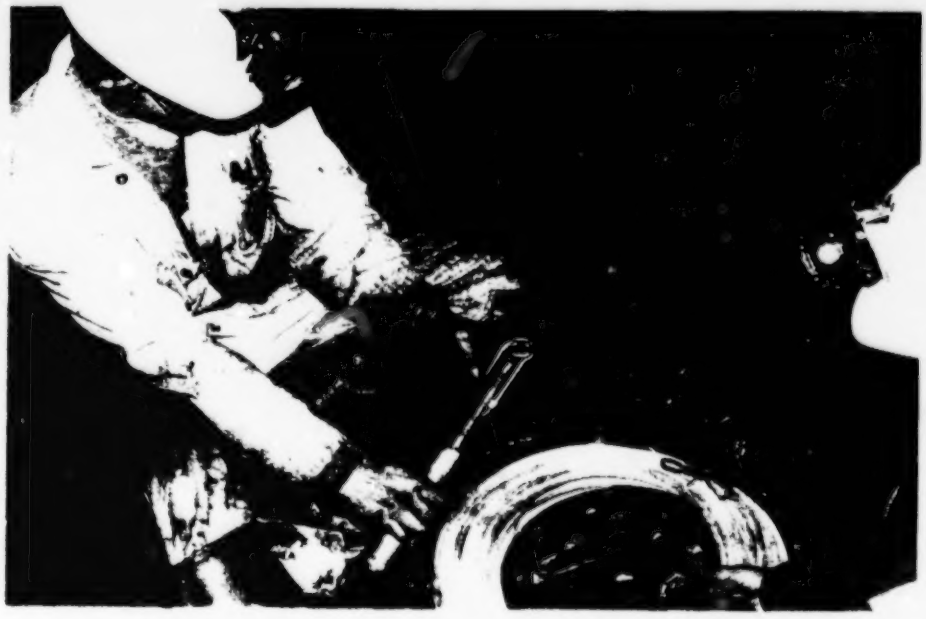

a) WIRE EXTENSOMETERS

b) WARNING DEVICE

Figure 10.6a: Displacement Monitoring Instrumentation

Rock Stressmeters

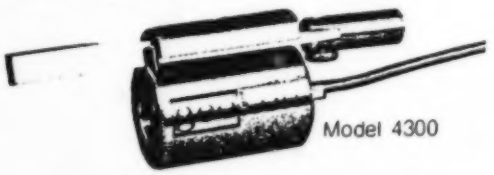

Model 4300

Model 4300 measures stress changes in rock. It uses the vibrating wire principle to measure the distortion of a stainless steel proving ring wedged inside a borehole in rock. Designed for installation in EX(1½-in.), AX(1⅞-in.), BX(2.36-in.) or NX(3-in.) boreholes, the stressmeter has a range of 0-10,000 psi and a sensitivity of ½-5 psi depending on hole size and rock modulus. High temperature versions of all sizes are available for use up to 200°C.

Pressure Cells

Model 4800C

Several versions of pressure cell are available using a variety of transducer types. **Earth Pressure Cells** measure total pressure in earth fills, embankments and mine backfills. They can also be used to determine pressures on retaining walls, building foundations, sheet pilings and tunnel linings. **Concrete Stress Cells** measure stresses in mass concrete, slurry walls, piles, tunnel linings etc. These cells are fitted with a post-stressing tube to ensure a good contact between cell and concrete.

Figure 10.6b: Stress Monitoring Instrumentation

CHAPTER ELEVEN
CONCLUSIONS

11.1 CONCLUDING REMARKS

The hangingwall and footwall at Ruttan was concluded to be in a state of relaxation, given the prevailing stress conditions and stope configuration. This, coupled with a foliated hangingwall, was determined to be the dominant failure mechanism. Optimum stope geometry was equated to stopes yielding lower observed dilution. The factors directly contributed to increased wall slough were:

* the rock quality of the individual critical wall contact;
* the exposed surface area;
* the rate at which the wall contact was exposed.

Figure 8.1 summarizes the empirically derived expressions as quantified through observation (133) recorded for the Ruttan database. It was concluded through multivariate analyses, that the predictive expressions were highly significant and correlative to the observed dilutions.

Dilution was found to be largely insensitive to the following factors:

* the stope span/width ratio;
* the mining depth;
* the method of open stoping (ITH versus conventional);
* the mine sequence (FW-HW).

The predictive equations were defined for the isolated, rib and en echelon configuration. Generally, it was found that the en echelon geometry yielded the lowest dilution (2% less than isolated) with the rib stopes exhibiting the greatest dilution (1.5% greater than isolated).

Further research should be directed in the following areas:

1. Attempt to develop a more comprehensive predictor for the blast induced dilution.

2. Develop alternate methods of recording stope dilution that do not rely solely on visual assessment.

3. Augment the present database by observations made at other mine operations. In particular, attempt to assess the effect of stope inclination, support and ground water on dilution.

The Ruttan operation has adopted the methods proposed in this study. It has been able to better predict stope dilutions, design optimum stope spans to better forecast the mining costs incurred due to wall instability. It is suggested that the empirical methods of design outlined in this study be attempted/calibrated for other operations where similar failure mechanisms prevail. It should be noted that the characteristics unique to the Ruttan operation be assessed prior to extending the study to other operations.

The author's contribution to the existing state of knowledge concerning open stope design is in the empirical approach to the development of a design methodology. That relationship being primarily a function of "exposed surface area, exposure rate and rock mass rating". The governing equations are applicable for the Ruttan operation, however the methodology is valid for all open stoping operations. The absolute magnitudes of stope design are expressed in terms of dilution. This parameter is difficult to access accurately, however once calibrated, it is a useful indicator of instability for any mine operation. The guidelines developed, Chapter 10, have been derived on the basis of relaxation existing in the immediate hangingwall. This results in ground slough which can be predicted and designed employing the concepts developed in this study.

LIST OF REFERENCES

Askew, J.E., McCarthy, P.L., and Fitzgerald, D.J. (1981). Mining With Backfill, CIMM Special Edition, PP 100-110.

Barker, R.M. and Hatt, (1972). Joint Effects in Bedded Formation for Roof Control, 14th U.S. Rock Mechanics Symposium, Penn State University, June 11-14, pp. 10.

Barrett, J.R., Grumitt, B. and Wical, M. (1979). Arch Formation and Pillar Yield in Jointed Rock, Int. Cong. on Rock Mech., Proc. 4th, Vol. 2, Montreaux, Suisse, pp. 10.

Barton, N., Lien, R. and Lunde, J. (1974). Engineering Classification of Rock Masses for the Design of Tunnel Support, Rock Mechanics, Vol. 6, No. 4, pp. 183-236.

Beer, G., Meek, J. L. (1982). Design Curves for Roofs and Hangingwalls in Bedded Rock Based on Voussoir Beam and Plate Solutions. Trans. Instn. Min. Metall., January, pp. 20.

Bieniawski, Z.T. (1983). Improved Design of Room and Pillar Coal Mines for U.S. Conditions, 1st Int. Conf. on Stability in Underground Mining, AIME, New York, pp. 19-51.

Bieniawski, Z.T. (1973). Rock Mechanics Design in Mining and Tunneling, A.A. Balkema Publishers, Accord, MA, pp. 272.

Blackwood, R.L. (1978). Diagnostic Stress Relief Curves in Stress Measurement by Overcoring, Int. J. Rock Mech., Min. Sci. & Geomech. Abstr. Vol., pp. 205-209.

Brady, B.H.G. and Brown, E.T. (1985). Rock Mechanics for Underground Mining, Allen and Unwin, Boston, pp. 527.

Brady, B.H.G. (1977). An Analysis of Rock Behaviour in an Experimental Stoping Block at Mt. Isa Mine, Queensland, Australia, Int. J. Rock Mechanics, Mng. Sci. Geomech., Vol. 14.

Bridges, M.C. (1982). Review of Open Stope Mining in Australia, 1st Int. Conf. Stability in Underground Mining, AIME, New York, pp. 15.

Brown, E.T. (1985). From Theory to Practice in Rock Engineering, Transactions of Instn. Mining and Metallurgy, April, pp. A67-A83.

Chen, D.W., Chen, J.Y. and Zavodni, Z.M. (1983). Stability Analysis of Sublevel Open Stopes at Great Depth, Proc. 23th U.S. Rock Mech. Symp., Texas.

Choquet, P. (1983). A Method of Estimating Loose Zone Extent Around Mine Openings for Support Assessment, CNCRM Symp. on Undergorund Support Systems, Sept., Sudbury, pp. 16.

Cook, N.G.W. and Jaeger, J. (1978). Fundamentals of Rock Mechanics, John Wiley & Sons, NY, pp. 183-194.

Coates, D.f. (1965). Rock Mechanics Principles, CANMET, Mines Branch Monograph 874, pp. 5.1 - 5.18.

Deere, D.U., Merritt, A.H. and Coon, R.F. (1968) Engineering Classification of In-Situ Rocks, Report by U. of Illinois to AFWL, No. AWFL-TW-67-144, NTIS No. AD8488798, pp. 272.

Duvall, W.I. (1977). General Principles of Underground Opening Design in Competent Rock, Monograph on Rock Mechanics Applications in Mining, AIME, New York, pp. 101-111.

Elissa, E.S. (1980). Stress Analysis of Underground Excavations in Isotropic and Stratified Rock Using the Boundary Element Method, Ph. D. Thesis, University of London.

Evan, W.H. (1940). The Strength of Undermined Strata, Trans. (Instn. Min. Metall., pp. 475-532.

Flint, F. and Skinner, B. (1974). Physical Geology, Wiley Inc., New York, New York, pp. 351-367.

Hedley, D.F. and Grant, F. (1972). Stope and Pillar Design for the Elliot Lake Uranium Mines, CIM Bulletin, Vol. 65, pp. 12.

Herget, G. (1980) Regional Stresses in the Canadian Shield-Summary, CANMET, Division Report MRP/MRL 80-559op), pp. 7.

Hoek, E. and Brown, E.T. (1980). Underground Excavations in Rock, Institution of Mining and Metallurgy, London, pp. 467-492.

Hoek, E. (1983). Strength of Jointed Rock Masses, Geotechnique 33, No. 3, pp. 187-223.

Interim Reports: File No. 07SQ.23440-4-9147. Project 3: Rock Mechanics Survey of Canadian Underground Mine Operators (Open Stope and Room and Pillar); Project 2/3: Data Base/Remote Monitoring; Project 5: Test Stope 800-26J.

Irad Gauge Inc. (1977). Vibrating Wire Stressmeter Instruction Manual, Lebanon, New Hampshire, pp. 40.

Kendorski, F.S., Cummings, R.A., Bieniawski, Z.T., and Skinner, E.H. (1983). Rock Mass Classification for the Planning of Caving Mine Drift Supports, Rapid Excavation and Tunneling Conference, AIME, New York, New York, pp. 28.

Kersten, R.W. (1985). The O-System of Tunnel Support Used for Underground Production Excavations, SANGORM Symposium on Rock Mass Characterization, Randburg, S.A., pp. 39-43.

Kersten, R.W. (1981). The Influence of Dilution on the Finanical Viability of a Massive Sulphide Deposit, 24th U.S. Symp. on Rock Mech., pp. 687-690.

Kristen, H.A.D. (1983). Combined Q-NATM System: The Design and Specification of Primary Tunnel Support, South African Tunneling, Vol. 6, No. 1, pp. 18-24.

Koch, G. and Link, R. (1980). Statistical Analysis of Geological Data, Volume II, Dover Publications Inc., New York, New York, pp. 1-152.

Laubscher, D.H. and Taylor, H.W. (1976). The Importance of Geomechanics Classification of Jointed Rock Masses in Mining Operations, Exploration from Rock Engineering, ed, Z.T. Bieniawski, A.A. Balkema, Rotterdam. Vol. 1, pp. 19-128.

Laubscher, D.H. (1976) Geomechanics Classification of Jointed Rock Masses - Mining Applications, Rhodesian Institution of Mining and Metallurgy, No. 86, pp. 8.

Laubscher, D.H. (1981). Selection of Mass Underground Mining Methods, Design and Operation of Caving and Sublevel Stoping Mines, AIME, New York, pp. 23-37.

Maconochie, D.J., Friday, R.G. and Thompson, R.R. (1981). An application of Monitoring and Numerical Modelling in Open Stope Mining, Fourth Austrialian Tunneling Conference, Melbourne, Austrialia, March, pp. 157-170.

Mathews, K., Hammett, R.D. and Stewart, S.B. (1983). Case Examples of Underground Mine Stability Investigations, Stability in Underground Mining, AIME, New York, pp. 829-846.

Mathews, K.E., Hoek, E., Wylie, D.C. and Stewart, S. (1981). Prediction of Stable Excavation Spans for Mining at Depths Below 1000 Meters in Hard Rock, CANMET Dept. of Energy, Mines and Resources, Canada, DSS Serial No./ OSQ80-0081DSS File No. 17SQ.23440-0-9020, pp 80.

Miller, H.D.S., Potts, E.L., and Szeki, A. (1976). In-Situ Stress Measurements in Halite in Chesire, Potash in North Yorkshire, and Slate at Dinorwic, Part II, Proc. Rock Engineering, University of Newcastle-upon-tyne, England, pp. 257-272.

Morrison, R.G.K. (1976). A Philosophy of Ground Control, published by Dept. Min. and Metal. Engng., McGill Univ., Montreal, pp. 125-160.

Moss, A.E.S. and Niemi, B. (1985). Investigation into Mining of a Main Crown Pillar, District Three Meeting, September, pp. 19.

Nicholas, D. (1981). Method Selection - A Numerical Approach, Design and Operation of Caving and Sublevel Stoping Mines, eds. D. Stewart, AIME, New York, pp. 39-54.

Ontario Ministry of Labour (1985). Provincial Inquiry into Ground Control and Emergency Preparedness in Ontario Mines. Report prepared by 1) Steffen, Robertson and Kirsten and 2) Golder and Assoc., Ontario Ministry of Labour, Sudbury, Ontario.

Page, C.H., Brenner, R.G. (1983). Stability of Large Open Stopes in Weak Rock, Stability in Underground Mining, AIME, New York, pp. 336-356.

PCBEM (1988), CANMET, DSS Serial No. OSQ84-00330, File No. 14SQ.23440-4-9147-1, pp. 53.

Pariseau, W.G., Fowler, M.E. and Johnson, J.C. (1984). Geomechanics of the Carr Fork Mine Test Stope, Geomechanics Applications in Underground Hardrock Mining, SME/AIME, New York, pp. 3-38.

Parker, J. (1973). Practical Rock Mechanics for Miners, EMJ, June, pp.78.

Potts, E.L.J., Szeki, A., Watson, S.H., Mottahed, P. (1979). The Evaluation of the Design Criteria for an Underground Roof Strata Considered as a Linear Arch Structure, Intl. Congress on Rock Mech., Proc. 4th, Vol. 2, Montreaux, Suisse.

Potvin, Y. and Miller, H.D.S. (1985). Pillar Design Methodology, presented at AGM-CIM, Vancouver, B.C.

Preston, J. (1985). Dupont Blast Studies at Ruttan, Internal Report.
Rotzien, J. and Miller, H.D.S. (1985). Report on In-Situ Stress Measurement at MacLellan Mine, Internal Report, University of British Columbia, pp. 150.

Smith, J.D. (1976-79). Progress Report, Ruttan Underground Rock Mechanics Study, Internal Report, Sherritt Gordon Mines.

Speakman, D., Chornoby, P., Holmes, G. and Haystead, B. (1976). Geology of the Ruttan Deposit, Internal Report - Sherritt Gordon Mines, pp. 25.

Spiegiel, M. (1972). Theory and Problems of Probability and Statistics, Schaum's Outline Series, McGraw Hill Co.,pp. 72.

St. John, C. M., Christianson, M., Petersen, D. L. (1980). Evaluation of Mine Parameters for Copper-Nickel Deposits of Northern Minnesota, U.S. Bureau of Mines, Open File Report No. 10-80, pp 87.

Terzaghi, K. (1943). Theoretical Soil Mechanics, John Wiley, New York, New York, pp. 510.

Vasey, J. (1983). Design and Support of Excavation Subjected to High Horizontal Stresses, Stability in Underground Mining, AIME, New York, pp. 428-449.

Vennard, J.K. and Street, R.L. (1975). Elementary Fluid Mechanics, John Wiley and Sons Inc., Toronto, pp. 326-327.

Wang, F.D., Danek, L.A. and Sun, M.C. (1971). Stability Analysis of Underground Openings Using a Coulomb Failure Criteria, Trans, Soc. Mining Eng., AIME, Vol. 250 pp. 317-321.

Wardle, L.J. (1980). Three-Dimensional Boundary Element Program for Mining Applications: MIN3D2 (3DBELM), CSIRO Publication, Technical Report No. 116, pp. 17.

Watson, J.O. and Cowling, R. (1985). Application of Three Dimensional Boundary Element Methods to Modelling of Large Mining Escavations at Depth, Paper presented to 5th Int. Conf. on Numerical Meth. in Geomech., Nagoya.

Worotnicki, G. and Walton, R. J. (1976). Hollow Inclusion Gauges for the Determination of Rock Stress In-Situ, Proc. ISRM Symp. on Investigation of Stress in Rock and Advances in Stress Measurement, Sydney, pp. 1-8.

Wright, D.F. (1980). Roof Control Through Beam Action and Arching, SME Mining Engineering Handbook, AIME, New York, Vol. 13, pp. 80-85.

APPENDIX I

A. DYNAMIC SITE CHARACTERISTICS

B. FILL CHARACTERISTICS

INTRODUCTION

This section is provided for purposes of completing the work scope as defined in Chapter 1.1. The results have not been employed directly in order to establish the design guidelines identified in Chapter 10. The reader is referred to Interim Report Project 2/3 - Data Base/Remote Monitoring for details.

A. DYNAMIC SITE CHARACTERIZATION

Dynamic strength refers to the ability of a rock to withstand failure when subjected to a changing load. This is critical in the design of optimum blast pattern configurations and in the control of rock burst damage. Three types of experiments are made to determine the behaviour of rock under dynamic loading and resonance, pulse propagation and impact (Cook, 1978).

An in-situ pulse propagation test was conducted by DuPont Canada Inc. (Preston, 1985), at Ruttan. In-situ dynamic site characteristics were determined for two ore types. This yielded information on how stress is attenuated when a rock unit id dynamically loaded by an explosive charge having a known weight and energy.

Water filled monitoring boreholes were used in conjunction with pressure sensors in order to monitor the blast induced stress build-up. The impacting stress wave causes the monitoring borehole to contract in size, producing the pressure rise. The pressure rise represents a true profile of stress transmitted according to the scaled attenuation characteristics of the rock type. Arrival times of P and S waves are measured from adjacent holes upon the initiation of a particular charge.

The dynamic rock properties are determined using the inter-relationships of P and S waves and the bulk density.

The dynamic moduli and poisson's ratio can be estimated in a semi-infinite medium by: EQNS 1

$$ED = Cs^2p[3(Cp/Cs)^2 - 4]/[(Cp/Cs)^2 - 1]$$

$$d = 1/2[(Cp/Cs)^2 - 2]/[(Cp/Cs)^2 - 1]$$

$$Kd = p(Cp^2 - 4Cs^2/3)$$

After Cook (1978)

where:

Ed - Dynamic Young's Module
d - Dynamic Poisson's Ratio
p - Bulk Rock Density
Kd - Dynamic Bulk Modulus
Cs - S Wave Velocity
Cp - P Wave Velocity

The dynamic compressive strength was calculated by measuring the borehole pressure that results in gases not being vented between the initiation hole and the point of observation. This venting would be through cracks formed by the crushing of the borehole wall in the vicinity of the point of initiation.

The dynamic tensile strength was back calculated by relating the observed back break for a particular burden to the computer estimated value given the dynamic site characteristics, hole diameter and explosive energy. The estimated back backbreak had been derived by DuPont's computer program, "Shear 2 Vers. 2" (Preston, 1985). Table 1 summarizes the dynamic site characteristics for a massive sulphide (J Zone) and chlorite schist semi-massive (C Zone) type ore. Generally, the dynamic strength properties were found to exceed the static values as is found in practice. In addition, the S wave magnitude was slightly more than one-half the P wave velocity, which is also typically found in practice (Preston, 1985). The velocity of wave propagation also reflects the degree of rock fracturing. This is depicted in Table 1 since the J Zone (higher wave velocity) is much more competent (less fractured) than the C Zone (lower wave velocity).

TABLE 1: DYNAMIC ROCK STRENGTH PROPERTIES AT RUTTAN (PRESTON 1985)

Rock Type	Young's Modulus (GPa)	Bulk Modulus (GPa)	Poisson's Ratio	Compressive Strength (MPa)	Tensile Strength (MPa)	P Wave Velocity m/s	S Wave Velocity m/s
Massive Sulphide (J Zone)	130 ± 20	61 ± 9	0.145	206 ± 31	9.3*	5,600	3,600
Semi-massive Sulphide (Chlorite Schist) (14C Stope-340L)	64 ± 10	52 ± 8	0.29	54→108 ± 16	3.4→6.9*	5,200	2,800

Values determined by in situ testing conducted by DuPont Canada Inc. Minimum data base 30 tests for each rock type

*Back calculated from observations of back break formation and dynamic site characteristics (Preston 1985)

B. FILL PROPERTIES

Laboratory tests on Ruttan backfill were conducted by Smith in 1979. The findings have been reproduced to be included in the Ruttan database. The conclusions are as follows:

1. The 60% recovery classified tailings has an effective grain size, D 10, of about 0.045 mm and a specific gravity of 3.5. It produces a backfill at a porosity of 0.45 and a dry density of about 1922 kg/m^3. Figure 1 shows the size distribution curve for this material.

2. The maximum percolation rate in this 60% classified material is estimated to be 9.6 cm/hr while the minimum percolation rate in a backfilled stope is estimated to be 3.1 cm/hr.

3. Results of standard shear box tests had shown that the friction angle for the backfill was 38 degrees. (Smith, 1989)

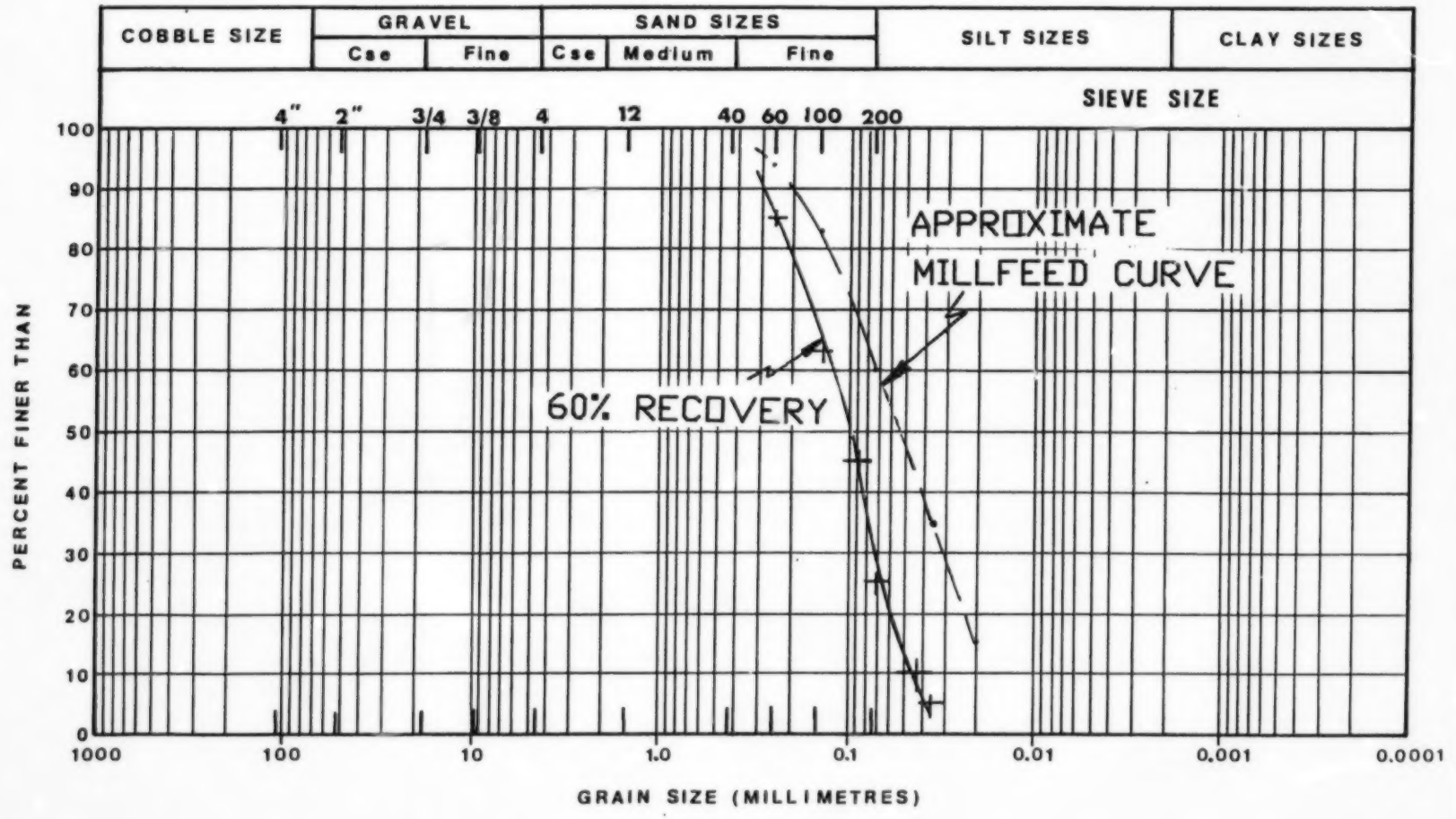

FIGURE 1: GRAIN SIZE ANALYSIS